

# **ELECTRODEPOSITION OF Ni-BASED ALLOY COATINGS AND THEIR ELECTROCHEMICAL BEHAVIOURS**

Thesis

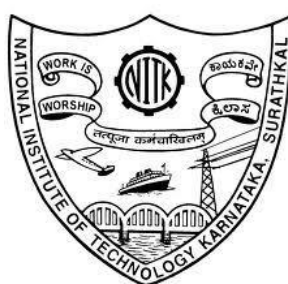
Submitted in partial fulfillment of the requirements for the  
degree of

DOCTOR OF PHILOSOPHY

By

**NEETHU RAVEENDRAN M**

**(Reg.No.177019CY002)**



DEPARTMENT OF CHEMISTRY  
NATIONAL INSTITUTE OF TECHNOLOGY KARNATAKA,  
SURATHKAL, MANGALURU – 575 025

DECEMBER, 2022



## DECLARATION

*By the Ph.D. Research Scholar*

I hereby *declare* that the Research Thesis entitled “**Electrodeposition of Ni-based alloy coatings and their electrochemical behaviours**”, which is being submitted to the **National Institute of Technology Karnataka, Surathkal** in partial fulfillment of the requirements for the award of the Degree of **Doctor of Philosophy in Chemistry** is a *bonafide report of the research work carried out by me*. The material contained in this Research Thesis has not been submitted to any University or Institution for the award of any degree.



**NEETHU RAVEENDRAN M**

Register number: 177019CY002

Department of Chemistry

National Institute of Technology Karnataka, Surathkal

Place: NITK-Surathkal

Date : 21/12/2022



## CERTIFICATE

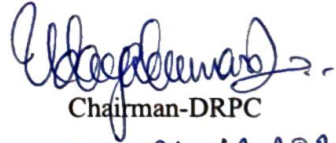
This is to *certify* that the Research Thesis entitled “**Electrodeposition of Ni-based alloy coatings and their electrochemical behaviours**”, submitted by **Neethu Raveendran M** (Register No: **177019CY002**) as the record of the research work carried out by her, is *accepted as the Research Thesis submission* in partial fulfillment of the requirements for the award of degree of **Doctor of Philosophy**.



**Prof. A. Chitharanjan Hegde**

Research guide

Date: 21.12.2022



Chairman-DRPC

Date: 21-12-2022  
डॉ. उदय कुमार डी.

Dr. UDAYA KUMAR D.

सह प्राध्यापक एवं विभागाध्यक्ष, रसायन शास्त्र विभाग  
Associate Professor and Head, Dept. of Chemistry  
राष्ट्रीय प्रौद्योगिकी संस्थान बंगलूर, सुरथकल  
National Institute of Technology Karnataka, Surathkal



*Dedicated to my parents for  
their endless love and support...*





## ACKNOWLEDGEMENT

---

I would like to express my sincere gratitude to my research supervisor Prof. A. Chitharanjan Hegde, Department of Chemistry for his continuous support and guidance throughout my research journey. His guidance and suggestions were the greatest strength to finish this work successfully. I would like to thank him for his encouragement and support to grow as a researcher. His support in each phase helped me a lot to finish this research journey successfully.

Further, I would like to thank my Research Progress Assessment Committee members, Prof. A. Nityananda Shetty, Department of Chemistry and Prof. H.D. Shashikala, Department of Physics for their invaluable suggestions and support during each assessment meeting, which helped me to bring my research work in a fruitful way.

A very special gratitude goes out to National Institute of Technology Karnataka, Surathkal for providing the Institute fellowship and financial support necessary for the completion of my research work.

I extend my profound gratitude to Dr. Udaya Kumar D., Head of the department of Chemistry and former HOD's Prof. D. Krishna Bhat and Prof. Arun M. Isloor for their great support during my research work.

Also, I would like to acknowledge all the teaching and non-teaching staff of Department of Chemistry, NITK, Surathkal, for their direct/indirect support and good wishes throughout my research work.

I thank CIF Manipal, CRF, NITK, and Mangalore University for their kind assistance in various characterization techniques.

My special thanks to my fellow labmates Ms. Cindrella N. Gonsalves, Mr. Yathish Rai, Ms. Harshini Sai, Dr. Akshatha Shetty and Dr. Abhilash P. for their immense support and cooperation, and love, which made this journey a special one in life.

I take this opportunity to thank my all friends from NITK like, Rasmi, Niveda, Panchami, Pushyaraga, Viprabha, among many for their company, love and support. I must also remember all my teachers till today, for passing their knowledge to me in shaping my mind and developing confidence in me.

Above all I would like to express my deep love and gratitude to my beloved family members, specially, to my father, mother, brother, grandmother and in-laws for their greatest support throughout of this journey. Finally, special thanks to my beloved husband, Mr.Smithin, for being my greatest strength and for his invaluable love, support which helped me to finish this journey successfully.

**NEETHU RAVEENDRAN M**

## ABSTRACT

This thesis titled '*Electrodeposition of Ni-Based alloy coatings and their electrochemical behaviours*' details the experimental results of investigation on electrodeposition and characterization of two newly proposed binary baths of nickel, namely NiW and NiCo for improved corrosion protection and electro-catalytic activity, through different new methods of electroplating. The research work presented here is primarily on optimization of two baths, using glycine as the common additive. Deposition conditions and operating variables have been optimized for best performance of alloy coatings against corrosion, and good electro-catalytic activity of alkaline water electrolysis of HER and OER (1 M KOH). The corrosion resistance and electro-catalytic activities of conventional (monolayer) alloy coatings developed using direct current were improved drastically through different modern methods of electroplating, like composition modulated multilayer (CMM) and magneto-electrodeposition (MED) methods. Experimental results showed that under optimal conditions, multilayer alloy coatings of both NiW and NiCo show several fold better corrosion resistance, compared to their monolayer counterparts, deposited from same bath for same time. Study of MED alloy coatings revealed that corrosion protection efficacy of monolayer alloy coatings can be increased to many fold of its magnitude by superimposing magnetic field ( $B$ ), both parallel and perpendicular, applied simultaneously to the process of deposition. At the same time, the electro-catalytic activity NiW and NiCo alloy coatings from their optimal baths, have been tested for their efficacy for both HER and OER during alkaline water electrolysis. The effect of addition of nanoparticles, namely Ag nanoparticles into NiCo bath has been studied for their HER activity. The corrosion resistance and electro-catalytic activity of Ni-based alloy coatings, and their nanocomposite coatings were compared in relation to their composition, surface morphology and phase structure. The process and product of electrodeposition were characterized using CV, CP, SEM, AFM, XRD, EDS and Elemental mapping techniques. The performance of alloy coatings, developed under different conditions have been compared, and discussed with Tables and Figures.

**Keywords:** *Electrodeposition, NiW, NiCo, Multilayer electrodeposition, Magneto-electrodeposition, corrosion study, HER and OER*



## CONTENTS

CHAPTER 1 .....	1
INTRODUCTION .....	1
1.1 ELECTRODEPOSITION .....	1
1.2 PRINCIPLES OF ELECTROPLATING .....	3
1.3 HULL CELL STUDY .....	5
1.4 ALLOY PLATING .....	7
1.4.1 Regular co-deposition .....	8
1.4.2 Irregular co-deposition .....	8
1.4.3 Equilibrium co-deposition .....	8
1.4.4 Anomalous co-deposition .....	9
1.4.5 Induced co-deposition .....	9
1.5 FACTORS AFFECTING THE ALLOY PLATING .....	9
1.5.1 Equilibrium potential .....	9
1.5.2 Current density .....	9
1.5.3 Temperature .....	10
1.5.4 Agitation .....	11
1.5.5 pH .....	11
1.5.6 Bath concentration .....	12
1.5.7 Plating Time .....	12
1.6 MODERN METHODS OF ALLOY PLATING .....	12
1.6.1 Composition Modulated Multilayer Alloy (CMMA) Coatings .....	13
1.6.2 MAGNETOELECTRODEPOSITION .....	16
1.7 CHARACTERIZATION OF ELECTRODEPOSITED ALLOY COATINGS .....	18
1.8 CORROSION .....	20
1.8.1 Mechanism of corrosion .....	21
1.8.2 Different forms of corrosion .....	22
1.8.3 Importance of corrosion control .....	23
1.8.4 Electrochemical techniques of corrosion monitoring .....	24
1.9 ELECTROCATALYSIS .....	29
1.9.1 Electrochemical Water Splitting Reaction .....	31
1.9.2 Electrochemical techniques for electrocatalytic water splitting reaction .....	33

CHAPTER 2 .....	37
LITERATURE REVIEW, SCOPE AND OBJECTIVES .....	37
2.1 Ni-based ALLOYS .....	38
2.1.1 Electrodeposition of NiW alloy .....	38
2.1.2 Electrodeposition of NiCo alloy .....	44
2.2 SCOPE AND OBJECTIVES .....	49
CHAPTER 3 .....	53
EXPERIMENTAL METHODS.....	53
3.1 SUBSTRATE PREPARATION FOR ELECTROPLATING .....	53
3.2 BATH OPTIMIZATION USING HULL CELL .....	54
3.3 DEVELOPMENT OF MONOLAYER COATING .....	55
3.4 DEVELOPMENT OF MULTILAYER ALLOY COATING .....	56
3.5 MAGNETOELECTRODEPOSITION .....	57
3.6 PERFORMANCE EVALUATION OF ELECTRODEPOSITED ALLOY COATINGS .....	59
3.6.1 Corrosion study .....	59
3.6.2 Electrocatalytic study.....	60
CHAPTER 4 .....	63
ELECTRODEPOSITION AND CHARACTERIZATION OF NiW ALLOY COATINGS .....	63
4.1 INTRODUCTION .....	63
4.2 EXPERIMENTAL.....	64
4.2.1 Optimization of NiW bath .....	64
4.3 RESULTS AND DISCUSSION .....	65
4.3.1 Chemical Composition.....	65
4.3.2 Surface Morphology .....	67
4.3.3 AFM Study.....	68
4.3.4 X-Ray Diffraction Study.....	69
4.3.4 Corrosion Study .....	70
4.4 CONCLUSIONS.....	74
CHAPTER 5 .....	75
ELECTRODEPOSITION OF MULTILAYER NiW ALLOY COATING FOR IMPROVED ANTICORROSION PERFORMANCE .....	75
5.1 INTRODUCTION .....	75

5.2 EXPERIMENTAL .....	77
5.3 RESULTS AND DISCUSSION .....	79
5.3.1 Optimization of CCCD's .....	79
5.3.2 Optimization of number of layers .....	81
5.3.3 Corrosion study .....	82
5.3.4 Comparison of corrosion response of monolayer and multilayer NiW alloy coating .....	86
5.3.5 SEM study after corrosion .....	87
5.3.6 Mechanism of corrosion in multilayer coatings.....	89
5.4 CONCLUSIONS.....	91
CHAPTER 6 .....	93
DEVELOPMENT OF NiW ALLOY COATINGS AND THEIR ELECTROCATALYTIC ACTIVITY FOR WATER SPLITTING REACTION.....	93
6.1 INTRODUCTION .....	93
6.2 EXPERIMENTAL.....	94
6.2.1 Electrodeposition of NiW alloy coatings .....	94
6.3 RESULTS AND DISCUSSION .....	95
6.3.1 Surface morphology and XRD study .....	95
6.3.2 Electrocatalytic activity of NiW alloy coatings .....	97
6.4 CONCLUSIONS.....	105
CHAPTER 7 .....	107
DEVELOPMENT OF COMPOSITION GRADED MULTILAYER NiCo ALLOY COATINGS AND THEIR CORROSION BEHAVIOUR .....	107
7.1 INTRODUCTION .....	107
7.2 MATERIALS AND METHODS.....	109
7.2.1 Optimization of NiCo bath.....	109
7.3 RESULTS AND DISCUSSION .....	111
7.3.1 Compositional analysis .....	111
7.3.2 Surface Morphology .....	113
7.3.3 AFM Study.....	114
7.3.4 X-Ray Diffraction Study.....	116
7.3.5 Corrosion study of monolayer NiCo Alloy Coatings .....	117
7.3.6 Improvisation of corrosion protection efficacy of monolayer NiCo alloy coatings by multilayer approach.....	121

7.3.7 Corrosion study of multilayer NiCo coating.....	124
7. 3. 8 Discussion on corrosion protection behaviour of monolayer and multilayer NiCo alloy coatings .....	127
7. 3. 9 Mechanism of corrosion in multilayer coating .....	128
7.4 CONCLUSIONS.....	129
CHAPTER 8 .....	131
IMPROVISATION OF CORROSION RESISTANCE OF NiCo ALLOY COATINGS THROUGH MAGNETO ELECTRODEPOSITION .....	131
8.1 INTRODUCTION .....	131
8.2 EXPERIMENTAL.....	132
8.2.1 Magneto-electrodeposition of NiCo alloy coatings .....	132
8.3 RESULTS AND DISCUSSION .....	134
8.3.1 SEM- EDS study.....	134
8.3.2 Effect of <i>B</i> on composition .....	136
8.3.3 XRD Study.....	138
8.3.4 AFM Analysis.....	140
8.3.5 Corrosion study .....	141
8.3.6 Comparison of ED and MED NiCo alloy coatings.....	145
8.3.5 Discussion.....	148
8.4 CONCLUSIONS.....	151
CHAPTER 9 .....	153
ELECTROCATALYTIC STUDY OF NiCo ALLOY COATINGS FOR WATER SPLITTING REACTION AND EFFECT OF Ag NANOPARTICLES ON ITS CATALYTIC ACTIVITY .....	153
9.1 INTRODUCTION .....	153
9.2 EXPERIMENTAL.....	155
9.2.1 Electrodeposition of NiCo alloy coatings .....	155
9.2.2 Characterization of NiCo alloy coatings.....	155
9.3 RESULTS AND DISCUSSION .....	156
9.3.1 Surface morphology and phase structure of alloy coatings .....	156
9.3.2 Electro-catalytic study .....	157
9. 4 EFFECT OF ADDITION OF SILVER NANO-PARTICLES .....	163
9.4.1 Development of NiCo-Ag composite coating.....	163
9.4.2 Characterization of NiCo-Ag composite coating.....	164



9.4.5 Electrocatalytic efficacy of NiCo-Ag composite coating .....	166
9.4 CONCLUSIONS.....	169
CHAPTER 10 .....	171
SUMMARY AND CONCLUSIONS .....	171
10.1 THESIS LAYOUT.....	171
10.2 EXPERIMENTAL.....	172
10.3 OPTIMIZATION OF NiW and NiCo ALLOY BATHS.....	173
10.4 ELECTRODEPOSITION OF NiW AND NiCo ALLOY COATINGS .....	174
10.4.1 Conventional monolayer alloy coatings.....	174
10.4.2 Development of multilayer and magneto-electrodeposited (MED) alloy coatings .....	175
10.5 CORROSION STUDY OF ELECTRODEPOSITED ALLOY COATINGS	175
10.6 ELECTROCATALYTIC STUDY OF ALLOY COATINGS.....	176
10.7 CONCLUSIONS.....	178
10.8 SCOPE FOR THE FUTURE WORK.....	180
REFERENCES .....	181
LIST OF RESEARCH PUBLICATIONS .....	199
PAPERS PRESENTED AT CONFERENCES .....	199
BIO-DATA .....	201



## LIST OF FIGURES

---

<b>Figure No.</b>	<b>Captions</b>	<b>Page No.</b>
1.1	Migration of hydrated metal ions to a cathode, surrender of the hydration sheath, formation of M-atoms, formation of crystal nuclei at the cathode surface	4
1.2	Schematic diagram showing a) Hull cell, b) positioning of cathode and anode in Hull cell (c) electrical field lines operating on the cathode during deposition	6
1.3	Hull cell Ruler	7
1.4	Schematic diagram showing composition modulated multilayer alloy coating having alternate layers of two different metals/alloys	13
1.5	Typical potentiodynamic polarization curve (Tafel's plot) leading to evaluate the corrosion rate by knowing the corrosion current ( $i_{corr}$ ) of given test specimen	29
1.6	Schematic representation mechanisms for Hydrogen evolution reaction	33
3.1	Diagrammatic representation showing the inclined positioning of cathode (Test panel) in Hull cell, responsible for varied current density along the length of cathode	54
3.2	Flow diagram showing different steps followed in optimization of an electrolytic bath using conventional Hull cell.	55
3.3	Electrochemical cell used for conventional electroplating (monolayer) of Ni-based alloy coatings by keeping anode and cathode parallel, using optimized bath.	56
3.4	Schematic representation showing development of electrodeposited alloy coatings, and power patterns used (below) under different conditions: a) Monolayer/homogeneous alloy coating affected due to constant current (DC), and b) Multilayer coating having alternate layers of alloys of different composition, affected due to pulsed DC.	57

3.5	Schematic diagram showing the experimental set up used magneto-electrodeposition (MED, under conditions of perpendicular and parallel magnetic field (B).	58
3.6	The schematic representation of the three-electrode corrosion cell used for corrosion study.	59
3.7	The experimental cell used electrodeposition of alloy coatings on the tip of copper rod for quantitate evaluation of electrocatalytic activity of HER and OER, using electrolyser.	60
3.8	The electrolyzer used for evaluation of electrocatalytic activity of electrodeposited alloy coatings in terms of its efficacy for HER and OER by knowing the volume of H <sub>2</sub> and O <sub>2</sub> liberated at cathode and anode during water electrolysis.	61
4.1	Dependency of composition of NiW alloy coatings on cathode current density, deposited from optimized bath.	66
4.2	Surface morphology of NiW alloy coatings deposited at different current densities. Increase of characteristic cracks with current density may be seen.	67
4.3	The AFM image showing the topography of NiW alloy coatings deposited from the optimized bath at: a) 1.0 Adm <sup>-2</sup> , b) 2.0 Adm <sup>-2</sup> , 3.0 Adm <sup>-2</sup> , and 4.0 Adm <sup>-2</sup> .	68
4.4	XRD patterns of NiW alloy coatings deposited at different current densities. A gradual increase of diffraction angle, shown by perforated vertical lines is attributed the internal strain of coatings due to increase of Ni content.	70
4.5	Nyquist plots of monolayer NiW alloy coatings deposited at optimized current densities.	71
4.6	Polarization behaviour of NiW alloy coatings deposited at different current densities from optimized bath.	73
5.1	Schematic representation of current pulses used for electrodeposition of different NiW alloy coatings: a) Direct current (DC) pulse for monolayer alloy coating, and b) Pulsed DC for multilayer alloy coating, and c)	

	Rapidly pulsed DC leading to the formation of almost monolayer coating due to diffusion of layers.	78
5.2	Nyquist plots of multilayer NiW alloy coatings having 10 layers of alternatively different composition deposited at different set of CCCD's.	80
5.3	Tafel's plots of multilayer NiW alloy coatings having 10 having 10 layers of alternatively different composition deposited at different set of CCCD's.	80
5.4	Nyquist plots of multilayer (NiW) <sub>1.0/3.0</sub> alloy coating having different number of layers deposited from the optimized bath.	82
5.5	Tafel's plots of multilayer (NiW) <sub>1.0/3.0</sub> alloy coating having different number of layers (from 10 to 300 layers), deposited form optimized bath.	83
5.6	Comparison of corrosion behaviour of monolayer and multilayer NiW alloy coatings (both optimal) with that of substrate through: a) Nyquist plots, and b) Tafel's plots	86
5.7	SEM image of electroplated NiW coatings after corrosion test displaying: a) uniform dissolution in case of monolayer alloy coating, and b) selective dissolution of alternate layers in case of multilayer coating.	87
5.8	A model multilayer diagram showing two alternate layers of (NiW) <sub>1.0</sub> and (NiW) <sub>3.0</sub> alloys, with their surface morphology, composition and XRD peaks (overlaid)	88
5.9	Representative diagram showing the mechanism of corrosion in NiW alloy coatings, deposited under different conditions: a) direct attract of the substrate in monolayer coating, b) delayed corrosion due to layered (optimal) structure of coating and c) direct attack due to diffusion of layers, affected by extreme layering	90
6.1	X-ray diffraction peaks and the corresponding SEM images of NiW alloy coatings deposited at different current densities. A slight shift of diffraction lines to right with increase of current density may be observed	96
6.2	AFM image of NiW alloy coating deposited at different current densities: (a) (NiW) <sub>1.0Adm<sup>-2</sup></sub> , and (b) (NiW) <sub>4.0Adm<sup>-2</sup></sub> . A change of surface homogeneity with change of current density may be seen	97

6.3	CV study of NiW alloy coatings corresponding to different c.d.'s showing their electro catalytic response when used as: a) cathode for HER, and b) anode for OER.	98
6.4	CP study for HER on the surface of NiW alloy coatings, deposited at different current densities (a), and (b) the volume of H <sub>2</sub> gas evolved at different current densities. Highest efficacy of (NiW) <sub>1.0 Adm<sup>-2</sup></sub> towards HER may be seen compared to other coatings.	100
6.5	CP study for OER on the surface of NiW alloy coatings, deposited at different current densities (a), and (b) the volume of O <sub>2</sub> gas evolved at different current densities. Highest efficacy of (NiW) <sub>4.0 Adm<sup>-2</sup></sub> towards OER may be seen compared to other coatings.	101
6.6	Electrocatalytic activity NiW alloy coatings deposited at different current densities in terms of the volume of H <sub>2</sub> and O <sub>2</sub> gas produced during electrolysis of water for duration 10 min.	103
6.7	Representational diagram showing inverse dependency of (NiW) alloy coating, deposited at different current density for HER and OER in alkaline water electrolysis	104
7.1	Variation in the Wt % of Ni and Co in NiCo alloy deposit with current density, deposited from optimized bath	112
7.2	Surface morphology of NiCo alloy coatings corresponding to different current densities deposited from optimal bath	114
7.3	AFM images of NiCo coating deposited at (a) 1.0 Adm <sup>-2</sup> , (b) 2.0 Adm <sup>-2</sup> , (c) 3.0 Adm <sup>-2</sup> and (d) 4.0 Adm <sup>-2</sup> showing increase of uniformity with current density	115
7.4	XRD patterns of NiCo alloy coatings deposited at different current densities from optimal bath	117
7.5	Nyquist plots of NiCo alloy coatings deposited at different current densities from optimized bath.	118
7.6	Polarization behaviour of NiCo alloy coatings deposited at different current densities from optimized bath	120

7.7	Nyquist plots of multilayer NiCo alloy coating having 10 layers of alloy of different composition, deposited at different set of CCCD's, from optimized bath	122
7.8	Tafel plots of multilayer NiCo alloy coating having 10 layers of alloys of different composition, deposited at different set of CCCD's, from optimized bath	122
7.9	Nyquist plots of multilayer (NiCo) <sub>2.0/4.0</sub> alloy coatings having different number of layers deposited from the optimized bath	124
7.10	Tafel's plots of multilayer (NiCo) <sub>2.0/4.0</sub> alloy coatings having different number of layers deposited form optimized bath.	126
7.11	Comparison of impedance and polarization behaviour of monolayer (NiCo) <sub>4 Adm<sup>-2</sup></sub> and multilayer (NiCo) <sub>1.0/3.0/120</sub> alloy coatings through: a) Nyquist plots and b) Tafel's plots	127
7.12	Cross-sectional SEM image of (NiCo) <sub>2.0/4.0/10</sub> coating showing the formation of layered coating (having 10 layers)	128
8.1	The experimental set up used for magneto-electrodeposition of NiCo alloy coating under condition of a) parallel, and b) perpendicular to B to the direction of electrical field. It may be noted that in a) lines of electric field and magnetic field are parallel, and in b) they are perpendicular to each other	133
8.2	Surface morphology of MED (NiCo) alloy coatings developed from the optimized bath under different intensity of B (parallel). In the inset is given (NiCo) <sub>4.0 Adm<sup>-2</sup></sub> alloy deposited without the effect of B, showing rough surface	135
8.3	Surface morphology of MED (NiCo) alloy coatings developed from the optimized bath under different intensity of B (perpendicular) In inset is given (NiCo) <sub>4.0 Adm<sup>-2</sup></sub> alloy deposited without the effect of B, showing rough surface	136
8.4	Variation in the Wt % of Ni and Co in ED and MED NiCo alloy coatings deposited from optimized bath. Increase of Ni content in the deposit with B may be seen.	137

8.5	XRD patterns of MED NiCo alloy coating obtained at different magnetic field strengths (parallel), under optimal current density from the optimized bath	138
8.6	XRD patterns of Ni-Co alloy coating obtained at different magnetic field strength (perpendicular), under optimal current density from the optimized bath. The same diffraction angles to all coatings deposited at different intensity of B indicates that coatings of same phase structures are formed during deposition	139
8.7	AFM image of NiCo alloy coatings deposited under different optimal conditions of electrodeposition :(a) ED(NiCo) <sub>4.0Adm</sub> <sup>-2</sup> , (b) MED(NiCo) <sub>4.0/0.3T/par</sub> , and (c)(NiCo) <sub>4.0/0.3T/per</sub> , from same bath.	140
8.8	Nyquist response for MED (NiCo) alloy coatings deposited at different intensity of B: (a) parallel, and (b) perpendicular, deposited from same bath	142
8.9	Potentiodynamic polarization behaviour of MED (NiCo) alloy coatings deposited at different conditions of magnetic field applied: (a) parallel and (b) perpendicular	144
8.10	Comparison of XRD patterns and microstructure of MED NiCo alloy coatings deposited under optimal conditions of parallel and perpendicular B, in comparison with ED NiCo alloy coatings, deposited from the same bath	147
8.11	Comparison of impedance responses of MED (NiCo) alloy coatings (under parallel and perpendicular B) in relation of ED (NiCo) coating deposited from same bath (all under optimal condition). Tafel's responses are given in the inset	148
8.12	Diagrammatic representation showing lines of ionic movement responsible for change in EDL thickness during electrodeposition of (NiCo) alloy coatings: a) ED (NiCo) Natural convection b) MED (NiCo) Parallel B, and c) MED (NiCo) Perpendicular B	149
8.13	Schematic representation showing: a) Process of magneto-electrodeposition and b) decrease of diffusion layer thickness ( $\delta$ ) due to	



	increase of limiting current density ( $i_L$ ) on superimposition of magnetic field, B	150
9.1	X-ray diffraction peaks of (NiCo) coatings, deposited at different current densities from the optimized bath. On the right are given their SEM image showing different surface morphology responsible for their different electro-catalytic activities	156
9.2	AFM image of (a)(NiCo) $_{1.0\text{Adm}^{-2}}$ and (b)(NiCo) $_{4.0\text{Adm}^{-2}}$ deposited from same bath for same duration, showing change of surface topography with deposition current density	157
9.3	CV curves for HER of (NiCo) coatings deposited at different current densities from optimized bath	158
9.4	Chrono-potentiograms for (NiCo) alloy coatings deposited at different current densities at applied cathodic current of - 3.0 A, showing different responses for HER	160
9.5	Cyclic voltammograms of OER on the surface of (NiCo) alloy coating, deposited at different current densities	161
9.6	Chronopotentiograms of (NiCo) alloy coatings deposited at different current densities showing different responses for OER	162
9.7	SEM image of (NiCo) alloy coating under different conditions: (a) (NiCo) $_{1.0\text{Adm}^{-2}}$ , (b) (NiCo-Ag) $_{0.5}$ , (c) (NiCo-Ag) $_{1.0}$ and (d) (NiCo-Ag) $_{2.0}$	164
9.8	Elemental mapping of (NiCo-Ag) composite coatings deposited from optimal bath having added with varied quantity of Ag nanoparticles: a) 0.5g/L, (b) 1.0g/L and (c) 2g/L. Presence of Ni, Co and Ag may be noted in all three coatings, confirming the incorporation of Ag in alloy matrix of (NiCo)	165
9.9	AFM image showing the surface roughness of a) (NiCo) $_{1\text{Adm}^{-2}}$ coating and b) (NiCo-Ag) $_{1.0}$ composite coating, deposited from same bath, A substantial difference in the topography of coatings may be seen due to addition of Ag nanoparticles	166
9.10	CV curves of HER on the surface of (NiCo-Ag) composite coatings deposited at $1.0\text{Adm}^{-2}$ from the optimized bath, having added with	167

different quantity of Ag nanoparticles. Highest cathodic peak current density (ipc) corresponding (NiCo-Ag)<sub>1.0</sub> indicates its highest efficacy for HER compared to other coatings

- 9.11 CP curves of HER on the surface of (NiCo-Ag) composite coatings deposited at 1.0 Adm<sup>-2</sup> on adding different amount of Ag nanoparticles into the optimized bath 168
- 10.1 Flow chart of the research work presented in the thesis 172
- 10.2 Schematic of the various deposition techniques used for development of different binary alloy coatings, using the same optimized bath 173
- 10.3 Histogram showing the corrosion rates (CR) of (NiW) and (NiCo) alloy coatings, achieved through different approaches in relation to that of their monolayer counterpart, deposited using DC, from same bath for same duration of time 176
- 10.4 Diagrammatic representation showing the relative performance of Ni-based alloy coatings as electro-catalyst for alkaline water electrolysis of HER and OER (deposited for same duration of time) 177

## LIST OF TABLES

---

<b>Table No.</b>	<b>Captions</b>	<b>Page No.</b>
4.1	Composition and operating conditions of optimised NiW bath	65
4.2	The surface roughness data of NiW alloy coatings developed at different current densities, using optimized bath	69
4.3	EIS data obtained by electrochemical equivalent circuit of NiW alloy coating developed at different current densities	72
4.4	Corrosion parameters of monolayer NiW coatings deposited at different current densities from standard bath	73
5.1	Corrosion parameters of multilayer NiW alloy coatings having 10 layers of alternatively different composition deposited at different set of CCCD's	81
5.2	Corrosion data of multilayer NiW alloy coatings having different number of layers deposited from the optimized bath.	84
6.1	Electro-catalytic kinetic parameters of NiW alloy coatings for HER and OER during alkaline water electrolysis, with metal contents in the deposit	99
7.1	Bath constituents and operating variables of optimized NiCo bath	110
7.2	AFM data of NiCo alloy coatings deposited at different current densities from optimized bath	116
7.3	EIS data from equivalent circuit of NiCo alloy coatings at different current densities	119
7.4	Corrosion parameters of NiCo coatings deposited at different current densities with wt. % metals content in the deposit, in relation to those in the bath	121
7.5	Corrosion parameters of multilayer NiCo alloy coatings having 10 alternate layers of alloys of different composition, deposited at different current density from optimal bath.	123

7.6	EIS data obtained by equivalent circuit simulation of NiCo alloy coating having different number of layers deposited from the optimized bath	125
7.7	Corrosion data of multilayer NiCo alloy coatings having different number of layers deposited from the optimized bath	126
8.1	Corrosion parameters of magneto-electrodeposited NiCo alloy coatings from optimized bath under different conditions of B, in relation to its monolayer counterpart	137
8.2	The surface roughness data of NiCo alloy coatings deposited under different optimal conditions of electrodeposition :(a) ED(NiCo) <sub>4.0Adm<sup>-2</sup></sub> , (b) MED(NiCo) <sub>4.0/0.3T/par</sub> , and (c) (NiCo) <sub>4.0/0.3T/per</sub> , from same bath.	141
8.3	EIS data obtained from equivalent circuit simulation of (NiCo) alloy coatings electrodeposited under different conditions of magnetic field (B	143
9.1	The electro-kinetic parameters of HER on the surface of (NiCo) alloy coatings deposited at different current densities, deposited from same bath	159
9.2	Electrochemical parameters obtained for OER on the surface of (NiCo) alloy coatings deposited at current densities	162
9.3	Electro-catalytic parameters of (NiCo-Ag) composite coatings in different composition for HER alkaline water electrolysis	168
10.1	Composition and operating parameters of optimized binary alloy baths used for electrodeposition and characterization of different alloys	174

## A. LIST OF ABBREVIATIONS

AC	Alternate current
AFM	Atomic force microscopy
c.d.	Current density
CMMA	Composition modulated multilayer alloy
CMA	Composition multilayer alloy
CP	Chronopotentiometry
CR	Corrosion rate
CV	Cyclic voltammetry
CVD	Chemical vapor deposition
DBT	Dual bath technique
DC	Direct current
ED	Electrodeposition
EDL	Electrical double layer
EDS	Energy dispersive X-ray spectroscopy
EIS	Electrochemical impedance spectroscopy
HER	Hydrogen evolution reaction
MED	Magneto electrodeposition
MHD	Magneto hydrodynamic
OCP	Open circuit potential
OER	Oxygen evolution reaction
PVD	Physical vapor deposition
SBT	Single bath technique
SCE	Saturated calomel electrode
SEM	Scanning electron microscopy
wt. %	Weight percentage
XRD	X - ray diffraction

## B. LIST OF SYMBOLS

$A \text{ cm}^{-2}$	Ampere per centimeter square
$\text{Adm}^{-2}$	Ampere per decimeter square
$i_{\text{pa}}$	Anodic peak current density
$\beta_a$	Anodic Tafel slope
$C_{\text{dl}}$	Capacitance double layer
$\eta_c$	Cathodic overpotential
$i_{\text{pc}}$	Cathodic peak current density
$\beta_c$	Cathodic Tafel slope
$R_{\text{ct}}$	Charge transfer resistance
$i_{\text{corr}}$	Corrosion current density
$E_{\text{corr}}$	Corrosion potential
$\delta$	Diffusion layer thickness
$i_o$	Exchange current density
$i_L$	Limiting current density
$C_B$	Concentration of ions
$F_L$	Lorentz force
$B$	Magnetic field intensity
$R_a$	Mean roughness
mA	Milliampere
mV	Millivolts
$R_P$	Polarization resistance
$R_q$	Root mean square roughness
$R_s$	Solution resistance
$E^\circ$	Standard electrode potential
E	Potential

# **CHAPTER 1**

## **INTRODUCTION**





# CHAPTER 1

## INTRODUCTION

---

*This chapter provides a brief introduction to the principles of electroplating of metals/alloys and their applications. The theory of electrodeposition with a special emphasis on principles of alloy deposition is explained. An overview of electroplating and different factors which can influence the process and product of electrodeposition is given. Introductory aspects of corrosion and electrocatalytic activity of metals/alloys are given. The importance of Ni-based alloy coatings as corrosion-resistant and electro-catalytic material is reviewed in brief. An introduction to different modern methods of electroplating such as composition modulated multilayer (CMM), and magnetoelectrodeposition (MED) to achieve higher performance efficiency of alloy coatings are given.*

### 1.1 ELECTRODEPOSITION

Electrodeposition is the process of coating a thin and uniform layer of a metal or alloy on top of a conducting substrate to modify its surface properties. Through this technique, one can modify the surface properties of any metals/alloy without changing its bulk properties. By the principle of electrolysis, it is a process that uses electrical current to reduce the cations of a desired material from an electrolyte and coat those materials as a thin film onto a conductive substrate surface. The properties of electrodeposited coatings generally depend on the plating variables such as bath composition, temperature, pH of the bath, stirring rate, the concentration of the additives, etc., and most importantly the current density at which plating is carried out. Electroplating is commonly done either to impart the desired physico-mechanical properties for a substrate such as better electrical, mechanical, corrosion resistance properties, wear, and frictional resistance, or to give a desired decorative appearance. Hence, the surface properties of a material can be tailored to one's requirement by proper manipulation of electrodeposition conditions. But due availability of advanced power sources and greater flexibility in the mass transport process, today electroplating technology has no

more remained a simple method to impart a better appearance to materials, it is an elegant approach to modify their the surface properties. Hence, today electroplating technology is responding in both revolutionary and evolutionary ways due to ever-increasing demand in the industry. It has turned into an important means for developing nano/microstructured materials, showing a variety of functional properties. Some of the technological areas in which electroplating finds an important area are macro and microelectronics, optics, optoelectronics, giant magnetoresistance (GMR), and sensors of most types, to name only a few among many (Schwarzacher 2006). The fundamental laws governing the process of electroplating are proposed as early as 1833 by Faraday (Poyner 1987), and are stated as follows:

**i) Faraday’s first law of electrolysis**

During electrolysis, the mass of a metal/alloy deposited/dissolved at an electrode surface is directly proportional to the quantity of electricity passed. If the mass of metal/alloy discharged/dissolved is ‘m’ in g, when quantity ‘Q’ electricity is passed through electrolyte solution, then it may be written as,

$$m \propto Q \quad \text{or } m = ZQ, \quad \text{or } m = Z (I \times t) \quad (1.1)$$

Here, Z is the constant of proportionality, called the electrochemical equivalent weight of the metal/alloy; and the quantity of electricity Q in coulombs is the product of current (I), expressed in ampere (A) and ‘t’ is the time of flow of current expressed in second. Faraday demonstrated that on passing 1 Faraday (96,485C) of charge, it can liberate 1 gram equivalent of the substance at the electrode surface. This means that 1C will liberate one gram equivalent of a substance/96,485, which is the electrochemical equivalent (Z) of the substance.

**ii) Faraday’s second law of electrolysis**

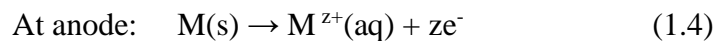
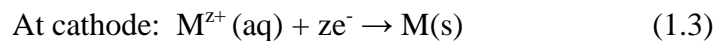
When the same quantity of electricity is passed through two different electrolyte solutions, A and B for the same duration of time, then the masses of the substances ( $m_A$  and  $m_B$ ) discharged at the electrodes are directly proportional to their equivalent masses. Hence, it may be written as

$$m_A/m_B = E_A/E_B \quad (1.2)$$

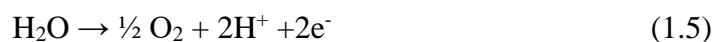
Where  $E_A$  and  $E_B$  are equivalent masses of A and B respectively.

## 1.2 PRINCIPLES OF ELECTROPLATING

Electroplating is an electrochemical process that involves the applying of a metallic coating over an electrically conducting substrate. It is carried out in an electrochemical cell, in which the substrate to be plated is acting as the cathode (negative electrode); and the anode (positive electrode) is either a non-metallic conductor such as graphite or coating metal itself, which completes the circuits and these two electrodes are immersed in an electrolyte and is also called as electrolytic bath containing the required metal ions either as a hydrated cation or as a complex ion. During deposition, the electrodes are connected to the power source and the direct current (DC) is allowed to pass through the circuit which acts as impelling force for the process of deposition. When the current passes through the circuit, the cations move towards the negatively charged cathode and there it is deposited as metal atoms. In the case of the sacrificial anode, it undergoes oxidation at the same time to replace the metal ions removed, and thereby maintain a constant metal ion concentration in the bath.



However, in the case of insoluble anode oxidation of water takes as below:



The electrodeposition of metal at the cathode surface depends on the rate of metal ion discharge from the electrolyte. Once the current starts flowing through the electrolytic cell, the metal ions accept an electron from the electrically conducting material at the solid-electrolyte interface and then deposit as metal atoms onto the surface of the cathode. The required electrons for the deposition process are provided either from an externally applied potential or the metal ions themselves derive either from metal salts added to the solution or by the anodic dissolution of the so-called *sacrificial anodes*, made of the same metal that is to be deposited on the cathode. Basically, electrodeposition is a very complex atomistic process, wherein metal ions (cations) from the electrolyte need to be deposited as metal atoms on the cathode surface. This process supposedly involves several steps, which are mentioned categorically as below:

- i) Transfer of hydrated metal ions or complex from the bulk solution to the cathode surface.
- ii) Stripping of the hydration sheath of metal ions after reaching the electrode/electrolyte interface.
- iii) Charge transfer with the formation of adsorbed atoms at the cathode surface.
- iv) Formation of the crystal nuclei by diffusion of adsorbed atoms at the cathode surface.
- v) Fusion of thermodynamically stable crystal nuclei to form a metallic layer on the surface of the cathode.

Thus individual steps involved in the overall process of electrodeposition are shown collectively in Figure 1.1, to understand the complex process of deposition in a simple way. Basically, in an electrode, the inner layer (the region close to the electrode) which contains solvent molecules and specifically adsorbed ions is known as the *inner Helmholtz plane* (IHP).

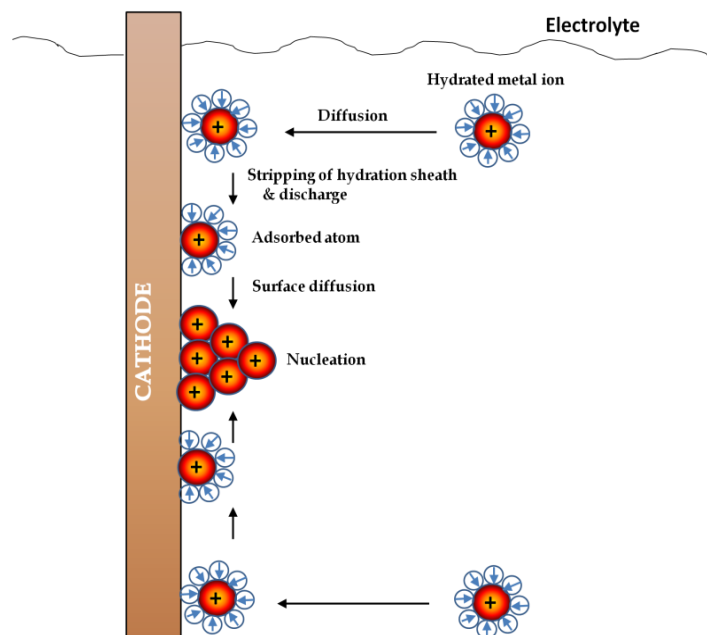


**Figure 1.1** - Migration of hydrated metal ions to a cathode, surrender of the hydration sheath, formation of M-atoms, formation of crystal nuclei at the cathode surface.

It passes through the centres of the specifically adsorbed ions. The *outer Helmholtz plane* (OHP) passes through the centres of solvated ions at the distance of their closest

approach to the electrode, which refers to the thickness of the *electrical double layer* (EDL). The diffusion of adsorbed ions to form adsorbed atoms takes place within the EDL, which forms spontaneously at the metal-solution interface. Although the metal ions lose most of their charge in this process, the residual charge remains on the part of their hydration sheath. In this state, and after passing through the electrolytic double-layer, they are adsorbed on the cathode surface where they form adsorbed atoms. Hence, a coherent metal film is formed on the cathode surface, and this process is known as nucleation, and subsequently, crystal growth takes place. This process is called electro-crystallization. Thus nucleation results from diffusion-controlled migration of the ad-atoms on the surface, and the growth process begins once the nuclei have reached a critical size (Kanani 2006).

### **1.3 HULL CELL STUDY**

The Hull cell is a kind of test cell intended to check operating parameters during the electrodeposition in the electroplating technology. The variables such as cathode c.d. range, the convergence of the added substances, the effect of additives, pH of the bath, and so on can be optimized by this method. Richard Hull innovated this method of testing and acquainted it with the business in 1939, and accordingly, the procedure is named as Hull cell method. The Hull cell is a trapezoidal shape container made of an insulating material such as Perspex or PVC material, having the capacity of holding 267 mL of solution. The representative diagram of the Hull cell, positioning of cathode and anode inside the Hull cell, and consequent electrical field lines on the cathode are shown in Figure 1.2 (a). In the Hull cell, the cathode of  $75 \times 100$  mm is angled with respect to the anode of  $60 \times 75$  mm size as shown in Figure 1.2 (b). Hence, when a current is applied across the anode and cathode, the resulting current density varies along the length of the cathode as shown in Figure 1.2 (c). The highest current density (HCD) side is closest to the anode, and the lowest current density (LCD) side is far from the anode. Based on the nature of the deposit obtained along the length of the cathode, one can fix the operating current density required to obtain the desired coatings, using Hull cell Ruler. The test is simple and quick to carry out and thereby this technique offers the possibility to alter the plating parameters, make additions or undertake treatments without interrupting production. Further, for analysis of the hull

cell plate, a plater need to have a certain amount of skill which can be achieved by practice.

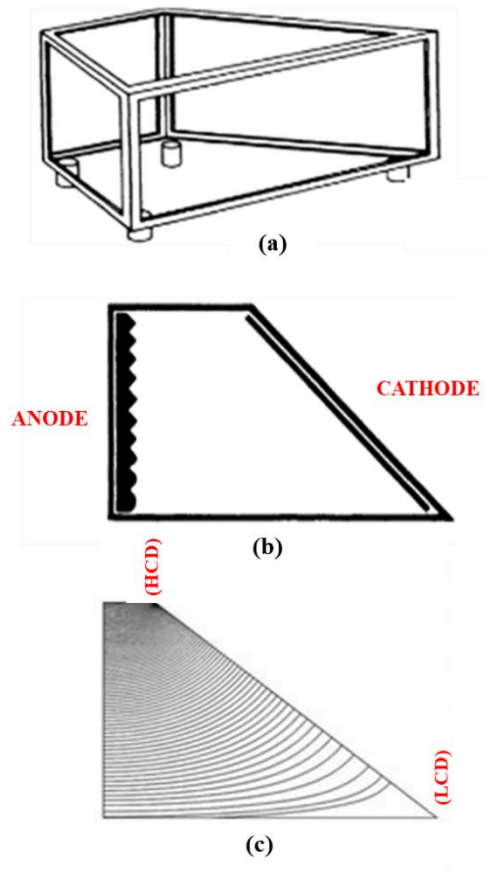


**Figure 1.2** - Schematic diagram showing a) Hull cell, b) positioning of cathode and anode in Hull cell (c) electrical field lines operating on the cathode during deposition.

The Hull cell study can be carried out using a given electrolytic bath by passing a definite quantity of cell current such as 1A, 2A, 3A, etc. The current density, corresponding to the region at which satisfactory deposition is obtained can be fixed by referring Hull cell ruler shown in Figure 1.3, depending on the cell current employed. The current density at a given point along the cathode panel can also be calculated using the formula,

$$I = C (5.10 - 5.24 \log L) \quad (1.6)$$

where 'I' is the current density in  $\text{Adm}^{-2}$  at any point on the cathode, 'C' is the current strength used for the test, and 'L' is the distance in cm from point of high current density (HCD) to the point on the cathode at which current density is desired to be known.

1 AMP	40	30	25	20	15	12	10	8	6	4	3	2	1	0.5
2 AMPS	80	60	50	40	30	24	20	16	12	8	6	4	2	1
3 AMPS	120	90	75	60	45	36	30	24	18	12	9	6	3	1.5
5 AMPS	200	150	125	100	75	60	50	40	30	20	15	10	5	2.5

*Figure 1.3 - Hull cell Ruler*

Thus Hull cell test helps the platter to save time, money, and error that occur during plating. Thus Hull cell is an invaluable analytical tool for preventive maintenance of electroplater. This tool allows to make corrections before problems occur in production and to troubleshoot after they have occurred. Hence Hull cell is one of the most trusted testing devices in modern electroplating even today, because of its simplicity and utility. Due to extensive, it is said that ‘a platter without a Hull cell is like an electrician without a voltmeter’ (Dini 1993).

#### **1.4 ALLOY PLATING**

By definition, an alloy is a substance that has metallic properties and is composed of two or more chemical elements of which at least one is a metal (Brenner 1963). Thus alloy plating is the co-deposition of two or more elements out of which one should be metal, and forming an alloy coating on the cathode surface. An alloy can exhibit qualities that are unobtainable with parent metals. This is particularly true for electrodeposited alloys. Some important properties of materials, such as hardness, ductility, tensile strength, Young’s modulus, corrosion resistance, solder-ability, wear resistance, and antifriction service, may be enhanced through electrodeposition of alloys (Jović, V.D., Lačnjevac, U.Č., Jović 2014). In addition, the mechanical, or the chemical properties of the electrodeposited alloy coating can be varied over a wide range than that of the pure metal (Brenner 1963a). Electrodeposited alloy coatings have a wide scope of uses in the hardware, metals, and surface finishing industry, and an enormous number of binary and ternary combinations of the alloy have been plated from aqueous electrolytes for microfabrication or surface finishing. The functional properties of alloy coatings depend on their chemical composition and structure. Hence,

one can mould the properties of alloy coatings based on the specific requirement. In addition to the factors responsible for single metal deposition, the plating process of alloy deposition also depends on many factors such as the potential difference between alloying elements, pH of the electrolytic bath, its composition, etc. Brenner, in his treatise (Brenner 1963) classified the alloy deposition processes into the following five types: a) Regular co-deposition, b) Irregular co-deposition, c) Equilibrium co-deposition, d) Anomalous co-deposition, and e) Induced co-deposition

#### **1.4.1 Regular co-deposition**

The Regular co-deposition usually occurs in an electrolyte having simple metal ions, but it can also take place from the electrolytic bath having complex ions. This co-deposition process is usually controlled by diffusion phenomena. The composition of the deposit depends on the metal ion concentration at the cathode diffusion layer which is further affected by the plating parameters. The composition of the noble metal in the deposit can be enhanced by increasing the metal content near the cathode surface and by other factors such as lowering the deposition current density, high bath temperature, an increased stirring of the bath during deposition, etc.

#### **1.4.2 Irregular co-deposition**

The electrolytic bath containing a complexing agent usually forms a complex ion with the metals present in it, and thereby bringing the electrode potential of the depositing metal closer and forming a solid solution of the corresponding metals. Also, the plating parameters have less effect on the composition of the deposit thus obtained. But, it may be affected by the concentration of the complexing agent present in the bath. Usually, this type of co-deposition is not controlled through diffusion phenomena, but, takes place by the characteristic potential of the depositing metals.

#### **1.4.3 Equilibrium co-deposition**

The deposition is carried out from an electrolytic bath in which the electrolyte and the depositing metals are existing in chemical equilibrium. At low current density, the ratio of the co-depositing metal remains the same as that of its ratio in the electrolyte. There are only a few alloy system such as copper-bismuth and lead-tin alloys deposited from an acid bath that comes under this category of co-deposition.



#### **1.4.4 Anomalous co-deposition**

This type of alloy deposition is characterized by the anomaly that less noble metal deposits preferentially than the more noble metal. Anomalous co-deposition is rather rare. It is most frequently associated with the electrodeposition of alloys containing one or more of the three metals of the iron group: iron, cobalt, or nickel. This type of alloy deposition is occurring at particular concentrations and operating parameters of the bath and is more common in alloys/mutual alloys of iron group metals.

#### **1.4.5 Induced co-deposition**

Some metals such as molybdenum, tungsten, or germanium cannot be deposited alone from their electrolytic solution. But the iron group elements including nickel, cobalt, iron, etc. can induce its deposition and form Ni-Mo, Ni-W, Fe-W, W-Co, etc. Metals that cannot deposit by themselves are known as *reluctant metals* and the metals which help the deposition of reluctant metals are known as *inducing metals*. The composition of the resulting alloy system does not completely dependent on the plating variables. Hence, the composition of the alloy coatings is quite vagarious and unpredictable (Brenner 1963).

### **1.5 FACTORS AFFECTING THE ALLOY PLATING**

Electroplating is relatively a simple and inexpensive technique widely used to produce alloy coating having improved appearance and enhanced properties such as corrosion resistance, wear resistance, conductance, etc. Though the technique is comparatively easy to carry out, the process involved in it is quite complex and it can be affected by many factors which are described below.

#### **1.5.1 Equilibrium potential**

The co-deposition of the metals takes place only when the deposition potential of the metal comes closer. Some factors can bring the potential of the depositing element closer. They are: (a) using solutions in which the metals are present as complex ions, (b) increasing the current density, (c) using addition agent, and (d) lowering the concentration of the more noble metal in the solution (Brenner 1963)

#### **1.5.2 Current density**

Current density, the current in amperes per unit area of the electrode, is one of the most important variables that can influence the electrodeposition process. During the

electrodeposition, the inadequate flow of current will result in poor deposit, while the excessive current flow does not bring the increased deposition rate and can throw some adverse effects. Thus in general, the effect of the operating variable does not follow any strict rule. Hence, the effect of current density also shows the same behaviour. Hence, the dependence of the composition of alloy coatings on the current density varies confounding. In the case of regular alloy systems, an increase in current density causes a decrease in noble metal content in the deposit. Whereas in other alloy plating systems, the variation of composition with the current density is quite unpredictable. This means with the variation in the current density the composition of more noble metal in the alloy coating may either increase, decrease, or remain unchanged (Brenner 1963).

### **1.5.3 Temperature**

The effect of temperature on electrodeposition, and hence on the composition of resulting alloy coatings can be due to the changes in different plating characteristics such as equilibrium potential, the concentration of the bath, polarization, cathode current efficiency, etc. The temperature has less effect on the equilibrium potential of the system. At the same time, to study the effect of temperature on the polarization, the actual deposition potential of the metal has to be determined. With the temperature rise, the deposition potential of the metal becomes nobler as polarization is decreased. Also, an increase in temperature increases the diffusion and convection movements of metal ions towards the cathode diffusion layer and thereby facilitates the deposition of metal on the substrate. In the case of a regular alloy coating system, elevation in temperature can increase the composition of the noble metal content in the alloy coating. But in the irregular plating system, the effect of temperature does not follow a particular trend. In the majority of cases, the rise in temperature favours the deposition of more noble metal in the deposit. In the case of anomalous co-deposition, the effect of temperature on the composition of alloy coatings depends on two opposing factors. One is polarization and the other is diffusion. With the increase in temperature, polarization decreases the less noble metal content, and the diffusion phenomena increase, and hence less noble metal content in the deposit. Hence, the actual trend in the variation of the composition of alloy coating with temperature is quite inconsistent. At the same time, the dependence of the composition of the alloy coating on temperature is predictable in the case of

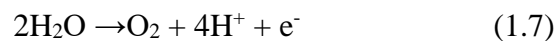
induced type of co-deposition, and it can be seen that the rise in temperature leads to a small increase in the reluctant metal composition.

#### **1.5.4 Agitation**

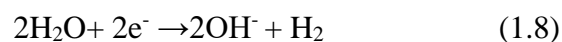
Agitation is the mechanical stirring of the electrolytic bath which can affect the composition of the alloy coating. It does not influence the electrochemical properties of the solution and the deposition mechanism. Generally, agitation of the electrolytic bath reduces the diffusion layer thickness near the cathode surface, and thereby a concentration polarization occurs between the cathode surface - solution interfaces. Since the diffusion layer thickness is decreased, there occurs a concentration gradient is developed between the diffusion layer and the bulk of the solution. This leads to the rapid movement of metal ions from the bulk towards the cathode surface and hence stimulates the deposition process. Agitation reduces the gas bubbles which can create pits in the deposit. But all these effects of agitation exhibit only when all other variables are properly optimized and maintained (Brenner 1963b).

#### **1.5.5 pH**

The effect of pH during the electrodeposition process and on the composition of the alloy coatings is usually uncertain and it varies from system to system. The pH of the electrolytic bath can highly influence the coating characteristics. Therefore, to get a fine deposit, the pH of the bath should be kept constant. The bath pH affects hydrogen evolution voltage, the precipitation of metal ions, and the decomposition of the metal ion complex from which the metal is deposited. In a complex bath, pH can affect various equilibrium processes. In the case of the insoluble anode, oxygen evolution takes place at the anode



On the other hand, at the cathode hydrogen evolution takes place followed by the formation of hydroxide ion



In the case of a neutral bath, if the anode current efficiency is greater than that of cathode current efficiency, the bath becomes more alkaline. While the bath pH

remains unchanged if the electrode efficiencies are similar. Hence the change in pH of a plating bath is a good indication of electrode efficiencies. In certain conditions, the hydrogen evolution increases the bath pH which further leads to the precipitation of metal hydroxides which get co-deposited with the metal being plated. An electrolyte containing simple metal ions is very sensitive to the variation in pH of the solution. In regular co-deposition where the metal ions are present as simple ions, the effect of pH on the composition of the alloy deposit is less. Whereas in irregular co-deposition the variation of pH has more effect on the composition of the alloy coatings (Brenner 1963; Kumar et al. 2015).

#### **1.5.6 Bath concentration**

Generally, bath concentration has a significant role in the electrodeposition process. In ordinary deposition conditions, when the bath concentration increases it leads to an increase in the metal ions concentration, which further increases the deposition rate of metal ions from the bath. In the case of alloy coating, the composition of metals in the alloy deposit depends on the concentration of the metal ions in the bath. In general, the ratio of the composition of metals in the alloy coatings differs considerably from their ratio in the bath. At the same time, there are alloy systems that show the same ratio of metal components in the alloy coating and the electrolytic bath (Brenner 1963; Kumar et al. 2015).

#### **1.5.7 Plating Time**

The plating time during the electrodeposition process can affect the thickness of the coating. Generally, with time the thickness of the coating increases. As stated earlier, according to Faraday's first law of electrolysis, quantity charge flow (Q) in the solution is directly proportional to the product of current flow (I), and flow time (t) as shown in the equation below (Kumar et al. 2015).

$$Q = I \times t \quad (1.9)$$

### **1.6 MODERN METHODS OF ALLOY PLATING**

Electrodeposition is a well-known coating technique in which one can modify the deposited property by introducing suitable additives into the plating bath, which can preferentially adsorb on specific crystallographic planes and alter the growth mechanism (Brenner 1963). Alternatively, properties and hence performance of alloy

coatings can be improved drastically by bringing variations in the mass transport process of metal ions towards the cathode during the process of electrodeposition. In this direction, the development of multilayer alloy coatings and magneto-electrolysis of alloy coatings are promising methods to synthesize the alloy coatings materials showing advanced properties (Tacken and Janssen 1995), compared to their conventional alloy coatings.

### 1.6.1 Composition Modulated Multilayer Alloy (CMMA) Coatings

A new class of materials with alternating layers of different metals/alloys of different compositions having a thickness of few nanometers with ultra-fine microstructure are known as compositionally modulated multilayer alloys (CMMA), or composition modulated multilayer (CMM), or simply multilayer coatings. CMMA coatings are the class of material with layered structures in which alloy coatings of different compositions are arranged alternatively. These multilayer materials exhibit extraordinary properties compared to their conventional alloy coatings. As a result of layering in atomic dimensions, multilayer coatings exhibit unusual and outstanding properties such as enhanced mechanical, magnetic properties, improved corrosion resistance, etc. which are not obtainable in normal metallurgical alloys. This class of materials shows improved properties in terms of magnetic behaviour, mechanical strength, wear, and corrosion resistance, elasticity, ductility, electrical, optical, and chemical properties which differ considerably from pure metals or their homogenous alloys.

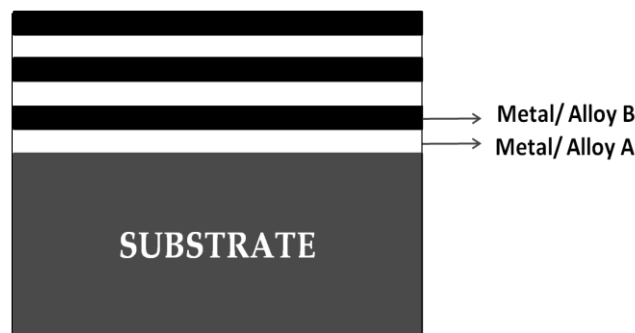


**Figure 1.4** - Schematic diagram showing composition modulated multilayer alloy coating having alternate layers of two different metals/alloys.

### **1.6.1.1 Methods of Production of Multilayer Coatings**

The composition modulated multilayer (CMM) coatings can be developed through either dry process or wet process.

#### ***a) Dry process or physical method***

The physical method or dry process includes the processes such as physical vapour deposition, chemical vapour deposition, sputtering, molecular epitaxy techniques, etc. These techniques have their advantage in different applications. But due to some disadvantages, like high capital cost, high energy cost, and less control over the process, this method is not much in practice unless it has a specific purpose. In that situation, the electrolytic method or wet process is the most sought after technique for the synthesis of multilayer coatings.

#### ***b) Wet process or electrolytic method***

In the wet process or electrolytic method, the production of CMM coating is carried out by the electrochemical method from an aqueous electrolyte having metal ions. Some of the added advantages of this process over the dry process are:

- Low cost of production and simplicity of the technique for mass-scale production
- Thick coatings can be deposited ( $>100\ \mu\text{m}$ ) with high deposition rates (up to about 5nm/minute)
- Even complicated geometries can be coated as current is the driving force of the process
- By using advanced power sources the deposition process can be controlled sensibly
- Being a cold process, the risk of inter-diffusion between the layers is low

Despite the above advantages, the complicated bath chemistry sometimes affects the coating quality. The electrodeposition process depends on different variables therefore its optimization and control are a little time-consuming. Under wet processes, multilayer coatings can be accomplished through either dual-bath technique (DBT), or single-bath technique (SBT) (Leisner et al. 1994), and their characteristic features are as below.

***i) Dual Bath Technique***

In the dual-bath technique, the deposition is carried from two separate electrolytic solutions. The substrate is altered between two solutions and forms the sublayers of coatings having varied thickness. Hence, it is an easy method to combine layers of two completely pure metals/alloys, using either pure metal or alloy plating solutions, respectively. Hence, this method allows commercially available plating solutions for the development of multilayer coatings. Though the dual-bath technique is simpler to use, it has its own limitations, like high time consumption, and chances of oxide layer formation on the coating surface. In this regard, the single bath technique is more convenient for the production of CMMA coatings (Leisner et al. 1994).

***ii) Single Bath Technique***

The most well-tried method for production of CMMA coatings is single - bath technique, where only one electrolyte (having two or more types of metal ions) is used and current (or other variables also) is made to pulse periodically during deposition. Sub-layers of small thickness are deposited from the electrolyte, containing two or more elements that are compatible with each other to deposit. The modulation in the composition is carried out by varying the current/potential conditions. Among that, the commonly used method is the dual current method, in which the current is altered between a high current and a low current. At low current densities, more noble metal deposition takes place. On the other side, at high current density, the limiting current density of more noble metal is exceeded and as a result, the alloy rich in less noble metal deposition occurs. Further, the increased time interval of current interruption between two values enhances the demarcation between the sublayers. In this technique, as the substrate is always dipped in the electrolyte the chances of mutual bath contamination are very less.

However, both dual-bath and single-bath techniques have their advantages and disadvantages, the disadvantages of the dual bath technique outweigh its benefits. Hence, the single bath technique is more commonly used for the easy development of multilayer alloy coatings (Leisner et al. 1994).

## **1.6.2 MAGNETOELECTRODEPOSITION**

The application of external magnetic fields on the electrochemical process has been studied for over 40 years (Monzon and Coey 2014). The enhancement of the mass transfer process leading to improved deposit quality and corrosion control are some of the practical applications of using a magnetic field in electrolytic process (Tacken and Janssen 1995). Generally, the process in which the splitting of a chemical compound or several compounds by the passage of electric current under the influence of an external magnetic field is called magneto-electrolysis (Fahidy 1983). Magneto-electrolysis is an interdisciplinary aspect that interrelates the concepts of electrochemistry, hydrodynamics, and magnetism. The process of electrodeposition under the influence of an applied magnetic field ( $B$ ) is called magneto-electrodeposition. This advanced method of deposition is currently gaining interest amongst researchers due to the greater possibility of electrodeposition, which is otherwise not possible. The forces and phenomenon emerging during the magneto-electrodeposition process are not yet completely comprehended and depicted, however, research is still going to develop a satisfactory explanation and mathematical equations and search for new utilization of magnetoelectrolysis (Kołodziejczyk et al. 2018).

The effect of the magnetic field on electrolysis is mainly due to its influence on mass transport, reaction kinetics, metal deposition/dissolution process, etc. During the electrolysis, the application of a magnetic field can enhance the mass transportation process by reducing the diffusion layer thickness. Hence, when a magnetic field is applied parallel to the process of electrodeposition, it can affect the process and product of electrodeposition by altering the limiting current density of metal ions involved. Thus, the effect of induced magnetic field on the process of deposition by changing the hydrodynamics of electrolyte solution is called magneto-hydrodynamic (MHD) effect. This phenomenon of MHD comes into play due to the combined effect of paramagnetic gradient and Lorentz force operating in the bath during electrodeposition (Monzon and Coey 2014).

### **1.6.2.1 Effect of Magnetic Field on Process of Electrodeposition**

The electrodeposition which is carried out under the influence of an external magnetic field is known as magneto-electrodeposition (MED). The superimposition of  $B$  in electrochemical processes has great practical importance. The applied magnetic field



can significantly affect the deposit characteristics like nucleation, growth, texture, phase composition, hardness, morphology, etc. (Monzon and Coey 2014). The degree of impact due to superimposition of  $B$  during MED on coating characteristics depends on the intensity and direction (parallel or perpendicular) of the applied magnetic field (Elias and Hegde 2017). As per the theory of MHD, when a constant magnetic field is applied parallel to the cathode surface, additional forces such as the Paramagnetic Force (FP), Field Gradient Force (FB), Lorentz Force (FL), Electrokinetic Force (FE), and the Magnetic Damping Force (FM) increase the rate of transport of ions to the electrode surface, thus increasing the mass transport current of electrode reaction. According to Hinds et al. (2001), the Lorentz force constitutes the largest contribution towards the increased mass transport among all other forces present in the MHD effect.

#### **1.6.2.2 Effect of Lorentz Force**

The effect of magnetic field on the process of electrodeposition is attributed to the principle of Lorentz force. According to this, if a charged particle ‘ $q$ ’ moving with velocity ‘ $v$ ’ through an electric field ‘ $E$ ’ and magnetic field ‘ $B$ ’ then the full electromagnetic force  $F_L$  acting (assuming metal ions as charged particles) is given by the relation,

$$F_L = qE + qvB \quad (1.10)$$

It may be noted that the first term is contributed by the electric field, and the second term is the magnetic force. The magnetic force has a direction perpendicular to both the velocity and the magnetic field. The magnetic force is proportional to ‘ $q$ ’ and to the magnitude of the vector cross product  $v \times B$ . In terms of the angle ‘ $\theta$ ’ between  $v$  and  $B$ , the magnitude of the force equals  $qvB \sin \theta$ . An interesting result of the Lorentz force is the motion of a charged particle in a uniform magnetic field. If  $v$  is perpendicular to  $B$  (i.e., with the angle  $\theta$  between  $v$  and  $B$  of  $90^\circ$ ), the particle will follow a circular trajectory with a radius of  $r = mv/qB$ . If the angle  $\theta$  is less than  $90^\circ$ , the particle orbit will be a helix with an axis parallel to the field lines. If  $\phi$  is zero, there will be no magnetic force on the particle, which will continue to move undeflected along the field lines. Thus, during magneto-electrodeposition, the Lorentz force may be comparable in magnitude to the buoyancy force driving the convection, and hence it enhances the convective motion of electrolyte towards the electrode surface. As a result, the

thickness of the Nernst layer decreases which is related to the increase of limiting current density (Fick's law). Under the influence of the applied magnetic field, the formation of the Navier-Stokes hydrodynamic layer occurs and it can affect the velocity of the electroactive species moving towards the working electrode (Kołodziejczyk *et al.* 2018).

The advantages of mass convection can be accomplished more conveniently by mechanical stirring. However, the connection between Lorentz force and local current density implies that it is feasible to produce a flow pattern magnetically on a scale that would be generally unreachable. As a result, the formation of high current density ( $j$ ) spots occurs, which further leads to the micro-MHD effect producing vortex. Another benefit is that electrolyte streams can be driven in microfluidic channels, where transverse redox currents flow occurs. Usually, the distribution of current density is non-uniform at the edges of the electrode surface and a regular MHD flow occurs around the edge when  $B$  is orthogonal to the surface of the electrode. Hence, this phenomenon leads to a non-uniform current distribution at the edges and results in secondary micro-MHD vortices that protrude into the diffusion layer (Monzon and Coey 2014)

## **1.7 CHARACTERIZATION OF ELECTRODEPOSITED ALLOY COATINGS**

The characterization of all coatings in terms of their structure at micro-level provides a keen understanding of the relationship between their structure (Girão *et al.* 2017). In the present study, the surface morphology and composition of electrodeposited coatings are studied by scanning electron microscopy (SEM) and Energy-dispersive X-ray spectroscopy (EDS) techniques. The micro or nanostructural features of alloy coatings, based on their surface roughness is carried out by Atomic Force Microscopy (AFM). Along with these techniques, the X-ray diffraction (XRD) technique is used to examine the phase structure of the deposit (Shetty and Hegde 2018).

SEM is a powerful tool to analyze both the morphological and micro or nano-structural details of alloy coatings (Di Girolamo *et al.* 2016). Generally in SEM, a high-energy electron beam is formed, and it is allowed to scan the sample surface to get its surface morphology images. Then, there occurs elastic and inelastic scattering due to the interaction of the electron beam with the sample. However, some parts of the

electron beam were left un-scattered. If the interaction between the sample and the electron beam is elastic, electrons reflect and are called backscattered electrons (BSE). But, inelastic interaction of the electron beam with the sample produces secondary electrons (SE) from the atoms of the sample itself. Hence, the image can be obtained by using secondary electrons as well as backscattered electrons. Since the BSEs originate from the deeper portion of the sample, BSE images are very sensitive to the variation in the atomic number in the sample, and a high atomic number of the element in the material leads to a brighter image. But, the SE that originates from the surface peripheral region, shows the image with details of the surface information. If the electron beam is generated from a thermionic emission gun it is called simple SEM; and if the electron beam source is a field emission gun, and is highly focused and narrow, giving rise to high-resolution images it is called FESEM image (Girão et al. 2017).

Micro-structural information is generally obtained using an energy dispersive X-ray spectrometer (EDS) detector attached to the SEM. When an incident electron beam interacts with the sample surface, it produces X-rays and the EDS detector measure the energy and intensity distribution of the X-ray signal. Generally, the incident electron knocks out an electron from the K shell of an atom in the sample. Then the electron vacancy created at the K shell ( $n=1$ ) is filled by the electrons in another shell of the atom and there occurs an electronic transition resulting in the emission of X-rays. The X-rays produced by the electronic transition to the K shell are called  $K_X$  rays, and to the L shell ( $n=2$ ) are  $L_X$  rays and to the M shell ( $n=3$ ) are called  $M_X$  rays and so on. These emitted X-rays are the characteristic of each chemical element in the sample, and are thus helpful in both qualitative and quantitative analysis by providing the identification of the elements present in the coatings, and their composition in it (Girão et al. 2017; Ul-Hamid 2018).

Atomic force microscopy (AFM) is one of the useful techniques to examine and estimate the surface structure of a material. Unlike other microscopic techniques, the AFM technique uses a sharp probe to scan the sample surface and develop a map of the height or topography of the sample surface. Hence, the light and electrons are not involved in the surface imaging (Eaton and West 2010). AFM analysis can be used to study the surface morphology and roughness of coating on a smaller scale

(Allahyarzadeh et al. 2016). This experimental information can be used to predict/assess the factors responsible for improved corrosion resistance/kinetics of electrocatalytic reactions of electrodeposited alloy coatings. (Shetty and Hegde 2018).

X-ray diffraction (XRD) is the commonly used non-destructive technique to study the phase structure of the electrodeposited coatings. It gives information about the phase structure, preferred crystal orientations, and other structural parameters including average grain size, crystallinity, strain, and crystal defects. During XRD analysis, the monochromatic X- rays are allowed to fall on the sample surface and it forms a diffraction pattern by constructive interference of X- rays scattered from the lattice planes of surface atoms. The X-ray diffraction takes place following Bragg's law,

$$n\lambda = 2d \sin \theta \quad ( 1.11)$$

Where  $n$  is an integer,  $\lambda$  is the wavelength of the incident X-rays,  $d$  is the interplanar distance and  $\theta$  is the angle of diffraction.

These diffracted X-rays are then detected, processed, and counted for structural information. All possible diffraction peaks are obtained by scanning the sample through a particular range of  $2\theta$  angles. Further, the obtained diffraction pattern can be analyzed by comparing it with diffraction data files, proposed in *Joint Committee of Powder Diffraction Standards* (JCPDS) (Allen J. Bard and Faulkner 2000; Bunaciu et al. 2015).

## 1.8 CORROSION

Corrosion is the destruction or deterioration of a material due to its interaction with the surrounding environment, and it is vexing problem observed in almost all metals and alloys, including non-metallic materials such as ceramics, polymers (Fontana 1987). But the term corrosion is generally referred to the chemical or electrochemical reactions between a metal or alloy and its exposing environment which leads to its destruction and decline in its properties (Yang 2008). Chemical corrosion occurs when the metal comes in contact with non-electrolytes which includes the conditions such as exposure to dry gases and high temperature. During chemical corrosion metal always transfers the electron to the substance in the surrounding environment. Whereas electrochemical corrosion is the redox reaction when the metal comes in contact with the electrolyte solution, and it generates the electrons which move from anode to cathode (Yang 2008).

### **1.8.1 Mechanism of corrosion**

Corrosion processes are most often electrochemical since the wet condition is quite common in the environment, due to humidity. Thus, a thorough understanding of the theory and electrochemical mechanistic steps of the corrosion process helps to mitigate the corrosion to large extent. A corrosion cell consisting of four components; Anode, Cathode, Electrolyte, and Metallic path is the fundamental requisite for corrosion to take place. The connection between anode and cathode through the solution and metal is achieved by the ionic path and electronic path, respectively. During an electrochemical corrosion reaction, corrosion occurs at the anode region, and the metal atoms are oxidized and go into the solution as metal ions. Hence, at this part the deterioration of the material takes place. As a result of oxidation reaction, electrons are generated which are responsible for the generation of corrosion current in the corrosion cell. The direct current going through the corrosion cell enters the solution at the anode. At the same time, at cathode reduction reactions take place by consuming the electrons released by the anodic reaction. The direct current flowing through the corrosion cell enters that metal at the cathode. The cations produced by the oxidation reaction at the anode move towards the cathode and anions move from cathode to anode. The direct current flow through the electrolyte solution occurs along the ionic path. This continuous movement of ions through the solution is responsible for the current flow through this portion of the corrosion cell. This process in turn is responsible for the corrosion, or dissolution of metal/alloy, by following Faraday's law.

Thus, the above four prerequisites comprise the corrosion cell, and the overall corrosion rate is constrained by the net equilibrium among all these parts of the corrosion cell. The oxidation reaction at the anode can just continue as fast as the electrons produced there can be utilized for the reduction reaction at the cathode. Hence, the slowdown in the redox reactions retards the anodic reaction. Any obstacle in the ionic current path, or the electronic current path will slow down the corrosion reaction by reducing the current flow through the corrosion cell. Hence, complete elimination of the ionic path by avoiding the wet condition stops the corrosion process, and elimination of the electronic path can also stop the corrosion reaction. Therefore, an effective control of corrosion can be achieved by the elimination of cathodic regions on material surface. If there is no place for the consumption of electrons generated by

the corrosion reaction(at cathode), there is no corrosion reaction is possible (Davis 2000).

### 1.8.2 Different forms of corrosion

Corrosion can be broadly classified based on the environment, mechanism of corrosion, and appearance of the corrosion product, and they are discussed below:

- *Nature of the corrodent*: According to this corrosion can be categorized as *wet corrosion* and *dry corrosion*. If a liquid or moisture is necessary for the former, and the second one usually takes place in dry conditions, which involve a reaction with high-temperature gases.
- *Mechanism of corrosion*: The direct chemical or electrochemical corrosion reactions comes in this category.
- *The appearance of the corroded metal*: Depending on the appearance of corroded metal, corrosion can be classified as either uniform or localized corrosion. When the metal deterioration takes place over the entire exposed surface area, it is considered as uniform corrosion; and if it takes place on a small surface are it is considered as localized.

Under wet, or aqueous corrosion (under which the majority of the corrosion types are falling), some eight forms of corrosion can be identified based on the appearance of corroded metal, and they are:

- *Uniform or general corrosion* - The uniform loss of metal occurs over the entire surface in an environment, such as a liquid (chemical solution, liquid metal), gaseous electrolyte (air, carbon dioxide, sulphide), or a hybrid electrolyte (solid and water, biological organisms).
- *Pitting corrosion* - It is a localized form of corrosion by which *cavities* or *holes* are produced inside the material.
- *Crevice corrosion* - This type of corrosion are found in cracks and crevices on the metal surface/joints.
- *Galvanic corrosion* - This type of corrosion takes place between dissimilar metal/alloys or microstructural phases, affected due difference in their electrode potential values.

- *Erosion corrosion* - In this type, corrosion of metal takes place due to effect of liquid flow or erosion in general. It may result in damaging of material including cavitation and fretting.
- *Intergranular corrosion* - Intergranular corrosion is characterized by the process of corrosion at intergranular regions where there is loose structural arrangement of atoms.
- *Dealloying* - This includes de-zincification and graphitic corrosion.
- *Cracking* - This type of corrosion includes stress-corrosion cracking, corrosion fatigue, and hydrogen damage.

The above eight types are only representative, but practically there are many other types of corrosion do exist, since corrosion is the result of interaction of metal and medium. The mechanism of corrosion depends on the environment to which a metal/material is exposed. Hence, in strict sense it may be stated that each type of corrosion is unique, depending on the environment. Therefore, few corrosions fit in more than one class and some other corrosions do not fall in any of the mentioned classifications. However, these categorizations and their comprehensive examination are very useful in corrosion process evaluation (Davis 2000; Perez 2004)

### **1.8.3 Importance of corrosion control**

The corrosion is a vexing problem in every use of every metal, and hence the corrosion reaction has become a major issue worldwide. Besides usual encounters, like deterioration of materials that the corrosion causes, it is also responsible for many indirect developments, like plant shutdowns, waste of valuable resources, loss or contamination of products, reduction in efficiency, and costly maintenance, etc. Likewise, it risks protection and restrains innovative advancement (Roberge 1999). Generally, all environments are corrosive to some extent. Some of such examples are air and moisture, fresh, salt, marine, mine-water, and industrial atmosphere like, steam and some gases such as chlorine, ammonia, sulphur dioxide, and fuel gases, many mineral acids and organic acids; alkalis, etc. Among them, inorganic materials are more corrosive than organic (Fontana 1987).

Corrosion is a natural spontaneous process taking place to meet the thermodynamic stability of material with the environment, and hence it is unavoidable.

However, there are approaches to control it by retarding the deterioration process. The corrosion control methodology for a particular material is supposed to be custom-made to the environment, its composition, and its structure. Generally, corrosion control methods can be roughly be classified as either active or passive. Examples of active corrosion control techniques incorporate inhibitors, external cathodic protection, with or without coatings, and sacrificial anodes. Whereas passive techniques include material selection, organic and inorganic coatings, and metallic coatings (including both barrier and sacrificial coatings). One more example of corrosion mitigation is by controlling the corrosive environment (oxygen, ions, etc.). For example in boilers, corrosion-causing oxygen is removed by adding hydrazine, and other constituents are eliminated by adding inhibitors (amines). The choice to utilize one method, or a combination of methods relies upon the sort of corrosion that is expected, the tolerance for risk, the expense of the technique, the material involved, the environment, and other factors related to the design of a structure. Among different existing corrosion mitigation techniques, the electrodeposited *metallic coatings* (of pure metal or alloy) approach, is considered to be the most commonly used method to protect active metal surfaces, from the effect of corrosion.

#### **1.8.4 Electrochemical techniques of corrosion monitoring**

Corrosion monitoring is the act of collecting the data on the progress of corrosion, or a measure of destructiveness by the surrounding environment, and is considered as a potential aid in the corrosion control process (Yang 2008). In electrochemical techniques, the potential developed during the electrochemical corrosion reaction is comparable to the driving force for the reactions and it decides the intensity of reactions that happen at the anode and cathode. The current generated during the electrochemical reaction indicates the reaction rate. Hence, higher the current or corrosion current, greater is the rate of corrosion. Using electrochemical techniques, it is possible to control the potential at particular levels and quantify the subsequent current. Equally, the potential can be estimated in working cells, when the current is controlled. The resistance or polarization elements through the cell also can be estimated. The measurement of these fundamental parameters of corrosion reactions gives an immense knowledge about the effect of corrosion on the material, and the impact of the environment on the corrosion behaviour as well as on the corrosion mechanism. The



measurement of potential, current, and resistance properties are carried out either individually or altogether. The electrochemical behaviour of any metal/alloy can easily be studied by two important methods, namely Tafel's extrapolation method, and electrochemical impedance method. Both these techniques give major inputs for the corrosion control process (Davis 2000).

#### **1.8.4.1 Electrochemical impedance spectroscopy (EIS)**

Electrochemical impedance spectroscopy (EIS), or alternate current (AC) method can be used to study the electrochemical responses of a corrosion cell using an alternate current of small amplitude over a wide range of frequencies. EIS technique is extremely helpful in describing the corrosion behavior of a test electrode. This technique can be used to measure the polarization resistance, most importantly to understand the electrochemical mechanism of corrosion reaction, and to find the way to control the corrosion, like in coatings (Perez 2004). The instrument utilized for EIS measures the impedance (AC analogue of DC resistance) in a wide frequency range, between a metallic test sample and counter electrode. In this method, a small perturbation of sinusoidal potential (<10 mV in amplitude) at a given frequency is applied to the free corrosion potential. The resulting alternating current with a phase difference  $\Phi$  is transferred to a frequency response analyser and the resulting output is the impedance response of the electrode. The test is carried out in a wide frequency range (e.g. from mHz to MHz range) and the whole impedance response is obtained as a spectrum (Yang 2008). The electrochemical impedance,  $Z(\omega)$  is the frequency-dependent proportionality factor in the relationship between the voltage signal and the current response,

$$Z(\omega) = E(\omega) / i(\omega) \quad (1.12)$$

where  $E$  = applied voltage dependent on the time,  $E = E_0 \sin(\omega t)$ ,  $i$  = the time dependent output current density,  $i = i_0 \sin(\omega t + \theta)$ ,  $Z(\omega)$  = the impedance ( $\text{ohm-cm}^2$ ) and  $t$  = time (s).  $Z(\omega)$  is a complex-valued vector quantity with real and imaginary components whose values are frequency dependent. It may be expressed as,

$$Z(\omega) = Z'(\omega) + jZ''(\omega) \quad (1.13)$$

Where  $Z'(\omega) = |Z(\omega)| \cos(\theta)$ , the real component of impedance and  $Z''(\omega) = |Z(\omega)| \sin(\theta)$  and  $j^2 = -1$ , (where  $j$  is the imaginary number). Hence, Equation 1.13 may also be written as,

$$|Z(\omega)| = (Z'(\omega)^2 + Z''(\omega)^2)^{1/2} \quad (1.14)$$

and phase angle,  $\theta$  as  $(\theta) = \tan^{-1} Z''(\omega) / Z'(\omega) \quad (1.15)$

The EIS technique is carried out in a frequency domain, and knowledge of the frequency dependence of impedance for a corroding system enables a determination of an appropriate equivalent electrical circuit for the electrode-electrolyte interface to describe that system. Such a circuit usually consists of a combination of resistance, capacitance, and inductance (Kelly et al. 2003). The EIS data analysis is usually carried out by studying the correlation between the impedance response, and the corresponding equivalent circuit representing the physical processes taking place in the system under investigation or through graphical representations. The measured impedance  $Z(\omega)$  contains two parts, a real part ( $Z'$ ), and an imaginary part ( $Z''$ ). A graphical plot of measured impedance showing the real part on the X-axis and the imaginary part on the Y-axis. Such plots are called by different names, like Nyquist Plot, Nyquist diagram, Nyquist response, impedance diagram, impedance spectrum, EIS spectrum, etc. Here the ordinate is negative, and each point on a Nyquist plot corresponds to the impedance at one frequency. Also, the low-frequency data lies on the right side of the plot, and the high-frequency data point is on the left side. Also, the diameter of the extrapolated semicircle in the Nyquist diagram corresponds to the charge transfer resistance,  $R_t$ , which is equivalent to the polarization resistance ( $R_p$ ). Thus, larger the diameter of semi-circle the greater is the polarization resistance ( $R_p$ ), and lower is the corrosion rate (Ribeiro and Abrantes 2016; Wagner 2011). The analysis of EIS data is usually carried out by fitting the Nyquist plot to an equivalent electrical circuit model. Based on the nature of the plot, a circuit model and initial circuit parameters are presumed and given as input by the analyst. The program then fits the best frequency response to the given Nyquist plot, to get corresponding circuit elements values. The accuracy of the data fitting is decided by how properly the fitting curve overlapped with the original plot. The acquired data set gives an idea about the process happening at the electrode-electrolyte interface during the corrosion reaction. Of the various equivalent circuits

that have been proposed to portray electrochemical interfaces, the equivalent circuit corresponding to the properly fitting curve will be selected to explain the mechanism of corrosion (Roberge 1999).

#### **1.8.4.2 Potentiodynamic Polarization (PDP) or Tafel Extrapolation Method**

The potentiodynamic polarization technique involves the measurement of an electrode response upon the application of a small electrochemical excitation. The technique usually gives the current-potential relationship as output data. When a small perturbation signal is applied to the electrode, the potential of the electrode varies from the corrosion potential. Hence the electrode is said to be polarized and the technique is known as the polarization method of determining corrosion rate. The method in which the potential of the electrode is varied at a constant rate and the current response of the sample is continuously monitored, and hence it is called potentiodynamic polarization method (Yang 2008). In the potentiodynamic polarization technique, the applied potential acts as a driving force for the anodic and cathodic process, also the nature of the potential scan determines the nature of the reaction that takes place at the electrode of interest, and the net change in the reaction rate is measured in terms of the current. During a DC polarization, the ionic conduction takes place through an electrolyte solution separating the working electrode and the counter electrode, while the potentiostat provides the path for electronic conduction. The potential applied at the working electrode is controlled by the potentiostat, and it also measures the current. At open circuit potential (OCP), a state corresponding to equilibrium (potential at which the total anodic current is equivalent to the total cathodic current), the measured or applied current will be zero.

The experimental setup required for potentiodynamic polarization study mainly contains three electrodes, the working electrode, the counter electrode, and the reference electrode. The working electrode is the test sample and the potential of the working electrode is measured with respect to the reference electrode. While the counter electrode is usually highly corrosion-resistant material such as Pt, and is used to transmit impressed current through the solution, either to or from the working electrode surface. The corrosion behaviour of a particular material in a given medium is evaluated by Tafel's extrapolation method, by polarizing the working electrode both

cathodically and anodically around its OCP. The potentiodynamic polarization experiment or Tafel extrapolation typically starts at a potential about 250 mV negative to OCP, and scans upward through the potential of zero current (which might be different than the original OCP to a value that is about 250 mV positive to the original OCP. Less polarization is required if the Tafel slope is low. The rate of polarization in a potentiodynamic scan is typically between 0.1 and 1 mV s<sup>-1</sup>. The linear portion of the curve in a positive potential direction from OCP is called an anodic Tafel slope, represented by  $\beta_a$ . The curve shows that for an active metal, as the electrode potential is made more positive or as the solution becomes more oxidizing, the metal dissolution increases. The cathodic branch of the polarization curve is the solid line at more negative potential than the OCP; a cathodic current to the metal specimen is measured. The slope of the linear portion of the polarization curve is the cathodic Tafel slope, represented by  $\beta_c$ . The total anodic and cathodic polarization curves corresponding to hydrogen evolution and metal dissolution are superimposed as dotted lines. One of the pieces of information often extracted from potentiodynamic polarization scans is the corrosion rate. To determine the corrosion rate from such polarization measurements, it is possible to extrapolate back from both the anodic and cathodic regions to the point where the anodic and cathodic reaction rates (i.e., currents) are equivalent. The current density at that point is the corrosion current density ( $i_{\text{corr}}$ ), and the potential at which it falls is the corrosion potential ( $E_{\text{corr}}$ ). A representative Tafel plot showing anodic and cathodic curves, anodic and cathodic slopes,  $i_{\text{corr}}$  and  $E_{\text{corr}}$  is shown in Figure 1.5.

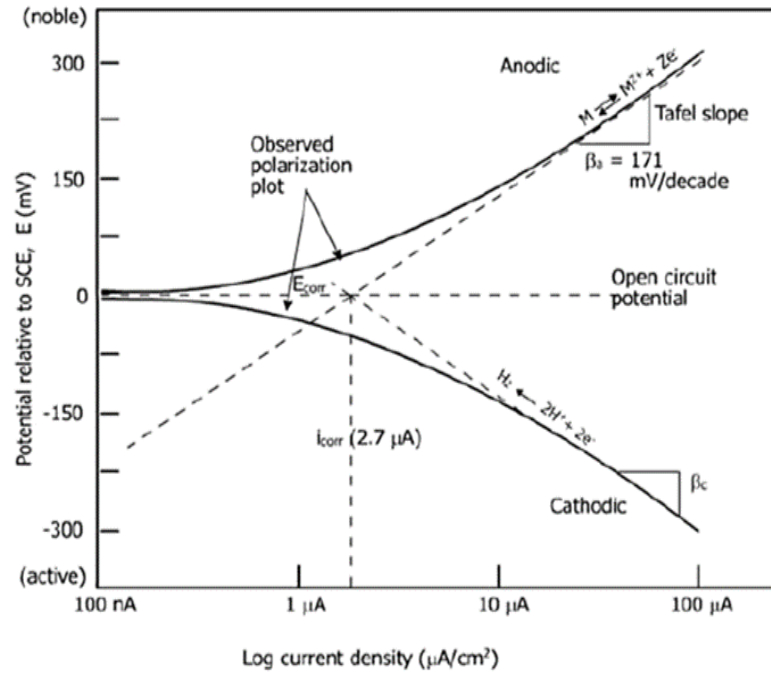


**Figure 1.5** - Typical potentiodynamic polarization curve (Tafel's plot) leading to evaluate the corrosion rate by knowing the corrosion current ( $i_{corr}$ ) of given test specimen (Davis 2000).

The corrosion rate (CR) can be calculated from the  $i_{corr}$  value using Equation 1.16.

$$CR(mm\,y^{-1}) = \frac{K \times i_{corr} \times EW}{\rho} \quad (1.16)$$

where K is a constant with value  $0.00327 \text{ mm g } (\mu\text{A cm year})^{-1}$ , defines the unit of corrosion rate ( $\text{mm y}^{-1}$ ),  $i_{corr}$  is the corrosion current density in  $\mu\text{A cm}^{-2}$ ,  $\rho$  is the density of the corroding material and EW is the equivalent weight of the metal/alloy. This method being involved with a large overpotential applied to the metal surface, it is considered to be a destructive method. This is particularly true during anodic polarization during which the metal surface may be permanently changed/damaged (Davis 2000; Yang 2008). However, in the EIS method, AC voltage of small amplitude is used ( $\pm 10\text{mV}$ ), it is a non-destructive technique.

## 1.9 ELECTROCATALYSIS

Electrocatalysis is the term that generally refers to the catalysis of electrode reactions (Trasatti 1995). It means the enhancement of the rate of electrochemical reactions with the reduction in the overpotential. It is because of catalytic acceleration of slow

chemical reaction, through fast charge transfer steps which together constitute an electrochemical reaction (Wendt et al. 1994). It should be noted that electrocatalytic reactions will normally involve both the formation and cleavage of the metal-adsorbate bond. Therefore, when the bond is of intermediate strength, the most effective catalysis occurs. Too low free energy of adsorption will lead to insufficient coverage by adsorbate for it to be an effective catalyst while too high a free energy of adsorption will cause the rate of the cleavage step to become too low. Generally, transition metal species play a significant role in the field of electrocatalysis because of their unpaired d-electrons and unfilled d-orbitals which are available for forming bonds with an adsorbate. It is to be expected that the free energy of adsorption will depend strongly on the number of unpaired d electrons per metal atom and also on their energy levels, and, hence, both on the choice of transition metal and its detailed environment. In the limit, the surroundings (i.e. the adjacent metal atoms in a metal or alloy, the ligands to a metal complex, or the oxide ions in an ionic lattice) and the adsorbate may be considered as ligands to the central transition metal ion acting as the catalyst centre, and the surroundings will moderate all the properties of the metal-adsorbate (Pletcher 1984).

*From the fundamental standpoint, important requirements of a well-performing electrocatalyst are:*

- i) Low intrinsic overpotential for the desired reaction (hydrogen or oxygen evolution)
- ii) The high active surface facilitates both good accessibility to the reactants and sufficiently fast removal of products (gases, liquids, ions)
- iii) High electrical conductivity (providing pathways for electrons)
- iv) Proper chemical stability (compatibility with the electrolyte)
- v) Electrochemical stability (i.e. not being corroded at high overpotentials)
- vi) Good mechanical stability (especially for high-temperature electrolysis)

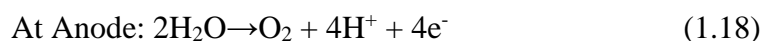
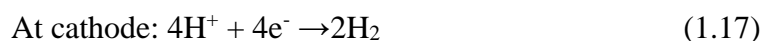
In addition to these requirements, which ensure high overall system efficiency, commercialization also requires long-term stability and low capital costs to compete with the conventional non-sustainable processes (Sapountzi et al. 2017).

### 1.9.1 Electrochemical Water Splitting Reaction

The majority of energy sources that we are relying on today are derived from fossil fuels such as coal, oil, and natural gas. Nonetheless, the consumption of non-renewable petroleum derivatives and the hurtful impacts of petroleum product usage on the climate need to lead to in-depth innovative technologies for the conversion and storage of sustainable and clean energy sources, like solar and wind. In this aspect, electrocatalytic water splitting to generate hydrogen has been considered as an alluring methodology (You and Sun 2018). Hydrogen is considered an efficient energy source as a fuel because of the following advantages it has: (a) Hydrogen is abundant in nature (in water) (b) It can be generated using either renewable or non-renewable sources, (c) It can be used as a fuel in both fuel cells and internal combustion engines, (c) It has high gravimetric energy density i.e. up to three times larger than liquid hydrocarbon-based fuel (however worth to note is its low volumetric energy density which caused safety issues with its pressurized storage), (d) It does not harm the environment since the only product of its oxidation is water (Sapountzi et al. 2017). During water electrolysis when hydrogen is produced, half the number of moles of oxygen is produced simultaneously as a by-product. Hence, if the production of hydrogen is more, then there will be more oxygen production simultaneously. In this case, oxygen can be used in both medical care, the chemical industry (blast furnaces, electric furnaces, and glass melting, gasification), and wastewater treatment (Kato et al. 2005).

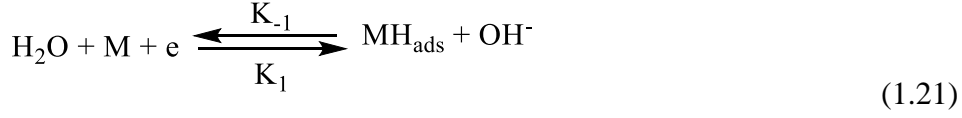
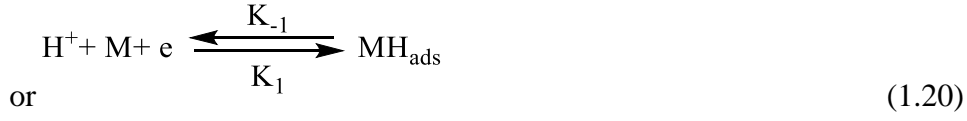
#### 1.9.1.1 Hydrogen Evolution Reaction (HER) and Oxygen Evolution Reaction (OER)

Generally, overall water splitting is based on two half-reactions: water oxidation and reduction as shown below (Tahir et al. 2017).

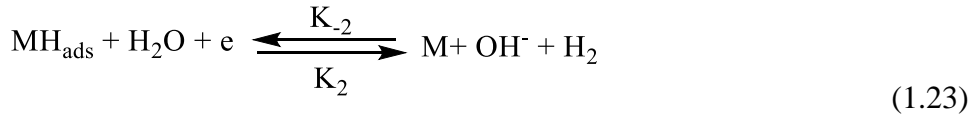
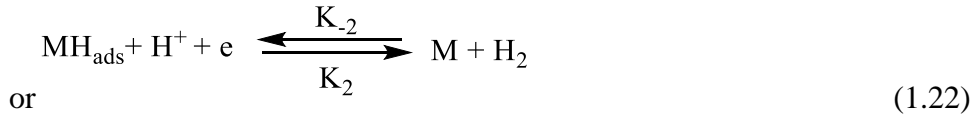


HER proceeds through three steps in acid and alkaline solutions, respectively:

*Step 1: electrochemical hydrogen adsorption, Volmer reaction*



*Step 2: electrochemical desorption, Heyrovsky reaction*

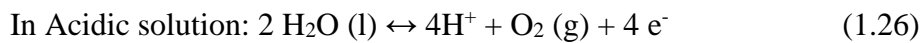
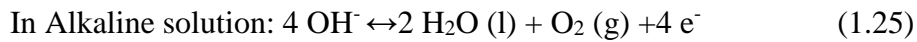


*Step 3: chemical desorption, Tafel reaction*



Where M represents the electrode material and  $\text{MH}_{\text{ads}}$  represents the hydrogen adsorbed on the electrode surface. The primary reaction for HER, which produces adsorbed H atoms on the electrode surface, is called the Volmer reaction. Based on the type of electrode, the hydrogen evolution takes place through Heyrovsky or Tafel reaction (Lasia 2010).

While the Oxygen Evolution Reaction is highly pH-dependent, and in acidic and neutral conditions two water molecules ( $\text{H}_2\text{O}$ ) are oxidized into four protons ( $\text{H}^+$ ) and oxygen molecule ( $\text{O}_2$ ), while hydroxyl groups ( $\text{OH}^-$ ) are oxidized and transformed into  $\text{H}_2\text{O}$  and  $\text{O}_2$  in basic environments (Tahir et al. 2017).





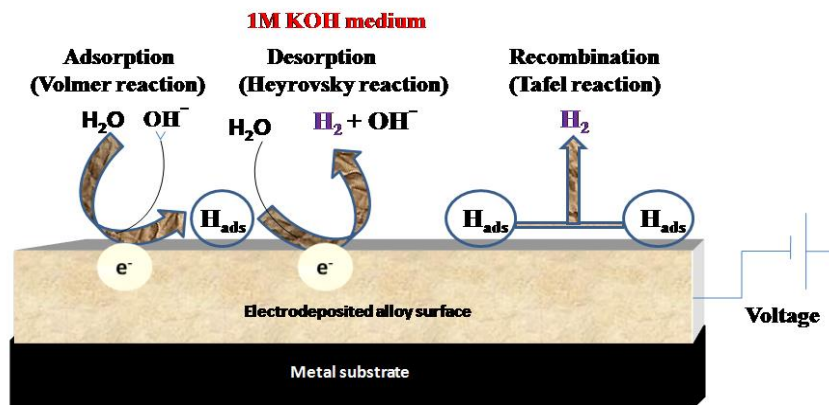


*Figure 1.6- Schematic representation mechanisms for Hydrogen evolution reaction.*

## 1.9.2 Electrochemical techniques for electrocatalytic water splitting reaction

### 1.9.2.1 Cyclic Voltammetry

Cyclic voltammetry (CV) is a technique for studying the electrochemical behavior of a system. It can give information about the thermodynamics of redox processes, rate of heterogeneous electron transfer reactions, and adsorption process. It can be used to study the electrochemical behaviour of different species diffusing to an electrode surface, interfacial process, and bulk properties of the material at the surface (Li and Miao 2013). The CV test is carried out by applying a linear potential sweep, which is a potential that increases/decreases with time to the working electrode. When the potential moves back and forth above the formal potential of the analyte, a current flow occurs through the electrode, which oxidizes or reduces the analyte. The experimental setup to carry out the CV analysis consists of three electrodes (working, reference, and auxiliary electrode) immersed in an electrolyte solution, which is connected to a potentiostat. The function of the potentiostat is to apply and maintain the potential between the working and reference electrode. Also, it measures the current generated at the working electrode. A recording device (such as a computer) records the resulting cyclic voltammogram and provides the data in the form of a graph of current versus potential (Rusling and Suib 1994; Swaminathan and Meiyazhagan 2020).

For an oxidation process to take place a positive potential ramp is applied to the working electrode and the electroactive species loses an electron at the electrode that results in the anodic peak current along with an oxidation peak at the given potential

( $E_{pa}$ ). At the same time when the applied potential at the working electrode is in the negative direction, the reduction process occurs at the electrode. This further leads to a cathodic peak current ( $i_{pc}$ ) at a potential ( $E_{pc}$ ) (Swaminathan and Meiyazhagan 2020). Hence, CV technique can be used to study the electrocatalytic activity of an electrode towards the HER and OER during the water-splitting reaction. To carry out HER and OER reactions, respectively a negative and positive potential ramp have to apply to the working electrode surface. The evaluation of the electrode as an electrocatalyst can be done by determining a set of parameters such as cathodic and anodic peak current from the Y-axis of the cyclic voltammogram for HER and OER respectively, and onset or discharge potential of the particular reaction that can find out by the extrapolation of voltammetric curve tangent with the X- axis which is the potential axis. Hence, the more cathodic peak current and low potential indicate the electrode is more active for the HER. Whereas in the case of OER, the anodic current indicates the activity of the electrode towards OER (Lupi et al. 2009; Ullal and Hegde 2014a).

### **1.9.2.2 Chronopotentiometry**

Chronopotentiometry (CP) is a technique used to study the mechanism and kinetics of an electrochemical reaction. In this technique, a constant current is applied between the working electrode and counter electrode for a particular time, and the potential developed at the working electrode is measured with respect to the reference electrode as a function of time. The electrolyte solution is usually kept unstirred and it contains supporting electrolytes in excess to facilitate the mass transport by diffusion mechanism. The variation in the transport process is inferred from the variation in the potential response (Peters 1971). This technique can be used to investigate the mechanism of a redox process occurring at the surface of electrodeposited alloy coatings during the electrochemical water-splitting reaction. Hence the role of the working electrode as an electro-catalyst to facilitate HER and OER can be well understood by the nature of the chronopotentiogram obtained. To study the HER activity of an electrode during water splitting, a cathodic current is passed through the working electrode which leads to the evolution of hydrogen at the electrode surface and the corresponding chronopotentiogram is obtained. Similarly, to carry out the OER at the electrode surface, an anodic current is passed and that liberates the oxygen gas. The corresponding chronopotentiograms obtained for both HER and OER manifest the

long-term stability of the electrode material towards the particular reaction and its robustness during the reactions (Elias and Hegde 2016, 2017).

So far, the Pt cathode possessing the near-zero overpotential is considered to be the most effective catalytic cathode. However, it is difficult to be practically applied, or industrialized due to its high cost and scarce resource. Therefore, seeking for low-cost, abundant, high efficient, and environmentally friendly catalytic cathode materials has become a research hotspot (Wang et al. 2019). In this regard, binary and ternary alloys of Ni, Fe, Co with metals, like W, Mo, La, etc. were tried as electrocatalysts for water splitting applications, i.e. either for HER or OER or for both (González-buch et al. 2013; Safizadeh et al. 2015). Experimental results demonstrated that these alloys are a good class of electrocatalytically active materials due to the synergistic effect of their good corrosion resistance and electronic configuration of individual metals (Elias et al. 2015).



## **CHAPTER 2**

### **LITERATURE REVIEW, SCOPE AND OBJECTIVES**



## CHAPTER 2

### LITERATURE REVIEW, SCOPE AND OBJECTIVES

---

*This chapter covers the literature review on electrodeposited Ni-based alloy coatings, of both binary and ternary alloys and their applications in both corrosion protection and electrocatalytic activity. Advancement in the area of modern methods of electrodeposition, namely multilayer-electrodeposition and magneto-electrodeposition were also reviewed. Finally, motivation behind the present work is given with scope and objectives of the titled thesis, stated at the end.*

The process of electrodeposition was made possible by the availability of the first voltage generator (Volta pile) and was invented shortly thereafter in 1803 by Brugnatelli. The first materials to be deposited were Au and Ag, and consequently, initial applications of this technique were limited to decorative purposes. The first process for producing an alloy coating was patented in England in 1838 by Elkington and Barratt. A diffusion coating of zinc and copper was formed by immersing copper articles attached to a piece of zinc which served as internal anode, into a boiling solution of zinc chloride. This process involved the deposition of zinc. The reaction occurred because the free energy liberated by the dissolution of zinc anode to form zinc ions was greater than the free energy required to deposit zinc ions into a copper lattice. As the process did not involve the simultaneous deposition of two metals, it is not alloy deposition. The first electrodeposition of alloys probably took place at the same time that cyanides were introduced into electroplating. De Ruolz is generally credited with having been the first to deposit brass and bronze. The bronze bath which was described in 1842 was apparently similar to the modern bath, which contains a cyanide copper complex and a stannate (Brenner 1963). Since that time electroplating technology has grown in length and breadth to meet various scientific, industrial-technological applications.

## 2.1 Ni-BASED ALLOYS

Although nickel electrodeposition has been studied since the beginning of 20th century, there has been an increased interest in recent years, and is now considered as one of the most frequently used methods in surface finishing treatments. Metals, alloys, and composite layers can be deposited electrochemically to form single or multi-component layers. Out of many Ni-based alloys, electrodeposition of NiW and NiCo alloy coatings are of great importance due to their excellent corrosion protection efficacy, and good electro-catalytic activity of HER and OER in alkaline water splitting applications.

### 2.1.2 Electrodeposition of NiW alloy

The electrodeposition of tungsten (W) is of considerable interest because of its unusual properties such as highest melting point metal, the lowest coefficient of linear thermal expansion, and the highest tensile strength. It has highest Young's modulus of elasticity value and is being exceeded by three of the platinum group metals, namely osmium, iridium, and ruthenium. In addition, it has high thermal conductivity and is exceeded only by five other metals. Tungsten is one of the densest metals, having a density about the same as gold, and is about 70 % denser than lead. Tungsten has got good corrosion resistance with unusual mechanical properties. It retains a considerable amount of hardness and strength at temperatures, where iron is as weak as lead. Thus, due to the unusual combination of many rare properties, tungsten has many engineering and industrial applications, despite its rare availability and high price (Brenner 1963). Due to the genuine reason that tungsten cannot be reduced from their aqueous solutions through electrodeposition, it can only be co-deposited in the presence of Fe group elements (like Ni, Co, and Fe), and such type of deposition is called the induced type of electrodeposition (Allahyarzadeh et al. 2016). Generally, here Fe-group metal is called *inducing metal*, and W is called *reluctant metal*.

The electrodeposition of tungsten alloys was first noticed by Fink and Jones during their experiment to electrodeposit pure tungsten. But, later Holt revealed that the alloy deposit obtained was an iron-tungsten alloy, formed from the iron impurity present in the electrolyte. In early stage, deposition of tungsten alloys mainly occurred from ammoniacal electrolytic bath, and it was first introduced by Gol'tz and Kharlamov. They prepared a bath by adding relevant metal ions containing salt, ammonium salt and ammonium hydroxide. But the coatings obtained were porous and dull due to poor



plating process, less metal ion concentration and high deposition current density. The next phase of progress in tungsten alloy electrodeposition was by incorporation of organic hydroxyl-acids such as citrate, tartrate, and malate into the ammoniacal baths. This further led to improved Faradaic efficiency and enhanced metal salt solubility in the bath. Accordingly, smooth, hard and thick Tungsten alloys were deposited at low current densities with improved current efficiency. The deposition of tungsten alloys from alkaline baths has been studied and developed by several authors, as an attempt to optimize the conditions to obtain high tungsten content and better quality of the alloy (Brenner 1963). Rauscher et al. (1993) investigated the corrosion resistance property of electrodeposited NiW alloy coatings in boiling HCl. They observed a remarkable corrosion resistance even in air. For the dissolution of NiW layers of thicknesses of 16 to 17 $\mu\text{m}$  with a tungsten content of 27 wt. %, more than 20 hours were found to be required.

Steffani et al. (1997) have developed ternary nickel-base alloy NiW-B alloy for surface corrosion and wear resistance to replace chromium plating, which uses environmentally hazardous solutions. Further, the corrosion test in acid medium of these alloys showed enhanced corrosion resistance compared with hexavalent chromium and electroless nickel deposits. Zhu et al. (2002) investigated the correlation of surface morphology changes of electrodeposited NiW alloy coating with its composition. It was found that with increasing composition of tungsten content, the phase structure of the coatings changes from polycrystalline fcc-Ni type structure to amorphous, followed by orthorhombic which is the characteristics of NiW alloy coatings. The surface morphology of NiW alloy coatings was found to be characterized by the presence of cracks/micro-cracks, probably due to hydrogen embrittlement and stress developed due to electro-crystallization. Thermal stability of NiW alloy coatings, developed by electrodeposition method was studied by Choi et al. (2003). In addition, Wu et al. (2003) assessed the effects of boric acid introduced into an ammonia-citric plating bath, both on the plating process and on the deposit characteristics. It was found that boric acid increased not only current efficiency but also the tungsten content of deposits, implying that boric acid may act as a surfactant to impede the proton reduction, and also form some complex with tungstate to be beneficial for tungsten co-electrodeposition.

Eliaz et al. (2005) in their work investigated the effect of bath chemistry, additives and operating parameters on surface morphology, composition and properties of NiW alloy coatings electrodeposited from citrate bath without the addition of ammonia and ammonium salts. The addition of nickel sulfamate found to increase the faradaic efficiency and decrease in tungsten content of the alloy, and to reduce the residual stress, hardness and surface roughness of the alloy coatings. Further, development of cracks on the coatings gradually found to be decreased with increase of deposition current density.

Gáliková et al. (2006) were developed NiW alloy coatings on the steel substrate at the temperature of 60°C. It was found that the content of tungsten in coatings was increased with the growing cathodic current density, which further increased its corrosion resistance property.

Electrodeposition of NiW alloy coatings from citrate-ammonium type electrolytes with relatively low tungstate concentration was studied by Anicai (2007). It was found that developed coatings exhibited good corrosion protection behaviour, and even after 240 hours of continuous immersion in chloride containing aggressive medium. It was observed that the exposed specimens didn't show any major surface deformation and pits. Chang et al. (2011) prepared NiW alloy coatings by electrodeposition technique with glycolic acid as a complexing agent for the first time. The experimental results showed that for the Ni -W alloy coatings with glycolic acid as complexing agent, the crystal grains are fine and compact and the surface is smooth. Compared to the coatings with conventional complexing agent of citric acid, the wear lost rate and corrosion rate decrease by 45% and 35%.

The electrodeposited materials with alternate layers of metals/alloys, consisting of a thickness of a few nanometres with ultra-fine microstructure, called composition modulated multilayer alloys (CMMA) produced by electrodeposition are gradually gaining interest amongst researchers recently (Yogesha and Chitharanjan Hegde 2011).

A comparative study of protective Ni-W alloy coatings, obtained by continuous (cc) and pulsed (pc) currents from citrate–ammonia media on copper surface was made by Sassi et al. (2012). The obtained coatings in both cases found to show improved electrical, mechanical and electrochemical proprieties to copper substrate. However, Ni–W films electrodeposited under pulsed current possessed better long-term stability.

Arganaraz et al. (2012) have made an extensive surface and structural characterization of electrodeposited Ni-W coatings deposited by galvanostatic pulse current on steel and copper substrates. The coatings were obtained at high current pulse frequency and show high micro hardness and absence of brittleness.

Arunsunai Kumar et al. (2012) employed pulse plating to obtain NiW alloy nano deposits from ammoniacal citrate bath, and studied the effect of peak current density, pH, tungstate ion concentration and temperature on cathodic current efficiency. Electrochemical polarization study revealed that the corrosion potential values of nickel increased with W addition by decreasing the corrosion current density values.

Udompanit et al. (2014) investigated the wear response of electro-fabricated composition-modulated multilayer NiW coatings. By regulating the pulse waveforms of the applied currents, the chemical composition and the individual layer thickness of the electrodeposited multilayer NiW alloy coatings were tailored. It was observed that the ball-on-disc test, and subsequent microstructural analysis indicated that the wear resistance and friction coefficient of multilayer NiW coatings are influenced by both composition and thickness of the individual alternating layer. Recently, Elias and Chitharanjan Hegde (2015) electrodeposited Ni-W coatings on mild steel (MS) in a laminar multilayer pattern from a citrate bath using single bath technique (SBT). Experimental results demonstrated that under optimal condition, multilayer Ni-W alloy coatings are about six time more corrosion resistant compared to its monolayer alloy coatings, obtained from same bath for same duration of time.

Wasekar et al. (2019) studied the corrosion behaviour of compositionally modulated nano-crystalline Ni-W alloy coatings, developed using by pulse current; and their corrosion protection efficacies, studied in 2N H<sub>2</sub>SO<sub>4</sub> solution was compared with that of conventional hard chrome coatings, and results are discussed. In addition, it was revealed that composition modulated Ni-W alloy coating is far more corrosion resistant compared to its single-layer counterpart.

From the experimental study on electrodeposition and characterization of tungsten based alloy coatings with Fe-group metals, it was found that these materials can behave as an excellent electrocatalytic material for HER and OER in water splitting applications. The experimental results demonstrated that these materials can be an alternative for replacement of expensive metals, like Pt and Pd. Many studies showed

that NiW alloy, furthermore W-based alloys prepared by electrodeposition method were found to exhibit the highest electro-catalytic activity and stability in long-term operations (Vernickaite et al. 2019). Arul Raj and Vasu (1990) developed a series of binary alloy coatings, namely nickel-molybdenum, nickel-zinc, nickel-cobalt, nickel-tungsten, nickel-iron and nickel chromium by electrodeposition method. The experimental studies revealed that those binary alloy coatings are good electro-catalyst for HER of alkaline water splitting applications in alkaline solution. It has been established that their electrocatalytic effects for HER is the order as, Ni-Mo > Ni-Zn (after leaching Zn in KOH) > Ni-Co > Ni-W > Ni-Fe > Ni-Cr > Ni plated steel.

González-buch et al. (2013) have developed the alloy coating of molybdenum, tungsten and cobalt with nickel in order to increase their intrinsic catalytic activity for HER. In all the cases, electrodeposits at very high current densities were found to be provided with macro-porous structure having quasy-cylindrical pores, and were attributed to the simultaneous evolution of hydrogen gas. The electro-catalytic studies showed that developed materials manifest apparently high catalytic activity than that reported for a smooth commercial poly-crystalline nickel electrode. Elias and Hegde (2015) developed electrocatalytically active NiW alloy coatings, through compositionally flexible electrodeposition method on copper substrate from tri-sodium citrate bath, using glycerol as the additive. The electrocatalytic study of HER and OER of alkaline water electrolysis in 1M KOH revealed that NiW alloy coatings deposited at low and high current densities showed, respectively superior performance towards OER and HER. This opposite electrocatalytic activity of NiW alloy coating towards HER and OER in overall water electrolysis is attributed to the noble metal contents of the alloy.

Benaicha et al. (2016) have developed the NiW alloys from citrate electrolyte and studied the effect of applied potential and solution pH on the composition limit and the properties of the deposits. Electrochemical measurements employing cyclic voltammetry (CV), potentiodynamic polarization and electrochemical impedance spectroscopy (EIS) were used to investigate the codeposition process, corrosion resistance and HER electrocatalytic properties of the deposits. It was found that Ni-W alloys deposited at -1.4 V/CSE (having about 14 at.% W) are good electrode materials as cathode for HER with substantial surface-adsorbed hydrogen while alloys plated at -

1.2 V/SCE (having about 32 wt.% W) were of excellent corrosion resistance in 3.5% NaCl solution.

The electrodeposited NiW alloy coating with as high as 22 Wt. % tungsten was found to exhibit an excellent wear resistance due to its enhanced hardness. Pramod Kumar et al. (2015) electrodeposited NiW alloy coatings from citrate bath containing salicylaldehyde as additive. The coating developed from the bath containing 100 ppm salicylaldehyde was found to be nano-crystalline, smooth and fine grained, analysed through XRD, SEM and AFM techniques. The same coating was found to show highest corrosion resistance as supported by the EIS and potentiodynamic polarization study. Lee et al. (2015) studied the electrodeposition of NiW thin films with tailored composition such as alternate layers of tungsten rich and tungsten poor multilayers, and thickness by controlling the parameters such as the deposition current density, bath pH and the deposition time. The effect of composition and the number of layers on the mechanical properties, like hardness and internal stress of the developed NiW alloy deposit were studied. The experimental results showed an enhanced hardness of NiW multilayer alloy coatings, with decreased internal strain compared to its monolayer counterpart.

Elias and Hegde (2017) electrodeposited high corrosion resistant NiW alloy coatings in presence of external magnetic field for the protection of mild steel, as substrate. The intensity and direction of the external applied magnetic field were manipulated to develop NiW alloy coatings of better corrosion resistance. It was demonstrated that the corrosion resistance property of NiW alloy coatings was enhanced to many folds by magneto-electrodeposition (MED) approach. The better corrosion stability of MED NiW alloy coatings were attributed increased W content of the alloy, affected due to enhanced mass transportation of W ions, and hence its increased limiting current density. Mollamahale et al. (2018) reported a study on electrodeposition of NiW nanoparticles with the aim of electrocatalytic activity enhancement of nickel material in acidic media for HER. The NiW electrocatalyst showed a high current density of  $10 \text{ mAcm}^{-2}$  at  $-205 \text{ mV}$  (vs. RHE) for HER, and an improved stability compared to that of tungsten-free Ni nanoparticles. The high catalytic activity of NiW nanoparticles stems from incorporation of the tungsten atoms into the nickel structure. Vernickaite et al. (2019) studied the electrocatalytic activity

of electrodeposited NiW, CoW and FeW alloys (0 - 30 at. % W) as an efficient cathode electrode for HER. The experiment was carried out in 30 wt. % NaOH, using linear voltammetry technique. It was observed that the electrocatalytic activity of mutual alloys of Ni, Co, Fe with W was more compared to the single iron group metals. Further, among them NiW alloy electrode with 30 wt. % W exhibited the highest electrocatalytic activity with lowest over potential, and highest exchange current density for HER.

### **2.1.2 Electrodeposition of NiCo alloy**

At the same time, the electrodeposition of mutual alloys of Fe - group elements, to name Fe, Ni and Co is comparatively easy to develop electrolytically due to two reasons: the standard electrode potentials of three metals are close together (Fe = - 0.44 volt; Co = - 0.28 volt and Ni = - 0.25 volt), and metals do deposit at higher polarization voltage. Moreover, mutual alloys Fe group metals follows famous anomalous type co-deposition with preferential deposition of less noble metal. The anomalous co-deposition is characterized by the fact that nickel, the most noble among the group is not readily deposit in presence of the other two metals. Instead, preferential deposition of less noble metal takes place. The experimental study of electrodeposition of NiCo alloy coatings revealed that NiCo alloy coatings exhibit enhanced hardness, adhesion, magnetic properties, wear and corrosion resistance, compared to even pure Ni coatings (Ganci et al. 2021). Burzyńska and Rudnik (2000) researched the role of different parameters such as deposition current density, cobalt ions concentration and additives (like saccharin and sodium lauryl sulfate etc.) in the electrolyte on the surface morphology and composition of alloy coatings. Moreover, it was found that as the deposition current density increased, the cobalt content of the alloy coatings decreased, in support of the natural behavior of anomalous type of co-deposition.

Golodnitsky et al. (2002) have electrodeposited NiCo alloy coatings from sulfamate bath containing acetate and citrate-anion additives. They found that the micro-hardness of electrodeposited alloy coatings is depends mainly on the concentration ratio of cobalt and nickel ions in the bath, as well as the pH of solution, in the bath. In addition, it was found that concentration of anions such as citrate included in the bath gives a coating with more structural stability and enhanced properties over a broad range of acidity and current density. Gang Wu , Ning Li , Derui Zhou , Kurachi Mitsuo (2004) experimented on electrolytic co-deposition of Co–Ni–Al<sub>2</sub>O<sub>3</sub> composite

coating from sulfamate electrolyte, having Co and Ni salts with  $\text{Al}_2\text{O}_3$  particles. The influence of plating parameters on the composition, surface morphology and performance of composite coatings was investigated. Gómez et al. (2005) have carried out electrodeposition of Co–Ni and Co–Ni–Cu alloys from a sulphate–citrate bath. They studied the effect on deposition parameters such as pH and the concentration of metal ions and the citrate on the process of electrodeposition. Wang et al. (2005) have studied the effect of cobalt content on structural, mechanical and tribological properties of NiCo alloy coatings, and reported an improved hardness and decreased wear resistance of alloy coatings, in relation to those of pure Ni coatings.

Development of Ni–Co/SiC nanocomposite coating through electrodeposition method was reported by Shi et al. (2006), where effect of varying the concentration of SiC nanoparticles were tried. Further, a detailed investigation was carried out to understand the effect of concentration of nanoparticles, deposition current density and temperature on the alloy composition. It was found that SiC nanoparticles are distributed uniformly in the NiCo matrix, which significantly improved the corrosion resistance, micro hardness and wear resistance of the alloy coatings. Srivastava et al. (2006) electrodeposited NiCo alloy coatings from sulphamate by varying the cobalt concentration in the bath. It was found that corrosion behaviour of alloy coatings changed significantly due to change in its cobalt content. The changed Co content was found to be responsible for changed microstructure, composition and surface morphology of alloy coatings. The coatings having 20 wt. % of Co was found to show more corrosion resistance compared other coatings, including plain Ni and plain Co coatings, irrespective of the substrate (like mild steel, brass) employed.

Electrodeposition of Ni-Co - carbon nanotubes (CNTs) composite coatings was studied by Shi et al. (2006). The experimental results showed that addition of CNTs brings a tremendous structural and compositional change in composite coatings. The uniformly distributed CNTs in the coatings found to enhance the hardness and tribological properties of composite coatings. Marikkannu et al. (2007) studied the effect of different additives such as, saccharine, dextrin, 1, 4-butyne diol, coumarin, 1, 3-naphthalene sulphonic acid, formaldehyde, glycine, crotonaldehyde in acetate bath for the electrodeposition of NiCo alloy coatings. It was found that both corrosion resistance and micro-hardness of alloy coatings were improved due to addition of

additives into the alloy matrix. Li et al. (2008) electrolytically synthesized NiCo alloy coatings from an electrolytic bath containing saccharine, as additive. It was found that hardness of alloy coatings has increased up to a particular concentration of both saccharine and cobalt. Hassani et al. (2009) studied the effect of deposition current density and additives, such as saccharine, sodium lauryl sulfate on the structure, the corrosion and tribological properties of the coatings. It was found that saccharine and sodium lauryl sulfate enhanced the corrosion resistance property of alloy coatings by improving its structural features. However, deposition current density was found to effect hardly the corrosion and tri-biological behavior of alloy coatings.

The effect of pH on composition of electrodeposited NiCo alloy coatings was investigated by Tian et al. (2011). It was found that the increase of pH increased the cathode efficiency, and the cobalt content of alloy. Lupi et al. (2011) reported a clear correlation between the surface morphology and electrochemical properties of NiCo alloy coatings with its composition. Karpuz et al. (2012) electrodeposited NiCo films from an electrolytic bath containing nickel sulfamate, cobalt sulfate and boric acid, and investigated the dependence of properties of the developed coatings with Co content of the alloy. A direct correlation between the cobalt content of alloy coatings and its magnetic properties was made, and results were discussed.

González-Buch et al. (2013) studied the electrodeposition of macro-porous Ni, Co and NiCo electrodes on stainless steel (AISI 304) substrate. It was found that under optimal condition, NiCo alloy coating is an excellent electro-catalytic material for HER of alkaline water electrolysis, and was found to be better than the commercially available smooth Ni electrode. NiCo deposits with 43 Wt. % Co was found to manifest the highest intrinsic activity for HER, due to synergetic effect of Ni and Co. She et al. (2014) developed a high corrosion resistant self-cleaning super hydrophobic NiCo alloy surface coating on AZ91D magnesium alloy through electrodeposition method. Lokhande and Bagi (2014) galvanostatically deposited NiCo alloy coatings from sulfate bath by varying the concentration of saccharine, as additive. It was found that addition of saccharine lead to the decrease of Co content in the alloy by increasing its hardness and corrosion resistance behavior. Cai et al. (2015) studied the effect of Co content on microstructure, composition, micro-hardness and corrosion behavior electrodeposited Ni-Co-Al alloy coatings. It was established that an increase of Co content in the ternary



Ni-Co-Al alloy coating results in decrease of grain size and its corrosion resistance behavior.

Zamani et al. (2016) studied the effect of cobalt content in the electrolytic bath on electrodeposition mechanism of alloy coatings by employing electrochemical impedance spectroscopy (EIS) technique as tool. It was observed that an increase of cobalt ion content in the bath increases the charge transfer resistance ( $R_{ct}$ ) and decreases the Warburg impedance. It was attributed, respectively to the increased cathode surface coverage due to formation of  $\text{Co(OH)}_2$  and increased rate of diffusion of metal ions toward cathode. Liu et al. (2016) Co-Ni alloy coatings were produced by two different electrodeposition techniques, and they are supercritical carbon dioxide ( $\text{Sc-CO}_2$ ) assisted electrodeposition, and conventional electrodeposition in air. The Co-Ni alloy coating electrodeposited in presence of  $\text{Sc-CO}_2$  shows smoother and brighter coatings with enhanced hardness and corrosion stability, when compared to its conventional alloy coating. Recently, corrosion protection efficacy of multilayer NiCo alloy coating was reported by Shetty and Chitharanjan Hegde (2017), where layered coating was accomplished by periodic modulation of ultrasound effect inside the bath, parallel to the process of electroplating. NiCo alloy coatings of high corrosion resistance were developed by optimizing deposition conditions, like composition (by altering the power density through sonicator probe) and thickness (by controlling the time duration of each pulse) of alternate layers. It was reported that corrosion resistance property of NiCo alloy coatings increased many fold of its magnitude, compared to its monolayer coatings. The increased corrosion resistance of multilayer coatings was ascribed to the formation of more number of interfaces, affected due to layering. However, at higher degree of layering an increase of corrosion rate was reported, which stands for the reason of interlayer diffusion due to very short deposition time (of each layer).

Bouzit et al. (2017) studied the electrodeposition of NiCo thin films on Cu substrate from chloride-sulphate bath, using thiourea as the additive. The effect of deposition current density on surface morphology, composition and phase structure of alloy coatings were studied using SEM, EDS and XRD techniques. The EDS supported composition information revealed that the bath follows anomalous type nature of codeposition with preferential deposition of less noble Co, than noble Ni. Variation in electro-catalytic activity of NiCo alloy coatings towards HER of alkaline water

electrolysis with its surface morphology was studied by Li et al. (2018). A series of NiCo alloy coatings, having Co content from 0% to 75% was deposited galvanostatically. It was found that out of all coatings, Ni-60% Co alloy shows excellent electro-catalytic behaviour towards HER. This behavior of alloy coating was accredited to the combined effect of (Ni and Co) and catalytically active site in the coating surface, due to its unique complex mesh structure. Zhang et al. (2020) developed a nanocrystalline NiCo alloy coating on the steel substrate by adopting the principle of electrochemical additive manufacturing (ECAM). The corrosion and hardness test showed that increase of Co content resulted in decrease of corrosion resistance and increase of hardness of alloy coating.

Elrouby et al. (2020) electrodeposited NiCo alloy coatings from neutral aqueous solutions of NiCl<sub>2</sub> and CoCl<sub>2</sub> salts as precursors at room temperature. The electrodeposited alloy coating found to act as a highly corrosion protective coatings on steel substrate in the hydrochloric acid solution. The coatings were examined via X-ray diffraction (XRD), indicating the formation of two main phases of (fcc) and (hcp). Electro-catalytic study of alloy coatings showed that they can be very good candidate for HER in HCl electrolyte. The effect of addition of nanoparticles (TiO<sub>2</sub>) into NiCo alloy matrix on its electro-catalytic reaction of HER was studied by Gómez et al. (2021). It was found that it forms a good class of material for HER of water electrolysis. At the same time, You et al. (2021) synthesized a high corrosion resistant NiCo-CeO<sub>2</sub> composite coatings. Wang et al. (2021) developed porous NiCo alloy coatings under conditions of different current densities and plating time. The surface morphology of alloy coatings were studied using SEM analyses, alongside its electro-catalytic activity towards HER. The electro-catalytic parameters were studied using different electrochemical methods, like EIS, linear polarization and potentiodynamic polarization and chronopotentiometry techniques. Further, experimental investigation established a strong link between the porosity of alloy coatings with electro-catalytic activity of HER.

Therefore, extensive literature review on electrodeposition of binary alloy coatings, it is confirmed that there are ample of reports on electrodeposition of Ni-based alloy coatings, keeping their corrosion protection efficacy and electro-catalytic activity into

consideration. The experimental study of electrodeposition and characterization of Ni-based alloy coatings revealed the following facts:

1. Ni-based alloy coatings of high corrosion resistance, and good electro catalytic activity can be developed from newly proposed baths, on proper manipulation of bath composition and operating parameters.
2. The corrosion protection efficacy and electro-catalytic activity of Ni-based alloy coatings can be tuned by proper manipulation of composition, phase structure and morphology of alloy coatings, through deposition current density.
3. The corrosion resistance of Ni-based alloy coatings can also be increased drastically with the advent of magneto-electrodeposition (MED). *i.e.* by superimposition of magnetic field ( $B$ ), applied simultaneously to the process of deposition.
4. The corrosion protection efficacy of Ni-based alloy coatings can be increased to many fold of its magnitude by composition modulated multilayer (CMM) coating approach. *i.e.*, by periodic pulsing of direct current during deposition.
5. The electrocatalytic activity of Ni-based alloy coatings can be improved significantly by proper manipulation of deposition current density, and incorporation of proper nano-materials into the electrolytic bath. *i.e.*, through composite coating technique.

## **2.2 SCOPE AND OBJECTIVES**

Having inspired by the technologic importance of Ni-based alloy plating, and exclusive claims of multilayer coating and magneto-electrodeposition techniques, electrodeposition of (Ni-M, where M = W and Co) alloy coatings on copper for better corrosion protection is intended to be achieved here. The optimization of two new baths namely NiW and NiCo will be tried, using suitable additives. NiM alloy coatings of high corrosion performance will be developed by exploring the advantages of multilayer and magneto-electrodeposition approach. The corrosion behaviour of monolayer and multilayer NiM alloy coatings will be studied, and reasons of facts responsible for enhanced corrosion protection of CMM alloy coatings will be analysed. The effect of magnetic field, applied both parallel and perpendicular to the process of electrodeposition will be studied, and experimental results will be detailed in the light

of magneto-convection effect. The incredible claims of electroplating (like effect of operating parameters) will be tried to explore effectively for electro-synthesis of NiW and NiCo alloys, as electrocatalytically active material. The electrocatalytic activity of these coatings, in terms of their efficacy for hydrogen evolution reaction (HER) and oxygen evolution reaction (OER) in complete alkaline water electrolysis will be studied.

As conventional metal plating is becoming insufficient to meet many of the recent technological demands, the NiM alloy coatings with new properties are to be tailored to cater the needs of advanced applications. The philosophy of the thesis is to maximize the corrosion protection ability and electrocatalytic activity of proposed alloy coatings, namely NiW and NiCo by proper manipulation of deposition conditions. In this direction, the title project is driven by following objectives:

1. To optimize two new electrolytic baths, namely NiW and NiCo for electrodeposition of bright and uniform corrosion resistant coatings by standard Hull cell method, using glycine as the additive.
2. To study the corrosion behaviour of all electrodeposited alloy coatings by electrochemical AC and DC methods in 3.5% NaCl solution, for comparison purpose.
3. To increase the corrosion protection efficacy of conventional monolayer NiW and NiCo alloy coatings (deposited using direct current (DC)) by multilayer approach using modulated DC (by pulsing DC in square wave pattern), and to discuss the factors responsible for their improved corrosion resistance.
4. To optimize coating configuration of multilayer alloy coatings (in terms of composition and thickness of individual layers) for their peak performance against corrosion.
5. To increase the corrosion protection ability of monolayer NiM (where M = Co) alloy coatings by exploring the phenomenon of magneto-convection. *i.e.* by superimposing magnetic field ( $B$ ), simultaneously to the process of electrodeposition.

6. To study the effect of both directions (parallel and perpendicular) and intensity of  $B$  on process and product of magneto-electrodeposition (MED) at constant current density, and to discuss the factors responsible for improved corrosion resistance of alloy coatings.
7. To study the electrocatalytic activity of NiW and NiCo alloy coatings, developed under different conditions in alkaline water electrolysis of HER and OER in 1.0 M KOH, by conventional cyclic voltammetry (CV) and chronopotentiometry (CP) methods, and to compare their performances.
8. To study the effect of incorporation of Ag nanoparticles on electro-catalytic performance of Ni-Co alloy coatings for water splitting applications, using CV and CP methods.
9. To compare and characterize the monolayer, multilayer and nanocomposite alloy coatings of Ni-M alloy coatings by various instrumental methods, such as SEM, EDS, XRD and AFM, and to analyse the reasons responsible for improved corrosion resistance and electro-catalytic responses.



**CHAPTER 3**  
**EXPERIMENTAL METHODS**

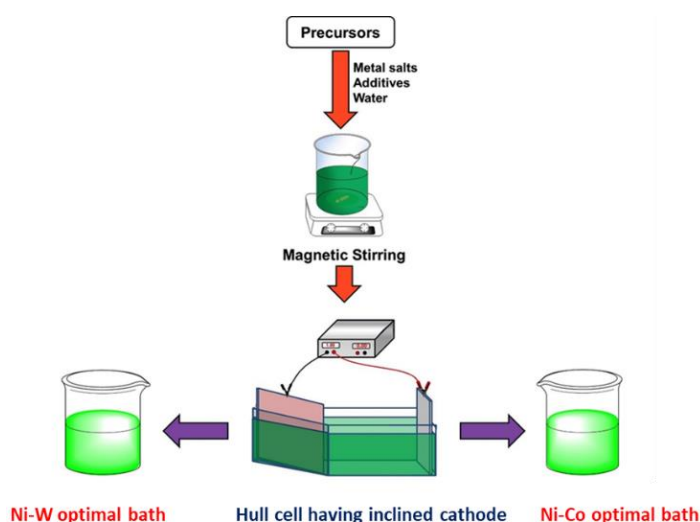




## CHAPTER 3

### EXPERIMENTAL METHODS

*This chapter speaks about the methods used for the production and characterization of electrodeposited Ni-based alloys and their nanocomposite coatings. The procedures adopted for optimization of electrolytic baths and deposition of alloys and their nanocomposite coatings are discussed followed by a concise description of the characterization techniques used. The experimental setup and the methods used to test the efficacy of the developed coatings for different applications such as corrosion resistance and electro-catalytic activity are described.*



#### 3.1 SUBSTRATE PREPARATION FOR ELECTROPLATING

The surface of the substrate used in the present study (copper plates and copper rod), having known active surface area were polished metallurgically to get mirror finish using emery coated mops of gradually decreasing grit size. The mirror-finished surface was decreased by trichloroethylene followed by air-drying. Electrodeposition was accomplished on known cleaned active surface area for given duration of time, by masking the remaining region using cellophane tape.

### 3.2 BATH OPTIMIZATION USING HULL CELL

The standard Hull cell method was used to optimize the bath constituents, their concentrations and operating variables (such as current density, pH, temperature) for deposition of a bright, uniform, and more corrosion-resistant alloy coatings on the substrate as described elsewhere (Kanani 2006). Hull Cell is a mini tank used to test of effect of plating variables on the nature of electrodeposits. Control of an electroplating process is achieved by making direct measurements on the solution itself, like temperature, current density, metal concentration, pH etc. In the Hull cell cathode is placed inclined to the surface of anode as shown in Figure 3.1.

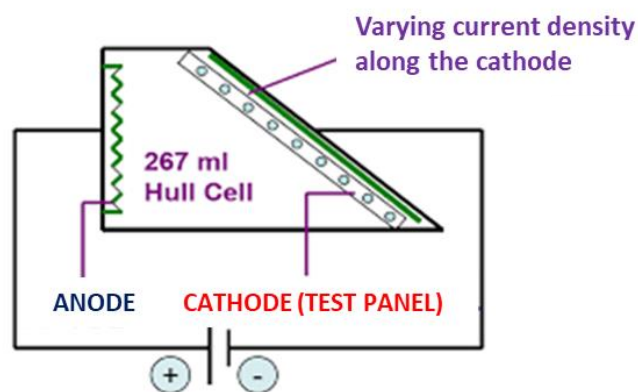


**Figure 3.1-** Diagrammatic representation showing the inclined positioning of cathode (Test panel) in Hull cell, responsible for varied current density along the length of cathode.

As current density varies along the length of the cathode, the nature of coating obtained along the length of cathode do changes, and is supposed to be the replica of the deposit developed at different current densities within the operating range of a specific bath, when it is kept parallel to anode. Using the advent Hull cell, the optimization of deposition conditions of two new baths, namely NiW and NiCo were accomplished. The Hull cell having 267 mL capacity was used, and cell current of 1A was used to fix the required current density from Hull cell Ruler.

In the present study, two new electrolytic baths, namely NiW and NiCo alloy have been formulated, using Hull cell. For optimization of bath composition and operating conditions, deposition of alloy coatings have been accomplished on cathode

by taking respective electrolyte in the Hull cell of 267 mL capacity. A cell current of 1A was used for duration of 5 min to get respective alloy coatings on cathode. All Hull cell experiments were carried out constant temperature of 303 K, with constant stirring of the electrolyte. After deposition, the cathode panels were removed from the electrolyte, rinsed with distilled water. It is then dried, and analyzed for its brightness, homogeneity and uniformity along the length of cathode. The visual examination of electrodeposited coatings (along the length of cathode) has been done, and was compared with the standard Hull cell Ruler to get the current density range at which the satisfactory deposition can be accomplished from the same bath by keeping cathode parallel to anode par. The sequence of work carried out in preparation of optimized bath solution to using Hull cell is shown diagrammatically in Figure 3.2.

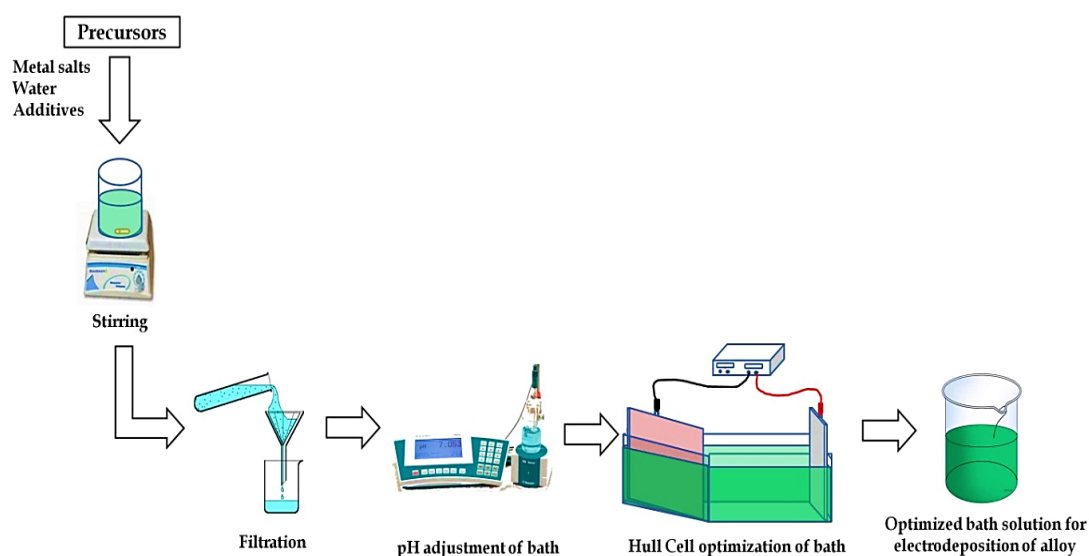


**Figure 3.2-** Flow diagram showing different steps followed in optimization of an electrolytic bath using conventional Hull cell.

### 3.3 DEVELOPMENT OF MONOLAYER COATING

The optimized baths of NiW and NiCo alloy were used for electrodeposition of respective alloy coatings on copper, through different approaches to achieve better corrosion and electrocatalytic performances. The conventional electrodeposition was carried out on a copper plate having an active surface area of  $3 \times 3 \text{ cm}^2$ , after the process of surface cleaning. The monolayer coatings were developed at optimal current densities in a rectangular PVC cell of 250mL capacity, keeping the polished copper plate as

cathode, and graphite plate (having same surface area as cathode) as anode. During regular electrodeposition, cathode and anode are kept parallel at a distance of 5 cm with provision for constant stirring of the electrolyte during plating. The electrochemical cell employed for regular electroplating, using optimized bath is shown in Figure 3.3. DC Power Analyzer (Agilent Technologies, N6705C, USA) was used as the power source for electrodeposition throughout the study. The pH of the bath was adjusted to the desired value by proper addition of either  $\text{NH}_4\text{OH}$  or  $\text{H}_2\text{SO}_4$ , depending on the requirement using a micro pH meter (Systronics, 362). All coatings were carried out for the same duration (600 s), keeping temperature and pH constant, for comparison purpose. After deposition, the electrocoated substrate is removed from the electrolyte, washed, dried and then desiccated, till further analyses.

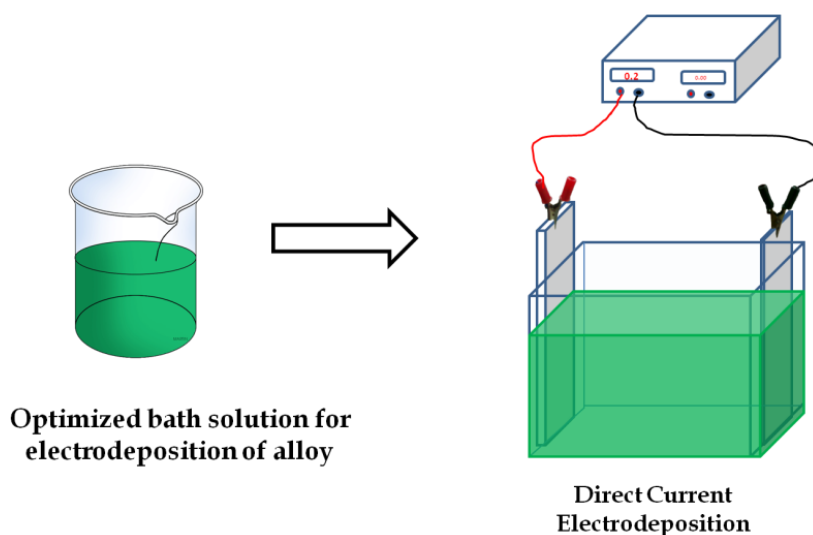


**Figure 3.3:** Electrochemical cell used for conventional electroplating (monolayer) of Ni-based alloy coatings by keeping anode and cathode parallel, using optimized bath.

### 3.4 DEVELOPMENT OF MULTILAYER ALLOY COATING

Multilayer coatings of NiW and NiCo alloy were electrodeposited by passing the DC in a pulsed manner between two current densities, using a DC power source (Agilent Technologies, N6705C, USA). The electrochemical cell setup used for the deposition remains same as that used for the monolayer counterpart, except the power pattern. In addition, alloy coatings were developed on the copper plates having the same active surface area ( $3 \times 3 \text{ cm}^2$ ) as that of the plate used in monolayer deposition. The duration of deposition was kept constant for both monolayer and multilayer alloy coatings to

compare their corrosion and electrocatalytic activity. The current pattern used for the deposition of monolayer and multilayer alloy coatings is shown schematically in Figure 3.4. It is important to note that, unlike in regular pulse plating, here cathodic current is made to pulse periodically between two preset values (lower and higher current densities). But in regular pulse plating, current is made to reach zero value for every change pulse.

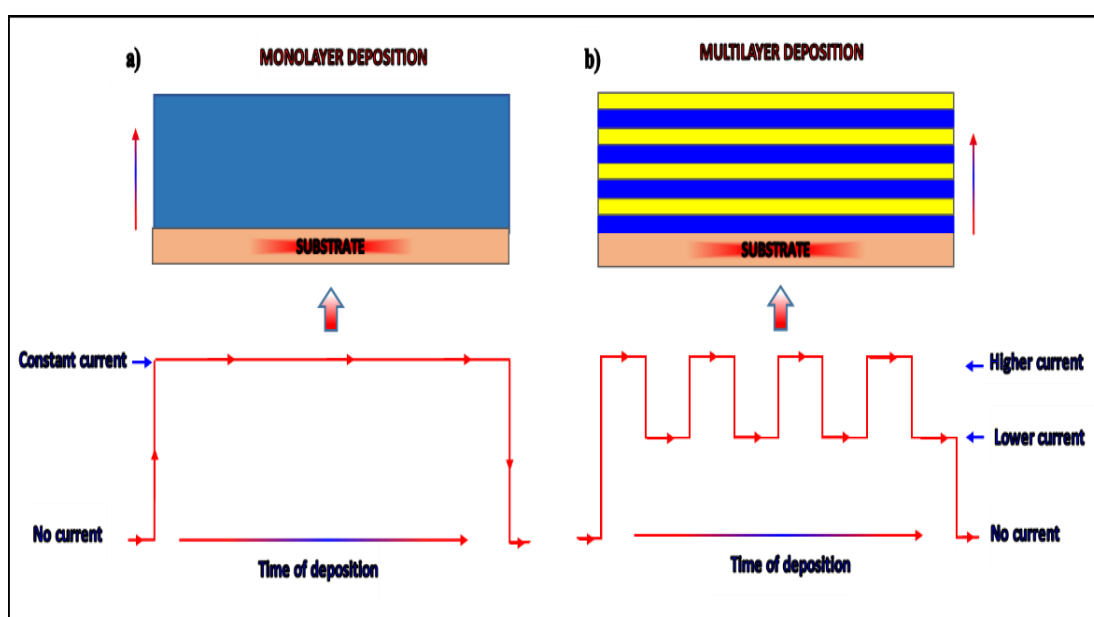


**Figure 3.4-** Schematic representation showing development of electrodeposited alloy coatings, and power patterns used (below) under different conditions: a) Monolayer/homogeneous alloy coating affected due to constant current (DC), and b) Multilayer coating having alternate layers of alloys of different composition, affected due to pulsed DC.

### 3.5 MAGNETOELECTRODEPOSITION

The magneto-electrodeposition (MED) of alloy coatings were carried out at a particular optimal current density, using the optimized bath by super-imposing magnetic field ( $B$ ). In other words, electrodeposition was allowed to take place under the combined effect of electric field ( $E$ ) and magnetic field ( $B$ ) by governing the principles of Lorentz force. The basic experimental setup used for magneto-electrodeposition do consists of an electrochemical cell, having cathode, anode and DC power source as described in the conventional monolayer plating process. But in magneto-electrodeposition, the

electrodeposition is carried out in conjunction with an electromagnet (Polytronics, Model: EM 100), with provision to vary both direction and intensity of  $B$ . The magneto-electrodeposition was accomplished by keeping deposition current density constant to see the effect of magnetic field ( $B$ ), in terms of its direction (parallel and perpendicular to the direction of flow of ions in the electric field) and intensity, in Tesla (T). Magneto-electrodepositions (MEDs) were carried out by varying both intensity (from 0.1T to 0.4T) and direction (parallel and perpendicular to the flow of ions), by keeping the current density constant. Experimental set up used for magneto-electrodeposition of alloy coatings at constant current density, using electrochemical cells is shown in Figure 3.5. It may be noted that a constant and uniform magnetic field is made to be applied on the process of electrodeposition, by keeping electrochemical cell in the space between magnetic poles. The direction of magnetic field is conveniently changed by rotating the electrochemical cell. *i.e.* by changing the plane of cathode with respect of the direction of magnetic field, as shown in Figure 3.5. All depositions were carried out for a constant time (600s), at constant pH and temperature (303 K) for the purpose of comparison of properties and performances of alloy coatings.

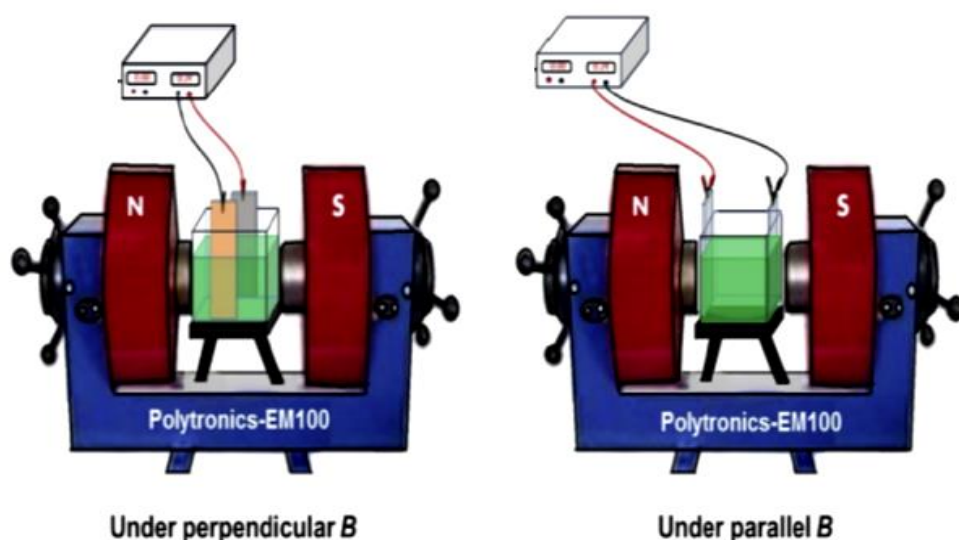


**Figure 3.5:** Schematic diagram showing the experimental set up used magneto-electrodeposition (MED, under conditions of perpendicular and parallel magnetic field ( $B$ )).

### 3.6 PERFORMANCE EVALUATION OF ELECTRODEPOSITED ALLOY COATINGS

The NiW and NiCo alloy coatings developed through different approaches from new baths are intended for better tolerance against corrosion, and good electrocatalytic performance for water splitting applications. Therefore, the corrosion resistance and electrocatalytic activity of electrodeposited alloy coatings were evaluated by various electrochemical techniques.

#### 3.6.1 Corrosion study

Corrosion behaviour of all developed Ni-based alloy coatings was studied in a corrosion cell (of 250mL capacity), having a three-electrode configuration, namely working electrode, counter electrode, and reference electrode. Here, electroplated substrate is made as working electrode (WE), saturated calomel electrode (SCE) as reference electrode (RE) and platinum electrode as counter electrode (CE). The experimental setup for the corrosion study of electrodeposited alloy coatings are shown in Figure 3.6.

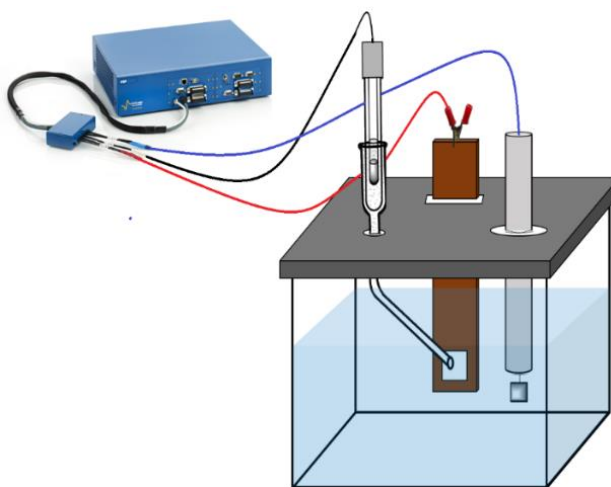


**Figure 3.6-** The schematic representation of the three-electrode corrosion cell used for corrosion study.

All electrochemical studies were carried out by using a computer-controlled instrument potentiostat/galvanostat (VersaSTAT-3, Princeton Applied Research). The corrosion behaviour of alloy coatings (having 1 cm<sup>2</sup> exposed surface area) was evaluated in 3.5% NaCl at 303 K. The corrosion studies were carried out by electrochemical impedance spectroscopy (EIS) technique followed by the

potentiodynamic polarization method. The EIS study was made in the frequency range of 10 kHz - 10 mHz by applying a small voltage perturbation of  $\pm 10\text{mV}$ . The corresponding Nyquist plots were analyzed in comparison with an equivalent circuit obtained by using ZSimpwin software and results are discussed. The corrosion behaviour of alloy coatings was evaluated by potentiodynamic polarization method, at a scan rate of  $1\text{mV/s}$  in a potential ramp of  $\pm 250\text{ mV}$  from OCP. The corrosion rate (CR) values are determined by Tafel's extrapolation method.

### 3.6.2 Electrocatalytic study

The electrocatalytic activity of alloy coatings for water splitting applications was assessed by electrodeposition it on the tip of copper rod (with exposed area  $1.0\text{ cm}^2$ ) instead of copper plate. This is with purpose of evaluating electrocatalytic efficacy of alloy coating, by quantifying the amount of hydrogen and oxygen produced when they are used as electrode in the custom-made electrolyser. The glass set up used for electrodeposition of Ni-based alloy coatings for the purpose of quantitate evaluation of electrocatalytic activity of HER and OER, using electrolyser is shown in Figure 3.7.

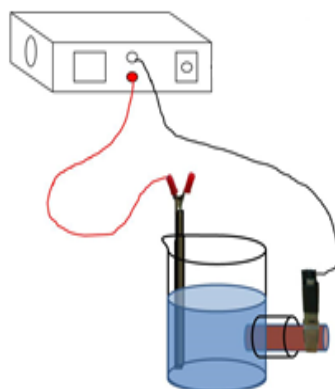


**Figure 3.7-** *The experimental cell used electrodeposition of alloy coatings on the tip of copper rod for quantitate evaluation of electrocatalytic activity of HER and OER, using electrolyser.*

The electrocatalytic efficacy of Ni-based alloy coatings for HER and OER of alkaline water splitting reaction was studied in a customized tubular glass cell equipped with three electrodes (electrolyser), in which platinized platinum is used as the counter electrode, saturated calomel electrode (SCE) as reference electrode, and alloy coated



copper rod as the working electrode. A Luggin's capillary with KCl bridge was used to establish a close contact between the working electrode and reference electrode, by minimize the ohmic polarization. The electrocatalytic activity of alloy coatings, in terms of its efficacy for HER (as cathode) and OER (as anode) are evaluated quantitatively by measuring the liberated  $H_2$  and  $O_2$  gases, using graduated burettes fitted on both ends of the electrolyser as shown in Figure 3.8

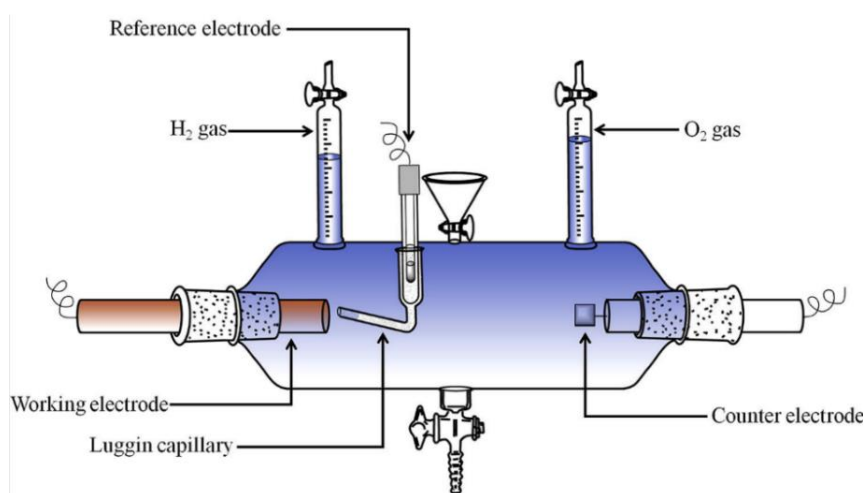


**Figure 3.8-** The electrolyzer used for evaluation of electrocatalytic activity of electrodeposited alloy coatings in terms of its efficacy for HER and OER by knowing the volume of  $H_2$  and  $O_2$  liberated at cathode and anode during water electrolysis.

This experimental setup enables the quantification of electrocatalytic activity of different alloy coatings (deposited at different conditions), in terms of their efficacy for HER and OER when using them as cathode and anode during water electrolysis. The electrocatalytic activity of all alloy coatings was studied by employing conventional cyclic voltammetry (CV). CV measurements were done in a potential window of 0.0 to -1.6 V for HER, and 0.0 to 0.75 V for OER, at a scan rate of  $0.05 \text{ Vs}^{-1}$ . The CP analysis was done by passing a constant current of - 0.3 A and 0.3 A for the 1800s for HER and OER, respectively. The electrocatalytic stability of NiW alloy coatings was tested by the chronopotentiometry method by monitoring the electrode reaction for 1800 s. The electrocatalytic efficiency of electrodes were evaluated quantitatively by measuring the volume of  $H_2$  and  $O_2$  evolved during electrolysis, by keeping other parameters constant, like  $1 \text{ cm}^2$  surface area of test electrode and duration of electrolysis as 300 s.



## **CHAPTER 4**

# **ELECTRODEPOSITION AND CHARACTERIZATION OF NiW ALLOY COATINGS**



## CHAPTER 4

### ELECTRODEPOSITION AND CHARACTERIZATION OF NiW ALLOY COATINGS

---

*This chapter reports the optimization of a new NiW alloy bath for development of a good corrosion resistant coatings using glycine as the additive. The effect of deposition current density on the composition, surface morphology and phase structures of alloy coatings are reported. The electrochemical impedance and potentiodynamic polarization methods are used for corrosion study. The composition, surface features and phase structures of alloy coatings, responsible for better corrosion protection of alloy coatings were analyzed through SEM-EDS, AFM and XRD techniques, and results are discussed.*

#### 4.1 INTRODUCTION

Ni-based tungsten (NiW) alloys are known for their excellent mechanical, tribological, and corrosion resistance properties. Compared to pure Ni, NiW alloys exhibit better hardness and abrasion resistance characteristics, hence find many practical applications, especially in the automotive and aviation industries, like in wheel bearings, magnetic heads, catalysts, etc. (Indyka et al. 2014). There are many reports on NiW alloy coating, demonstrating the fact that baths follow induced type of co-deposition, with less dependency of deposit features on bath composition and operating parameters (Benaicha et al. 2016; Eliaz et al. 2005b; Indyka et al. 2014; Lee et al. 2015b). In the majority of practical NiW plating baths, generally a complexing agent is used to improve the quality of the deposit. The purpose of a complexing agent is to impart finer-grained, smoother, and brighter coatings by improving the throwing power of the bath. Apart from this, complexing agents are used to approximate the electrode potentials of metals to enable the co-deposition by forming proper complex ions with metals to be deposited (Eliaz and Gileadi 2008). In solutions of complex ions, whether the solution is acid or alkaline, the electrode potentials of all metals are shifted to more negative (less noble) potentials, and this often brings them closer together, and thereby permitting

an active metal to be coated by a more noble metal, without the latter deposition by immersion (Kanani 2006).

Thus there are many reports available in the literature on electrodeposition of and characterization of NiW alloy coatings to impart better properties to the substrate, to name few to impart better electrical, magnetic, mechanical and corrosion resistance properties. In this direction, this chapter reports the optimization of new alkaline NiW alloy bath, using glycine as the additive for production of high corrosion resistant alloy coating of NiW on copper. The experimental results of investigation are presented below.

## **4.2 EXPERIMENTAL**

### **4.2.1 Optimization of NiW bath**

A new alkaline NiW alloy bath consisting of potassium sodium tartrate (PST) ( $\text{KNaC}_4\text{H}_4\text{O}_6 \cdot 4\text{H}_2\text{O}$ ), or Rochelle salt, sodium tungstate ( $\text{Na}_2\text{WO}_4 \cdot 2\text{H}_2\text{O}$ ), nickel sulphate ( $\text{NiSO}_4 \cdot 6\text{H}_2\text{O}$ ), ammonium chloride ( $\text{NH}_4\text{Cl}$ ), and glycine ( $\text{NH}_2\text{-CH}_2\text{-COOH}$ ) has been proposed. PST was used as complexing agent to enable the induced type of codeposition of NiW. No detergents or wetting agents, were used for improving the uniformity of alloy coating. All reagents are individually dissolved in double distilled water, and then mixed and stirred well for complete dissolution. The pH of the bath was adjusted to 8.5 using  $\text{H}_2\text{SO}_4$  and  $\text{NH}_4\text{OH}$ , with a Micro-pH Meter (Systronics-362), before each deposition. The composition and processing parameters for electrodeposition of a bright, uniform and sound coating of NiW alloy were optimized using a standard Hull cell method described elsewhere (Kanani 2006). The composition and operating conditions of an optimized alkaline NiW tartrate bath to produce bright and uniform coating is given in Table 4.1.

**Table 4.1- Composition and operating conditions of optimised NiW bath**

Bath composition	Concentration (g/L)	Operating parameters
NiSO <sub>4</sub> . 6H <sub>2</sub> O	14.3	pH : 8.5
Na <sub>2</sub> WO <sub>4</sub> .2H <sub>2</sub> O	22.5	Temperature: 303 K
KNaC <sub>4</sub> H <sub>4</sub> O <sub>6</sub> .4H <sub>2</sub> O	100.0	Anode : graphite
NH <sub>4</sub> Cl	50.0	Cathode: copper
NH <sub>2</sub> -CH <sub>2</sub> -COOH (Glycine)	4.3	Current density : 1.0 Adm <sup>-2</sup> - 4.0 Adm <sup>-2</sup> Deposition time : 600 s

### 4.3 RESULTS AND DISCUSSION

Monolayer NiW alloy coatings were developed on polished copper substrate, using the optimized bath (Table 4.1) at different current densities, keeping temperature constant. The electrodeposited coatings are washed, rinsed and air dried, and then subjected different analyses.

#### 4.3.1 Chemical Composition

The performance of any alloy coatings is principally determined by its composition. In this connection, compositional analysis of electrodeposited alloy coatings have been undertaken using EDS technique. The change of metal contents in the deposit with deposition current density is shown diagrammatically in Figure 4.1.

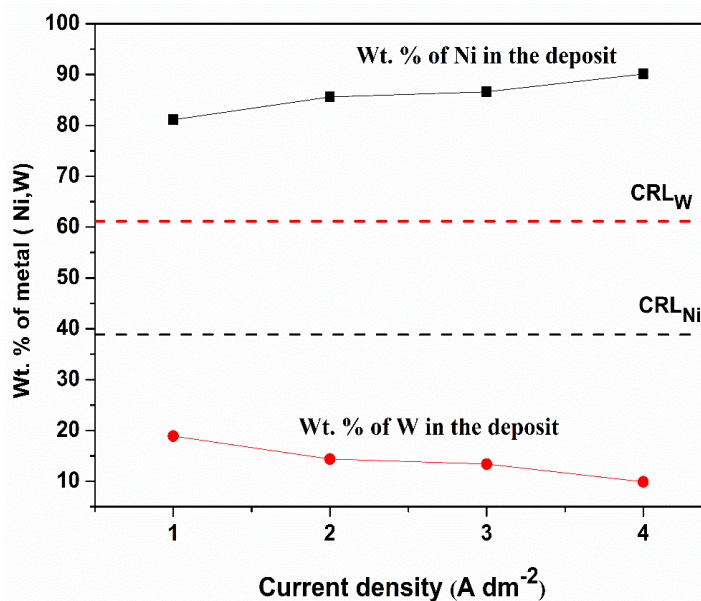


**Figure 4.1-** Dependency of composition of NiW alloy coatings on cathode current density, deposited from optimized bath.

It may be noted that, wt. % of Ni in the deposit increased steadily with current density, and reached its maximum value (90.1 wt. %) at 4.0  $\text{Adm}^{-2}$ , and conversely wt. % of W in the deposit decreased with current density. The wt. % of Ni and W in the bath (calculated on the basis of weight of the salt taken) is shown by horizontal perforated lines in the Figure 4.1, as composition reference line (CRL) of the bath. It may be noted that wt. % of Ni in the deposit is much higher than that in the bath; whereas wt. % W in the deposit is much lower than in the bath. This study of composition change with current density confirmed that the proposed bath follows induced type of co-deposition, and is supported by two observed facts: *i*) change metal contents in the deposit with current density is very small, and *ii*) the wt. % of more noble Ni in the deposit is increasing with current density. Here, it may be recalled that as transition metal ions, like W and Mo cannot be electrodeposited as such from their aqueous solutions, but they can only be co-deposited in the presence of Fe - group metals, like Fe, Ni, Co. Accordingly, in alloy deposition W and Mo are called reluctant metals, and Fe-group metals as inducing metals. Though co-deposition of binary alloys of transition metals with Fe-group metals commonly follow induced type of co-deposition, sufficient number of exceptions do available in the literature (Brenner 1963). From this observation, it may be concluded that the proposed NiW bath follows peculiar induced



type of co-deposition, where Ni induced the reluctant W to co-deposit in the entire range of current density studied, with no sign of regular type of co-deposition.

#### 4.3.2 Surface Morphology

The surface micrographs of NiW alloy coatings corresponding to different current densities (from  $1.0 \text{ Adm}^{-2}$  to  $4.0 \text{ Adm}^{-2}$ ) are examined under SEM, and are shown in Figure 4.2.

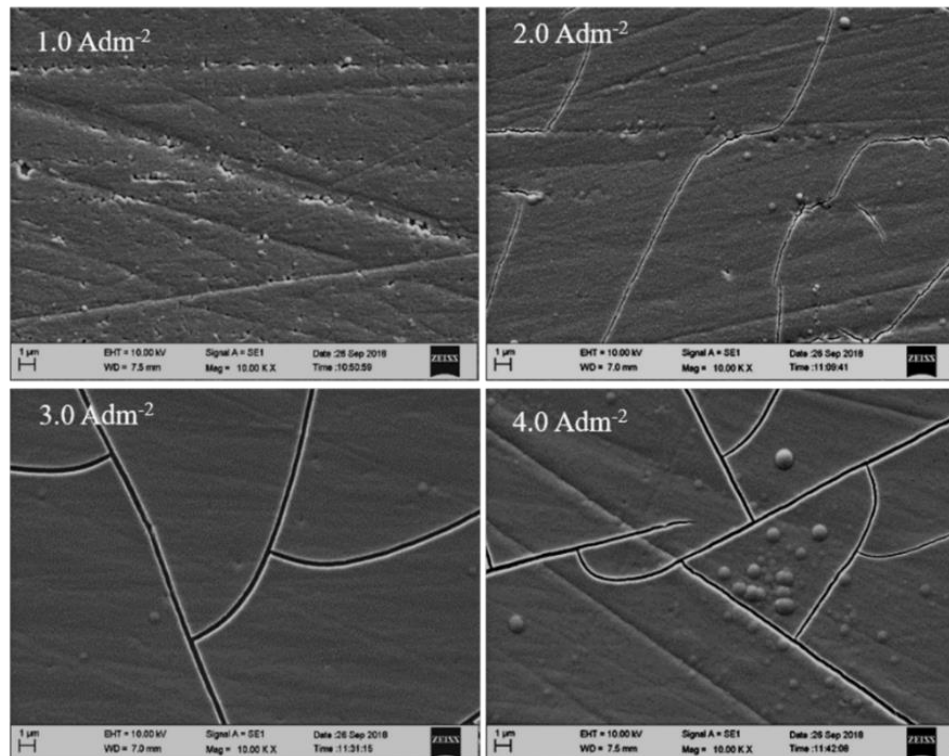


**Figure 4.2-** Surface morphology of NiW alloy coatings deposited at different current densities. Increase of characteristic cracks with current density may be seen.

It may be observed that smoothness of alloy coating increased with current density, but ended up with formation of deep cracks. These observed cracks, having definite patterns are due to hydrogen embrittlement, and they are characteristics of W-based alloy coatings. The hydrogen embrittlement is due to liberation of  $\text{H}_2$  gas which is trapped inside deposits during plating. This  $\text{H}_2$  gas is later released from the alloy lattice due to high tensile stress, leaving the cracks on the surface (Wasekar et al. 2016). Hence, more distinct cracks are observed on coatings as the current density is increased (due to liberation of more hydrogen) as seen in Figure 4.2.

### 4.3.3 AFM Study

The surface roughness is an equally important factor to influence the properties of alloy coatings. Hence, the surface topography of electrodeposited alloy coatings are studied using three dimensional Atomic Force Microscopy (AFM) technique. Accordingly, the AFM image of NiW alloy coatings, deposited at different current densities are shown in the Figures 4.3.

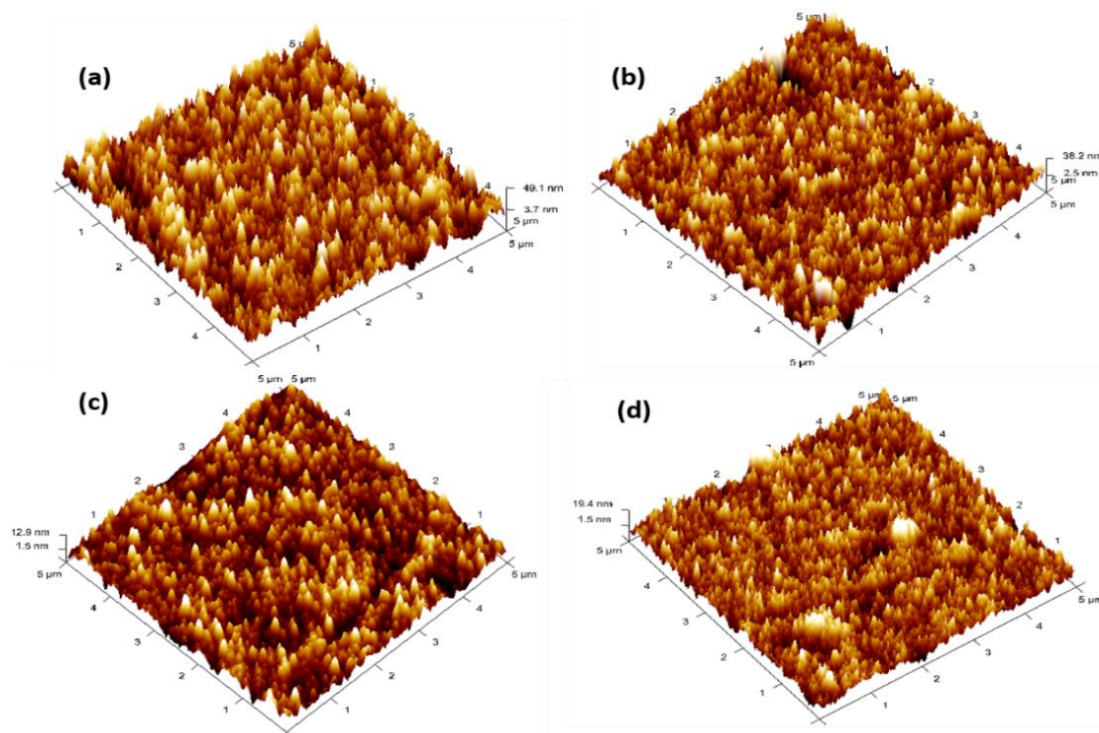


**Figure 4.3-** The AFM image showing the topography of NiW alloy coatings deposited from the optimized bath at: a)  $1.0 \text{ Adm}^{-2}$ , b)  $2.0 \text{ Adm}^{-2}$ , c)  $3.0 \text{ Adm}^{-2}$ , and d)  $4.0 \text{ Adm}^{-2}$ .

The topographical study of any coatings may be carried out by measuring their average roughness ( $R_a$ ) and root mean square roughness ( $R_q$ ) values (Ashraf et al. 2016). Accordingly,  $R_a$  and  $R_q$  values of electrodeposited NiW alloy coatings, corresponding to different current densities are measured, considering their  $5 \mu\text{m} \times 5 \mu\text{m}$  surface area, and experimental data are reported in Table 4.2. It may be seen that the surface smoothness of NiW alloy coatings increased with current density, as seen in AFM images from Figure 4.3 (a) through Figure 4.3 (d), and is supported by values of  $R_q$  and  $R_a$  (Table 4.2).

**Table 4.2 - The surface roughness data of NiW alloy coatings developed at different current densities, using optimized bath**

Coating configuration	R <sub>q</sub> (nm)	R <sub>a</sub> (nm)
(NiW) <sub>1.0Adm<sup>-2</sup></sub>	12.8	10.1
(NiW) <sub>2.0Adm<sup>-2</sup></sub>	10.3	7.6
(NiW) <sub>3.0Adm<sup>-2</sup></sub>	5.2	4.5
(NiW) <sub>4.0Adm<sup>-2</sup></sub>	4.9	3.7

#### 4.3.4 X-Ray Diffraction Study

The phase structure of electrodeposited NiW alloy coatings was studied by XRD, and the corresponding X-ray diffractograms are shown in Figure 4.4. The diffracting planes corresponding to each observed peaks are also shown (JCPDS No. 01-072-2650). It may be noted that XRD signals corresponding different current densities are found to follow the same pattern, *i.e.* with same diffraction angle ( $2\theta$ ). This confirms the fact that solid solution of Ni in W is formed during deposition, regardless of the current density at which they are formed. This constancy of diffraction angles for all alloy coatings indicates that the coatings formed are solid solutions of individual metals (Hosokawa et al. 2004). These solid solutions are characterized by the fact that atoms in the lattice of a metal are substituted by atoms of another metal. This substitution changes the dimensions of the unit cell, without changing the type of the cell, and this substitution may occur either over a limited range of compositions, or over a complete range of compositions from one pure metal to another (Cullity 1956).

In addition, it may be noted that the observed all XRD peaks are well defined (narrow). This indicates that all coatings formed are crystalline, and forms a solid solution of W in Ni that consists of W atoms substitutionally dissolved in the fcc structure of Ni. A gradual increase in the intensity of peak with current density may be ascribed an increase of the Ni content in the deposit. (Table 4.2 and Figure 4.3). Further, a slight shift in the scattering angle ( $2\theta$ ) was found to be at a higher current density as seen in Figure 4.4. This shift of scattering angle was afforded by the internal strain of

coatings due to increase of Ni content, which increased with the current density. This is supported by the composition data, given in Table 4.2.

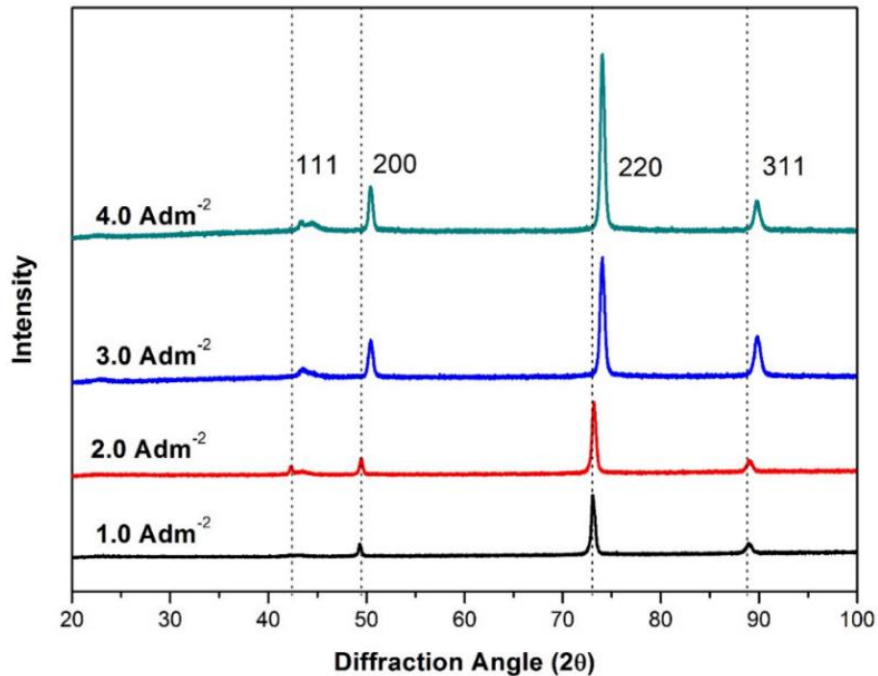


**Figure 4.4-** XRD patterns of NiW alloy coatings deposited at different current densities. A gradual increase of diffraction angle, shown by perforated vertical lines is attributed the internal strain of coatings due to increase of Ni content.

#### 4.3.4 Corrosion Study

The very objective of this work is to formulate a new NiW bath for production of alloy coatings of high corrosion resistance. In this regard, NiW alloy coatings deposited at different current densities from the optimized bath are subjected electrochemical corrosion study, namely Electrochemical Impedance Spectroscopy (EIS) and potentiodynamic polarization methods, experimental results are discussed below.

#### 4.3.4.1 Electrochemical Impedance study

EIS is a commonly used technique to study the corrosion behavior of surface coatings (Mehta 2013). Nyquist (complex plane) plots are the most often used in the EIS study because they allow for an easy prediction of the circuit elements, required to explain behavior of electrode- electrolyte interface (Lasia 1999). Accordingly, Nyquist plots of NiW alloy coatings deposited at different current densities are shown in Figure 4.5. Generally Nyquist plots gives valuable information with regard to the process of corrosion, and it helps to understand the plausible mechanism of corrosion taking place at the interface of coatings and corrosion medium. The similarity in the shape of the Nyquist plot indicates the resemblance of corrosion process in all the coatings under study (Liu et al. 2013).

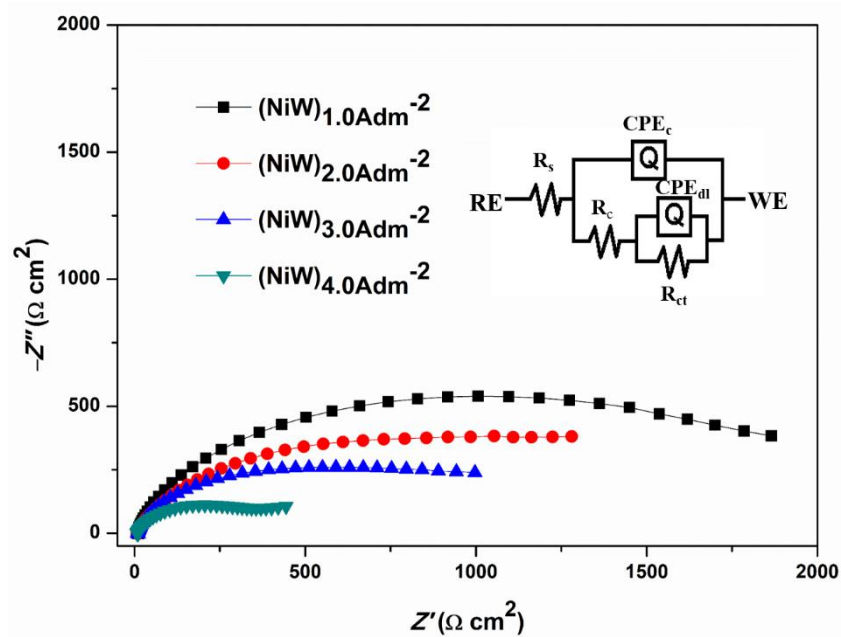


**Figure 4.5-** Nyquist plots of monolayer NiW alloy coatings deposited at optimized current densities.

Hence, based on the shape of Nyquist plots, it may be inferred that NiW alloy coatings formed at different current density follows same corrosion mechanism. Based on the shape of impedance loops, electrochemical equivalent (ECE) circuit has been stimulated, and is shown in inset of Figure 4.5. The electric circuit elements obtained to this model are, coating resistance  $R_c$ , CPE (Q) as constant phase element of the alloy coatings,  $R_{ct}$  and  $CPE_{dl}$  as constant phase element of the coatings-substrate interface.

The  $R_c$  and  $R_{ct}$  altogether constitute the polarization resistance, shows the corrosion behaviour of the coatings (Xing et al. 2020).

**Table 4.3 - EIS data obtained by electrochemical equivalent circuit of NiW alloy coating developed at different current densities**

Coating configuration	$R_s$ ( $\Omega$ )	$R_c$ ( $\Omega$ )	$Q_c$ ( $\mu F$ )	$R_{ct}$ ( $\Omega$ )	$Q_{dl}$ ( $\mu F$ )
$(NiW)_{1.0 \text{ Adm}^{-2}}$	8.78	1051	388	794	579
$(NiW)_{2.0 \text{ Adm}^{-2}}$	7.27	793	650	587	991
$(NiW)_{3.0 \text{ Adm}^{-2}}$	8.63	534	1091	466	1091
$(NiW)_{4.0 \text{ Adm}^{-2}}$	7.62	317	1143	156	1805

From the circuit element values reported in Table 4.3, it may be noted that both coating resistance ( $R_c$ ) and charge transfer resistance ( $R_{ct}$ ) of alloy coating decreases with increase of deposition current density. It implies that the corrosion resistance behavior of alloy coatings decreases as the deposition current density increases. Hence, it may be concluded that NiW alloy deposited at  $1.0 \text{ Adm}^{-2}$  represented as  $(NiW)_{1.0 \text{ Adm}^{-2}}$  is of highest corrosion resistance compare all other coatings. This may be attributed to less number of cracks observed on its surface. But, the obvious cracks observed on the surface of coatings at higher current densities are responsible for their lower corrosion resistance.

#### 4.3.4.2 Potentiodynamic Polarization Method

Follow to EIS study, potentiodynamic polarization study of all four NiW alloy coatings have been carried out, and their polarization behaviours are shown in Figure 4.6. The corrosion rates of alloy coatings are calculated directly from corrosion current ( $i_{corr}$ ) values, obtained through extrapolation of anodic and cathodic polarization curves. The corrosion rate of all NiW alloy coatings, with other corrosion parameters are reported in Table 4.4. Corrosion rate data demonstrated that NiW alloy corresponding to  $1.0 \text{ Adm}^{-2}$  is the most corrosion resistant (with least corrosion rate). The least corrosion rate is of  $(NiW)_{1.0 \text{ Adm}^{-2}}$  is further supported by its more noble (cathodic)  $E_{corr}$  value as shown

in Figure 4.6. Highest corrosion resistance of NiW alloy coating, deposited at  $1.0 \text{ Adm}^{-2}$  may be accredited to its high W content, compared to all other coatings, as shown in composition data shown in (Table 4.3). But coatings deposited at higher current densities are found to be more corrosive, which may be due to a lower W content and increased cracks on the surface (see Figure 4.2).

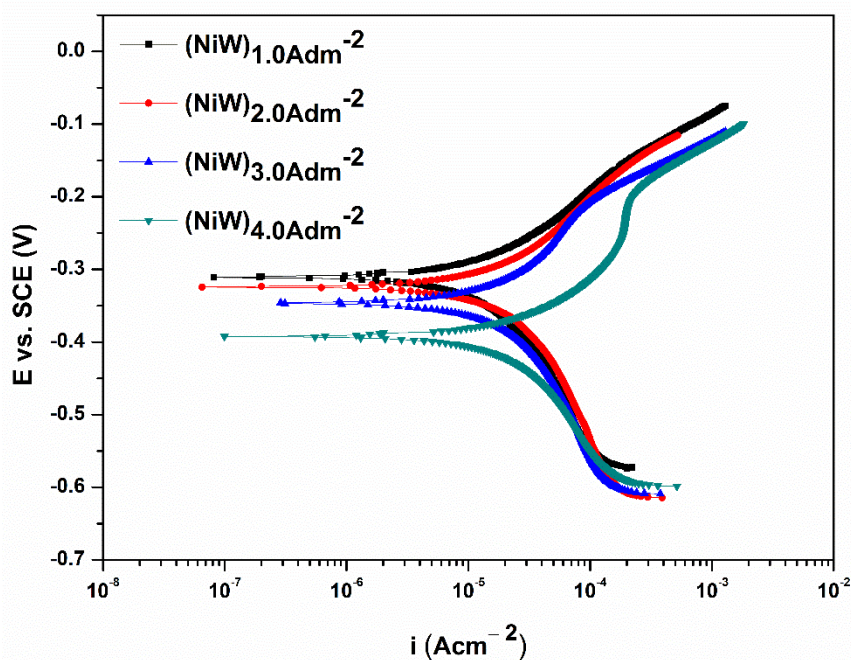


**Figure 4.6-** Polarization behaviour of NiW alloy coatings deposited at different current densities from optimized bath.

**Table 4.4 - Corrosion parameters of monolayer NiW coatings deposited at different current densities from standard bath.**

c.d. ( $\text{Adm}^{-2}$ )	wt. % of Ni	wt.% of W	$-E_{\text{corr}}$ (V vs. SCE)	$i_{\text{corr}}$ ( $\mu\text{A cm}^{-2}$ )	$R_p$ ( $\Omega$ )	$\text{CR} \times 10^{-2}$ ( $\text{mm y}^{-1}$ )
(NiW) <sub>1</sub> $\text{Adm}^{-2}$	81.1	18.9	0.311	15.25	1845	14.89
(NiW) <sub>2</sub> $\text{Adm}^{-2}$	85.6	14.4	0.324	21.81	1380	21.86
(NiW) <sub>3</sub> $\text{Adm}^{-2}$	86.5	13.5	0.346	27.94	1216	27.30
(NiW) <sub>4</sub> $\text{Adm}^{-2}$	90.1	9.9	0.329	41.48	473	42.61
<i>Bath</i>	38.9	61.1				

#### 4.4 CONCLUSIONS

*Based on the experimental observations following conclusions are made:*

1. A new alkaline NiW alloy bath has been formulated using potassium sodium tartrate as complexing agent, and glycine as additive.
2. Bright and uniform coatings were developed at different current densities (from 1.0 to 4.0  $\text{Adm}^{-2}$ ) and their corrosion performances were evaluated by electrochemical AC and DC methods.
3. The composition data revealed that proposed NiW bath follows induced type of co-deposition in range of current density studied, confirmed by EDS study.
4. Electrodeposited NiW alloy coatings are found to have characteristic cracks on the surface which pronounced with increase of current density, evidenced by SEM study. The formation of is due to the combined effect high tensile stress and entrapped  $\text{H}_2$  gas.
5. Constancy of XRD peaks of all NiW coatings confirmed that solid solution of Ni in W has formed, regardless of the deposition current densities.
6. The corrosion study demonstrated that NiW alloy deposited at 1.0  $\text{Adm}^{-2}$  represented as  $(\text{NiW})_{1.0 \text{ Adm}^{-2}}$ , having 18.9 wt. % W is the most corrosion resistant, when compared to other.



## **CHAPTER 5**

# **ELECTRODEPOSITION OF MULTILAYER NiW ALLOY COATING FOR IMPROVED ANTICORROSION PERFORMANCE**



## CHAPTER 5

### ELECTRODEPOSITION OF MULTILAYER NiW ALLOY COATING FOR IMPROVED ANTICORROSION PERFORMANCE

---

*The composition modulated multilayer (CMM), or simply multilayer NiW alloy coatings of better corrosion resistance have been developed using the same optimized bath, reported in previous chapter. Here, the attractiveness of electroplating linked to cathodic current density has been explored to develop multilayer NiW alloy coatings. The multilayer coatings of different configurations, in terms of composition and thickness of individual layers have been developed by proper modulation of amplitude and duration of square current pulse, respectively. The deposition conditions were optimized to get coatings of highest corrosion resistance. The experimental study revealed that under optimal condition, multilayer NiW coating having (NiW)<sub>1.0/3.0/120</sub> configuration is almost six times more corrosion resistant than its monolayer coating, deposited from same bath for same duration. The reason for improved corrosion performance of multilayer NiW alloy coating was explained in the light of effect of layering and composition of each layer, confirmed by scanning electron microscopy (SEM) analysis, energy dispersive spectroscopy (EDS) and X-ray diffraction (XRD) study. Mechanism of corrosion in multi-layer coating, in relation to its monolayer coating is given, and results are discussed.*

#### 5.1 INTRODUCTION

Recent advances in nanostructured multilayer coatings have been led by the development of new synthetic methods, that provide control over the number and composition of individual layers (Bang and Suslick 2010). The use of periodically pulsed current, from highly sensitive power source offers a facile and versatile route for synthesis of nanostructured multilayer coatings showing extraordinary properties, not possible by conventional methods. Multi-layered coating is a new class of materials, having alternate layers of different metals, or alloys of different composition/phase structures (Bull and Jones 1996; Thangaraj et al. 2009a; Ueda et al. 1999; Wilcox and

Gabe 1993). These coating having layers in nanometre scale, hence they are also called as nano-laminated, or composition modulated coatings. Actually, composition modulated multilayer alloy (CMMA) coatings are consisting of thin layers of alloys of same metals, but of different composition. They exhibit a wide range of applications owing to their unique technological properties, different from those of both pure metals and their monolayer alloys. The basic physical phenomena associated with periodic modulation of cathodic current density during deposition is responsible for development of coatings in layered manner with changed composition, instead of a homogeneous one. The pulse electrodeposition method has a merit that it is possible to control the composition and layer thickness of multilayer coating in atomic scale by varying the amplitude of cathodic current (pulse), which is responsible for composition change; and deposition time, responsible for thickness of deposit (Yahalom and Zadok 1987).

Thus by knowing the advent of multilayer alloy coatings, compared to monolayer alloy coatings (developed through conventional method using direct current), a more anti-corrosive NiW alloy coatings was tried to develop from the same optimized bath through multilayer approach, by pulsing periodically the cathode current density (between two values) during plating. The composition and thickness of alternate layers of alloys are manipulated by proper modulation of current densities (pulsing) and duration of pulse (time), respectively. The multilayer coatings of NiW alloy having lamellar structures of nanometre scale were developed under different conditions of current densities (current pulse) and number of layers, using optimized bath. The corrosion protection efficacy of multilayer NiW alloy coatings were evaluated by electrochemical AC and DC methods. The effect of composition of alternate layers, and degree of layering on corrosion protection efficacy of multilayer alloy coatings have been discussed. The multilayer coatings of different configurations, in terms of composition and thickness of individual layers have been developed by proper modulation of amplitude and duration of square current pulse, respectively. The coating configuration of multilayer alloy coatings has been optimized for best performance against corrosion. The reasons of facts responsible for better performance of multilayer NiW alloy coatings against corrosion are explained, and results are discussed.

## 5.2 EXPERIMENTAL

All electrodepositions reported here are carried out in a PVC cell of 200 mL capacity, using high sensitive DC Power Analyser (Agilent Technologies, N6705C, USA). Copper plates having (7.5 cm × 3.0 cm × 0.2 cm) dimension were polished metallurgically to get mirror finish, and then degreased using trichloroethylene as solvent. Anode and cathode were kept parallel 5 cm apart during deposition. Pure graphite plate, having the same surface area, as cathode was used as an anode. All multilayer NiW alloy coatings were carried out galvanostatically on cathode using pulsed DC, of known amplitude. Electrodeposition is accomplished on 3.0 × 3.0 cm<sup>2</sup> active surface area (keeping other part insulated by cellophane tape) of cathode, using the optimized bath reported in Table 3.1. After each deposition, coatings are rinsed thoroughly with distilled water several times, dried in hot air, and then desiccated until further testing.

Driven by the fact that there can be a significant improvement in the corrosion performance of multilayer alloy coatings, when coating is changed from monolayer to multilayer type (Benaicha et al. 2016; Tsyntsaru et al. 2012), multilayer NiW alloy coatings were deposited from optimized bath using pulsed current. Multilayer coatings of different configurations have been developed with different set of cyclic cathode current densities (CCCD's), *i.e.* two current densities between which cathode pulse is made to cycle repeatedly to form coatings in layered pattern. All other conditions of deposition are kept constant as that of monolayer coating. The power pattern used for deposition of multilayer NiW alloy coating is shown by a representative diagram in Figure 5.1 (b) and (c), with the homogeneity of alloy coating formed therefrom at different degree of layering, on the right. The wave pattern of direct current (DC) used for development of conventional monolayer alloy coating is also shown in Figure 5.1(a), with the homogeneity of the coating formed therefrom, for comparison purpose. In this study, monolayer NiW alloy coating showing the least corrosion rate, deposited at optimal current density (at 1.0 Adm<sup>-2</sup>) is represented as (NiW)<sub>1 Adm<sup>-2</sup></sub>. In addition, nano-laminated multilayer coatings, having layers of alloys of different composition are represented as (NiW)<sub>1.0/3.0/n</sub> (here 1.0 and 3.0 stands for CCCD's, and 'n' is the number of layers formed during total plating time. *i.e.*, 600 s. This pulsed DC coating should not

be confused with conventional pulse plating, where the current reduces to zero for every cycle, as explained in the literature (Ganesan et al. 2007).

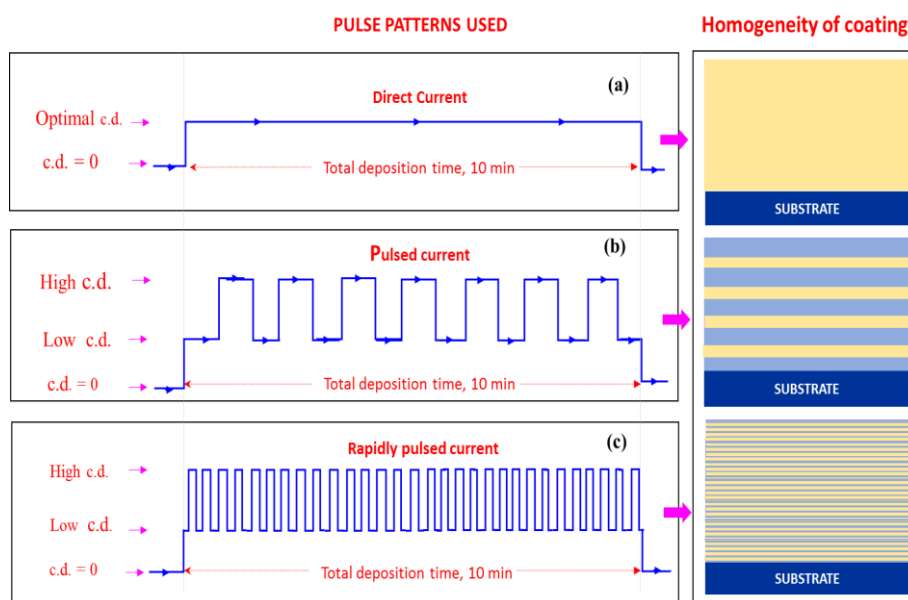


**Figure 5.1-** Schematic representation of current pulses used for electrodeposition of different NiW alloy coatings: a) Direct current (DC) pulse for monolayer alloy coating, and b) Pulsed DC for multilayer alloy coating, and c) Rapidly pulsed DC leading to the formation of almost monolayer coating due to diffusion of layers.

All coatings (both monolayer and multilayer) reported here are electrodeposited for 600 s at constant temperature (303 K) and pH 8.5, for comparison purpose. The corrosion behaviour of all multilayer coatings was evaluated in the same corrosion medium (3.5% NaCl solution), as in monolayer NiW alloy coatings. Potentiodynamic polarization and electrochemical impedance spectroscopy (EIS) methods were used to measure their corrosion tendency, in a three-electrode cell. After desiccator drying of electroplated multilayer NiW alloy coatings, they are subjected to corrosion tests using potentiostat/galvanostat (VersaSTAT 3, Princeton Applied Research). The surface morphology, and formation of layers of/in NiW alloy coatings were confirmed by scanning electron microscopy (SEM, Zeiss Ultra 55, Germany). Composition of the NiW alloy coatings corresponding to different cathode densities were analysed using Energy dispersion X-ray spectroscopy (EDS) technique, (Oxford EDS, X-act). The composition-dependent crystal structures of NiW alloy coatings were characterised by

X-ray diffraction (XRD, Rigaku-miniFlex 600), with  $\text{CuK}_\alpha$  radiation,  $\lambda = 1.5418 \text{ \AA}$ , as the X-ray source.

### 5.3 RESULTS AND DISCUSSION

The corrosion study of monolayer NiW alloy coatings, deposited from the optimized bath at different current densities (Chapter -1), revealed that monolayer NiW alloy coating deposited at  $1.0 \text{ Adm}^{-2}$ , represented as  $(\text{NiW})_{1 \text{ Adm}^{-2}}$  is of highest corrosion resistance. Here, it may be recalled that from the principle of multilayer coating that properties of any multilayer coatings largely depends on the composition and thickness of individual layers. In other words, it is important to have clear demarcation between the compositions of individual layers. The clear demarcation between alternate layers is possible only by proper gradation of layers, by selection of proper cyclic current densities (to get layers of different compositions). In this regard, optimization of alternate layers of alloys (in terms of composition) are carried out using different set of CCCD's, and experimental results are shown below.

#### 5.3.1 Optimization of CCCD's

The preliminary work on electrodeposition and characterisation of NiW alloy coating showed that the proposed bath could able to develop coatings of different composition, morphology and phase structure, as reported in Table 4.4. The composition of NiW alloy vary from 18.9 wt. % to 9.9 wt. % of W over current density from 1.0 - 4.0  $\text{Adm}^{-2}$ . To enhance the anticorrosion performance of monolayer NiW alloy coatings by multilayer approach, multilayer NiW alloy coatings were deposited at different sets of CCCD's. To optimize CCCD's for development of the most corrosion resistant NiW alloy coatings, to begin with they are developed at three different sets of CCCD's by keeping 10 layers (chosen arbitrarily), and their corrosion performances were evaluated by both EIS and potentiodynamic polarization techniques. The corresponding Nyquist and Tafel plots of NiW alloy coatings having 10 layers, with different set of CCD's are shown in Figure 5.2 and Figure 5.3, respectively. The consequent corrosion data are shown in the Table 5.1. This procedure of coating at three different sets of CCCD's gives a provision to optimize the composition of individual layers, for best configuration of multilayer coatings to show the highest corrosion resistance.

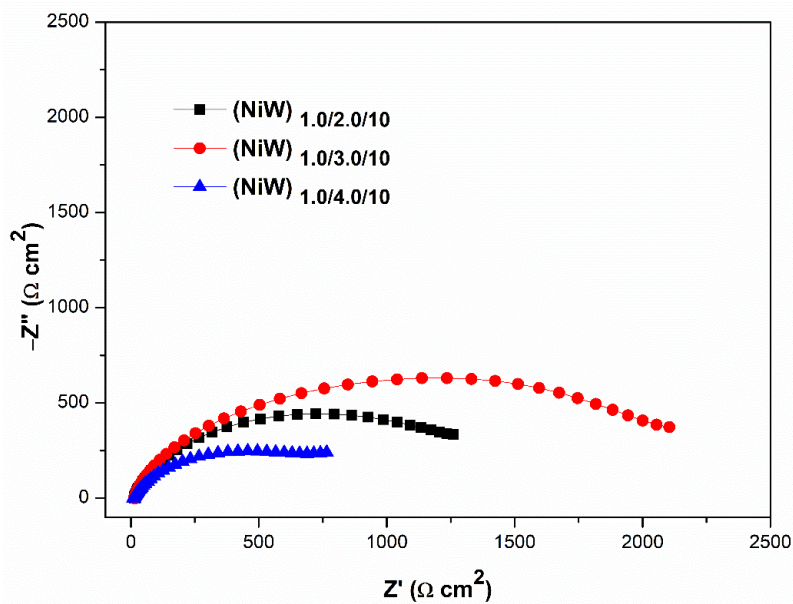


**Figure 5.2-** Nyquist plots of multilayer NiW alloy coatings having 10 layers of alternatively different composition deposited at different set of CCCD's.

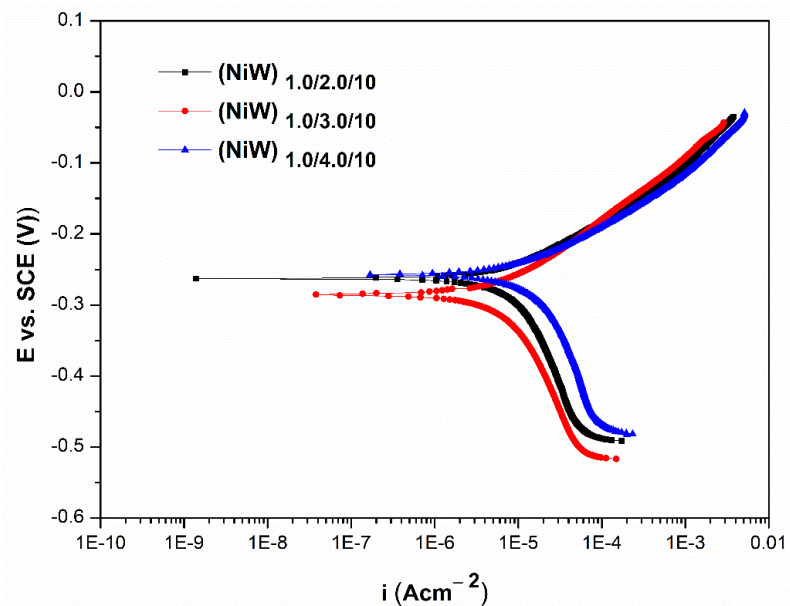


**Figure 5.3 -** Tafel's plots of multilayer NiW alloy coatings having 10 layers of alternatively different composition deposited at different set of CCCD's.



**Table 5.1 - Corrosion parameters of multilayer NiW alloy coatings having 10 layers of alternatively different composition deposited at different set of CCCD's**

Coating configuration	wt. % of Ni	wt.% of W	$-E_{\text{corr}}$ (V vs SCE)	$i_{\text{corr}}$ ( $\mu\text{A cm}^{-2}$ )	$\text{CR} \times 10^{-2}$ ( $\text{mm y}^{-1}$ )	$R_{\text{P}}$ ( $\Omega$ )
(NiW) <sub>1.0/2.0/10</sub>	83.3	16.7	0.262	8.52	8.42	2088
(NiW) <sub>1.0/3.0/10</sub>	83.8	16.2	0.285	4.51	4.44	2423
(NiW) <sub>1.0/4.0/10</sub>	85.6	14.4	0.257	14.56	14.63	1874
(NiW) <sub>1.0 Adm<sup>-2</sup></sub>	81.1	18.9	0.311	15.25	14.89	1845

The corrosion data reported in Table 5.1 indicates that all multilayer NiW alloy coatings show least CR compare to its monolayer counterpart, deposited from same bath. Further, among three sets of CCCD's tried, the least CR was observed in one set CCCD's, corresponding to 1.0 and 3.0 Adm<sup>-2</sup>, as cyclic current pulses. The least CR of (NiW)<sub>1.0/3.0/10</sub> configuration indicates that its layers are of most optimal composition for better corrosion resistance. At the same time, coating having (NiW)<sub>1.0/4.0/10</sub> configuration shows almost same CR as that of its monolayer alloy coating (Table 5.1). This indicates that these CCCD's are not suitable for further layering to bring proper modulation in composition. Therefore, 1.0 Adm<sup>-2</sup> and 3.0 Adm<sup>-2</sup> have been selected as optimal CCCD's for further layering.

### 5.3.2 Optimization of number of layers

It is well known fact that many properties, including corrosion properties of alloy coatings can be improved by increasing interfacial structures through multilayer technique. Hence, to take the benefit of multilayer coating to the fullest of its possibility, multilayer NiW alloy coatings are electrodeposited with increased number of layers. By considering 1.0 Adm<sup>-2</sup> and 3.0 Adm<sup>-2</sup> as optimal CCCD's for the optimized bath, multilayer NiW alloy coatings are developed with different degree of layering. In other words, multilayer NiW alloy coating were developed by periodic pulsing of the current between 1.0 Adm<sup>-2</sup> and 3.0 Adm<sup>-2</sup> to form coating of desired number of layers. Accordingly, multilayer NiW alloy coating having 10, 30, 60, 120 and 300 layers were developed using the same bath, and their corrosion behaviours were evaluated. Here,

these number of layers were conveniently chosen, to examine the effect of layering on its corrosion protection efficacy, within the limitation of power source used in this study.

### 5.3.3 Corrosion study

EIS and potentiodynamic polarization methods were used to study the corrosion behaviour of multilayer NiW alloy coatings of different configurations, and their experimental results are reported below.

#### 5.3.3.1 EIS study

Electrochemical impedance spectroscopy (EIS) technique is a very powerful technique to determine the electrical properties of materials, and to understand the mechanism involved in the kinetics of charge transfer process at electrode-electrolyte interface (MacDonald 1987). In a typical Nyquist plot, the complex electrical impedance ( $Z$ ) of a sample is measured as a function of frequency over a wide frequency range, typically several orders of magnitude. *i.e.*, in range of mHz to MHz (Shoar Abouzari et al. 2009). Accordingly, Nyquist plots of multilayer NiW alloy coatings having different number of layers have been studied, and are shown in Figure 5.4.

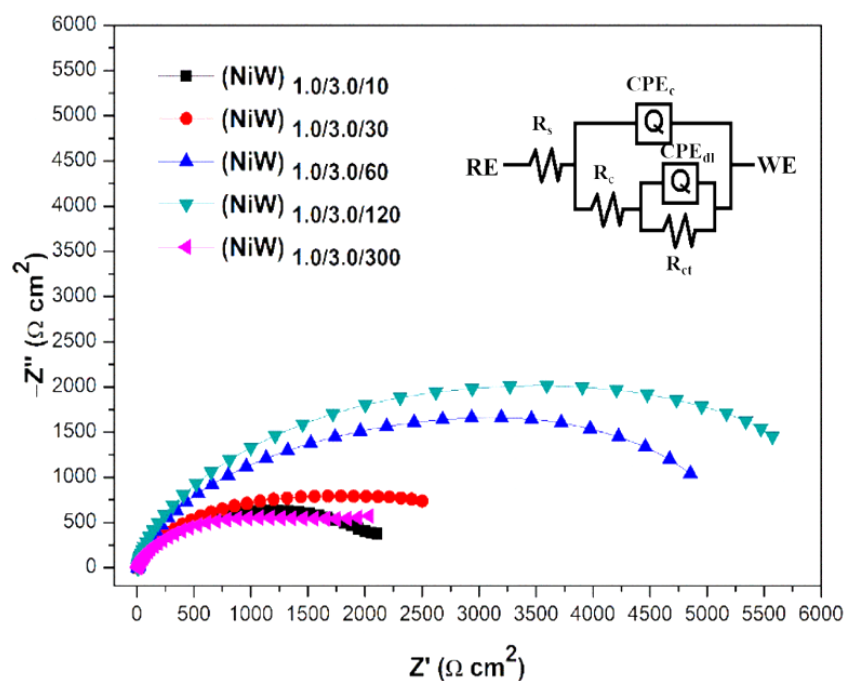


**Figure 5.4** - Nyquist plots of multilayer (NiW)<sub>1.0/3.0</sub> alloy coating having different number of layers deposited from the optimized bath.

Electrochemical impedance response clearly shows that the value of polarization resistance ( $R_p$ ) increased progressively with number of layers up to 120 layers, and then decreased. The decreased diameter of capacitive loop corresponding to  $(\text{NiW})_{1.0/3.0/300}$  clearly indicates that corrosion protection of multilayered NiW alloy coating decreases at higher degree of layering.

### 5.3.3.2 Potentiodynamic polarization study

Potentiodynamic polarization behaviour of multilayer NiW alloy coatings, having different number of layers were studied, and are shown in Figure 5.5. Corrosion rates were calculated by Tafel's extrapolation method. The corrosion data of multilayer NiW alloy coatings, having different configurations, i.e., different number of layers are reported in Table 5.5, with their corrosion rate (CR) values. The corrosion rate of monolayer NiW alloy coating, abbreviated as  $(\text{NiW})_{1.0 \text{ Adm}^{-2}}$  developed by conventional method is also given for comparison purpose.

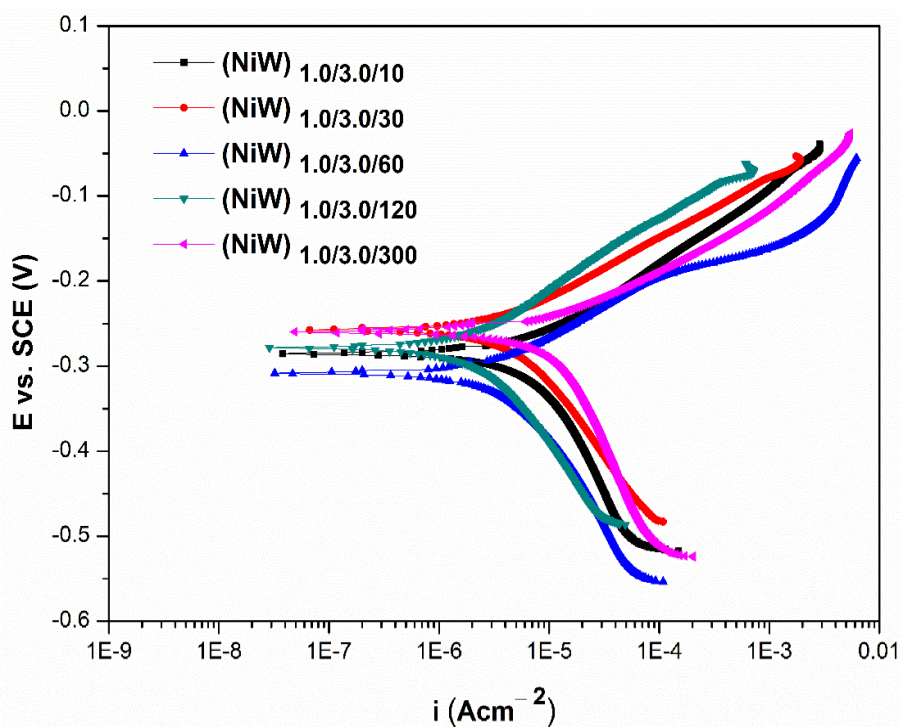


**Figure 5.5-** Tafel's plots of multilayer  $(\text{NiW})_{1.0/3.0}$  alloy coating having different number of layers (from 10 to 300 layers), deposited from optimized bath.

The corrosion data, evaluated through Tafel's extrapolation method are reported in Table 5.2. It verifies that the anticorrosion performance of multilayer NiW alloy coating increased with number of layers up to 120 layers, and then started decreasing. The least CR corresponding to (NiW)<sub>1.0/3.0/120</sub> configuration indicates that it is the optimal configuration of the coating for best performance against corrosion. The total thickness of multilayer (NiW)<sub>1.0/3.0/120</sub> alloy coating is found to be about 6 μm, as measured from thickness tester, and later verified from Faraday law. Hence, it may be estimated that the average thickness of individual layers is in range of 50 nm. Therefore, it may confirmed that best anticorrosion performance of multilayer NiW alloy coating is possible due to alternate layers of alloys of different composition, in nano-meter thickness.

**Table 5.2: Corrosion data of multilayer NiW alloy coatings having different number of layers deposited from the optimized bath.**

Coating configuration	$-E_{\text{corr}}$ (V vs. SCE)	$i_{\text{corr}}$ ( $\mu\text{A cm}^{-2}$ )	$\text{CR} \times 10^{-2}$ ( $\text{mm y}^{-1}$ )	$R_{\text{P}}$ ( $\Omega$ )
(NiW) <sub>1.0/3.0/10</sub>	0.285	4.51	4.48	2423
(NiW) <sub>1.0/3.0/30</sub>	0.257	3.80	3.77	3360
(NiW) <sub>1.0/3.0/60</sub>	0.308	2.53	2.88	5496
<b>(NiW)<sub>1.0/3.0/120</sub></b>	<b>0.278</b>	<b>2.46</b>	<b>2.44</b>	<b>6070</b>
(NiW) <sub>1.0/3.0/300</sub>	0.260	4.94	4.91	2042
<b>(NiW)<sub>1.0 Adm</sub><sup>-2</sup></b>	<b>0.311</b>	<b>15.25</b>	<b>14.89</b>	<b>1845</b>

Further, it may be noted that CR of multilayer coatings having 300 layers, *i.e.*, coating having (NiW)<sub>1.0/3.0/300</sub> configuration has decreased compared to that having 120 layers. This decrease of CR at higher degree of layering, *i.e.*, at 300 layers may be attributed to very short pulsing period (2 s), where modulation of composition is not likely to happen. This increase of CR at high degree of layering may be explained in the light of reported work (Yogesha and Hegde 2011). According to this, as a larger numbers of layers are allowed to form in same time duration, the time for the deposition

of each layer, for example,  $(\text{NiW})_{1.0/3.0}$  is small (as total time for deposition remains same, 600 s). Owing to short pulse duration (2 s), there is no sufficient time for metal ions ( $\text{Ni}^{+2}$  and  $\text{WO}_4^{-2}$ ) to relax (against diffusion under applied c.d.) and to deposit on the cathode by forming a distinct interface. Consequently, multilayer coating tend to become a monolayer; and shows same anticorrosion performance as monolayer one. The development of monolayer (homogeneous) alloy coating at higher degree of layering, due to rapid change of current pulse (small pulse duration) is shown diagrammatically in Figure 5.1c. It may be seen that when power source is made to pulse very rapidly, the alloy coating takes place homogeneously with no demarcation between layers, for the reason as explained earlier.

It is important to note that against to our earlier reports (Thangaraj et al. 2009; Ullal and Hegde 2014), in present tartrate bath optimal number of layers for best performance of NiW alloy coating is only 120 layers. This early attainment of homogeneity of the multilayer coating is due to the inherent limitation of the induced type of codeposition, prevailing in the bath. This is originated by the use of complexing agent ( $\text{KNaC}_4\text{H}_4\text{O}_6 \cdot 4\text{H}_2\text{O}$ ) in the bath, which enabled the codeposition of Ni and W. The complexing agent does form a complex with the ions of the electrolyte, and accordingly bring the electrode potential value of Ni and W more closely. In other words, complexing agent approximates (getting closer) electrode potentials of the different metals by converting the simple ions of more noble metal into complex ions with lower potential; and thereby prevents the immersion deposition and improve the nature of deposit (Brenner 1963). Therefore, due to narrow potential window of deposition potentials of individual metals, affected due to complexing agent, range of composition modulation by pulsing the c.d. is very small. This is supported by narrow compositional change of monolayer NiW alloy coatings with c.d. as reported in Table 4.4.

Hence, it may be summarised that anticorrosion performance of multilayer alloy coating increased with number of layers. However, and on extreme thinning of layers (by increasing the number of layers) anticorrosion performance decreased, due to diffusion of layers. The optimal number of layers for the best anticorrosion performance is a function of bath composition, depending on the kind chemistry involved in it.

### 5.3.4 Comparison of corrosion response of monolayer and multilayer NiW alloy coating

The anticorrosion behavior of monolayer (NiW) and multilayer (NiW) alloy coatings (deposited under optimal conditions) are compared with that of uncoated copper (substrate), through Impedance responses and Tafel's plots, and are shown in Figure 5.6. It may be noted from both Tafel and impedance behaviors, that (NiW)<sub>1.0</sub> alloy coating (monolayer) is more corrosion resistant than the substrate, whereas (NiW)<sub>1.0/3.0/120</sub> alloy coating (multilayer) is still more corrosion resistant compared to its monolayer counterpart. It is confirmed by change of their charge transfer resistance ( $R_{ct}$ ) values in case of impedance plot, and  $i_{corr}$  values and  $E_{corr}$  values (in Tafel's plot), as may be seen in Figure 5.6.

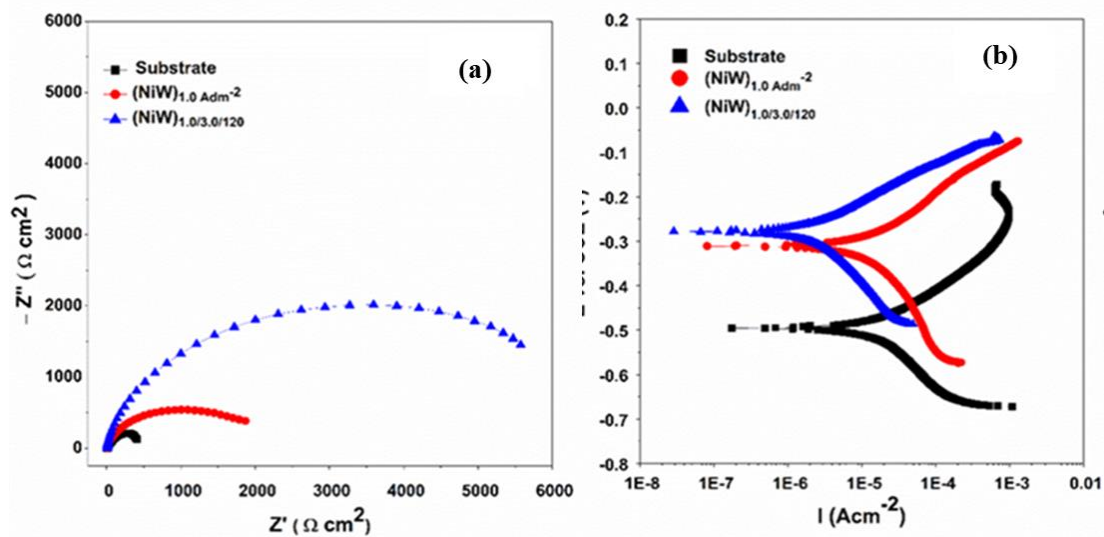


**Figure 5.6-** Comparison of corrosion behaviour of monolayer and multilayer NiW alloy coatings (both optimal) with that of substrate through: a) Nyquist plots, and b) Tafel's plots.

The Nyquist plots shown in Figure 5.6 (a) testimonies that (NiW)<sub>1.0/3.0/120</sub> alloy coating has far more better corrosion stability compare to both substrate and monolayer (NiW)<sub>1.0</sub> alloy coating. The actual CR's corresponding to substrate, monolayer (NiW)<sub>1.0</sub> and multilayer (NiW)<sub>1.0/3.0/120</sub> alloy coating, under optimal conditions are given in Table 5.2. Thus, it may be concluded that under optimal conditions, multilayer NiW alloy coating is roughly six times more corrosion resistant than its monolayer counterpart, deposited from same bath for same duration.

### 5.3.5 SEM study after corrosion

To confirm the development of coating in layered fashion, and to examine the reason responsible for better anticorrosion performance of multilayer coatings, electrodeposited coatings, after corrosion test were subjected to SEM study. The coatings having  $(\text{NiW})_{1.0}$  and  $(\text{NiW})_{1.0/3.0/120}$  configuration were made to corrode by subjecting it to the anodic polarization at + 250mV vs. OCP in 3.5% NaCl solution. The corroded specimen was washed with distilled water, then examined under SEM. The surface morphology of monolayer  $(\text{NiW})_{1.0}$  and multilayer  $(\text{NiW})_{1.0/3.0/120}$  alloy coatings, after corrosion test are shown in Figure 5.7.

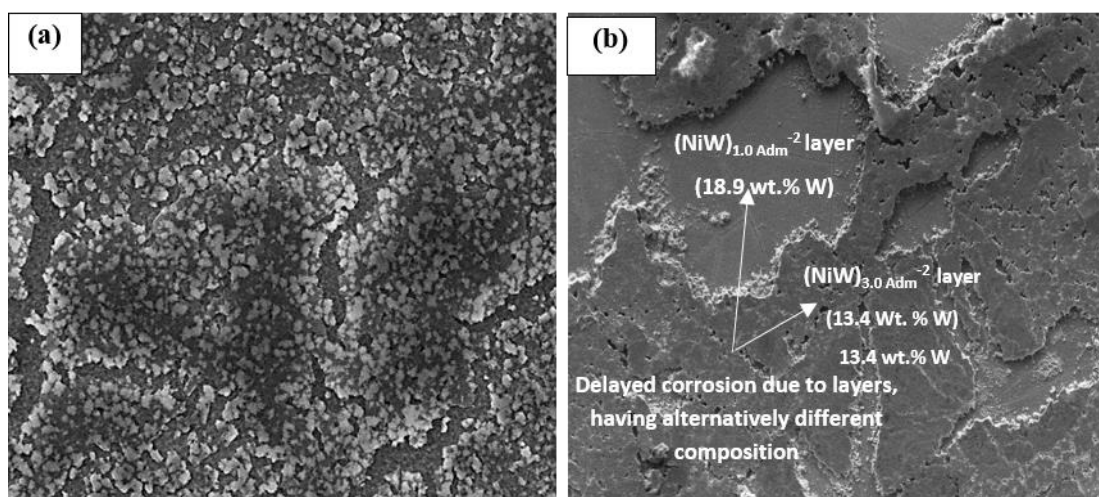


**Figure 5.7-** SEM image of electroplated NiW coatings after corrosion test displaying: a) uniform dissolution in case of monolayer alloy coating, and b) selective dissolution of alternate layers in case of multilayer coating.

It may be seen that in case monolayer  $(\text{NiW})_{1.0}$  alloy coating, corrosion has taken place uniformly, with no discrimination as shown in Figure 5.7 (a). But in case of multilayer  $(\text{NiW})_{1.0/3.0/120}$  corrosion has taken place non-uniformly, where electrolyte attacked the coating layer by layer as shown in Figure 5.7 (b). The possibility of better anticorrosion performance of multilayer coating is due to alternate layers of alloys having composition corresponding to  $(\text{NiW})_{1.0}$  and  $(\text{NiW})_{3.0}$  coatings. It may be seen that top ending layer corresponding to  $(\text{NiW})_{3.0}$ , having 13.4 wt.% W gets corroded easily, but it is retarded in next layer corresponding to  $(\text{NiW})_{1.0}$ , having 18.9 wt.% W. Thus a small change in wt. % W content in alternate layers of alloy is responsible for delayed corrosion of multilayer NiW alloy coatings. As a whole, the protection efficacy

of multilayer  $(\text{NiW})_{1.0/3.0/120}$  coatings is due to the barrier effect of layer having high wt. % W (18.9%) and sacrificial effect of layer having low wt. % W (13.4 %).

It is well known that successful synthesis of multilayer coatings lies in development of coatings having clear demarcation between layers, in terms of their surface morphology, composition and phase structure (Dobrzański and Lukaszewicz 2007). In this regard, Figure 5.8 depicts a model multilayer coating, having four layers of alloys in which two layers of same compositions are layered alternatively.

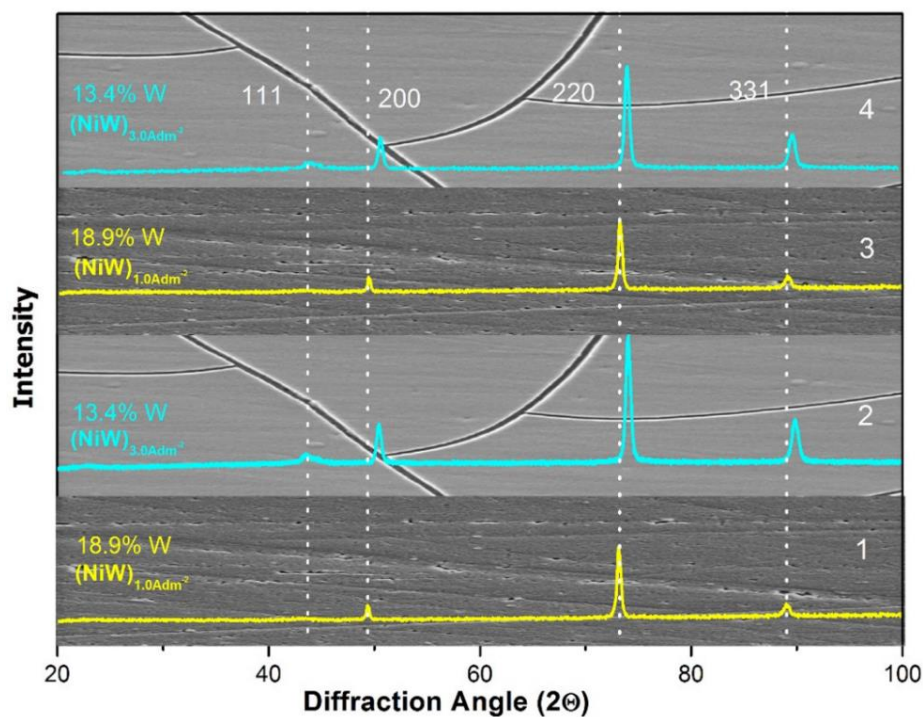


**Figure 5.8-** A model multilayer diagram showing two alternate layers of  $(\text{NiW})_{1.0}$  and  $(\text{NiW})_{3.0}$  alloys, with their surface morphology, composition and XRD peaks (overlaid).

Referring to present study, it may be seen that layers labelled as 1, 3 are corresponding to monolayer  $(\text{NiW})_{1.0}$ , having same composition and phase structure; and layers labelled as 2, 4 are corresponding to monolayer  $(\text{NiW})_{3.0}$ , having same composition and phase structure. Here, surface morphology, composition and position of XRD peaks of two consecutive layers are different as may be seen in Figure 5.8, which is responsible for development of phase boundary between layers. Hence, it is important to note that discrete phase boundary between layers (1, 2, 3 and 4), affected due to pulsing of current during deposition is responsible for improved anticorrosion



property of multilayer coatings. Thus, it may be concluded that compositional modulation between consecutive layers is the pre-requisite for delayed corrosion of multilayer coatings.

### **5.3.6 Mechanism of corrosion in multilayer coatings**

Thus the better anticorrosion performance of multilayer NiW alloy coatings in relation to its monolayer alloy coating was attributed to the selective dissolution of layers of different compositions, as envisaged by (Ganesan et al. 2007; Yogesha and Hegde 2011). The mechanism of corrosion protection in case of multilayer coating (under condition of optimal and extreme layering), in relation to monolayer alloy coating can be explained through a pictorial representation as shown in Figure 5.9. Electrodeposited NiW alloy coating are considered to have different degree of homogeneity depending on the type of current pulses used. In case of monolayer NiW alloy coating, represented as  $(\text{NiW})_{1.0}$  the coating being homogeneous or non-nanostructured, corrosion occurs unabatedly and electrolyte (corrosion medium) reaches the substrate very quickly, as shown in Figure 5.9(a). But in case of multilayer coating developed under optimal condition, represented as  $(\text{NiW})_{1.0/3.0/120}$ , owing to the presence of well-defined phase boundaries between layers, the electrolyte spreads both laterally and vertically, as shown in Figure 5.9(b). Due to multilayer structure, the lower layer will come in contact with the electrolyte only after the destruction of top layers as may be seen in Figure 5.9(b), and the corrosion spreads over the interface latterly, and process continues layer after layer. Consequently, substrate will get exposed to the corrosion medium only after the destruction of all top layers, and hence the corrosion occur slowly compared to monolayer coating. The increase in anticorrosion performance of multilayer coating with number of layers, of course up to certain numbers is due to increase in the number of interfaces formed due to layering.

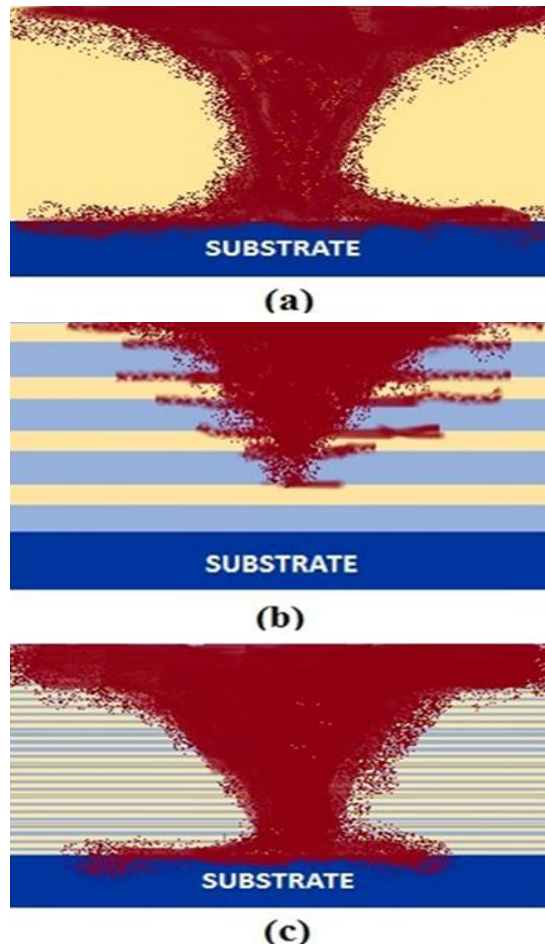


**Figure 5.9-** Representative diagram showing the mechanism of corrosion in NiW alloy coatings, deposited under different conditions: a) direct attack of the substrate in monolayer coating, b) delayed corrosion due to layered (optimal) structure of coating and c) direct attack due to diffusion of layers, affected by extreme layering.

Thus it may be concluded from the Figure 5.9 (b) that the time required for the electrolyte to reach the substrate by penetrating through the multilayer coating is much greater than that through the monolayer coating. However, multilayer coating electrodeposited under condition of rapid pulsing of DC, the layers are so thin that diffusion of multilayer layers taking place as shown in Figure 5.9(c), this situation make the multilayer coating to turn into monolayer one, with no better corrosion protection value than that of monolayer. This is supported by observed high CR value of multilayer NiW alloy coating having configuration,  $(\text{NiW})_{1.0/3.0/300}$ .

## 5.4 CONCLUSIONS

*In the pursuit of improving the anticorrosion behaviour of monolayer NiW alloy coatings, developed from newly formulated NiW alloy bath through multilayer approach using square current pulses, following conclusions are arrived.*

1. Multilayer NiW alloy coatings have been developed from a single bath by periodic modulation of current density, during process of deposition. The composition and thickness of alternate layers have been optimized by proper modulation of current densities (pulse amplitude) and duration of pulse (time), respectively.
2. The improved corrosion performance of multilayer alloy coatings are attributed to the increased number of interfaces, affected due to formation of layers of alloys having low and high W content, due to change of current density during deposition.
3. Under optimal condition, multilayer NiW alloy coating, having (NiW)<sub>1.0/3.0/120</sub> configuration is approximately six times more corrosion resistant than its monolayer coating, deposited from the same bath for same duration.
4. The corrosion stability of multilayer NiW alloy coatings were found to be increased with degree of layering only up to certain extent, and then started decreasing.
5. Increase of CR of multilayer NiW coating at higher degree of layering (at 300 layers) is attributed to the diffusion of layers, as their no significant compositional change of individual layers are likely to happen due to rapid change of current density.
6. SEM study of corroded surface of monolayer and multilayer NiW alloy coating demonstrated that the better corrosion performance of multilayer coating is due to selective dissolution of alternate layers of alloys, having low and high W content.



## **CHAPTER 6**

# **DEVELOPMENT OF NiW ALLOY COATINGS AND THEIR ELECTROCATALYTIC ACTIVITY FOR WATER SPLITTING REACTION**



## CHAPTER 6

### DEVELOPMENT OF NiW ALLOY COATINGS AND THEIR ELECTROCATALYTIC ACTIVITY FOR WATER SPLITTING REACTION

---

*This chapter reports the electrocatalytic activity of NiW alloy coatings (monolayer) deposited from the newly optimized bath towards alkaline water electrolysis. Electrodeposited NiW alloy coatings were used as electrode material for hydrogen evolution reaction (HER) and oxygen evolution reaction (OER) of water splitting applications in 1 M KOH. Cyclic voltammetry (CV) and chronopotentiometry (CP) techniques were used to quantify their electrocatalytic activities. Experimental results demonstrated the inverse dependency of electrocatalytic behavior of alloy coatings towards HER and OER, depending on their composition. The surface features, structural and compositional change of coatings, responsible for improved electrocatalytic activity were examined using Scanning electron microscopy (SEM), X-ray diffraction (XRD) and Energy dispersive X-ray spectroscopy (EDS) techniques. Experiment results revealed that NiW alloy deposit can be used as a potential candidate for water splitting applications.*

#### 6.1 INTRODUCTION

Electrocatalytic water splitting is considered to be a promising method for generation of clean hydrogen. In order to realize this goal, a more effective catalysts for hydrogen evolution reaction (HER) and oxygen evolution reaction (OER) are required. In this regard, many researchers are engaged in developing efficient materials for conversion of water, nitrogen and carbon dioxide into high energy carriers such as hydrogen (H<sub>2</sub>), oxygen (O<sub>2</sub>), ammonia, hydrocarbon etc. (Tahir et al. 2017). Among these, electrocatalytic water splitting reaction is of high concern due to its low cost, less pollution and high efficiency (Wang et al. 2019). Though noble metal based electrocatalysts were used for water splitting reaction so far, its prohibitive cost and less availability restricted its thorough use in most of the applications. Today scientific community is looking forward for production electrode materials, at low cost and high

abundance, and showing high efficiency for water splitting reactions, as electrocatalyst (Pu et al. 2016). In this direction, binary and ternary alloys of Ni, iron (Fe), cobalt (Co) with metals, like tungsten (W), molybdenum (Mo), lanthanum (La) etc. have been tried as electrocatalysts for water splitting applications, *i.e.*, either for HER or OER, or for both (González-buch et al. 2013; Safizadeh et al. 2015). Experimental results demonstrated that these alloys are good class of electrocatalytically active materials due to both good corrosion resistance and electronic configuration of individual metals (Elias et al. 2015). Keeping above points in view, the electrocatalytic efficacy of NiW alloy coatings, electroplated on copper substrate using newly optimized bath (Table 4.1), under different conditions of current densities have been studied. The electrocatalytic activity of alloy coatings, using them as cathode for hydrogen evolution reaction (HER); and as anode for oxygen evolution reaction (OER) for alkaline water splitting applications have been studied, using cyclic voltammetry (CV) and chronopotentiometry (CP) techniques. Quantification of their electrocatalytic activities were made by knowing the amount of H<sub>2</sub> and O<sub>2</sub> liberated, using a specially designed water electrolyser. The experimental studies have been carried out for optimization of deposition conditions for development of best electrode material of NiW alloy coatings, as cathode and anode for water electrolysis, and results are discussed.

## **6.2 EXPERIMENTAL**

### **6.2.1 Electrodeposition of NiW alloy coatings**

The electrolytic bath having nickel sulphate hexahydrate (NiSO<sub>4</sub> · 6H<sub>2</sub>O), sodium tungstate dihydrate (Na<sub>2</sub>WO<sub>4</sub> · 2H<sub>2</sub>O), potassium sodium tartrate tetrahydrate (KNaC<sub>4</sub>H<sub>4</sub>O<sub>6</sub> · 4H<sub>2</sub>O), ammonium chloride (NH<sub>4</sub>Cl) and glycine (NH<sub>2</sub>-CH<sub>2</sub>-COOH) is used for deposition NiW alloy coating. The bath was prepared in distilled water, using laboratory reagent (LR) grade chemicals. The bath conditions and operating parameters were arrived by standard Hull cell method. The bath composition and operating parameters of the optimized bath used in the present study is given in Table 4.1. The NiW alloy coatings were developed at different cathode current densities, like from 1.0 to 4.0 Adm<sup>-2</sup>, using specially made glass vessel, shown in Figure 3.7. Here, for electrocatalytic study electrodeposition of NiW alloy coating is carried out on the cross-sectional area of mirror finished copper rod, having exposed surface area of 1cm<sup>2</sup> as



cathode; and graphite sheet as anode. DC Power Analyzer (Agilent Technologies, N6705C, USA) was used as power source for deposition. All coatings were carried out for same duration (600 s), keeping temperature and pH constant for comparison purpose. The pH of the bath was adjusted to 8.5 using pH meter (Systronics-362), by addition of either sulphuric acid ( $H_2SO_4$ ) or ammonium hydroxide ( $NH_4OH$ ) solution. NiW alloy coatings were deposited at different current densities and their electro-catalytic behaviours towards alkaline water splitting (for both HER and OER) were studied in 1M KOH, using a custom-made tubular glass set up having three electrodes, shown in Figure 3.8. The conventional cyclic voltammetry (CV) techniques was employed to study the electrocatalytic activity of alloy coatings, using computer controlled potentiostat, VersaSTAT 3-400 (Princeton Applied Research, USA). The electrocatalytic stability of NiW alloy coatings was tested by chronopotentiometry (CP) method by monitoring the electrode reaction for 1800 s. The efficiency of electrode reactions for both hydrogen evolution reaction (HER) and oxygen evolution reaction (OER) of water splitting reactions were evaluated quantitatively by measuring the volume of  $H_2$  and  $O_2$  evolved on  $1\text{ cm}^2$  surface area of the test electrode for 300 s.

## 6.3 RESULTS AND DISCUSSION

### 6.3.1 Surface morphology and XRD study

The surface feature of NiW alloy coatings corresponding to different current densities was examined using SEM, through secondary electron images. The micro cracks, characteristic of NiW alloy coatings were found on the surface, as shown in the Figure 6.1. It may be seen that the extent of cracks/porosity has increased with deposition current density, which likely to be responsible for their enhanced catalytic property due to increased effective surface area. By principle, the electro-catalytic activity of alloy coatings are generally based on their composition. *i.e.*, it depends on the wt. % of constituting metals. Hence, the composition of NiW alloy coatings deposited from optimized bath at different current densities are reported in Table 6.1, determined by energy dispersion spectroscopy (EDS) analyses. The XRD peaks are the characteristics of the material, and speaks about its crystallinity and phase structure. Accordingly, XRD study of NiW alloy coatings corresponding to different deposition conditions are made, and is shown in Figure 6.1. From the literature, it is known that electrochemically

deposited NiW alloy, having less than 20 wt.% W forms a single phase solid solution of W in Ni (Obradović et al. 2001). Thus from the nature of XRD patterns, it may be inferred that electrodeposited NiW alloy coatings, developed at all current densities (from 1.0 to 4.0  $\text{Adm}^{-2}$ ) are found to be the solid solution of W in Ni. Therefore, XRD patterns of all NiW alloy coatings looks similar, irrespective of the current density at which they are deposited.

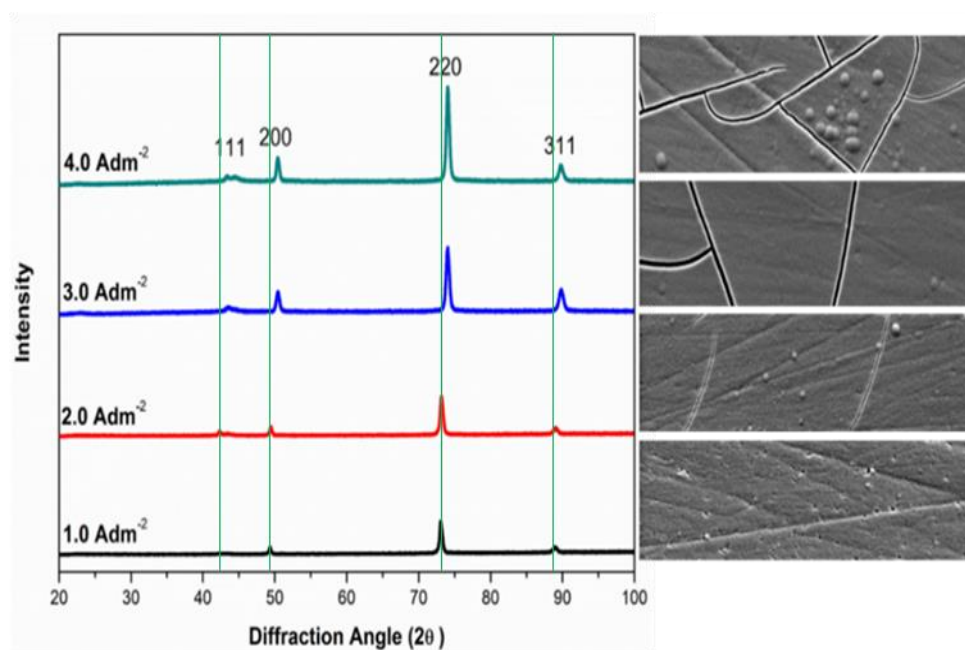


**Figure 6.1-** X-ray diffraction peaks and the corresponding SEM images of NiW alloy coatings deposited at different current densities. A slight shift of diffraction lines to right with increase of current density may be observed.

A slight shift of diffraction line positions to the right was observed with increase of current density. It may be explained from the composition data of alloy coatings (Table 6.1) as below. As the wt. % Ni the deposit increased with current density, it is accompanied by a decrease in cell volume, as Ni atom is smaller than W atom, which leads to bring change in strain inside the lattice structure (Cullity 1956). In continuous solid solutions of NiW alloy, since the lattice parameter of the solution is directly proportional to the atomic percent of solute present, the diffraction peaks were found to be shifted to the right, in proportion of the increase of Ni in the deposit. Thus XRD peaks are shifted more and more towards right (higher  $2\theta$  side) as Ni content of the deposit increased with current density. *i.e.*, peaks are moving away from the vertical

lines. The observed shift of diffraction lines to the right, without any change of phase structure with increase of current density is due to change of alloy composition.

A significant change in the surface of alloy coatings due to change of deposition current density is further confirmed by AFM analyses. The three dimensional AFM image of (NiW) alloy coatings, deposited at extreme two situations of current density (in the present study), *i.e.*, coatings corresponding to  $(\text{NiW})_{1.0 \text{ Adm}^{-2}}$  and  $(\text{NiW})_{4.0 \text{ Adm}^{-2}}$  are shown in Figures 6.2 (a) and 6.2 (b), respectively. The experimental data revealed that there is a decrease of surface roughness with increase of deposition current density, evident from the observed average roughness values of  $(\text{NiW})_{1.0 \text{ Adm}^{-2}}$  and  $(\text{NiW})_{4.0 \text{ Adm}^{-2}}$  coatings as 10.0 nm and 3.7 nm, respectively.

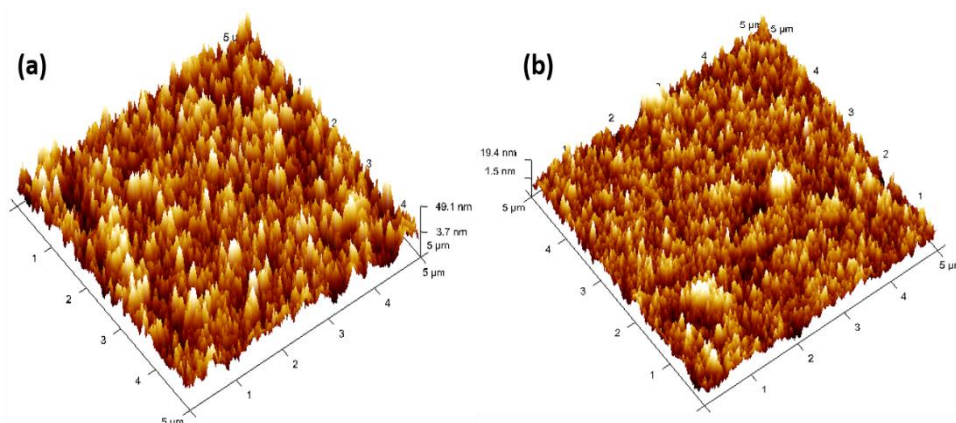


**Figure 6.2-** AFM image of NiW alloy coating deposited at different current densities: (a)  $(\text{NiW})_{1.0 \text{ Adm}^{-2}}$ , and (b)  $(\text{NiW})_{4.0 \text{ Adm}^{-2}}$ . A change of surface homogeneity with change of current density may be seen.

### 6.3.2 Electrocatalytic activity of NiW alloy coatings

The electrocatalytic activity of NiW alloy coatings, deposited at different current densities have been studied using them as electrodes, both cathode and anode for hydrogen evolution reaction (HER) and oxygen evolution reaction (OER), respectively in alkaline water electrolysis (1.0 M KOH).

#### 6.3.2.1 Cyclic voltammetry study

Cyclic voltammetry (CV) technique provides useful information with regard to electron transfer-initiated chemical reactions and redox activity of working electrode, which includes electro catalysis (Mizushima et al. 2005). In this regard, CV study of NiW alloy

coatings deposited at  $1.0 \text{ Adm}^{-2}$  -  $4.0 \text{ Adm}^{-2}$  were done for both HER and OER in a potential range of 0 V to -1.6 V and 0 V to 0.75 V, respectively at a scan rate of  $0.05 \text{ Vs}^{-1}$ . The resulted cyclic voltammogram are shown in Figure 6.3, and corresponding electro-catalytic data are reported in Table 6.1.

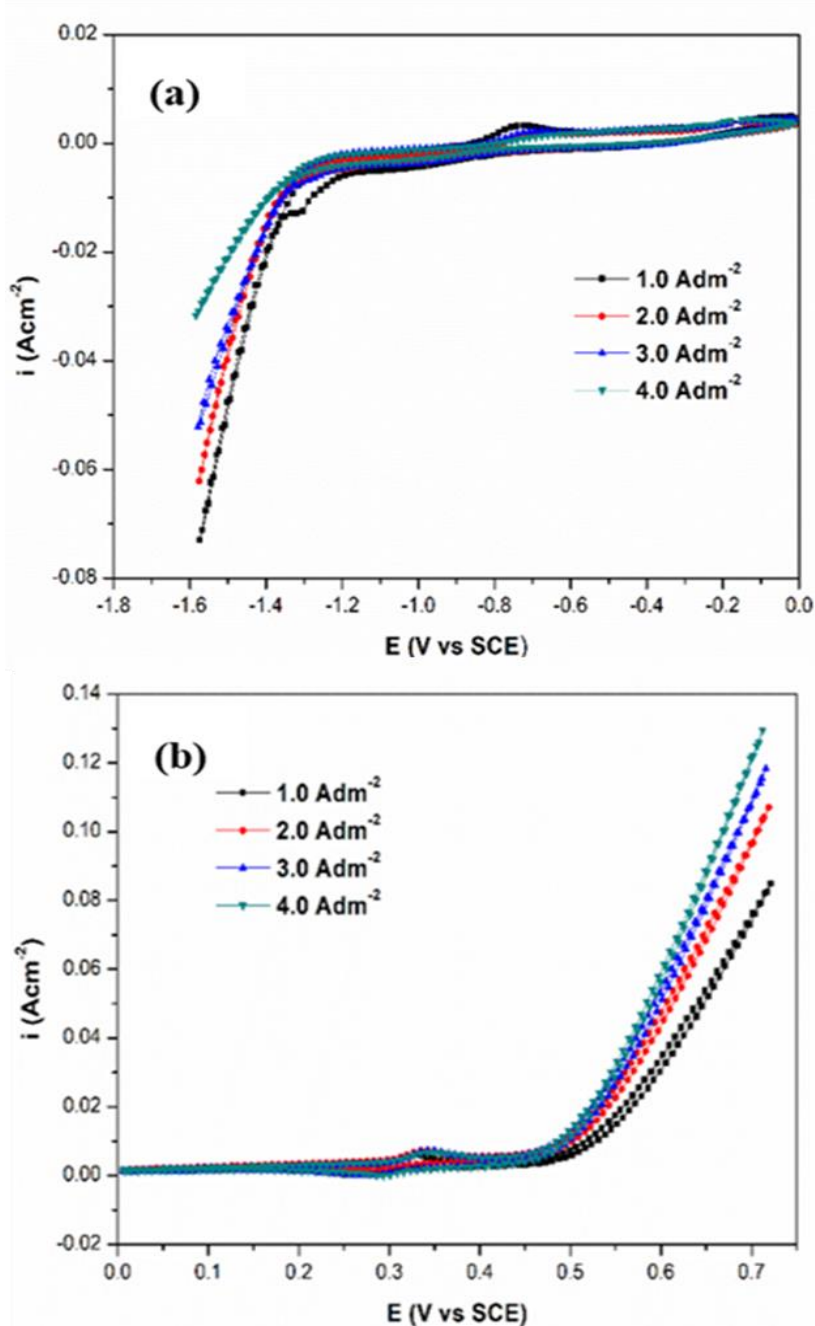


**Figure 6.3-** CV study of NiW alloy coatings corresponding to different c.d.'s showing their electro catalytic response when used as: a) cathode for HER, and b) anode for OER.

The CV plot shown in Figure 6.3(a) clearly shows that onset potential for HER increased as the deposition current density increased. It may be seen that NiW coating deposited at 1.0  $\text{Adm}^{-2}$  (having 81.1 wt. % Ni and 18.9 wt.% W) shows the least onset potential with the highest cathodic peak current density ( $i_{pc}$ ) for HER. It may further be noted that the value of  $i_{pc}$  reaches its minimum value when deposition current density is increased to 4.0  $\text{Adm}^{-2}$ , with decreased wt. % of W in the deposit as shown in Table 6.1.

**Table 6.1- Electro-catalytic kinetic parameters of NiW alloy coatings for HER and OER during alkaline water electrolysis, with metal contents in the deposit**

Deposition c.d. ( $\text{Adm}^{-2}$ )	Wt. % of Ni in the deposit	Wt. % of W in the deposit	HER		OER	
			Cathodic peak c.d. ( $i_{pc}$ ) ( $\text{Acm}^{-2}$ )	Onset potential (V vs. SCE)	Anodic peak c.d. ( $i_{pa}$ ) ( $\text{Acm}^{-2}$ )	Onset potential (V vs. SCE)
1.0	81.1	18.9	-0.074	-1.20	0.084	0.513
2.0	85.6	14.4	-0.063	-1.25	0.107	0.494
3.0	86.6	13.4	-0.052	-1.29	0.118	0.480
4.0	90.1	9.9	-0.032	-1.33	0.130	0.470

Thus, highest value of  $i_{pc}$  of NiW alloy corresponding to 1.0  $\text{Adm}^{-2}$  may be attributed to its highest W content. Thus NiW alloy having high W content is likely to favour the HER on its surface, and is due to less hydrogen over voltage of W (Elgrishi et al. 2018). On the other hand, same NiW alloy coatings (deposited at 1.0  $\text{Adm}^{-2}$  - 4.0  $\text{Adm}^{-2}$ ) observed to follow opposite trend for OER, when used them as anode, and is evident from the CV plots shown in Figure 6.3(b). It may be seen that NiW alloy coating corresponding to 4.0  $\text{Adm}^{-2}$  shows the least onset potential with the highest anodic peak current density ( $i_{pa}$ ) for OER, compare to other coatings. Thus, highest value of  $i_{pa}$  of NiW alloy corresponding to 4.0  $\text{Adm}^{-2}$  may be attributed to its highest Ni content, compared to all other coatings (Table 6.1). Thus increased efficacy of NiW alloy coating of OER towards high current density is due to increase of Ni content in the alloy, which is in compliance with reported work (Elias et al. 2015).

### 6.3.2.2 Chronopotentiometry study

In this technique, potential of the working electrode is measured as a function of time with respect to reference electrode, by passing a constant current between two electrodes

(P.J.Hillson 1952). The chronopotentiometry study of NiW alloy coatings at  $1.0 \text{ Adm}^{-2}$  -  $4.0 \text{ Adm}^{-2}$  were done by passing a constant current of  $-0.3 \text{ A}$  and  $0.3 \text{ A}$  for 1800s for HER and OER, respectively. The electro-catalytic performance of NiW alloy coatings were evaluated by quantitatively by measuring volume of  $\text{H}_2$  and  $\text{O}_2$  evolved on  $1 \text{ cm}^2$  surface area, for 300 s. The chronopotentiograms of NiW alloy coatings, deposited at different current densities for HER is shown in Figure 6.4 (a), and volume of  $\text{H}_2$  gas evolved during the process of electrolysis (300 s) is shown as bar chart, in Figure 6.4(b).

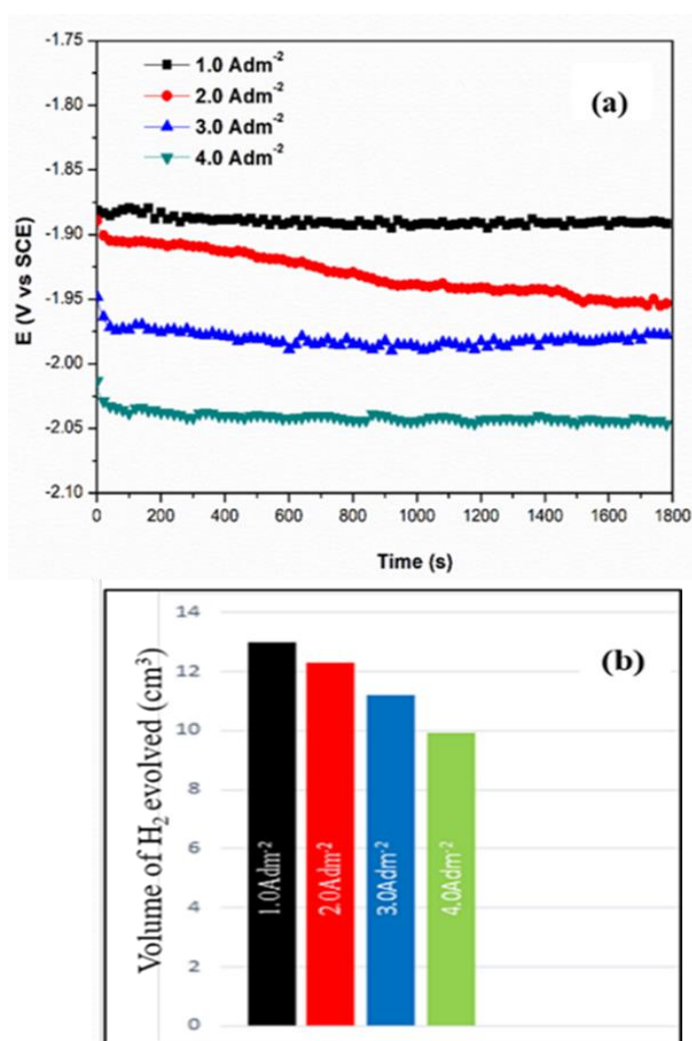


**Figure 6.4-** CP study for HER on the surface of NiW alloy coatings, deposited at different current densities (a), and (b) the volume of  $\text{H}_2$  gas evolved at different current densities. Highest efficacy of  $(\text{NiW})_{1.0 \text{ Adm}^{-2}}$  towards HER may be seen compared to other coatings.

The constancy of chronopotentiogram of all coatings over a time 1800 s, shown in the Figure 6.4 speaks about their stability in the medium of study, and their robustness to work as electro-catalyst. Among all, NiW alloy coating deposited at  $1.0 \text{ Adm}^{-2}$ , i.e.,  $(\text{NiW})_{1.0 \text{ Adm}^{-2}}$  exhibited the best electrocatalytic activity for HER with maximum amount of  $\text{H}_2$  gas evolution, compared to all other coatings, as may be seen in Table 6.1., and Figure 6.5.

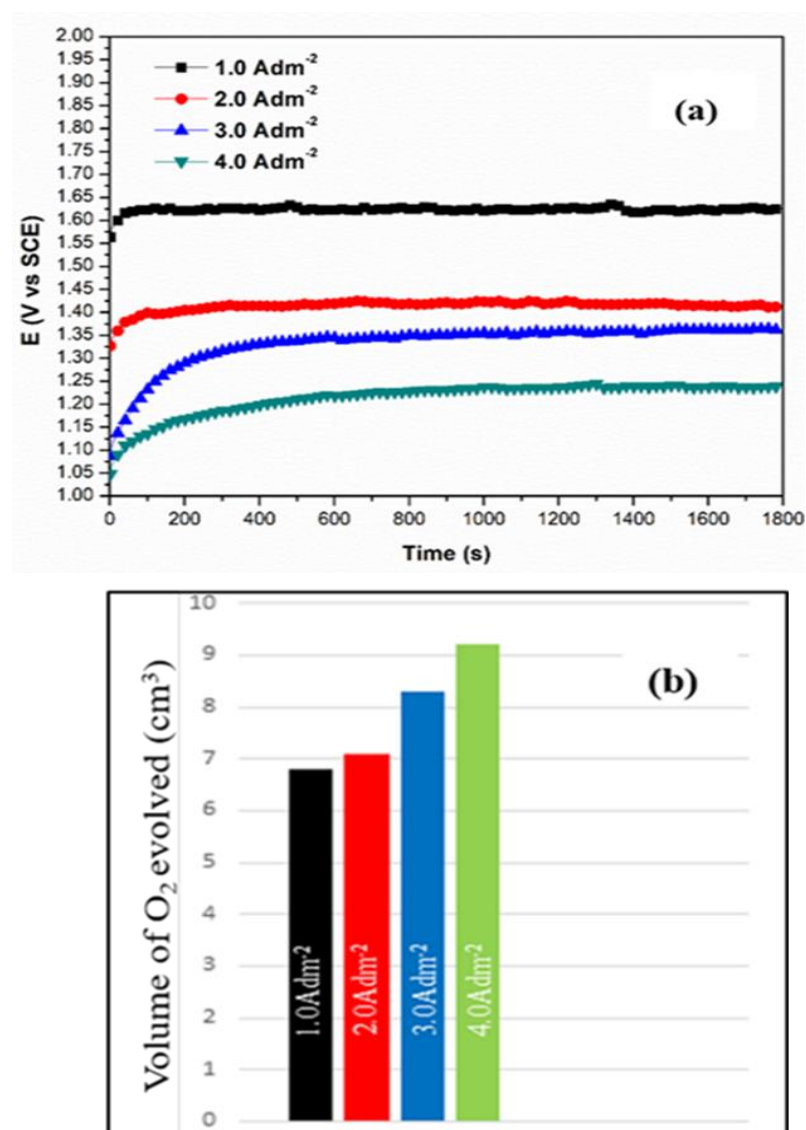


**Figure 6.5-** CP study for OER on the surface of NiW alloy coatings, deposited at different current densities (a), and (b) the volume of  $\text{O}_2$  gas evolved at different current densities. Highest efficacy of  $(\text{NiW})_{4.0 \text{ Adm}^{-2}}$  towards OER may be seen compared to other coatings.

It may be seen in Figure 6.4(a), all NiW alloy coatings showed a sudden decrease in potential in the beginning of electrolysis, and eventually reached a steady state. This is due to the attainment of equilibrium between reduction of  $H^+$  from electrolyte on the electrode surface and  $H_2$  gas evolution from the surface. Here, it may be noted that  $(NiW)_{1.0 \text{ Adm}^{-2}}$  attained the steady state equilibrium immediately, compared to other coatings (Figure 6.4(b)). This confirmed the fact that  $(NiW)_{1.0 \text{ Adm}^{-2}}$  coating is electrocatalytically more stable and active for HER, and is the best electrode material for HER, compared to other coatings (Covington 1973; Ullal and Hegde 2014a). Similarly, chrono-potentiograms of NiW alloy coatings, deposited at different current densities for OER is shown in Figure 6.5 (a), and volume of  $O_2$  gas evolved during the process of electrolysis (300 s) is shown as bar chart, in Figure 6.5(b). It may be seen that NiW coating at  $4.0 \text{ Adm}^{-2}$ , *i.e.*,  $(NiW)_{4.0 \text{ Adm}^{-2}}$  showed more activity as catalyst for OER, with highest volume of  $O_2$  gas evolved at lesser positive potential, compared to all other coatings. This may be attributed to the high Ni content of the alloy, responsible for increased oxidation of  $OH^-$  ions (Elias et al. 2015). From the nature of chrono-potentiogram corresponding to all coatings (Figure 6.5 (b)), it may be noted that when current is applied, initially there is a potential hike due to the sudden depletion of  $OH^-$  ions from the electrolyte at the electrode surface. Later, the oxidation of  $OH^-$  to  $O_2$  gas processed uninterruptedly, and the formation of  $O_2$  gas at the electrode surface and its evolution from the surface found to occur steadily, which lead to the potential of the system to remain unchanged. The volume of  $H_2$  and  $O_2$  liberated on the surface of NiW deposited at different current densities are shown in Figure 6.6. From the nature of diagram, it may be noted that, volume of  $H_2$  decreased with W content of the alloy, and volume  $O_2$  increased with Ni content of the alloy. Thus, it is evident that electrocatalytic activity of NiW alloy coating for HER and OER has inverse dependency of their composition. *i.e.*, the composition favouring HER is not favourable for OER, and vice versa.

### **6.3.2.2 Inverse dependency of electrocatalytic efficacy of HER and OER with composition**

The electrocatalytic activity of NiW alloy coatings for both HER and OER, deposited at different current densities are summarized in Table 6.1. From the data, it may be noted



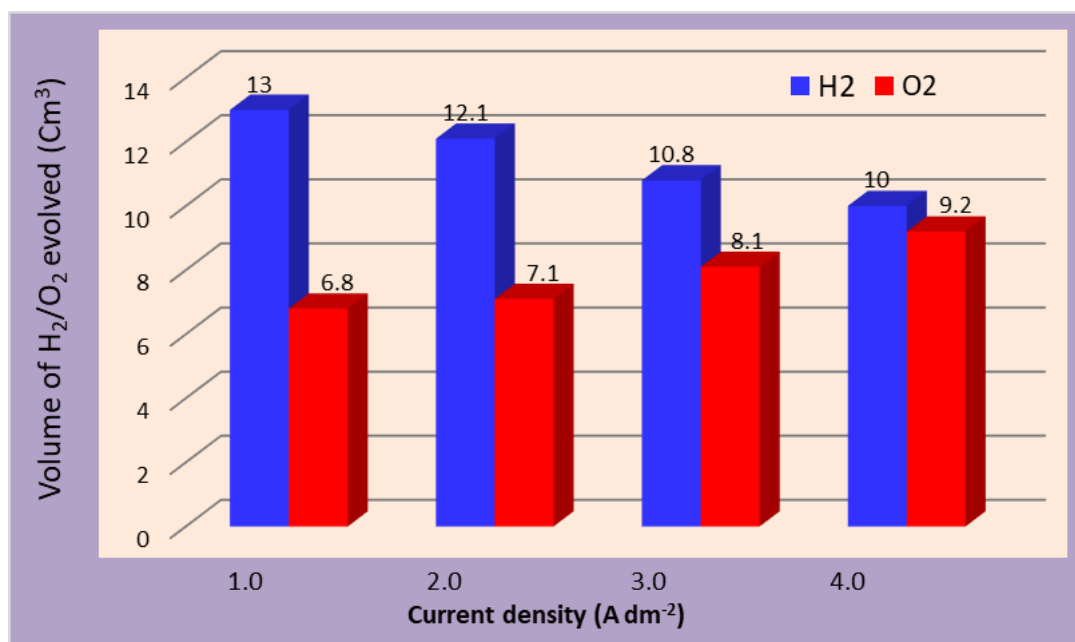


**Figure 6.6-** Electrocatalytic activity NiW alloy coatings deposited at different current densities in terms of the volume of H<sub>2</sub> and O<sub>2</sub> gas produced during electrolysis of water for duration 10 min.

that as the deposition current density is increased (or as Ni content of the deposit increased), the electrocatalytic efficacy of NiW alloy coatings for HER (cathodic process) increased; whereas for OER (anodic process), it decreased. This inverse dependency of electrocatalytic efficacy of HER and OER with Ni content of alloy coatings may be accredited to the redox behavior of alloy coatings, having different composition. It may be explained in terms of the tendency of the electrons to transmit between working electrodes (test electrodes) and counter electrode. It may be recalled that in electrochemical study, working electrode is an electrical conductor, and by means of an external power source (potentiostat), voltage can be applied to it to modulate the energy of the electrons in the electrode. Hence, driving force of a particular reaction can be controlled, and the ease with which thermodynamic and kinetic parameters can be measured (Elgrishi et al. 2018). In the backdrop of the above principle, a conceptual diagram showing the efficacy of NiW alloy coatings, having different Ni content towards HER and OER during alkaline water electrolysis is given in Figure 6.7. It may be noted that during alkaline water electrolysis, H<sub>2</sub> and O<sub>2</sub> gases are liberated on

working electrode (NiW alloy coatings having different compositions), when relatively negative and positive potentials are applied, respectively through the potentiostat.

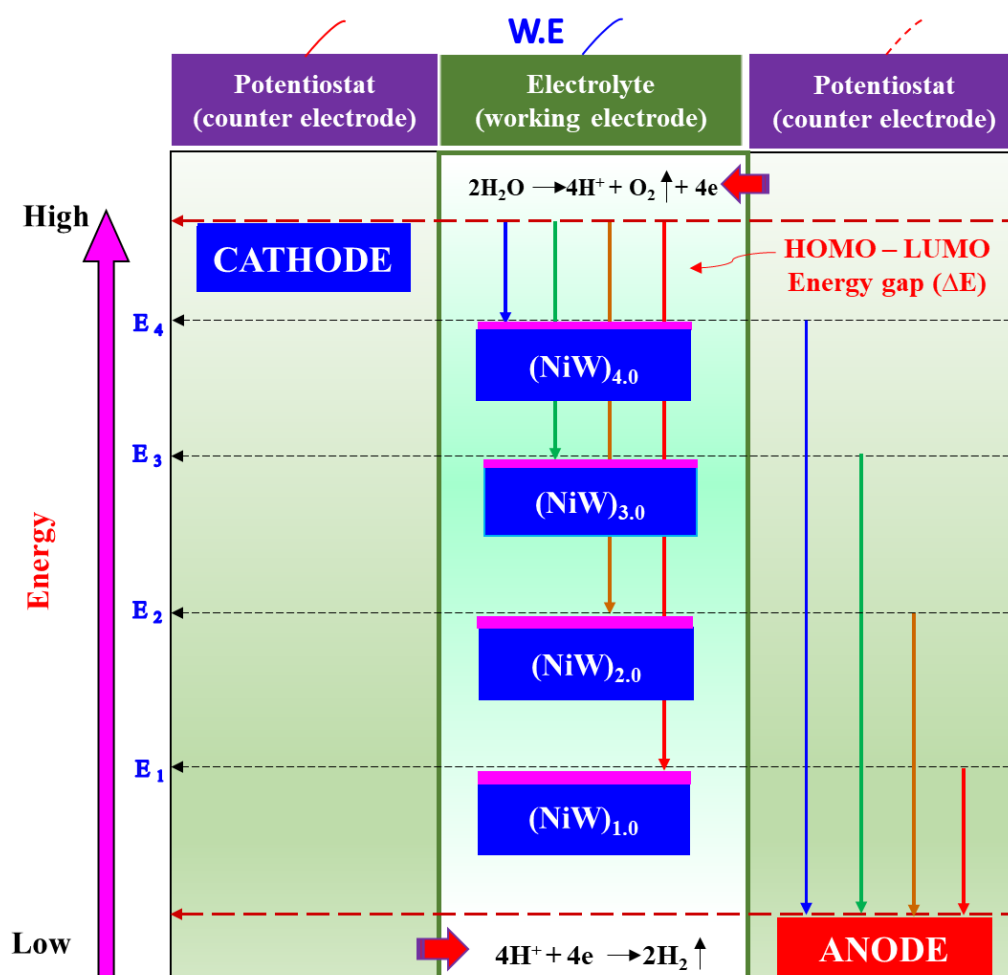


**Figure 6.7-** Representational diagram showing inverse dependency of NiW alloy coating, deposited at different current density for HER and OER in alkaline water electrolysis.

When electrons in the NiW alloy coatings are at a higher energy than the Lowest Unoccupied Molecular Orbital (LUMO) of the electrolyte constituent ( $\text{H}^+$ ), electron from the electrode is transferred to electrolyte constituent to release  $\text{H}_2$ . Similarly, when electrons in the NiW alloy coating is at lower energy than the Highest Occupied Molecular Orbital (HOMO) of electrolyte constituent ( $\text{OH}^-$ ), electron from the electrolyte constituent is transferred to electrode to release  $\text{O}_2$ . Thus, depending on the Ni content, or depending on the deposition current density, NiW alloy coatings can

assume different electrode potential values ( $E_1$ ,  $E_2$ ,  $E_3$  and  $E_4$ ) along the energy axis (depending on the Ni content), as shown in Figure 6.7, and hence different energy gap ( $\Delta E$ ) between HOMO-LUMO. Therefore, transferring of electrons takes place from HOMO to LUMO to favor either HER or OER, depending on its composition. If the efficacy of NiW alloy coating, deposited at a particular current density, say at  $1.0 \text{ Adm}^{-2}$  (having the least Ni content) is more favourable for HER (due to high energy gap  $\Delta E$ ), and less favourable for OER (due to small energy gap  $\Delta E$ ), as shown in Figure 6.7. But NiW alloy coating, deposited at  $4.0 \text{ Adm}^{-2}$  (having highest Ni content) is more favourable for OER, and less favourable for HER, as may be seen in Figure 6.7. Thus it may be summarized that a mutually opposite electrocatalytic activity of NiW alloy coatings towards HER and OER, which changes with deposition current density is attributed to the change in composition of the alloy, in terms of their Ni and W content. In other words, the driving force of electrochemical reaction of water splitting of both HER and OER of NiW alloy coating is a function of energy difference between working electrode and counter electrode, and show mutually opposite trends.

#### **6.4 CONCLUSIONS**

*The electrocatalytic activity of NiW alloy coatings, deposited from newly formulated bath at different current densities have been studied, and following observations are made as conclusions:*

1. Electrodeposited NiW alloy coatings, at different current densities were used as electrode material for hydrogen evolution reaction (HER) and oxygen evolution reaction (OER) of water splitting applications in 1 M KOH.
2. Experimental results demonstrated that electro-catalytic activity of alloy coatings for both HER and OER are highly dependent on its composition, depending on the current density at which they are deposited.
3. Quantitative measurement of  $\text{H}_2$  and  $\text{O}_2$  gases evolved at cathode and anode revealed that NiW alloy having least and highest Ni content is good electrode material, respectively for HER and OER, supported by cyclic voltammetry and chronopotentiometry study.
4. Mutually opposite electrocatalytic activity of NiW alloy coatings towards HER and OER with deposition current density is attributed to the difference in the

energy gap between HOMO - LUMO states of electrode materials, depending on their composition, in terms of their Ni and W content.

5. The surface feature, phase structure and compositional change of NiW alloy coatings, responsible for highest electrocatalytic activity of HER and OER were examined, using Scanning electron microscopy (SEM), X-ray diffraction (XRD) and Energy dispersive X-ray spectroscopy (EDS) techniques.

## **CHAPTER 7**

# **DEVELOPMENT OF COMPOSITION GRADED MULTILAYER NiCo ALLOY COATINGS AND THEIR CORROSION BEHAVIOUR**



## CHAPTER 7

# DEVELOPMENT OF COMPOSITION GRADED MULTILAYER NiCo ALLOY COATINGS AND THEIR CORROSION BEHAVIOUR

---

### 7.1 INTRODUCTION

Electroplating of metals and alloys are widely used in many industries, with distinct advantages compared to most other coating technologies. It is the simplest of all approaches for production of binary/ternary alloy coatings for better corrosion protection of base metals with greater ease of flexibility in terms of their structure, composition and surface roughness (Kanani 2006). Electroplated Zn-Fe group metals (Ni, Co and Fe) alloys and mutual alloys of Fe group metals exhibit better corrosion resistance properties compared to individual pure metals (Brenner 1963; Fratesi et al. 1997) , and their electrodeposition follows peculiar anomalous type of codeposition. The phenomenon of anomalous codeposition was first noticed by Brenner (Brenner 1963) in electrodeposition of Zn-Fe group metal alloys, where it was found that less noble metal is deposited preferentially than the more noble metal, under most common plating conditions. This type of codeposition is attributed to the suppression of deposition of more noble metal by hydroxides of less noble metal, formed at the interface of cathode and the medium (Thangaraj et al. 2009). Among electroplated coatings of binary alloys of Fe- group metals, nickel-cobalt (NiCo) alloy is of highest attention from many years. This is mainly due to its good brightness, smooth and uniform surface properties, high thermal properties, good electronic properties (Chi et al. 2005) and good heat exchanging behaviours (Wang et al. 2005). Apart from electrocatalytic behaviour (Kamel et al. 2021), good material property even at high temperatures, excellent adhesive behaviour, good chemical stability and high temperature corrosion stability (Bahadormanesh et al. 2011; Hassani et al. 2009; Shi et al. 2006b; Tian et al. 2011).

Currently, the research in surface coating technology mainly shifted to the

creation of layered structures rather than monolayer coatings in order to provide greater corrosion protection. Several research works have been published in this area, by applying pulsed current densities during the deposition process which allows the formation of coatings with periodic changes in composition. In fact, the different amplitude current densities are frequently employed because they are simple to manage, and equipment used to implement changes is simple and accurate (Elias and Chitharanjan Hegde 2015; Thangaraj et al. 2009; Venkatakrisna and Chitharanjan Hegde 2010). The electroplated NiCo alloy is prominent engineering materials, widely used for aesthetic and protective purposes in harsh environments, having water or corrosive materials (Ma et al. 2013; Pérez-Alonso et al. 2015). Endowed with superior material properties, many researchers have extensively studied the production and properties of NiCo alloy coatings. NiCo alloy coatings with varying cobalt content was electrodeposited from sulfamate by Srivastava and others (Srivastava et al. 2006). The influence of saccharin on process and product of electroplating of NiCo alloy coatings have been reported in the literature (Hassani et al. 2008; Lokhande and Bagi 2014). It was found that grain size, and hence properties of alloy coating are controlled by both diffusion of ad-ions and current density used for deposition. Recently, NiCo alloy coatings of high corrosion resistances have been developed from an acid bath, using suphanilic acid as the additive, through ultrasound induced codeposition (Shetty and Chitharanjan Hegde 2017).

Electrodeposition of mutual alloys of Fe group metals, including NiCo found to follow predominantly the anomalous type of codeposition. The less noble Co metal gets deposited at the expense of nobler Ni. The operating parameters like current density, bath temperature, utilization of organic components, the concentration of solution constituents results in an amendment in the kinetics of the deposition process, the structure, and appearance of the deposits (Kamel 2007). But contrary to this, there are several reports in the literature that few baths show both regular and anomalous type of codeposition, depending on certain conditions of bath concentration, complexing agents and operating variables (like pH, current density, temperature, agitation) (Brenner 1963). *i.e.* a given bath under some conditions of current density and temperature follows normal type, and under other conditions follows anomalous type. Hence, due to possible normal and anomalous type of codeposition in a given bath (depending on the



conditions provided), search for development of new electrolytic baths is ever increasing. Hence, possibilities of both normal and anomalous type of codeposition can be used advantageously to bring better material properties to alloy coatings NiCo by proper manipulation of bath chemistry and deposition current density. In addition, the experimental results revealed that corrosion resistivity of NiCo alloy coating has a strong dependency on its composition, surface morphology and phase structure.

In this regard, the present study includes the formulation of a new NiCo bath for development of conventional monolayer alloy coatings of better corrosion resistance, using constant current, or direct current (DC). Further, the corrosion resistance of monolayer NiCo alloy coatings was attempted to increase by multilayer approach by periodic pulsing of the current densities between two amplitudes, during process of deposition. The corrosion performance of alloy coatings, both monolayer and multilayer coatings was tested using electrochemical AC and DC techniques. The deposition conditions for multilayer coating are manipulated, in both composition and thickness of individual layers layered deposition to get coatings of best performance. The composition, phase structure and surface morphology of alloy coatings corresponding to different conditions were analysed using, respectively EDS, XRD, SEM and AFM techniques. The reasons for better performance of multilayer alloy coatings, in relation to that of monolayer alloy coatings were explained, and results are discussed.

## **7.2 MATERIALS AND METHODS**

### **7.2.1 Optimization of NiCo bath**

A simple and new NiCo alloy bath containing potassium sodium tartrate ( $\text{KNaC}_4\text{H}_4\text{O}_6 \cdot 4\text{H}_2\text{O}$ ), or Rochelle salt, cobalt sulphate ( $\text{CoSO}_4 \cdot 7\text{H}_2\text{O}$ ), nickel sulphate ( $\text{NiSO}_4 \cdot 6\text{H}_2\text{O}$ ) and glycine ( $\text{NH}_2\text{-CH}_2\text{-COOH}$ ) has been proposed. All reagents were dissolved in double distilled water, individually and then mixed and stirred well for complete dissolution. The bath pH was adjusted to 3.0 using either  $\text{H}_2\text{SO}_4$  or  $\text{NH}_4\text{OH}$  (depending on the requirement), using Micro-pH Meter (Systronics-362). The standard Hull cell method was employed for the optimization of bath composition and plating variables, discussed elsewhere (Kanani 2006). The bath chemistry and operating variables of NiCo bath, required to get smooth and uniform NiCo alloy coatings (optimized) is given in Table 7.1.

**Table 7.1- Bath constituents and operating variables of optimized NiCo bath**

Bath composition	Concentration (g/L)	Operating Parameters
NiSO <sub>4</sub> . 6H <sub>2</sub> O	100.0	pH: 3.0
CoSO <sub>4</sub> . 7H <sub>2</sub> O	20.0	Temperature: 303K
KNaC <sub>4</sub> H <sub>4</sub> O <sub>6</sub> .4H <sub>2</sub> O	16.6	Anode: Graphite
NH <sub>2</sub> -CH <sub>2</sub> -COOH (glycine)	3.3	Cathode: Copper
		current density: 1.0 Adm <sup>-2</sup> - 4.0 Adm <sup>-2</sup>
		duration of deposition time: 600 s

Electrodeposition of NiCo alloy coatings were performed in a 200 mL capacity cell (made of PVC) using DC Power Analyzer (Agilent N6705C, USA). Copper plates of 7.5 cm × 3.0 cm × 0.2 cm dimensions were polished to get mirror finish. The surface is then cleaned using cotton swab, dipped in Trichloroethylene solvent. A graphite plate was used as anode. NiCo alloy coatings of different composition were developed galvanostatically on a 3.0 × 3.0 cm<sup>2</sup> cathode, at different current densities from the optimized bath, keeping anode and cathode parallel. Electroplated substrates were rinsed using distilled water, and then dried in hot air. Lastly, it is dried in a desiccator, till it is taken to further analysis. The duration of all depositions was kept constant to validate the relative performance of all coatings. Both monolayer and multilayer NiCo alloy coatings were developed Galvanostatically, using optimized bath, given in Table 7.1. Multilayer NiCo alloy coatings were developed by pulsing of cathode current density, periodically. The composition modulated multilayer (CMM) NiCo alloy coatings, having different Ni content were developed. The monolayer NiCo alloy coating deposited at a particular current density 'x' is denoted as (NiCo)<sub>x</sub>; and the CMM NiCo alloy coatings are represented as (NiCo)<sub>2.0/4.0/n</sub>. Here, 2.0 and 4.0 denote cathode current density (in Adm<sup>-2</sup>), and 'n' is the number of layers formed during total plating time. *i.e.*, 600 s.

All coatings (both monolayer and multilayer) reported here are electrodeposited for 600 s at constant temperature (303 K) and pH 3.0, for comparison purpose. The corrosion behavior of alloy coatings were tested in a three-electrode cell (having 3.5%

NaCl solution) by electrochemical methods using Electrochemical Workstation (VersaSTAT-3). After desiccator drying, electrodeposited coatings were subjected to electrochemical impedance spectroscopy (EIS) study first, using AC voltage of small amplitude ( $\pm 10$  mV) in the frequency range of 100 kHz to 10 mHz. Then corrosion rates of alloy coatings were evaluated by Tafel's extrapolation method, by having potentiodynamic polarization curves. Potentiodynamic polarization was carried out in a potential window of  $\pm 250$  mV, from the open circuit potential (OCP) at a scan rate of  $1 \text{ mVs}^{-1}$ . Change in the surface features and composition of alloy coatings with current density were examined using scanning electron microscopy (SEM), interfaced with Energy Dispersion X-ray Spectroscopy (EDS) facility (Oxford EDS, X-act). The surface roughness of alloy coatings were analyzed using Innova SPM Atomic Force Microscope. The surface of alloy coatings was mapped in tapping mode, using antimony doped silicon cantilever having a force constant in the range of 20 - 80  $\text{Nm}^{-1}$ . The composition-dependent crystal structures of alloy coatings were analyzed using X-ray diffraction (XRD) study (Rigaku, Miniflex 600, with  $\text{CuK}\alpha$  radiation having  $\lambda = 1.5418$  Å, as the X-ray source).

## 7.3 RESULTS AND DISCUSSION

### 7.3.1 Compositional analysis

Generally, composition of electrodeposited alloy coatings is a function of a large number of variables, the main ones of which are bath composition and bath operation conditions (Fratesi et al. 1997). In addition, the corrosion protection efficacy of any binary/ternary alloy coatings depends on its composition. In this regard, the composition of NiCo alloy coatings corresponding to different current densities are reported in Table 7.4, and is shown graphically in Figure 7.1. The composition reference line (CRL) corresponding to contents of two constituting metals (Ni and Co) in the bath, denoted respectively as  $\text{CRL}_{\text{Ni}}$  and  $\text{CRL}_{\text{Co}}$  are also shown in Figure 7.1, as perforated horizontal lines. Hence, from the nature of graph showing metals content in the deposit, in relation to those in the bath, it may be concluded that the present NiCo bath follows phenomenon of anomalous codeposition with preferential deposition of less noble metal (Co). It is supported by two facts: *i*) The Co (less noble metal) content of alloy deposited at all current densities is much higher than that in the bath (16.7 %)

and ii) Wt.% of Ni (more noble metal) in the deposit increased with current densities. This increase of Ni content in the deposit with increase current density may be explained by principles of electroplating of binary alloys of Fe group metals as envisaged by Brenner (Brenner 1963).

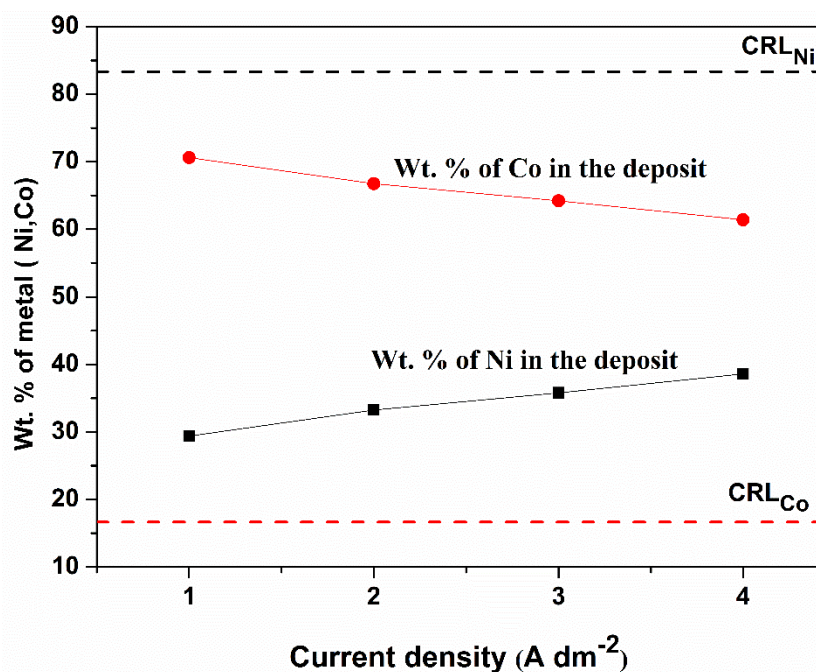


**Figure 7.1** - Variation in the Wt % of Ni and Co in NiCo alloy deposit with current density, deposited from optimized bath.

It was explained by the fact that in alloy deposition, Wt.% of less noble metal (Co), or more precisely a more readily deposit able metal in the deposit can be increased by any change of coating conditions – fast agitation, increase in temperature, or increase in the salt content in the bath, or decreasing the current density. All these acts tend to oppose the depletion  $\text{Co}^{+2}$  ions in the cathode diffusion layer. Hence, as the current density is increased, cathode diffusion layer becomes relatively more depleted of less noble  $\text{Co}^{+2}$  ions. Hence,  $\text{Ni}^{+2}$  ions deposited preferentially. Therefore, it may be summarized that increase in the Wt.% Ni in the electrodeposited NiCo alloy coatings with current density is attributed to the depletion of more readily depositable  $\text{Co}^{+2}$  ions at the cathode diffusion layer. Here, it should be noted that Ni content of the alloy, at all current densities studied are falling well below its content in the bath (83.3 %),

shown as  $CRL_{Ni}$  in the Figure 7.1. Further, it may be noted that under no conditions of deposition, *i.e.* at all current densities studied, the bath followed normal type of codeposition, with having less Wt.% Co (less noble) in the deposit than in the bath. However, from the composition data shown in Table 7.3, it may also be inferred that NiCo codeposition is tending towards the normal type as the current density is increased, but not reached it as Ni content of the deposit is much lower than that in the bath even at highest current density ( $4.0 \text{ Adm}^{-2}$ ).

### 7.3.2 Surface Morphology

Figure 7.2 shows SEM micrographs of NiCo alloy coatings on copper, corresponding to different current densities. It may be seen that surface morphologies shows decreasing grain size when current density increased from  $1.0 \text{ Adm}^{-2}$  to  $4.0 \text{ Adm}^{-2}$ . Decrease in the grain size due to increase of current density may be explained from the theory of electrocrystallization process as follows: The process of electrodeposition takes place in two consecutive and coupled stages, called nucleation and growth process. The first of this is formation of thermodynamically stable crystal nuclei at certain points on the cathode, followed by their growth. Both process of nucleation and crystal growth can be expressed in terms of a characteristic overvoltage, generally known as crystallization overvoltage (Kanani 2006). The nucleation usually contributes more to the overvoltage than the growth stage due to the reason that former is having a higher activation energy. Hence, at lower current density crystal growth takes place preferentially than new nucleation (as activation energy for growth process is less when compared to nucleation). Hence, NiCo coating corresponding to  $1.0 \text{ Adm}^{-2}$ , denoted as  $(NiCo)_{1.0 \text{ Adm}^{-2}}$  is more rough, with more irregularities as shown in Figure 7.2. But as the current density increased, crystallization overvoltage is increased to increase in rate of kinetics of nucleation (as activation energy for nucleation is high). Consequently, the size of crystallites decreased to form a smooth and uniform, as seen in the coating corresponding to  $4.0 \text{ Adm}^{-2}$ , denoted as  $(NiCo)_{4.0 \text{ Adm}^{-2}}$  in Figure 7.2. Thus, roughness of NiCo alloy coatings towards lower current densities may be attributed to higher rate of crystal growth, than rate of nucleation (due to less crystallization overvoltage); and smooth (relatively) NiCo alloy coatings towards higher current densities is due to higher rate of nucleation, than rate of crystal growth. Thus, variation in the uniformity of alloy coatings depends on the relative rates of kinetics of nucleation and crystal

growth, depending the current density used for deposition.

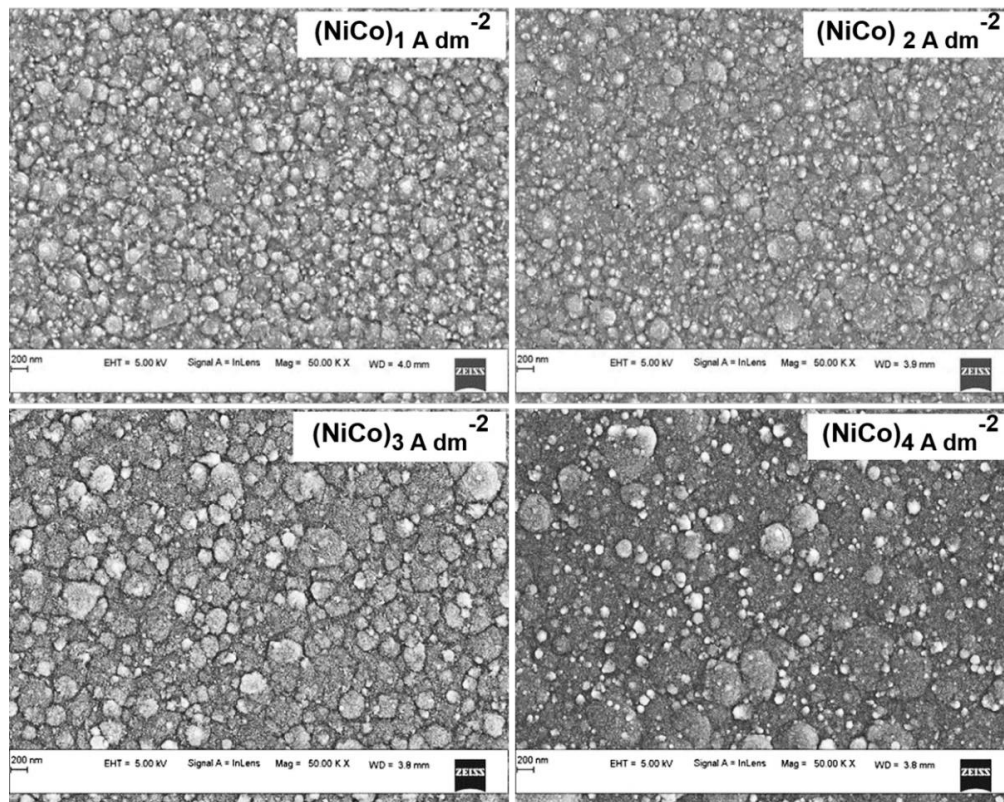


**Figure 7.2** - Surface morphology of NiCo alloy coatings corresponding to different current densities deposited from optimal bath.

### 7.3.3 AFM Study

The surface roughness is an important factor that can influence the properties of coatings. Hence, the surface topography of electrodeposited coatings were studied using three dimensional Atomic Force Microscopy (AFM) technique. The three dimensional AFM image of NiCo alloy coatings, deposited at different current densities are shown in the Figures 7.3. (a), (b), (c) and (d). The topographical characterization is carried out by measuring the amplitude parameters such as average roughness ( $R_a$ ) and root mean square roughness ( $R_q$ ) value (Ashraf et al. 2016), and corresponding data analysed for area of  $10\mu\text{ m} \times 10\mu\text{ m}$  is outlined in the Table 7.2. The AFM images prospects for the compactness of deposited alloy coatings, depending on the deposition current densities.

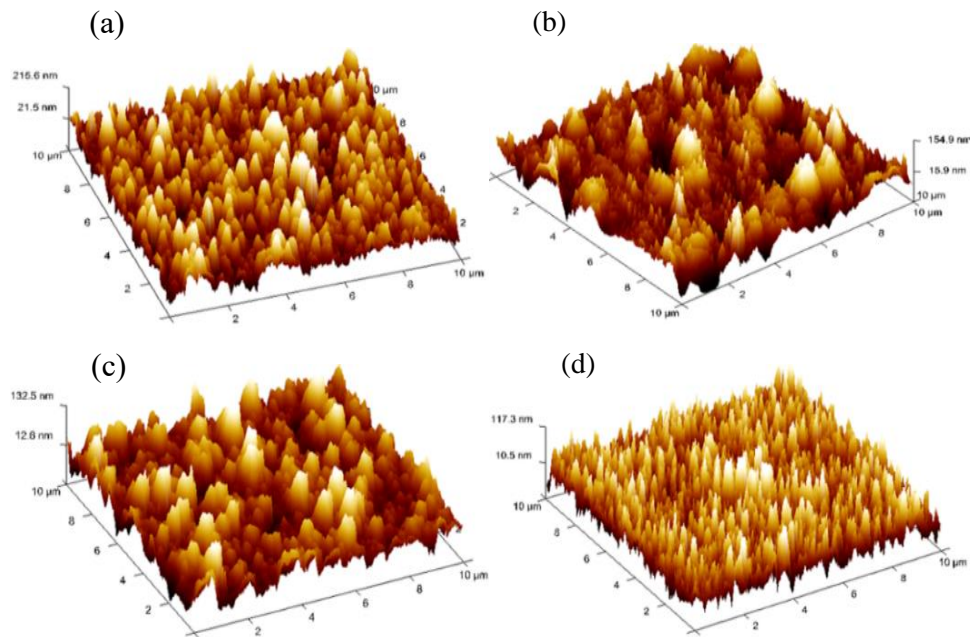


**Figure 7.3** - AFM images of NiCo coating deposited at (a)  $1.0 \text{ Adm}^{-2}$ , (b)  $2.0 \text{ Adm}^{-2}$ , (c)  $3.0 \text{ Adm}^{-2}$  and (d)  $4.0 \text{ Adm}^{-2}$  showing increase of uniformity with current density.

It may be recalled that  $R_q$  corresponds to the surface roughness, obtained by squaring each height value of the peak, then taking the square root of the mean. It is a measure of the asymmetry of the surface deviation about the mean plane; and  $R_a$  is measure of the deviation of a surface from a mean height and is globally well accepted parameter for surface roughness. Accordingly, it may be seen that surface roughness of electrodeposited NiCo alloy coatings were decreased with increase of current density as can be seen in the AFM images depicted in the Figure 7.3, and the corresponding roughness data ( $R_q$  and  $R_a$ ), reported in Table 7.2.

**Table 7.2 - AFM data of NiCo alloy coatings deposited at different current densities from optimized bath**

Coating configuration	Root mean square roughness, $R_q$ (nm)	Average roughness, $R_a$ (nm)
(NiCo) $_{1.0}$ Adm $^{-2}$	54.8	42.7
(NiCo) $_{2.0}$ Adm $^{-2}$	36.5	24.9
(NiCo) $_{3.0}$ Adm $^{-2}$	33.7	26.4
(NiCo) $_{4.0}$ Adm $^{-2}$	30.8	24.5

### 7.3.4 X-Ray Diffraction Study

The phase structure of electrodeposited NiCo alloy coatings was analyzed by XRD technique, and the corresponding X-ray peaks are shown in Figure 7.4. The examination by X-ray patterns confirmed that all coatings are well-crystalline, and found to have two different phases, a face-centered cubic (fcc) and hexagonally close-packed (hcp) in the entire range of current density studied (Karimzadeh et al. 2019; Mbugua et al. 2020). The coatings showed well-defined characteristics peaks at 44.5, 51.77 and 76.2, corresponds to (111), (200) and (220) lattice planes, respectively. These are characteristic planes of face centered cubic structure of NiCo alloy coatings (Radhakrishnan et al. 2021). Thus XRD study showed that the crystal structure is a combination of fcc and hcp with the appearance of (002), (110) and (112) peaks, which reflects the lattice planes of hcp cobalt apart from the above mentioned fcc reflections. Further, the intensity of hcp lattice plane reflection decreases with increasing deposition current density (Karimzadeh et al. 2019; Srivastava et al. 2006). This observation is in agreement with the principle of anomalous codeposition, followed in mutual alloys of Fe group metals. *i.e.* deposition of more readily depositable metal (Co) is suppressed with increase of current density due to less availability of  $Co^{+2}$  ions (or more availability of  $Ni^{+2}$  ions) at cathode film (Salehi et al. 2014).



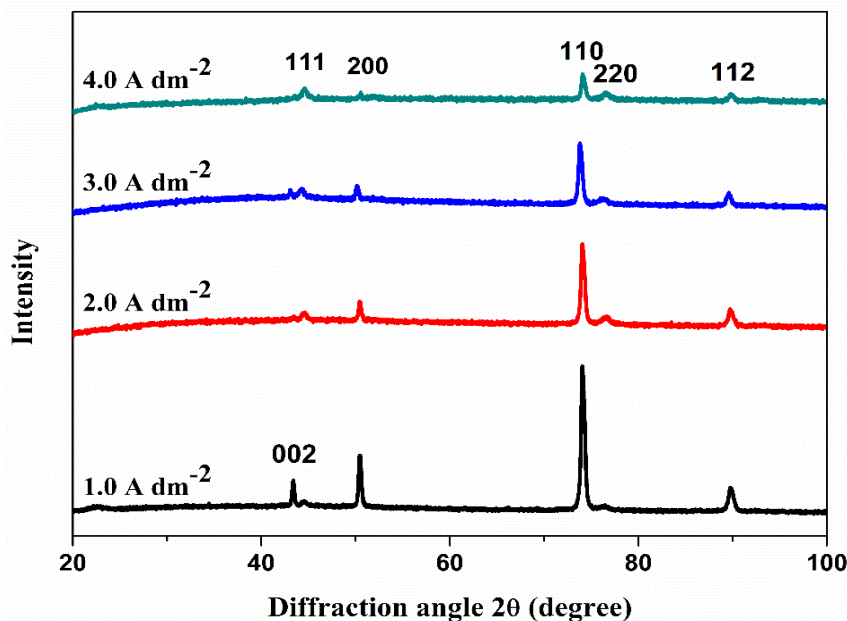


*Figure 7.4 - XRD patterns of NiCo alloy coatings deposited at different current densities from optimal bath*

In addition, the calculated average crystallite size was found to be 24.93 nm, 22.04 nm, 18.06 nm and 14.8 nm for NiCo alloy coatings, deposited, respectively at  $1.0\text{Adm}^{-2}$  –  $4.0\text{Adm}^{-2}$ . It may also be seen that the crystallite size decreases with increase in deposition current density, which further reduced the strain in the crystal lattice and reduced the defects. This reduced defects of coating is responsible for highest corrosion resistance of NiCo alloy coatings, deposited at higher current density (at  $4.0\text{Adm}^{-2}$ ).

### **7.3.5 Corrosion study of monolayer NiCo Alloy Coatings**

As first part of this chapter is focused on optimization of bath conditions and operating variables for development of more corrosion resistant monolayer NiCo alloy coatings, their corrosion behaviors studied by Electrochemical Impedance Spectroscopy (EIS) and potentiodynamic polarization methods. It may be pointed out that all the electrochemical potentials referred in this work are in the scale of saturated calomel electrode (SCE), and all experimental results are discussed as below.

#### **7.3.5.1 EIS Study**

EIS is a commonly used technique for detailed study the corrosion behavior of surface coatings (Mehta 2013). Nyquist, or complex plane plots are the most often used in the

EIS study because they allow an easy prediction of the circuit elements, required to explain behavior of electrode - electrolyte interface (Lasia 1999). Accordingly, Nyquist plots of NiCo alloy coatings deposited at different current densities are shown in Figure 7.5, and the circuit inside is the corresponding equivalent circuit obtained by impedance experimental data fitting. This circuit elements helps in the interpretation of Nyquist plot, in order to understand the plausible corrosion process takes place at the corrosion medium/coatings and or substrate interface.

The similarity in the shape of the Nyquist plots indicates the resemblance of corrosion process taking place in all NiCo alloy coatings under study (Liu et al. 2013). The circuit description code (CDC) for the equivalent circuit proposed for the coated samples are  $R(Q(R(QR)))$  (Srivastava et al. 2006). The electric circuit elements obtained in this model are coating resistance ( $R_c$ ), constant phase elements (CPEs) of the alloy coatings; Charge transfer resistance ( $R_{ct}$ ) and constant phase element of coatings-substrate interface ( $CPE_{dl}$ ). The  $R_c$  and  $R_{ct}$  altogether constitute the polarization resistance, which amounts to the corrosion behavior of coatings (Xing et al. 2020). The circuit elements of the common circuit shown in Figure 7.5 is summarized in Table 7.3.

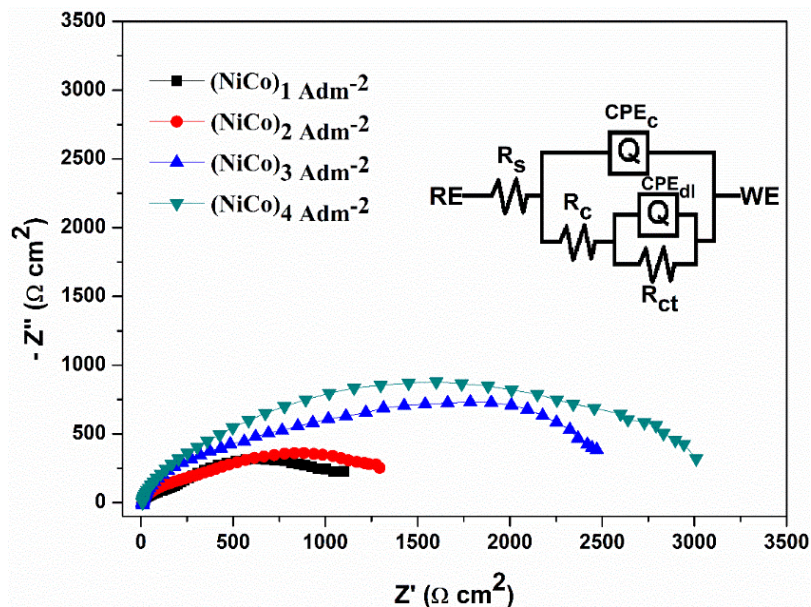


**Figure 7.5** - Nyquist plots of NiCo alloy coatings deposited at different current densities from optimized bath.

It may be seen that both  $R_c$  and  $R_{ct}$  increased with increasing the deposition current density. It implies that the corrosion resistance of alloy coatings increases with

its Ni content, and reaches its maximum at  $4.0 \text{ Adm}^{-2}$ , compared to all other coatings. This progressive increase of corrosion resistance of alloy coatings with current density may be attributed to progressive increase of Ni content. In addition, increased corrosion resistance of NiCo alloy coatings towards high current density is due to decreased surface roughness and crystallite size, supported by AFM, FESEM and XRD analysis, respectively.

**Table 7.3 - EIS data from equivalent circuit of NiCo alloy coatings at different current densities.**

<b>Coating configuration</b>	<b><math>R_s</math> (<math>\Omega</math>)</b>	<b><math>R_c</math> (<math>\Omega</math>)</b>	<b><math>Q_c</math> (<math>\mu\text{F}</math>)</b>	<b><math>R_{ct}</math> (<math>\Omega</math>)</b>	<b><math>Q_{dl}</math> (<math>\mu\text{F}</math>)</b>
$(\text{NiCo})_1 \text{ Adm}^{-2}$	6.63	148.6	113.1	1109	1227
$(\text{NiCo})_2 \text{ Adm}^{-2}$	8.06	203.0	79.90	1472	918
$(\text{NiCo})_3 \text{ Adm}^{-2}$	8.63	334.9	74.81	2132	632
$(\text{NiCo})_4 \text{ Adm}^{-2}$	8.75	510	54.49	2736	256

### 7.3.5.2 Potentiodynamic polarization method

After EIS study, NiCo alloy coatings are subjected to potentiodynamic polarization study, and corresponding polarization curves are shown in Figure 7.6. The corrosion rates (CR) of all alloy coatings were evaluated by Tafel's extrapolation method, by taking the composition based equivalent weight of the alloy. The composition and corrosion data of each alloy coating is reported in Table 7.4.

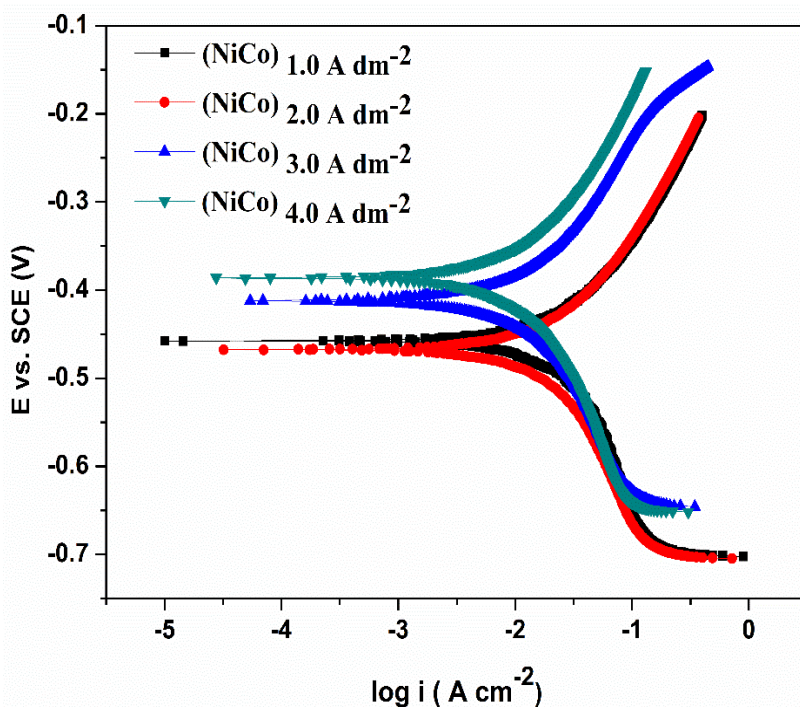


**Figure 7.6** - Polarization behaviour of NiCo alloy coatings deposited at different current densities from optimized bath.

The CR values, calculated through Tafel's method testimonies once again that (NiCo)<sub>4.0 Adm<sup>-2</sup></sub> offers highest corrosion resistance (least CR), compared all other coatings. Moreover, the highest corrosion stability of (NiCo)<sub>4.0 Adm<sup>-2</sup></sub> coating is further supported its highest corrosion potential ( $E_{\text{corr}}$ ) value, as shown in Figure 7.6. Thus, from surface analysis, compositional information and corrosion data (evidenced by both EIS and potentiodynamic polarization methods) of NiCo alloy coatings, it may be stated that that the least of CR of (NiCo)<sub>4.0 Adm<sup>-2</sup></sub> coating is affiliated to decreased surface roughness (Figure 7.3), and highest noble metal (Ni) content (38.6 Wt.%) as shown in Table 7.4.

**Table 7.4 - Corrosion parameters of NiCo coatings deposited at different current densities with wt. % metals content in the deposit, in relation to those in the bath (given at the bottom)**

current density ( $\text{Adm}^{-2}$ )	wt. % of Ni	wt.% of Co	$-E_{\text{corr}}$ (V vs. SCE)	$i_{\text{corr}}$ ( $\mu\text{A cm}^{-2}$ )	$\text{CR} \times 10^{-2}$ ( $\text{mm y}^{-1}$ )
1.0	29.4	70.6	0.456	23.2	25.1
2.0	33.3	66.7	0.467	18.2	19.7
3.0	35.8	64.2	0.413	14.8	16.0
4.0	38.6	61.4	0.388	13.3	14.4
<i>Wt. % of metals in the bath</i>					
	83.3	16.7			

### **7.3.6 Improvisation of corrosion protection efficacy of monolayer NiCo alloy coatings by multilayer approach**

Taking the advent of multilayer coating technology, the corrosion protection performance of NiCo alloy coatings was tried to increase by coating in layered fashion, by periodic pulsing of DC. Multilayer NiCo alloy coatings were developed from the optimized bath (Table 7.1) by making the power source to switch between two cathode current densities, periodically. It may be noted that in the present study, the current density is made to cycle (pulse) between two values, and those current densities are conveniently called ‘cyclic cathode current densities’ (CCCD’s), as described elsewhere (Raveendran and Hegde 2021). The composition and thickness of individual layers of multilayer coating were altered, precisely and conveniently by cyclic modulation of the current densities and duration, respectively.

#### **7.3.6.1 Optimization of CCCD’s**

The basic principle of multilayer coatings is that their best performance are attainable on fulfilling two important requirements. One is that a clear cut compositional demarcation between two layers, and other one is that the thickness of individual layers must be as thin as possible. Therefore, before going for increased number of layers of NiCo alloy coating, it is necessary to optimize the composition of alternate layers. In this regard, optimization of CCCD's have been done using the optimized bath. This step

involves the development of multilayer coating having 10 layers (arbitrarily chosen value), at different set of deposition current densities, and their corrosion performances were evaluated by EIS and potentiodynamic polarization method. The EIS response and potentiodynamic polarization curves of representative NiCo alloy coatings having 10 layers are shown in Figures 7.7 and 7.8, respectively, and corresponding corrosion data is reported in the Table 7.5.

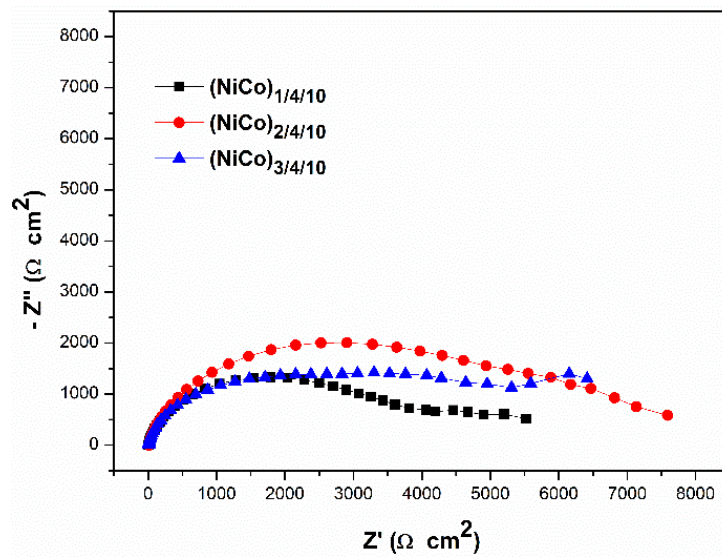


**Figure 7.7** - Nyquist plots of multilayer NiCo alloy coating having 10 layers of alloy of different composition, deposited at different set of CCD's, from optimized bath.

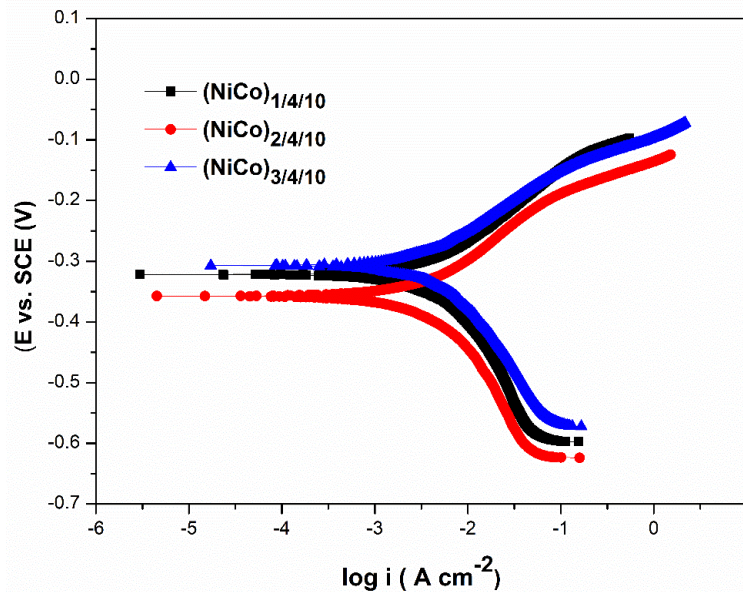


**Figure 7.8** - Tafel plots of multilayer NiCo alloy coating having 10 layers of alloys of different composition, deposited at different set of CCD's, from optimized bath.

**Table 7.5 - Corrosion parameters of multilayer NiCo alloy coatings having 10 alternate layers of alloys of different composition, deposited at different current density from optimal bath.**

Coating configuration	wt. % of Ni	wt.% of Co	$-E_{\text{corr}}$ (V vs SCE)	$i_{\text{corr}}$ ( $\mu\text{A cm}^{-2}$ )	$R_{\text{ct}}$ ( $\Omega$ )	CR $\times 10^{-2}$ ( $\text{mm y}^{-1}$ )
(NiCo) <sub>1.0/4.0/10</sub>	34.00	66.00	0.319	4.12	2250	4.45
(NiCo) <sub>2.0/4.0/10</sub>	35.93	64.07	0.355	2.90	3296	3.14
(NiCo) <sub>3.0/4.0/10</sub>	34.2	62.80	0.301	3.17	4626	3.43
(NiCo) <sub>4.0 Adm<sup>-2</sup></sub>	38.60	61.40	0.388	13.32	2736	14.41

On comparing the corrosion rate values, reported in Table 7.5, it may be noted that all NiCo multilayer coatings, off course all with only 10 layers are showing better anticorrosion behaviour, compared to its monolayer coating, developed from the same bath. It may also be noted that among many sets of CCCD's tried, the least CR was observed in one set of CCCD's. *i.e.*, at 2.0 and 4.0 Adm<sup>-2</sup>. This least CR corresponding to (NiCo)<sub>2.0/4.0/10</sub> configuration is pointing to the fact that its layers are of most optimal composition for getting the highest corrosion resistance. Therefore, 2.0 Adm<sup>-2</sup> and 4.0 Adm<sup>-2</sup> have been selected as optimal CCCD's for further layering.

### 7.3.6.2 Effect of layering

To explore the best anticorrosion performance of multilayer coatings developed by pulsing the deposition current densities between 2.0 Adm<sup>-2</sup> and 4.0 Adm<sup>-2</sup>, further layering was carried out. Accordingly, multilayer NiCo alloy coating having 10, 30, 60, 120,300 and 600 layers were developed using the same bath, and their corrosion behaviours were evaluated. Here, it is important to note that these number of layers were conveniently chosen to examine the effect of increasing the number of layers, within the limitation of power source, used to drive the process of deposition.

### 7.3.7 Corrosion study of multilayer NiCo coating

The same EIS and potentiodynamic polarization methods were used to test effect of layering on the corrosion stability of multilayer NiCo alloy coatings, and experimental observations are discussed as below.

#### 7.3.7.1 EIS study

EIS is a versatile AC technique used to characterize electrochemical processes taking place at the electrode-electrolyte interface. Impedance ( $Z$ ) is AC analogue of DC resistance, and is the vector ratio of potential to current. Here, a sinusoidal potential of a given frequency is applied, and its current is measured. EIS data can be presented in Nyquist format, where the negative of the imaginary component ( $-Z''$ ) is plotted against the real component ( $Z'$ ). Out of different electrochemical techniques available for studying the corrosion of metals, EIS study is extensively used to understand the reaction mechanism. Accordingly, Nyquist plots of multilayer NiCo alloy coatings, having different number of layers are shown in Figure 7.9.

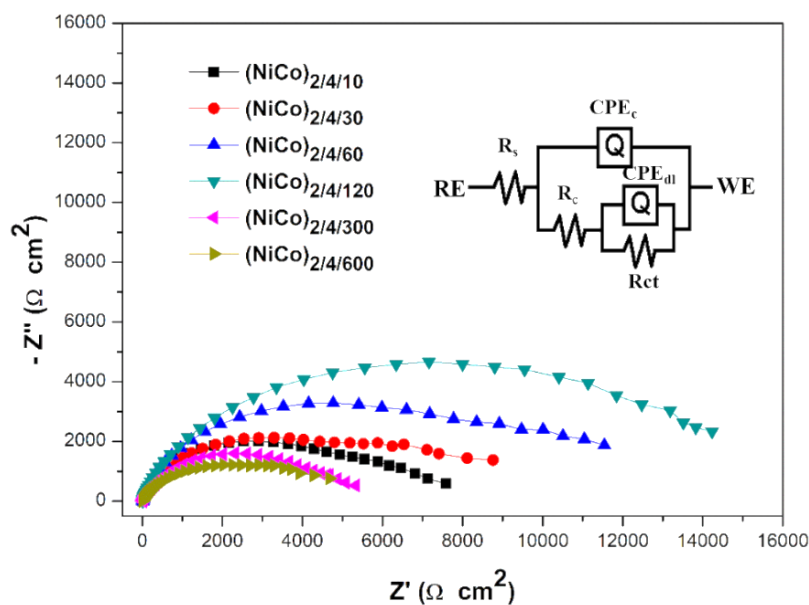


**Figure 7.9** - Nyquist plots of multilayer  $(\text{NiCo})_{2.0/4.0}$  alloy coatings having different number of layers deposited from the optimized bath.

The similar Nyquist responses, shown in Figure 7.9 indicates that same corrosion protection mechanism holds well, in coatings of all configurations. The Impedance response of multilayer coatings alloy coatings are further analyzed through



electrochemical equivalent circuit, shown in the inset of Figure 7.9. The magnitude of different circuit elements, responsible for improved corrosion protection are compiled in Table 7.6. Here,  $R_s$  represents the solution resistance, if  $R_c$  and  $Q_c$  denotes the resistant and capacitance of the coatings, respectively. Further,  $R_{ct}$  represents the resistance of double layer, and  $Q_{dl}$  is the constant phase element of charge transfer at the coatings/substrate interface.

**Table 7. 6 - EIS data obtained by equivalent circuit simulation of NiCo alloy coating having different number of layers deposited from the optimized bath**

Coating configuration	$R_s$ ( $\Omega$ )	$R_c$ ( $\Omega$ )	$Q_c$ ( $\mu F$ )	$R_{ct}$ ( $\Omega$ )	$Q_{dl}$ ( $\mu F$ )
(NiCo) <sub>2.0/4.0/10</sub>	8.74	3838	88.99	3296	290.5
(NiCo) <sub>2.0/4.0/30</sub>	8.33	3124	82.02	6154	250.3
(NiCo) <sub>2.0/4.0/60</sub>	8.94	5618	80.89	6359	242.6
(Ni Co) <sub>2.0/4.0/120</sub>	8.41	3822	48.87	12068	86.01
(NiCo) <sub>2.0/4.0/300</sub>	8.03	705.8	78.46	4611	134.1
(NiCo) <sub>2.0/4.0/600</sub>	8.28	383.8	128. 3	4714	253.6
(NiCo) <sub>4.0 Adm<sup>-2</sup></sub>	8.75	511.2	54.33	2836	256.0

It may be noted that the absence of Warburg impedance element in the circuit indicates the corrosion process is a charge transfer process instead of a diffusion controlled. In addition, the value of solution resistance ( $R_s$ ) remained to be constant as the same electrolyte solution was used throughout. EIS response clearly shows that the value of coating resistance ( $R_c$ ) increased progressively with number of layers up to 120 layers, and then decreased. The decrease in diameter of the capacitive loop of (NiCo)<sub>2.0/4.0/300</sub> multilayer coating clearly reveals the decreased corrosion stability of alloy coatings at higher degree of layering. *i.e.* at 600 layers.

### 7.3.7.2 Potentiodynamic polarization study

Potentiodynamic polarization behaviour of developed coatings were demonstrated in the form of Tafel plots in Figure 7.10. The corrosion data of multilayer NiCo alloy coatings, having different configurations are reported in Table 7.7, along with the CR of monolayer (NiCo)<sub>4.0</sub> coating, for comparison purpose. As may be seen, that  $i_{corr}$  value

has decreased with increasing the number of layers from 10-120 layers, and further it increased. The maximum anticorrosion performance was exhibited by the NiCo alloy coatings having 120 layers with least corrosion rate (CR) as may be seen in Table 7.10. The CR of multilayer NiCo alloy coatings was found to be decreased with further increase in number of layers. This decrease of corrosion stability of multilayer coatings at higher degree of layering (as confirmed by both EIS and potentiodynamic polarization study) may be attributed to diffusion of layers, due to short layering period as explained earlier (Section 5.3.6).

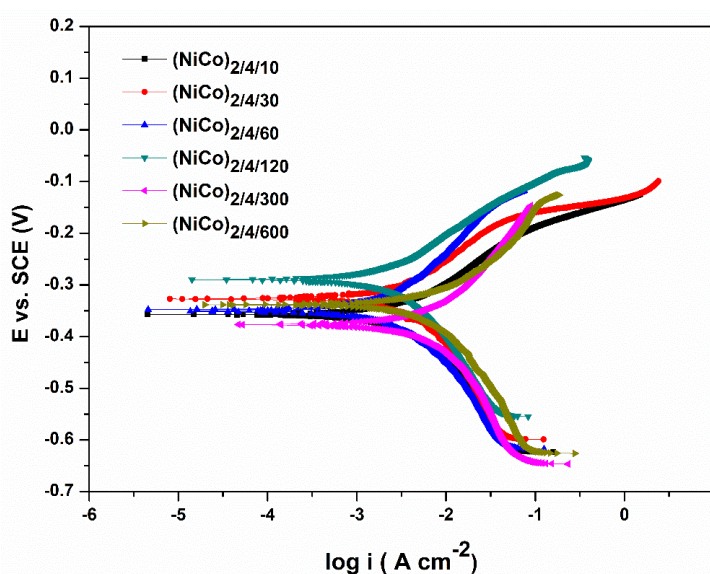


**Figure 7.10** - Tafel's plots of multilayer (NiCo)<sub>2.0/4.0</sub> alloy coatings having different number of layers deposited from optimized bath.

**Table 7.7-** Corrosion data of multilayer NiCo alloy coatings having different number of layers deposited from the optimized bath.

Coating configuration	-E <sub>corr</sub> (V vs. SCE)	i <sub>corr</sub> (μA cm <sup>-2</sup> )	CR x10 <sup>-2</sup> (mm y <sup>-1</sup> )
(NiCo) <sub>2.0/4.0/10</sub>	0.355	2.90	3.14
(NiCo) <sub>2.0/4.0/30</sub>	0.326	2.76	2.99
(NiCo) <sub>2.0/4.0/60</sub>	0.347	2.29	2.48
(NiCo) <sub>2.0/4.0/120</sub>	0.289	1.59	1.72
(NiCo) <sub>2.0/4.0/300</sub>	0.375	8.37	9.06
(NiCo) <sub>2.0/4.0/600</sub>	0.341	10.18	11.01
(NiCo) <sub>4.0 Adm</sub> <sup>-2</sup>	0.311	15.25	14.89

### 7. 3. 8 Discussion on corrosion protection behaviour of monolayer and multilayer NiCo alloy coatings

The corrosion protection ability of monolayer and multilayer NiCo alloy coatings (both optimized for best performance) were compared through impedance and potentiodynamic polarization methods, and corresponding plots are shown in the Figure 7.11. The Nyquist and Tafel's plots clearly revealed that multilayer  $(\text{NiCo})_{2.0/4.0/120}$  alloy coating is far more corrosion resistant than its monolayer counterpart  $(\text{NiCo})_{4.0}$ .

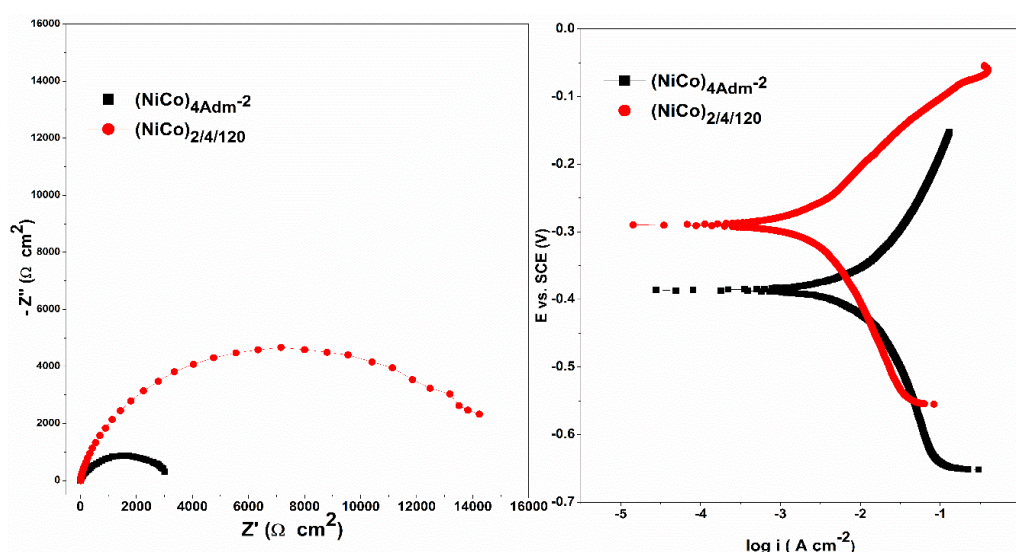


**Figure 7.11-** Comparison of impedance and polarization behaviour of monolayer  $(\text{NiCo})_{4\text{Adm}^{-2}}$  and multilayer  $(\text{NiCo})_{1.0/3.0/120}$  alloy coatings through: a) Nyquist plots and b) Tafel's plots.

It may be seen that in case of Nyquist plot, a drastic increase of coating resistance value ( $R_{ct}$ ) was found, compared to its monolayer counterpart. Similarly, a significant change of  $i_{\text{corr}}$ ,  $E_{\text{corr}}$  and corrosion rate values were observed in case Tafel's plots, indicating multilayer NiCo alloy coating is highly corrosion resistant, compared to its monolayer coating. Thus on comparing the CR's of monolayer and multilayer NiCo alloy coatings, it may be inferred that under optimal condition, multilayer NiCo alloy coating is about thirteen times more corrosion resistant than its monolayer coating, deposited from same bath for same duration. However, at high degree of layering, *i.e.*, at 300 and 600 layers, it was observed that corrosion resistance of multilayer coatings were decreased. Which means, initially, the increasing the number of layers imparts the

barrier property for the multilayer coating against corrosion. But on high degree of layering, due to very less time of deposition of each layer (2 s and 1s for 300 layer and 600 layers, respectively) the multilayer coating acts as a monolayer.

### 7. 3. 9 Mechanism of corrosion in multilayer coating

The formation of layered structure in multilayer coating, produced by pulsing the current densities between two values are confirmed by taking the cross-sectional view of multilayer coating. The cross-sectional view of multilayer NiCo alloy, having 10 layers are shown in Figure 7.12.

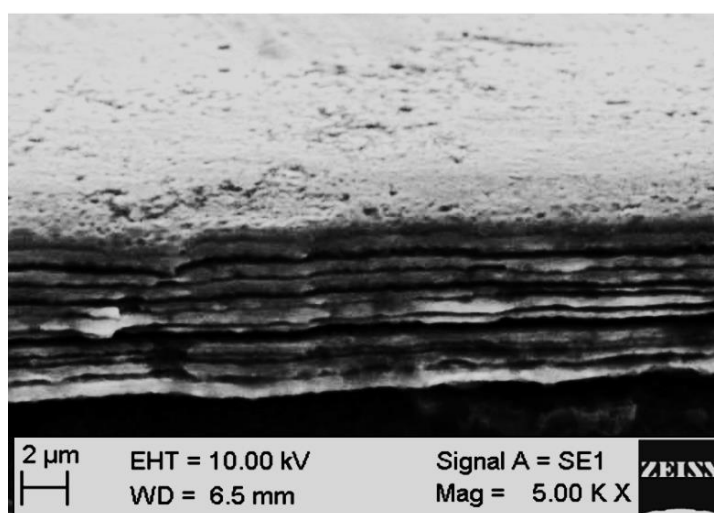


**Figure 7.12** - Cross-sectional SEM image of  $(NiCo)_{2.0/4.0/10}$  coating showing the formation of layered coating (having 10 layers).

Thus, better anticorrosion performance of multilayer NiCo alloy coatings in relation to its monolayer alloy coating was attributed to the selective dissolution of layers of different compositions. In case of multilayer coating the corrosion medium penetrates through micro paths which continues through the interfaces of adjacent layers which exhibit different structural morphology and chemical composition. Hence, in case of multilayer coating the localized corrosion spread to the surrounding areas rather than penetrating into the interior structures and finally to the substrate. This lateral spreading of corrosion medium leading to lagging of corrosion rate in multilayered coatings. As a result, by increasing the number of layers, much time is needed to penetration the corrosive agent within the coatings and reaching into the substrate. Thus, the corrosion resistance enhances by increasing the number of layers. However, in case of monolayer

coatings, the vertical penetration of the corrosive agent takes place which leads higher corrosion rate of monolayer coatings, compared to the multilayered one. However, again at higher degree of layering, due to the diffusion of layers proper demarcation between the layers were not observed, and leads to decrease of corrosion resistance if alloy coatings (Bahadormanesh et al. 2017; Raveendran and Hegde 2021; Shourgeshty et al. 2017).

#### 7.4 CONCLUSIONS

The work of formulation of a new electrolytic bath for development of more corrosion resistant NiCo alloy coatings, and its improvisation by multilayer approach led to the following conclusions:

1. A bright and uniform NiCo alloy coatings have been electroplated from the optimized bath at varied current densities, and condition for development of highest corrosion protection has been proposed.
2. The compositional study of alloy coatings confirmed that bath follows anomalous type of co-deposition in the limit of current density studied ( $1.0 - 4.0 \text{ Adm}^{-2}$ ), with more wt. % of Co in the deposit, than in the bath.
3. Hike in the Ni content of the alloy with current density is due to preferential deposition of Ni, supported by XRD analysis is due to depletion of less noble metal ions ( $\text{Co}^{+2}$ ) at cathode layer.
4. The corrosion study revealed that monolayer  $(\text{NiCo})_{4.0 \text{ Adm}^{-2}}$  alloy coating is less corrosive compared to all other coatings. It stands for the reason of its highest Ni content (38.6 Wt. %), which increased surface smoothness of the alloy coating, evidenced by EDS-SEM and AFM study.
5. The corrosion resistance property of monolayer NiCo alloy coating was further enhanced by multilayer approach by periodic modulation of current density, during process of deposition.
6. The deposition conditions of multilayer coating was optimized to maximize its performance against corrosion by proper modulation of composition and thickness of individual layers by pulsing the current density (pulse amplitude) and duration of pulse (time), respectively.

7. The surface feature, phase structure and compositional change of NiCo alloy coatings of both monolayer and multilayer type were examined, using Scanning electron microscopy (SEM), Atomic force microscopy (AFM), X-ray diffraction (XRD), and Energy dispersive X-ray spectroscopy (EDS) techniques.
8. The corrosion stability of multilayer (NiCo) alloy coatings were found to be increased to the extent of 120 layers, and then started decreasing. This decrease of CR at higher degree of layers was attributed to the diffusion of individual layers, affected due to short pulsing period.
9. Under optimal condition, multilayer NiCo alloy coating, having 120 layers is about thirteen times more corrosion resistant than its monolayer coating, deposited from same bath for same duration.

## **CHAPTER 8**

# **IMPROVISATION OF CORROSION RESISTANCE OF NiCo ALLOY COATINGS THROUGH MAGNETO- ELECTRODEPOSITION**





## CHAPTER 8

### IMPROVISATION OF CORROSION RESISTANCE OF NiCo ALLOY COATINGS THROUGH MAGNETO- ELECTRODEPOSITION

---

*Having limited by low limiting current density ( $i_L$ ) of Ni in the proposed NiCo bath, the corrosion resistance of NiCo alloy coatings, developed under the optimal condition was attempted to enhance further through magneto-electrodeposition method. This chapter devoted to explain how corrosion resistances of NiCo alloy coatings can be improved drastically with magnetic field ( $B$ ), applied simultaneously to the process of deposition. Experimental results manifested that magneto-electrodeposited (MED) NiCo alloy coatings developed under parallel and perpendicular  $B$  are respectively, about 4 and 13 times less corrosive than electrodeposited (ED) alloy coatings developed from the same bath, for same time. Properties of MED alloy coatings have been analysed by SEM-EDS and XRD studies. The reasons responsible for improved corrosion resistance of MED coatings were explained through  $B$  controlled diffusion of more noble of  $Ni^{2+}$  ions, and magnetic field-controlled limiting current density ( $i_L$ ) of metal ions. It was observed that the effect of  $B$  is more pronounced in case of perpendicular than parallel. Improved corrosion resistance property of NiCo alloy coatings were explained on the basis of Lorentz force ( $F_L$ ) coupled magneto-hydrodynamic (MHD) effect. The experimental results are discussed in the light of changed composition, phase structure, surface morphology of alloy coatings, affected due to magneto-convection effect, and results are discussed.*

#### 8.1 INTRODUCTION

The effect of magnetic field on the process of electrodeposition of metal, alloys, polymer and composite coatings were the main area of interest for many researcher for past several years. The application of magnetic field on electrochemical deposition process can improve the mass transfer process, deposit quality and thereby its corrosion behaviour. It is well established fact that under normal conditions of electrodeposition,

NiCo bath follows anomalous type of codeposition, where less noble metal (cobalt) is preferentially deposited, compared to the more noble metal (nickel). As envisaged by Brenner, this phenomenon of anomalous type of co-deposition is mainly due to formation hydroxide of less noble metal (Co) on the surface of substrate, which suppresses the deposition of more noble metal (Ni). Thus the inherent limitation of anomalous codeposition of NiCo alloy coating was tried to alleviate using the advantage of magnetic field effect. The advantage of magnetic field effect on the process of electrodeposition was reviewed in detail by Fahidy *et al* (Fahidy 1983). It has been described that the applied magnetic field primarily effects the transport of ions towards cathode, and consequently alters the thickness of electrical double layer (EDL). This change in mass transport process is responsible for change of surface morphology of the deposit, by altering the thickness of the double layer. Thus, corrosion performance of NiCo alloy coatings can be improved, by altering the mass transport process during their deposition, at the electrode-electrolyte interface. This can be brought by taking the advantage of magnetic field effect, called magnetoelectrodeposition, and the effect is called magnetohydrodynamic (MHD) effect. Thus, superposition magnetic field develops a new route for developing material of better corrosion properties. The effect on deposit characteristic mainly dependant on intensity and direction (parallel and perpendicular) of applied magnetic field. Therefore, in continuation of our work presented in pervious Chapter -7, an attempt has been made to enhance the corrosion resistance properties of monolayer NiCo alloy coating by magnetoelectrodeposition method. Effect of inducing the magnetic field, both intensity and direction on the corrosion behaviour of NiCo ally coatings have been studied, and results are presented here.

## **8.2 EXPERIMENTAL**

### **8.2.1 Magneto-electrodeposition of NiCo alloy coatings**

Initially, monolayer NiCo alloy coatings are electrodeposited at different current densities from the optimized bath using direct current (DC). *i.e.*, by applying only electric field. The current density, at which the NiCo alloy coating showed the least corrosion rate was identified. It was found that monolayer NiCo alloy coating deposited at  $4.0 \text{ Adm}^{-2}$ , abbreviated as ED (NiCo)<sub>4.0 Adm<sup>-2</sup></sub> has the highest corrosion resistance,

compared to all other coatings. Then, magneto-electrodeposited NiCo alloy coatings, abbreviated as MED NiCo are electrodeposited in conjunction with the effect of magnetic field. MED NiCo alloy coatings were achieved by employing a DC power source (DC Power Analyzer, Agilent Technologies, Model: N6705) at the required current density in conjunction with an electromagnet (Polytronics, Model: EM 100) to induce magnetic field effect during process of electrodeposition. The bath pH was kept constant as 3.0; and before each deposition it was adjusted to 3.0, using either  $\text{NH}_4\text{OH}$  or  $\text{H}_2\text{SO}_4$ .

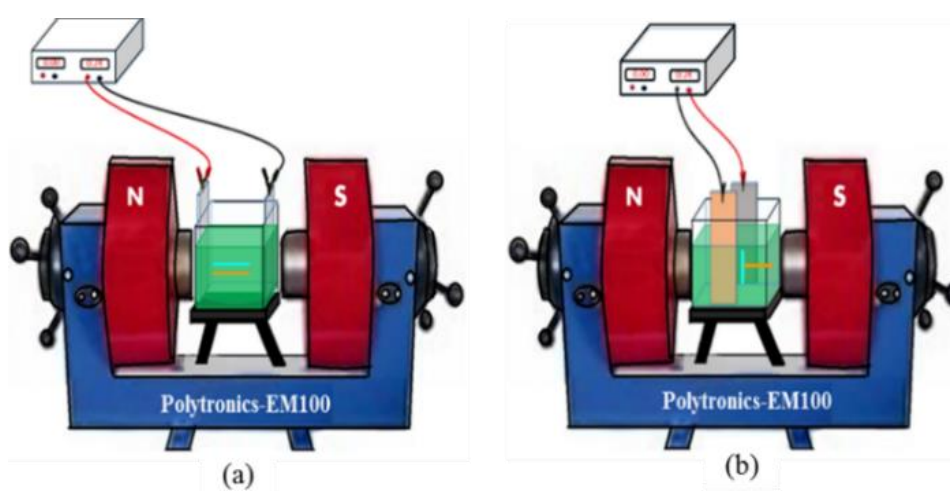


**Figure 8.1-** The experimental set up used for magneto-electrodeposition of NiCo alloy coating under condition of a) parallel, and b) perpendicular to  $B$  to the direction of electrical field. It may be noted that in a) lines of electric field and magnetic field are parallel, and in b) they are perpendicular to each other.

It is well-known fact that the magnetic field introduction during the electrodeposition process can bring significant change in the composition, phase structure and surface morphology of alloy coatings. Keeping this in mind, the corrosion resistance properties of NiCo alloy coatings were tried enhance by inducing magnetic field, in different direction (parallel and perpendicular the direction of electric field) and intensities, expressed in Tesla (T) from 0.1 T - 0.4T. The experimental set up used for magneto-electrodeposition of NiCo alloy coatings are shown in Figure 8.1. To understand the influence of induced magnetic field on process of deposition, the

deposition current density was kept constant. *i.e.*,  $4.0 \text{ Adm}^{-2}$ , which was fixed as the optimal current density, from the previous study.

During the magnetoelectrodeposition, the customized cell having electrolyte of optimized bath (Table 3.1) was centrally placed, between the poles of two electromagnet, as shown Figures 8.1 (a) and (b). It shows two situations, where magnetic field applied is parallel and perpendicular the direction of flow of ions, respectively. The graphite anode, having same exposed area as cathode was used, and were kept 5 cm apart from each other. All coatings were washed using distilled water, followed by air drying. The magneto electrodeposited NiCo alloy coatings were analysed for the composition, phase structure, surface roughness and surface morphology. Further, the corrosion resistance properties of electrodeposited coatings were evaluated in 3.5% NaCl medium, by EIS and potentiodynamic polarization methods. Here for convenience, electrodeposited and magnetoelectrodeposited NiCo alloy coatings are represented as ED (NiCo) and MED (NiCo) alloy coatings, respectively. Further magnetoelectrodeposited NiCo alloy coatings are conveniently represented as  $(\text{NiCo})_{x/y/\text{Par or Per}}$ , where subscript 'x' and 'y' represent, respectively the current density and magnetic field density; and 'Par' and 'Per' stands for parallel and perpendicular magnetic field.

## 8.3 RESULTS AND DISCUSSION

### 8.3.1 SEM- EDS study

To understand the effect of magnetic field on the process of electro-crystallisation, NiCo alloy coatings were deposited under different intensity of  $B$  (both parallel and perpendicular in the range of 0.1T - 0.4T), at a constant current density of  $4.0 \text{ Adm}^{-2}$  (optimal c.d. of the bath), and were subjected to SEM-EDS analyses. The corresponding SEM images obtained are shown in Figures 8.2 and 8.3, and their composition data are reported in Table 8.1. From Figures 8.2 and 8.3, it may be noted that uniformity of alloy coatings has improved drastically due to superimposition of magnetic field. For comparison purpose, surface morphology of  $(\text{NiCo})_{4.0 \text{ Adm}^{-2}}$  coating, developed without the effect of  $B$  is shown in the inset of Figures 8.2 and 8.3. From the SEM micrograph of NiCo alloy coatings, it may be noted that applied magnetic field affects the resulting

deposit morphology substantially (both parallel and perpendicular) by reducing the grain structure. Further, degree of uniformity of coatings was found to be increased with increase of intensity of  $B$ , as may be seen in both Figures 8.2 and 8.3. Thus, SEM images shown in Figures 8.2 and 8.3 demonstrates increase of uniformity of coatings while changing the magnetic field, in both strength and directions. However, effect is more pronounced in case of perpendicular  $B$ . In addition, at higher limits of  $B$ , *i.e.* at 0.4T the surface roughness of coating again started increasing as shown in Figure 8.3. The highest corrosion resistance of MED (NiCo)<sub>4.0/0.3T/Per</sub> coating could be due to this surface smoothness. However, the coatings developed in presence of parallel magnetic field shows comparatively less smoothed surface than coatings produced under perpendicular  $B$ . It may be noted that there is an innate relationship between surface morphology and corrosion resistance property of alloy coatings. However, at 0.4T, the corrosion rate increases in both cases, due to excessive porosity of the coating, affected due to excessive evolution of H<sub>2</sub> on its surface.

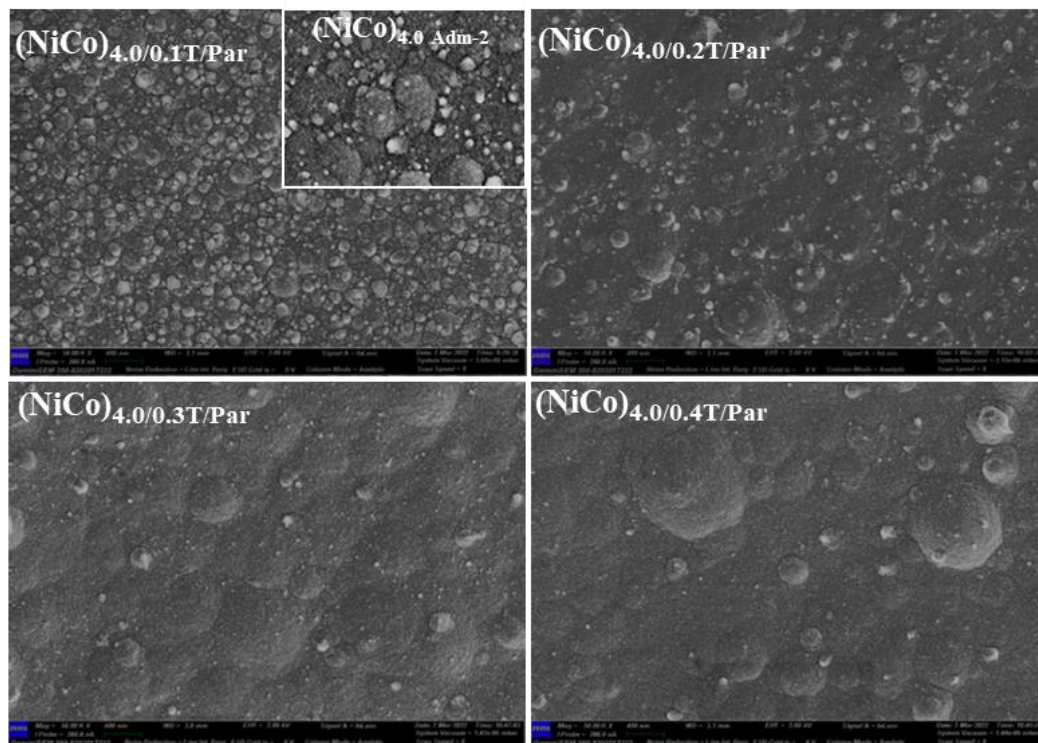


**Figure 8.2** - Surface morphology of MED (NiCo) alloy coatings developed from the optimized bath under different intensity of  $B$  (parallel). In the inset is given (NiCo)<sub>4.0</sub> Adm<sup>-2</sup> alloy deposited without the effect of  $B$ , showing rough surface.

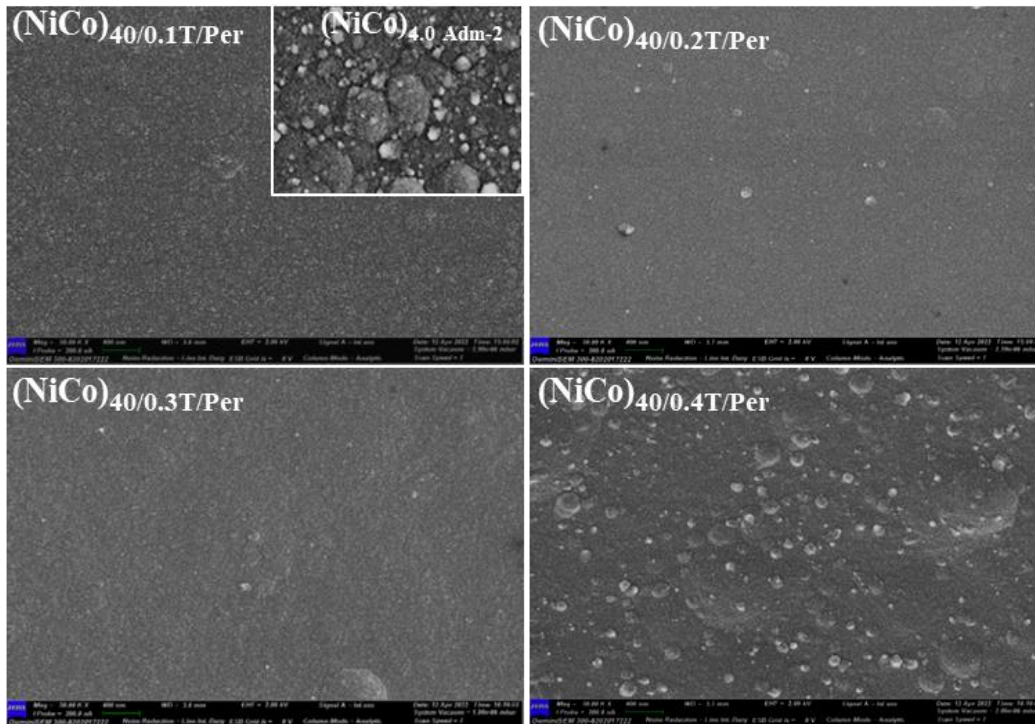


**Figure 8.3-** Surface morphology of MED (NiCo) alloy coatings developed from the optimized bath under different intensity of  $B$  (perpendicular) In inset is given  $(\text{NiCo})_{4.0} \text{Adm}^{-2}$  alloy deposited without the effect of  $B$ , showing rough surface.

### 8.3.2 Effect of $B$ on composition

The change in the Wt. % of noble metal (Ni) content of alloy coatings (generally responsible for its good corrosion resistance behaviour) with intensity and direction of  $B$  are shown Table 8.1. From the composition data, it may be noted that Wt. % Ni in the deposit increased drastically with intensity of  $B$ , in both parallel and perpendicular magnetic field. It may be recalled that the Wt. % Ni in the ED (NiCo) alloy coating, developed without the effect of  $B$  is 38.60 and is shown in Table 8.1. The variation of Wt.% of Ni and Co in the MED (NiCo) alloy coatings with intensity of  $B$  (for both parallel and perpendicular field) is shown diagrammatically in Figure 8.4. Here, horizontal lines represent the Wt. % of individual metals in the ED (NiCo) alloy coatings.

**Table 8.1 – Corrosion parameters of magneto-electrodeposited NiCo alloy coatings from optimized bath under different conditions of  $B$ , in relation to its monolayer counterpart**

Coating configuration	Wt. % Ni in the deposit	Wt. % Co in the deposit	$-E_{\text{corr}}$ (V vs SCE)	$i_{\text{corr}}$ ( $\mu\text{A cm}^{-2}$ )	$\text{CR} \times 10^{-2}$ ( $\text{mmy}^{-1}$ )
(NiCo) <sub>4.0/0.1T/Par</sub>	38.93	61.07	0.367	12.19	13.19
(Ni-Co) <sub>4.0/0.2T/Par</sub>	49.57	50.43	0.384	10.67	11.53
(Ni-Co) <sub>4.0/0.3T/Par</sub>	55.81	44.19	0.293	3.51	3.78
(Ni-Co) <sub>4.0/0.4T/Par</sub>	55.24	44.76	0.358	6.32	6.83
<i>Under perpendicular field</i>					
(NiCo) <sub>4.0/0.1T/Per</sub>	58.91	41.09	0.316	3.05	3.29
(Ni-Co) <sub>4.0/0.2T/Per</sub>	62.03	34.97	0.336	2.25	2.43
(NiCo) <sub>4.0/0.3T/Per</sub>	64.72	32.28	0.278	0.96	1.03
(NiCo) <sub>4.0/0.4T/Per</sub>	63.53	36.47	0.291	1.08	1.17
<b>(NiCo)<sub>4.0 Adm<sup>-2</sup></sub></b>	<b>38.60</b>	<b>61.40</b>	<b>13.32</b>	<b>2736</b>	<b>14.41</b>

Thus, from the nature of graph it may be noted that Wt.% of noble Ni increased with intensity of  $B$ , in both parallel and perpendicular magnetic field. However, this increase of Ni with intensity of  $B$  is more pronounced in case of perpendicular field. A slight decrease of Ni content at very high intensity of  $B$  (0.4T), was found in both parallel and perpendicular magnetic field as shown in the Figure 8.4.

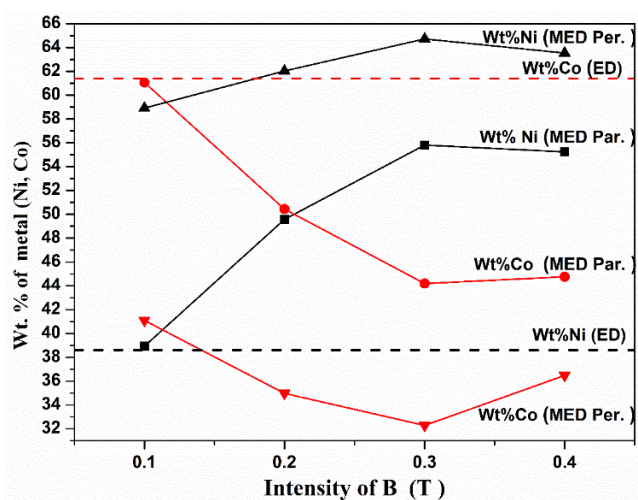


**Figure 8.4-** Variation in the Wt % of Ni and Co in ED and MED NiCo alloy coatings deposited from optimized bath. Increase of Ni content in the deposit with  $B$  may be seen.

### 8.3.3 XRD Study

The XRD patterns of MED NiCo alloy coatings, developed at different field strengths, under parallel and perpendicular direction are given, respectively in Figures 8.5 and 8.6. It was observed that MED NiCo alloy coatings, regardless of the intensity and direction of the field exhibit the same crystal structures, consisting of both fcc and hcp phases. The lattice planes at (111), (200), (220) and (311) are reflections of fcc phase, whereas peaks (110) and (112) corresponds to the planes of hcp lattice.

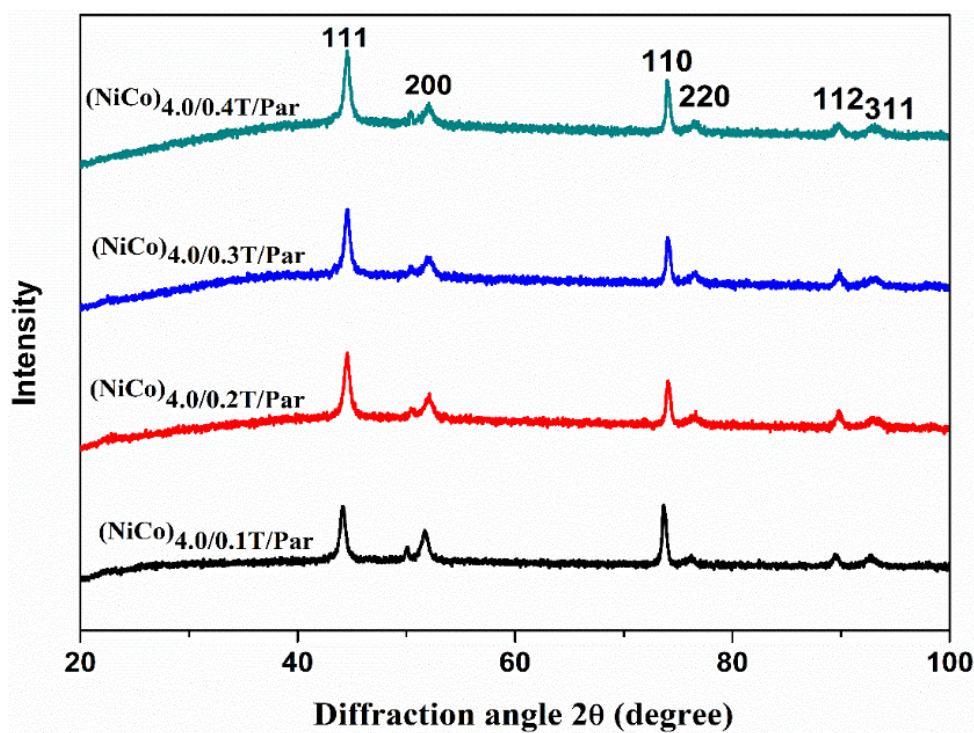


*Figure 8.5- XRD patterns of MED NiCo alloy coating obtained at different magnetic field strengths (parallel), under optimal current density from the optimized bath.*

It may be noted that the intensity of reflections was found to be change slightly with intensity of  $B$ , and in line with changed composition of the alloy (Table 8.1). Hence, from the intensity of peaks corresponding to hcp lattice plane, it may be inferred that decrease of peak intensity with increase of  $B$  is due to the decrease of cobalt content in the deposit. Parallely, the observed increase of intensities of fcc lattice planes with intensity of  $B$ , and is in agreement with increase of Ni content in the deposit.



Thus, XRD study of MED NiCo alloy coatings, under both parallel and perpendicular  $B$  reveals that applied magnetic field has an important role on composition of the alloy coatings, but not with their phase structures. Hence, it may be summarized that magneto electrodeposition of NiCo alloy coating is more a diffusion controlled, consequent to magnetic field controlled, without effecting the crystallinity of alloy coatings.

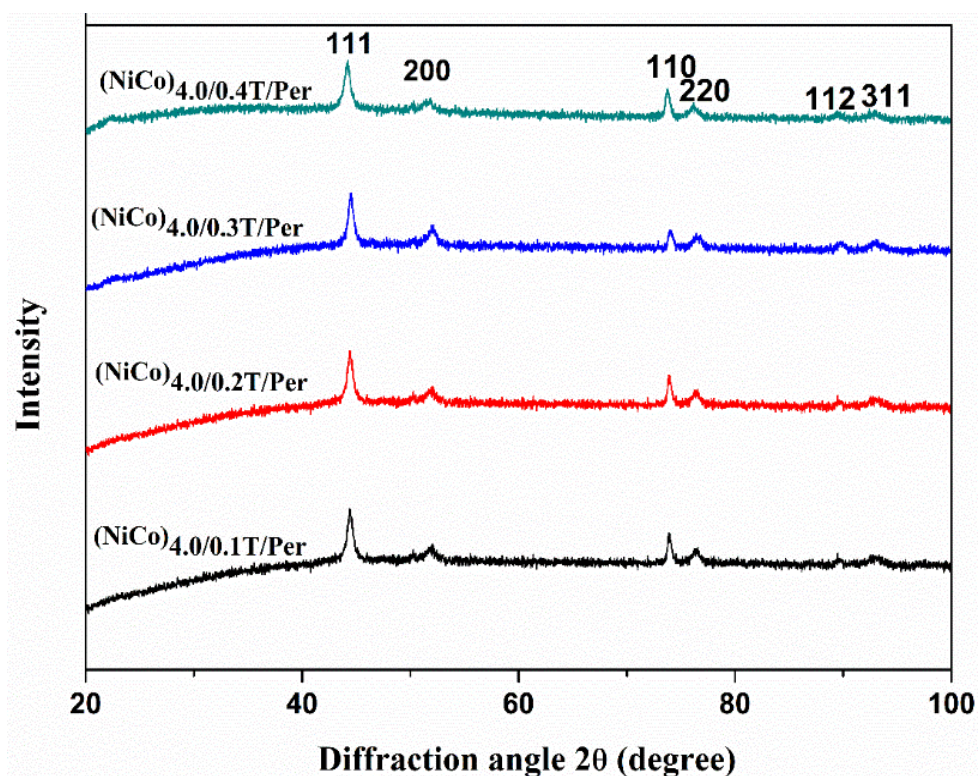


**Figure 8.6** - XRD patterns of Ni-Co alloy coating obtained at different magnetic field strength (perpendicular), under optimal current density from the optimized bath. The same diffraction angles to all coatings deposited at different intensity of  $B$  indicates that coatings of same phase structures are formed during deposition.

The crystallite size of MED NiCo alloy coatings was calculated using the Scherrer's formula. It was found that crystallite size of MED Ni-Co alloy coatings, under parallel and perpendicular conditions of  $B$  are, respectively 14.4nm and 13.4nm. This reduced crystallite size, in case of coatings developed under perpendicular  $B$  is responsible for decreased lattice strain, which is responsible for increased corrosion resistance of alloy coatings (Bakhit and Akbari 2013; Srivastava et al. 2006).

### 8.3.4 AFM Analysis

AFM is a powerful technique used for taking the topography of any surface. In this technique a sharp probe is made to scan mechanically across the surface, and the motion of probe is captured with a computer. The probe's motion is then used to create a three-dimensional image of the surface. Accordingly, AFM image of NiCo alloy coatings deposited under three optimal conditions, *i.e.* ED (NiCo)<sub>4.0</sub>Adm<sup>-2</sup>, MED (NiCo)<sub>4.0/0.3T/par</sub> and (NiCo)<sub>4.0/0.3T/per</sub> are taken in 10µm × 10µm area, and is shown in Figure 8.7. The surface roughness parameters, such as average roughness (R<sub>a</sub>) and root mean square roughness (R<sub>q</sub>) values obtained are tabulated in Table 8.2.

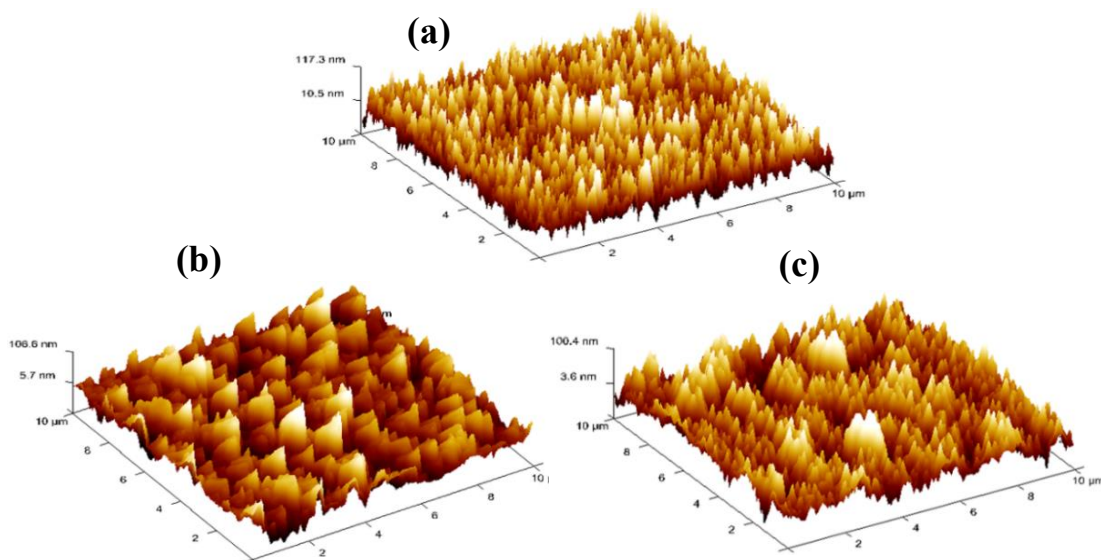


**Figure 8.7** - AFM image of NiCo alloy coatings deposited under different optimal conditions of electrodeposition : (a) ED(Ni-Co)<sub>4.0</sub>Adm<sup>-2</sup>, (b) MED(Ni-Co)<sub>4.0/0.3T/par</sub>, and (c) (Ni-Co)<sub>4.0/0.3T/per</sub>, from same bath.

The AFM image, shown in Figure 8.7 demonstrate that coatings deposited with and without the effect of magnetic field has significant difference. It may be noted that the surface roughness decreased substantially on superimposition of magnetic field, evident from data in Table 8.2. Moreover, effect is more pronounced when magnetic field is applied in perpendicular direction. This observation is in agreement with the surface information of alloy coatings, obtained through FESEM analyses.

**Table 8.2 - The surface roughness data of NiCo alloy coatings deposited under different optimal conditions of electrodeposition:(a) ED(Ni-Co)<sub>4.0Adm<sup>-2</sup></sub>, (b)MED(Ni-Co)<sub>4.0/0.3T/par</sub>, and (c)(Ni-Co)<sub>4.0/0.3T/per</sub>, from same bath.**

Coating configuration	R <sub>a</sub> (nm)	R <sub>q</sub> (nm)
(NiCo) <sub>4.0Adm<sup>-2</sup></sub>	24.5	30.8
(NiCo) <sub>4.0/0.3T/par</sub>	22.5	28.4
(NiCo) <sub>4.0/0.3T/per</sub>	20.9	26.6

### 8.3.5 Corrosion study

The corrosion resistance properties of the developed NiCo alloy coatings under natural and forced convection (by applying magnetic field) were analysed by the electrochemical techniques AC and DC techniques, and experimental results are discussed below.

#### 8.3.5.1 EIS study

EIS technique has been used as the tool to study the corrosion protection efficacy of magneto-electrodeposited (NiCo) alloy coatings in the 3.5% NaCl solution, as common corrosion medium. Nyquist plots of alloy coatings, deposited under the influence of both parallel and perpendicular magnetic field are shown in Figure 8.8. Further, the impedance responses were tried to understand in terms of the ongoing physicochemical process, responsible for better corrosion resistance by fitting the EIS data into an equivalent circuit. The circuit description code (CDC) for the equivalent circuit proposed for the coated samples are  $R_s(Q_c(R_c(Q_{dl}R_{ct})))$  (Srivastava et al. 2006). The circuit parameters associated with the fitted electrochemical equivalent circuit (EEC) is mentioned in Table 8.3. The electric circuit elements obtained in this model are, coating resistance  $R_c$ , constant phase element (CPE) of the alloy coatings ( $Q_c$ ), charge transfer resistance ( $R_{ct}$ ) and constant phase element (CPE) of the coatings-substrate interface ( $Q_{dl}$ ). It may be noted that the value of  $R_c$  and  $R_{ct}$ , put together constitute the polarization resistance of alloy coatings, and they are responsible for their corrosion resistance behaviors (Hefnawy et al. 2018; Xing et al. 2020) .

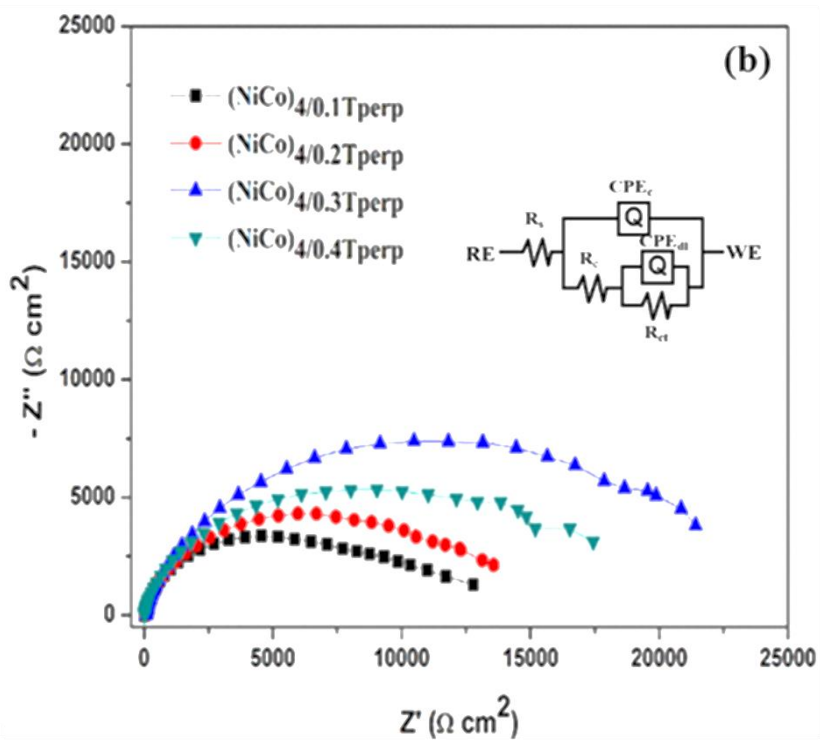
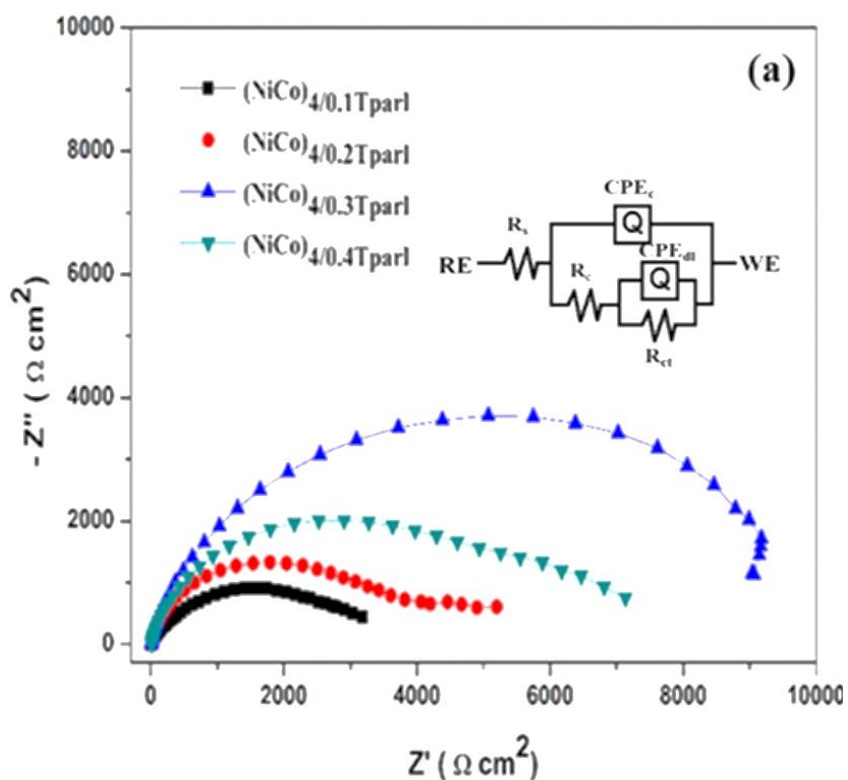


**Figure 8.8** - Nyquist response for MED (NiCo) alloy coatings deposited at different intensity of  $B$ : (a) parallel, and (b) perpendicular, deposited from same bath.

The diameter of capacitive loops of Nyquist plots represents the polarization resistance of the work electrode (Liu et al. 2016). Hence, it may be seen that in both parallel and perpendicular  $B$ , axial radius of the semicircle keeps increasing with the intensity of  $B$ , till 0.3 T and then decreased. This clearly suggests that the polarization resistance ( $R_p$ ) of MED coatings increased with intensity of  $B$ . But at high intensity of  $B$ , the value of  $R_p$  was found to be decreased once again. This is further supported by the data listed in the Table 8.1. Hence the  $(\text{NiCo})_{4.0/0.3\text{T/Per}}$  coating, with highest polarization resistance and less capacitance value shows that it is the least corrosive compared to all other coatings. Further, NiCo alloy coatings developed under all other parallel magnetic field are comparatively less corrosion resistant than  $(\text{NiCo})_{4.0/0.3\text{T/Per}}$ .

**Table 8.3 - EIS data obtained from equivalent circuit simulation of (NiCo) alloy coatings electrodeposited under different conditions of magnetic field ( $B$ )**

Coating configuration	$R_s$ ( $\Omega$ )	$R_c$ ( $\Omega$ )	$Q_c$ ( $\mu\text{F}$ )	$R_{ct}$ ( $\Omega$ )	$Q_{dl}$ ( $\mu\text{F}$ )
$(\text{NiCo})_{4.0/0.1\text{T/Par}}$	8.31	412.3	72.67	3067	266.0
$(\text{Ni-Co})_{4.0/0.2\text{T/Par}}$	8.48	2896	90.81	2250	270.4
$(\text{Ni-Co})_{4.0/0.3\text{T/Par}}$	8.78	4014	45.41	5912	74.95
$(\text{Ni-Co})_{4.0/0.4\text{T/Par}}$	8.88	3939	89.28	3260	513.8
$(\text{NiCo})_{4.0/0.1\text{T/Per}}$	8.67	6318	71.54	5686	314.4
$(\text{Ni-Co})_{4.0/0.2\text{T/Per}}$	8.43	4625	44.96	9964	103.3
$(\text{NiCo})_{4.0/0.3\text{T/Per}}$	8.78	6742	19.75	14730	44.51
$(\text{NiCo})_{4.0/0.4\text{T/Per}}$	8.36	6635	50.15	12990	114.1

The increased corrosion resistance of alloy coatings may be explained on the basis of their alloy composition, surface roughness and crystallite size. As mentioned above, an increased cobalt content towards higher  $B$ , lead to an increase of electrochemical activity, roughness and strain of the NiCo alloy matrix, and hence these factors are found to be responsible for their decreased corrosion resistance (Bakhit et al. 2014). The inhibition efficiency values obtained from the EIS measurements were congruent with those obtained from the polarization measurements (San et al. 2012).

### 8.3.5.2 Potentiodynamic polarization study

The potentiodynamic polarization behaviour of the magnetoelectrodeposited NiCo coatings, corresponding to different intensities of magnetic field applied in both parallel and perpendicular directions are shown in the form of Tafel's plot in the Figures 8.9 (a) and (b).

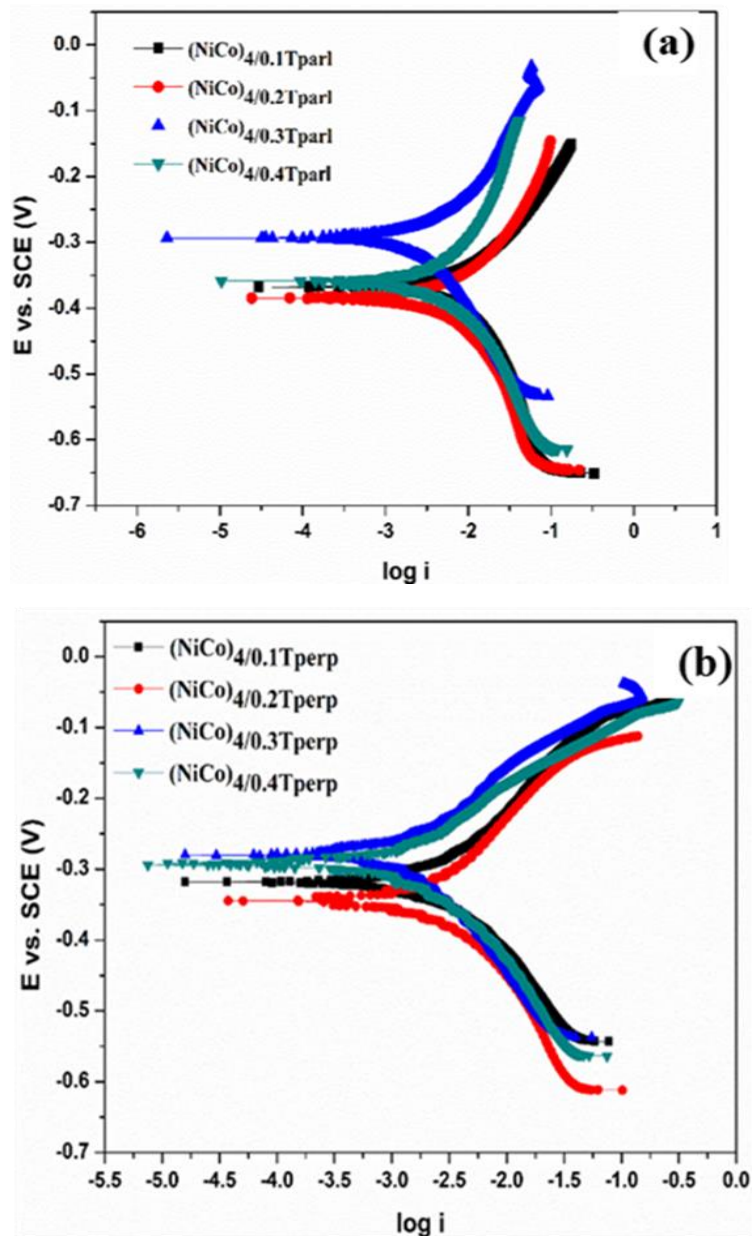


**Figure 8.9** - Potentiodynamic polarization behaviour of MED (NiCo) alloy coatings deposited at different conditions of magnetic field applied: (a) parallel and (b) perpendicular.

The rate of corrosion were calculated by Tafel's extrapolation method and corresponding data are reported in the Table 8.1. It was observed that irrespective of the direction of the magnetic field applied, its increasing strength, *i.e.*, up to 0.3T, the  $i_{\text{corr}}$  and corresponding corrosion rate value decreased, but there after it showed a rise in its values. Hence, it may be realized that super imposition of magnetic field during electrodeposition process can enhance the corrosion resistance properties of alloy coatings by brining changes in the deposit characteristics such as composition and surface morphology affected due to magneto-convection The increasing corrosion resistance of the coating is attributed to the increase in wt. % of nobler Ni in the deposit, due to superimposition of magnetic field. It was observed that CRs of MED (NiCo) alloy coatings decreased with the intensity of  $B$  only up to 0.3T, under both parallel and perpendicular  $B$ . But, on applying  $B$  greater than its limiting value (of the bath), it started giving a negative impact on the deposit characteristics, may be due increase in the hydrogen evolution reaction (HER) at the optimal current density. As a result, the coatings were shown to be rougher at higher limits of induced  $B$  (at 0.4T) with decreased nobler metal content. Hence, alloy coatings at higher intensity of  $B$  showed greater CR in both parallel and perpendicular fields (Table 8.1). In conclusion, MED (NiCo)<sub>4.0/0.3T/Per</sub> coating has the least corrosion rate ( $1.03 \times 10^{-2} \text{ mm y}^{-1}$ ) and MED (NiCo)<sub>4.0/0.3T/Par</sub> with CR value of  $3.78 \times 10^{-2} \text{ mm y}^{-1}$ . Hence, it may be noted that high CR value ( $14.41 \times 10^{-2} \text{ mm y}^{-1}$ ) of monolayer (NiCo) alloy coating, represented as (NiCo)<sub>4.0 Adm</sub><sup>-2</sup> has been improved to greater extent by magneto-electrodeposition.

The lower corrosion rate of magneto-electrodeposited (NiCo)<sub>4.0/0.3T/Per</sub> compared to MED (NiCo)<sub>4.0/0.3T/Par</sub> may be due to the additional magnetic convective effect of Lorentz force. In the case of parallel  $B$ , Lorentz force is applied to the charge density of the diffusion layer, a non-electrostatic field parallel to the surface of the working electrode is generated, and the solution moves near the interface. Whereas, in case of perpendicular magnetic field, the magneto convection is maximum due to the net effect of both non-electrostatic and electrostatic, due to that the magnetic convection effect is maximized for perpendicular  $B$ .

### 8.3.6 Comparison of ED and MED NiCo alloy coatings

The change of Ni and Co content in the magneto-electrodeposited NiCo alloy coatings under different conditions, in comparison with conventionally electrodeposited NiCo

alloy coatings is shown in the Figure 8.4. The horizontal lines in the graph indicate the metal (Ni and Co) content in ED coatings at  $4.0 \text{ Adm}^{-2}$ , where  $B = 0 \text{ T}$ . But it may be seen that on superimposition of  $B$  (both parallel and perpendicular), the noble metal (Ni) content of the deposit increased drastically, while decreasing its less noble metal (cobalt), in the beginning, and started decreasing at higher limits of  $B$  as shown in shown in Figure 8.4. At optimal intensity of  $B$  (0.3 T), of both parallel and perpendicular  $B$ , Ni content of alloy coatings is found to be 55.81 and 67.72 wt. %, respectively, compared to 38.6 wt. % corresponding to conventional ED coating. Hence, increase of Ni content in the deposit, affected due to magnetic field effect is responsible for improved corrosion resistance of MED NiCo alloy coatings. At optimal intensity of  $B$ , the Ni content of the deposit is found to be much high, and found to follow normal type of co-deposition, against anomalous type of co-deposition that the bath follows under normal conditions ( $B = 0 \text{ T}$ ). This drastic increase of Ni content in the deposit at higher limits of  $B$  (0.3T) is due to increase of its limiting current density value, affected due to magneto-convection effect.

The surface microstructure and the phase structure of ED  $(\text{NiCo})_{4.0 \text{ Adm}^{-2}}$ , MED  $(\text{NiCo})_{4.0/0.3\text{T}/\text{Par}}$  and  $(\text{NiCo})_{4.0/0.3\text{T}/\text{Per}}$  alloy coatings, showing the highest corrosion resistances (all optimal) are shown comparatively in Figure 8.10. It may be seen that smoothness of alloy coatings, responsible for better corrosion resistance has improved as the mode of deposition is changed, from conventional type to magneto-electrodeposition type. It may be seen from the SEM image that NiCo alloy coating deposited under no effect of magnetic field is rougher than those developed under magnetic field effect. When  $B$  is oriented perpendicular to the electrode surface, the magneto convection effect is found to be maximum due to inclusion of Lorentz force. Hence, coating corresponding to MED  $(\text{NiCo})_{4.0/0.3\text{T}/\text{Per}}$  configuration found to be the most uniform (Figure 8.10), with least corrosion rate.



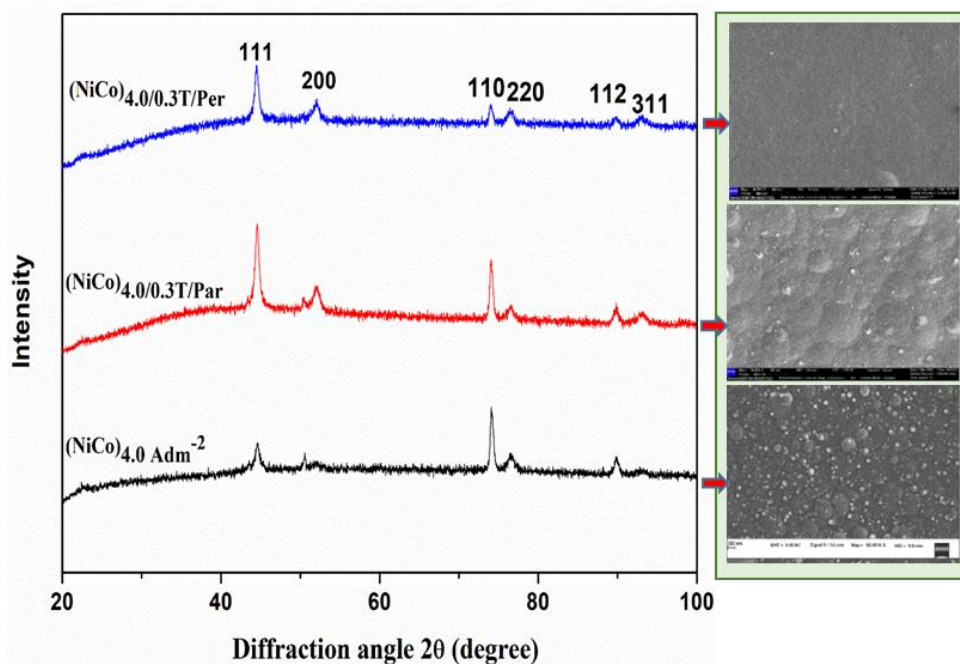


**Figure 8.10** - Comparison of XRD patterns and microstructure of MED NiCo alloy coatings deposited under optimal conditions of parallel and perpendicular  $B$ , in comparison with ED NiCo alloy coatings, deposited from the same bath.

The observed facts amounts to state that the Lorentz force acting, under condition of perpendicular  $B$  is responsible to increase the mass transfer process towards cathode. This in turn is responsible for decrease in diffusion layer thickness in the vicinity of the electrode. Hence, it may be concluded that induction of magnetic field during deposition, improved the corrosion resistance of alloy coatings by smoothening its surface.

The corrosion resistance behaviour of ED  $(\text{NiCo})_{4.0} \text{Adm}^{-2}$ , MED  $(\text{NiCo})_{4/0.3\text{T}/\text{Par}}$  and MED  $(\text{NiCo})_{4/0.3\text{T}/\text{Per}}$  coatings showing the least CR (optimal) are shown in Figure 8.11. The Nyquist plots, with distinct difference in the diameter of the capacitive loops indicates that magneto-electrodeposited NiCo alloy coatings (both parallel and perpendicular) are far more corrosion resistant than their conventional alloy counterpart. This further supported by their potentiodynamic polarization response shown in the inset of Figure 8.11, with having a clear difference between their  $i_{\text{corr}}$  and  $E_{\text{corr}}$  values.

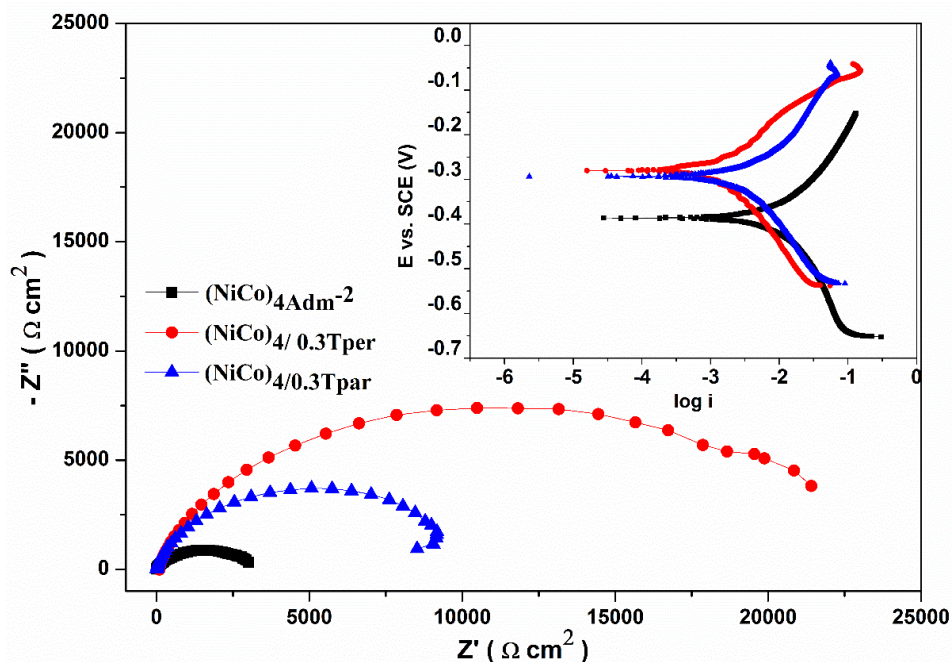


**Figure 8.11** - Comparison of impedance responses of MED (NiCo) alloy coatings (under parallel and perpendicular B) in relation of ED (NiCo) coating deposited from same bath (all under optimal condition). Tafel's responses are given in the inset.

Thus from the data it may be summarized that, if ED (NiCo)<sub>4.0 Adm</sub><sup>-2</sup> alloy coating, having 38.6 wt.% Ni showed CR =  $14.4 \times 10^{-2} \text{ mmy}^{-1}$ , MED coatings having MED (NiCo)<sub>4.0/0.3T/Par</sub> and (NiCo)<sub>4.0 /0.3T/Per</sub> configurations, with having respectively 55.81 wt.% Ni and 64.72 wt.% Ni, showed CR's =  $3.78 \times 10^{-2} \text{ mmy}^{-1}$  and  $1.03 \times 10^{-2} \text{ mmy}^{-1}$ , respectively.

### 8.3.5 Discussion

The MED approach adopted for improving corrosion resistance property of ED NiCo alloy coating was driven by the following facts. The factor responsible for improved corrosion resistance of MED NiCo alloy coatings is by increasing wt. % Ni in the deposit, and is discussed as below. The effects of plating variables on the composition of the deposit are determined by changes in the concentrations of metal ions in the cathode diffusion layer (CDL), and is predictable from simple diffusion theory, and is shown schematically in Figure 8.13. According to this, the limiting current density ( $i_L$ ) is the measure of maximum reaction rate that cannot be exceeded because of a limited

diffusion rate of metal ions in solution. In other words, it is current density at which the rate of electrodeposition is maximum. In the region of the  $i_L$  when the electrode process is mass-transfer controlled, the value of the current density is given by Equation (8.1)

$$i_L = \frac{nFD_z C_B}{\delta} \dots \dots \dots (8.1)$$

Where, n is the valency of the metal ions, and F is the Faraday constant (96400 C), D is the diffusion coefficient of the reacting species,  $C_B$  is the concentration and  $\delta$  is the thickness of electrical double layer (EDL). The lines of ionic movement responsible for change of EDL thickness, during conventional electrodeposition (ED) and magneto-electrodeposition (MED) are shown in Figure 8.12.

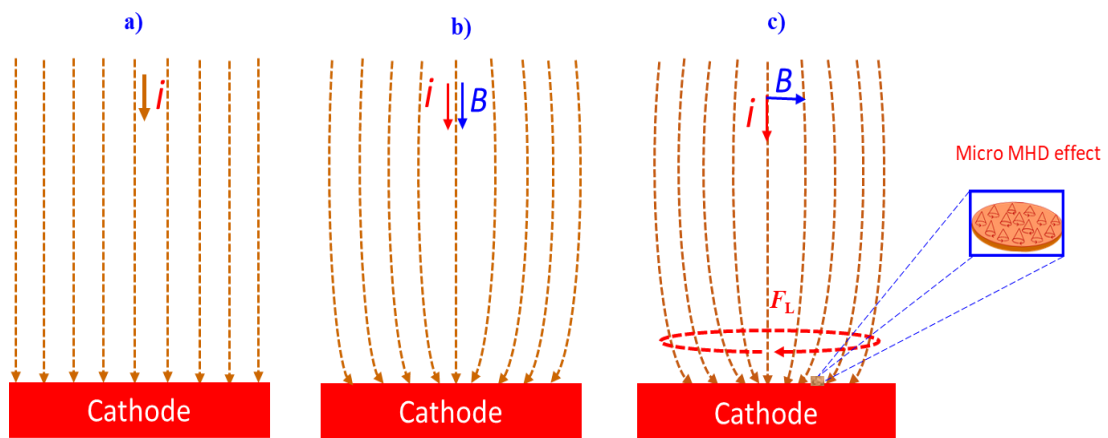


**Figure 8.12** - Diagrammatic representation showing lines of ionic movement responsible for change in EDL thickness during electrodeposition of (NiCo) alloy coatings: a) ED (NiCo) Natural convection b) MED (NiCo) Parallel B, and c) MED (NiCo) Perpendicular B.

It may be noted that during conventional ED, lines of ionic movement are parallel, and perpendicular to the plane of the cathode, as shown in Figure 8.12(a). When magnetic field applied is parallel to the direction of movement ions, an increase in the rate of mass transport is affected due to formation of a hydrodynamic boundary layer at the E-E interface due to the tangential velocity, induced by the field that actually decreases the diffusion layer thickness, and increases the flux of the ionic species (Ganesh et al. 2005). This this situation is shown in Figure 8.12(b). When the applied  $B$  is perpendicular to the direction of movement of ions, the improved deposition patterns of MED coatings may be attributed to the magnetohydrodynamic (MHD)

effect, which may be explained from the Lorentz force, due to the interaction of velocity field of charged species with electromagnetic field. The total force on a charged particle, moving in an electromagnetic field is the Lorentz force, and it is given by,

$$F_L = qE + qvB\sin\theta \dots\dots\dots (8.2)$$

Where,  $F_L$  is the Lorentz force,  $q$  the charge of an ion,  $E$  the electric field strength,  $v$  the velocity of the ions and  $B$  the magnetic flux density. When a  $B$  is applied perpendicular to the direction of flow of ions (where  $\sin 90 = 1$ ), the Lorentz force is exerted on the moving ions, and thereby induces a convective flow of the electrolytic solution. This convective force operating during magneto-electrodeposition, with perpendicular field is shown in Figure 8.12(c).

Thus increase of mass transport process due to applied magnetic field is responsible for increase of  $i_L$ , which in turn responsible for reduction of diffusion layer thickness. The process of magneto-electrodeposition and decrease of diffusion layer thickness ( $\delta$ ) due to superimposition of magnetic field ( $B$ ) is shown in Figure 8.13, in relation to that in the conventional electrodeposition.

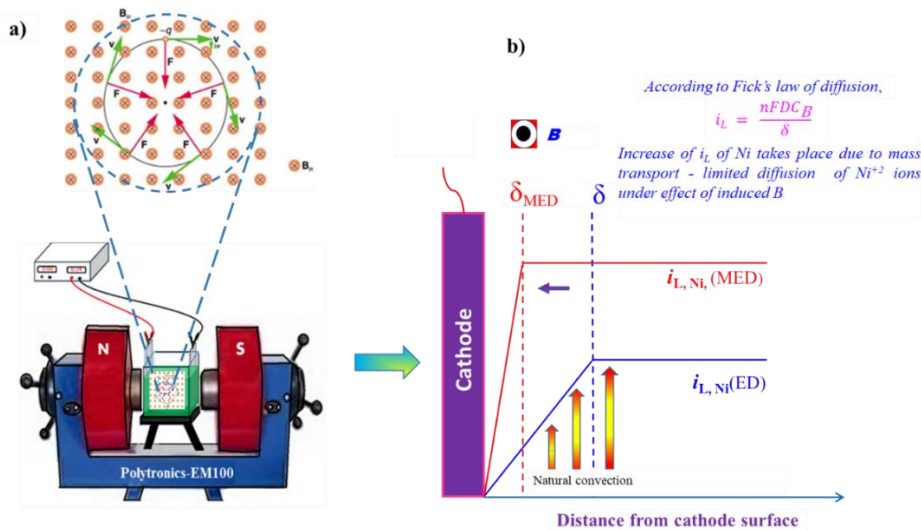


**Figure 8.13-** Schematic representation showing: a) Process of magneto-electrodeposition and b) decrease of diffusion layer thickness ( $\delta$ ) due to increase of limiting current density ( $i_L$ ) on superimposition of magnetic field,  $B$

Thus in the light of principles of magneto-electrodeposition, it may be summarized that (NiCo)<sub>4.0/0.3T/per</sub> coating obtained in a perpendicular direction was found to be more corrosion resistant, compared NiCo alloy coatings of other configurations. The highest effect of perpendicular field, compare to parallel field is due to the combined effect of non-electrostatic force and Lorentz force. The Lorentz force is at its maximum when field is applied perpendicular to the direction of flow of ions (Equation 8.2). This is responsible for highest decrease of EDL thickness during deposition. The thickness of cathode film decreased from  $\delta_0$  to  $\delta_D$ , as the mode of the coating is changed from ED to MED type as shown in Figure 8.12 (b). In addition, increase of Ni content of the alloy, due to increase of its  $i_L$  is responsible for increased corrosion resistance of MED NiCo alloy coatings.

#### 8.4 CONCLUSIONS

In an effort to increase the corrosion protection efficacy of ED (NiCo) alloy coatings, magneto-electrodeposited (MED) (NiCo) alloy coatings have been developed by from the optimized bath by inducing the magnetic field (both parallel and perpendicular), simultaneous to the process of deposition. The experimental results of investigations are accredited to arrive the following conclusions:

1. The corrosion protection efficacy of conventional ED (NiCo) alloy coatings can be increased drastically through magneto-electrodeposition (MED) approach, by inducing the magnetic field  $B$ , simultaneously to the process of electrodeposition.
2. The corrosion rate of (NiCo) alloy coatings were found to be decreased due to superimposition of  $B$ , applied both parallel and perpendicular to the line movement of ions. However, effect is more pronounced in case of perpendicular  $B$  and is attributed to the combined effect of Lorentz force and magneto-convection.
3. Under optimal conditions, MED (NiCo) alloy coating is about fourteen-times more corrosion resistant compared to its electrodeposited (ED) counterpart, deposited from same bath, at same current density.

4. Drastic improvement in the corrosion protection efficacy of MED (NiCo) alloy coatings, (under both parallel and perpendicular field) is attributed to the drastic increase of wt.% Ni content in the deposit.
5. The Ni content in the deposit is found to be increased with  $B$  (in both parallel and perpendicular field) due to increase of its limiting current density ( $i_L$ ) value, affected due to magneto convection effect.
6. The constancy of XRD patterns of MED (NiCo) alloy coatings, regardless of the direction and intensity of  $B$  is due to formation of solid solution of NiCo alloy. Only change of intensity of XRD peaks were found, due to change in the composition of alloy, keeping scattering angles constant.
7. The improved corrosion resistance of MED (NiCo) alloy coatings, in relation to its conventional alloy coatings were attributed to their changed composition, and surface morphology, supported by EDS, AFM and SEM study, respectively.

## **CHAPTER 9**

# **ELECTROCATALYTIC STUDY OF NiCo ALLOY COATINGS FOR WATER SPLITTING REACTION AND EFFECT OF Ag NANOPARTICLES ON ITS CATALYTIC ACTIVITY**





## CHAPTER 9

### ELECTROCATALYTIC STUDY OF NiCo ALLOY COATINGS FOR WATER SPLITTING REACTION AND EFFECT OF Ag NANOPARTICLES ON ITS CATALYTIC ACTIVITY

---

*The present chapter is devoted to study the electrocatalytic applications of NiCo alloy coatings in alkaline water electrolysis. The NiCo alloy coatings deposited from the optimal bath at different current densities were used, as electrode material as both cathode and anode for hydrogen evolution reaction (HER) and oxygen evolution reaction (OER), respectively. The electrocatalytic performance of alloy coatings were evaluated in 1M KOH medium using cyclic voltammetry (CV) and chronopotentiometry (CP) techniques. The factors responsible for changed electrocatalytic activity of NiCo alloy coatings, developed at different current densities were explained in terms of their changed surface morphology, composition and phase structure, analysed through SEM, AFM, EDS and XRD techniques. The effect of addition of Ag nanoparticles into bath on electrocatalytic activity of HER has also been studied. A significant improvement in the electrocatalytic activity of HER was found. The enhanced electrocatalytic activity of NiCo-Ag co-electrodeposited composite coating was found to be affiliated to the incorporation Ag nanoparticles into alloy matrix, confirmed by elemental mapping of coatings. The deposition conditions for best electrocatalytic activity of NiCo and (NiCo-Ag) coatings were proposed, and results are discussed.*

#### 9.1 INTRODUCTION

Electrochemical water splitting is a viable technique to generate clean energy from the unlimited water supply, and is of great significance in the continuous progress of carbon - neutral energy technologies and mitigation of environmental impact (Peng et al. 2021). Hence, synthesis of high performance and economical viable electro-catalysts for overall water splitting applications is of high priority. The electrocatalytic properties of electrode materials mainly depends on the density of active sites embedded in it, which are responsible for their redox activities (Wu et al. 2004). The simple production

of such electrode materials is one of the most important challenges of the scientific community (Ashraf et al. 2020). Generally, platinum and other noble metal oxides, like IrO<sub>2</sub>, RhO<sub>2</sub>, PtO<sub>2</sub> and RuO<sub>2</sub> are used as best electrode material for hydrogen and oxygen evolution reactions, but their prohibitive cost impedes their wide spread use for industrial scale application (Sapountzi et al. 2017). In this regard, the transition metals and their alloys are used as best electrode materials for water splitting reactions. Since, Ni and its alloys have been considered as efficient electrode materials due to their special properties, such as low cost, high-strength, good wear resistance and good electrocatalytic activity (Wang et al. 2005). The electrodeposited alloys of transition metals, like Ni, Co, Fe, Mo are proved to be the efficient electro catalysts towards water splitting reaction than bare Ni coatings (Fan et al. 1994; Rosalbino et al. 2008). Apart from this, many reports are available in literatures to support the fact electro-catalytic efficiency of electrode materials can be improved drastically by incorporation of colloidal nano-particles into the metal/alloy matrix, through nanoparticles co-electrodeposition.

In this direction, NiCo alloy coatings electrodeposited from optimized bath of NiCo (Table 7.1) has been subjected to electrocatalytic study. NiCo alloy coatings were accomplished on copper substrate from acid sulphate bath at different current densities, and their efficacy for water electrolysis of HER and OER were studied. The performance of NiCo deposit, as bipolar electrode material has been evaluated quantitatively, and electrocatalytic kinetic parameters were assessed by conventional cyclic voltammetry (CV) and chronopotentiometry (CP) methods. Further, in view of many reports on improved electrocatalytic activity of nanoparticle induced transition metals alloy coatings, it was planned to improve the electro-catalytic performance NiCo for HER by incorporating the Ag nanoparticles into the bath. Here, NiCo-Ag composite coatings have been developed through co-electrodeposition, where Ag nanoparticles are dispersed in optimized NiCo bath. The electro-catalytic efficiency of composite coatings was investigated, in relation to its binary alloy matrix to evaluate effect of Ag nanoparticles. The electro-catalytic activity of NiCo alloy and NiCo-Ag composite coatings were evaluated under different conditions of their depositions. Different factors responsible for varied electro-catalytic activity are correlated with their

composition, phase structure and surface topography, evidenced through EDS, XRD, AFM and SEM analyses, and experimental results are discussed.

## **9.2 EXPERIMENTAL**

### **9.2.1 Electrodeposition of NiCo alloy coatings**

The electrolytic bath having nickel sulphate hexahydrate ( $\text{NiSO}_4 \cdot 6\text{H}_2\text{O}$ ), cobalt sulphate heptahydrate ( $\text{NiSO}_4 \cdot 7\text{H}_2\text{O}$ ), potassium sodium tartrate tetrahydrate ( $\text{KNaC}_4\text{H}_4\text{O}_6 \cdot 4\text{H}_2\text{O}$ ), and glycine ( $\text{NH}_2\text{-CH}_2\text{-COOH}$ ), is used for deposition of NiCo alloy coating. The bath was prepared in distilled water using laboratory reagent (LR) grade chemicals. The bath conditions and operating parameters were arrived by standard Hull cell method. The composition and operating parameters used in the present study is given in Table 7.1. The (NiCo) alloy coatings were developed at 1.0 to 4.0  $\text{Adm}^{-2}$  current densities on the cross sectional area of mirror finished copper rod, having exposed surface area of  $1\text{cm}^2$  as cathode; and graphite sheet as anode. The experimental set up used for electrodeposition of (NiCo) alloy coatings for electrocatalytic study is shown in Figure 3.7. DC Power Analyzer (Agilent Technologies, N6705C, USA) was used as power source for deposition. All coatings were carried out for same duration (600 s), keeping temperature and pH constant, for comparison purpose. The pH of the bath was adjusted to 3.0 using pH meter (Systronics-362), on addition of either sulphuric acid ( $\text{H}_2\text{SO}_4$ ) or ammonium hydroxide ( $\text{NH}_4\text{OH}$ ) solution, depending on the requirement.

### **9.2.2 Characterization of NiCo alloy coatings**

The compositional and structural characterization of (NiCo) alloy coatings were carried out using EDS, SEM, AFM and XRD analyses. Further, their electrocatalytic behaviours towards alkaline water splitting (for both HER and OER) were studied in 1M KOH, using a custom made tubular glass set up having three electrodes (Figure 3.8). The conventional CV and CP techniques were employed to study the electrocatalytic efficacy of alloy coatings, using computer controlled potentiostat, VersaSTAT 3-400 (Princeton Applied Research, USA). The electrocatalytic stability of the developed coatings were tested by chronopotentiometry method, by monitoring the electrode reaction for duration of 1800 s. The efficiency of electrode reactions, both as cathode

and anode, for HER and OER were evaluated quantitatively by measuring the volume of H<sub>2</sub> and O<sub>2</sub> evolved on 1 cm<sup>2</sup> surface area of the test electrode for 300 s.

### 9.3 RESULTS AND DISCUSSION

#### 9.3.1 Surface morphology and phase structure of alloy coatings

Knowing the fact that electrocatalytic activity of alloy coatings are based on their composition, surface roughness and porosity, the composition of NiCo alloy corresponding to different current densities are reported in Table 9.1, obtained by EDS analyses. The phase structure of NiCo coatings corresponding to different current densities were also examined by XRD techniques and corresponding X-ray peaks are shown in Figure 9.1. The observed lattice planes (111), (200), (220) which are characteristic planes of face centered cubic structure of NiCo alloy (Radhakrishnan et al. 2021). The phase diagram of NiCo alloy system found to have two different phases, a face-centered cubic (fcc) and a hexagonally close-packed (hcp) phases, in compliance with its composition (Karimzadeh et al. 2019; Mbugua et al. 2020). Further, the intensity of hcp lattice plane reflection decreases with increasing deposition current density. This observation is in agreement with the decrease of cobalt content in the deposit with current density (Karimzadeh et al. 2019; Srivastava et al. 2006).

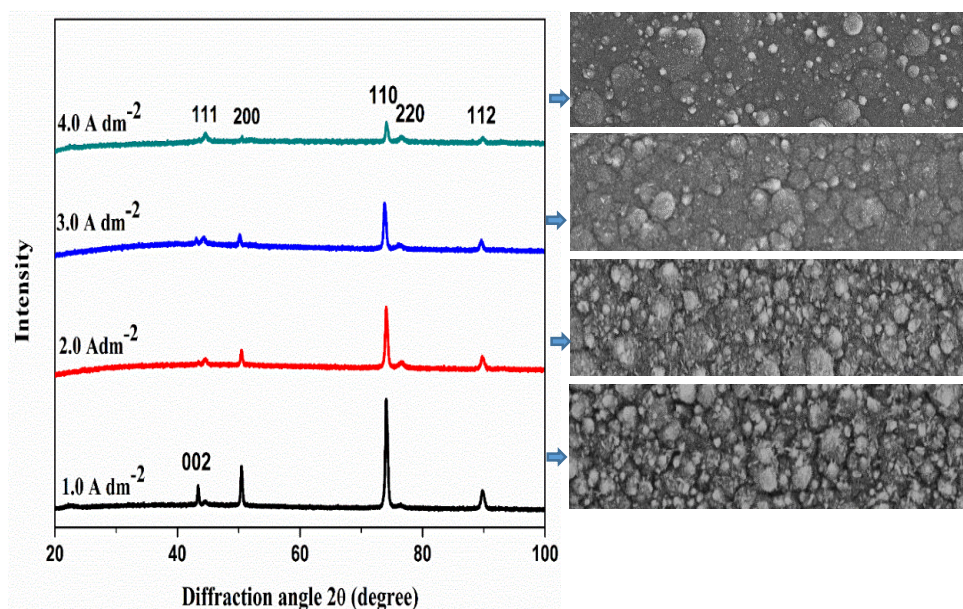


**Figure 9.1** - X-ray diffraction peaks of NiCo coatings, deposited at different current densities from the optimized bath. On the right are given their SEM image showing different surface morphology responsible for their different electro-catalytic activities.

In addition, surface morphology of alloy coatings was found to change drastically with deposition current densities, shown on the right in Figure 9.1. The granular structure of alloy coatings, corresponding to lower current density was found to change to fine grained type. This change may be attributed to the decrease of cobalt content in the alloy, with increase of current density. Significant topographical change of NiCo alloy coating with deposition current density is further conformed by Atomic Force Microscopy (AFM) image, shown in Figure 9.2. Three dimensional AFM image of NiCo alloy coatings deposited at extreme situation of current density, namely at  $1.0 \text{ Adm}^{-2}$  and  $4.0 \text{ Adm}^{-2}$ , abbreviated as  $(\text{NiCo})_{1.0 \text{ Adm}^{-2}}$  and  $(\text{NiCo})_{4.0 \text{ Adm}^{-2}}$  are shown in Figures 9.2 (a) and 9.2 (b), respectively. Experimental data revealed that the average roughness of  $(\text{NiCo})_{1.0 \text{ Adm}^{-2}}$ , and  $(\text{NiCo})_{4.0 \text{ Adm}^{-2}}$  are, respectively 42.7 nm and 24.5 nm. Hence, AFM study confirmed that surface roughness of alloy coatings decreased drastically with deposition current density. This is in compliance with decreased electrocatalytic behaviour of NiCo alloy coatings, with increase of deposition current densities.

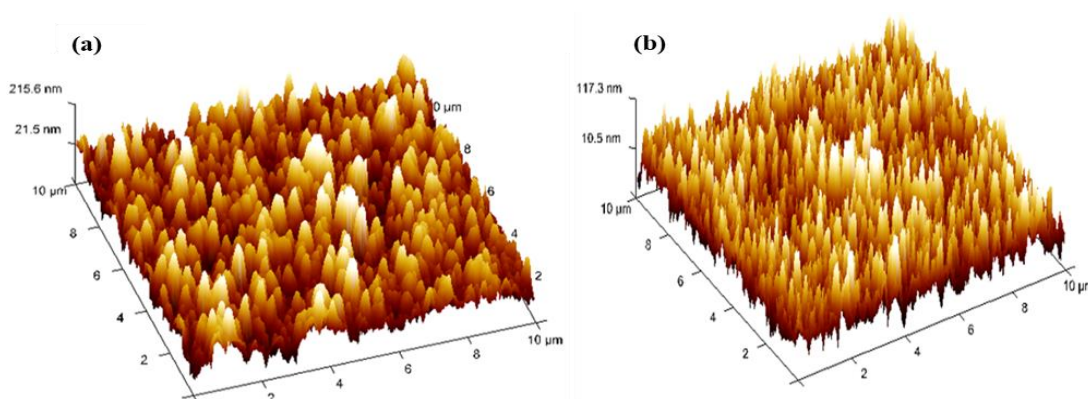


**Figure 9.2-** AFM image of (a)  $(\text{NiCo})_{1.0 \text{ Adm}^{-2}}$  and (b)  $(\text{NiCo})_{4.0 \text{ Adm}^{-2}}$  deposited from same bath for same duration, showing change of surface topography with deposition current density.

### 9.3.2 Electro-catalytic study

#### 9.3.2.1 Hydrogen Evolution Reaction

The steady state equilibrium is one of the simplest approach to study the water splitting ability of electro-catalysts. Hence, NiCo alloy coatings obtained at different current densities were subjected to electro-catalytic study of HER in 1M KOH medium. The

experimental data were investigated through cyclic voltammetry (CV) and chronopotentiometry (CP) techniques, and are discussed in the following sections.

*i) Cyclic voltammetry study*

The electrocatalytic behaviour of NiCo coatings have been studied for HER, by making the coatings as cathode in the electrolyser. The CV study was made in a potential range of 0.0 V to -1.6 V, at 50mV/sec scan rate for 20 cycles. The CV curves of alloy coatings, deposited at different current densities are as shown in the Figure 9.3, and corresponding kinetic parameters of HER listed in the Table 9.1.

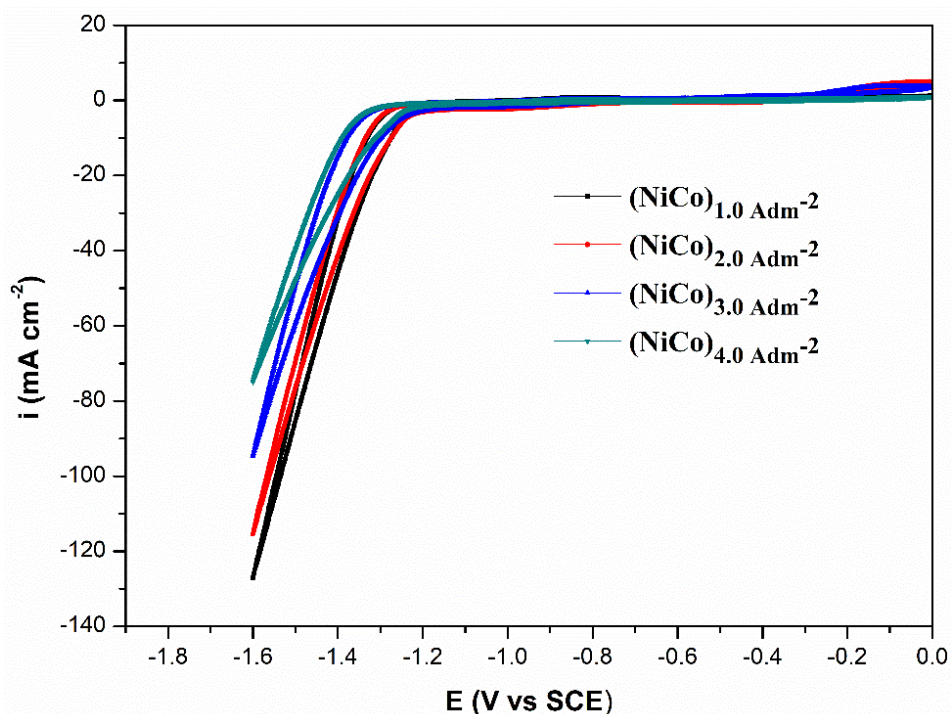


**Figure 9.3** - CV curves for HER of NiCo coatings deposited at different current densities from optimized bath.

During CV study, it was observed that the current responses steadily decreased with increase in number of cycles, and finally reached a stable value near -1.6 V. This decrease of current density may be attributed to resistance offered by the hydrogen gas, formed on the surface of cathode. A stable and reproducible CV curves were found at the end, indicating a state of equilibrium between attached and detached hydrogen gas on the electrode surface. *i.e.* a state of steady liberation of H<sub>2</sub> gas from the surface of cathode.

The current density corresponding to this equilibrium is called cathodic peak current density, denoted by  $i_{pc}$  and the potential at which desorption of hydrogen gas started is called onset potential. From the CV curves, shown in Figure 9.3 it may be noted that (NiCo) alloy coating deposited at  $1.0 \text{ Adm}^{-2}$  showed the highest cathodic peak current density with least onset potential for HER, compared to all other coatings. Hence, it may be inferred that this particular coatings having  $(\text{NiCo})_{1.0 \text{ Adm}^{-2}}$  configuration has highest efficacy for HER. This highest efficacy of  $(\text{NiCo})_{1.0 \text{ Adm}^{-2}}$  coatings for HER may be attributed to its highest Co content, which is responsible for more number of active sites for evolution of hydrogen. It is important to note that the tendency of HER of alloy coatings bears a close relationship with its surface roughness, and is evident from its highest average roughness value. The average roughness value of (NiCo) alloy coatings were found to be decreased with increase in current density, as shown in Figure 9.2.

**Table 9.1 – The electro-kinetic parameters of HER on the surface of NiCo alloy coatings deposited at different current densities, deposited form same bath**

Coating configuration	Wt. % of Co content of the deposit	Cathodic peak c.d. ( $i_{pc}$ ) ( $\text{mA cm}^{-2}$ )	Onset potential for H <sub>2</sub> evolution (V vs SCE)	Volume of H <sub>2</sub> Evolved in 300 s ( $\text{cm}^3$ )
$(\text{NiCo})_{1.0 \text{ Adm}^{-2}}$	70.6	-128.7	-1.32	12.3
$(\text{NiCo})_{2.0 \text{ Adm}^{-2}}$	66.7	-116.8	-1.33	12.1
$(\text{NiCo})_{3.0 \text{ Adm}^{-2}}$	64.2	-94.4	-1.35	11.7
$(\text{NiCo})_{4.0 \text{ Adm}^{-2}}$	61.4	-75.6	-1.37	10.4

**ii) Chrono-potentiometry study**

NiCo coatings deposited at different current densities were subjected to chronopotentiometry analysis also to monitor the potential change as a function of time by applying a constant current between test electrode and reference electrode. The CP Study was carried out by applying a constant current of 0.3A, on working electrode for a time period of 1800 s, and corresponding CP curves are shown in the Figure 9.4.

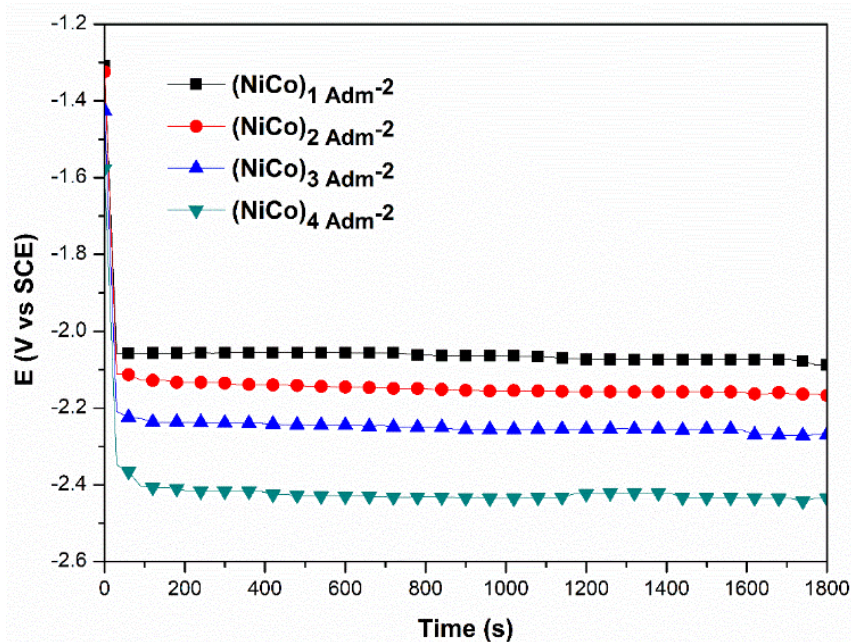


**Figure 9.4** – Chrono-potentiograms for NiCo alloy coatings deposited at different current densities at applied cathodic current of - 3.0 A, showing different responses for HER.

From the nature of CP curves, shown in Figure 9.4, it is clear that initially there is sudden decrease of potential with time, in all coatings. There is sudden decrease of potential in the beginning of electrolysis, and eventually reached a steady state, in case of all coatings, deposited at different current densities. This is due to the attainment of equilibrium between reduction of  $\text{H}^+$  ions from electrolyte on the electrode surface, and  $\text{H}_2$  gas liberation from the surface. Here, the coating developed at  $1.0 \text{ Adm}^{-2}$  attained the steady state very quickly, compared to other coatings. This behaviour confirmed that NiCo coating at  $1.0 \text{ Adm}^{-2}$  is electrocatalytically more active and stable for HER, and hence a better electrode material for HER. Further, the electrocatalytic behaviour of NiCo coatings are evaluated quantitatively on the basis of the amount of hydrogen liberated for initial 300s, on its surface. The quantity of hydrogen evolved on the surface of alloy coatings deposited at  $1.0 \text{ Adm}^{-2}$ ,  $2.0 \text{ Adm}^{-2}$ ,  $3.0 \text{ Adm}^{-2}$  and  $4.0 \text{ Adm}^{-2}$  are shown in Table 9.1. Experimental data demonstrated that  $(\text{NiCo})_{1.0 \text{ Adm}^{-2}}$  alloy coating is most favourable for HER, compared to coatings at other current density. Thus, CP study demonstrated that NiCo alloy coatings, deposited at  $1.0 \text{ Adm}^{-2}$  is the best electrode material for HER, which is in compliance with CV study.



### 9.3.2.2 Oxygen Evolution Reaction

The electrocatalytic behaviour of NiCo alloy coatings at different current densities were tested for their efficacy for OER by using them as anode, in the same line as for HER. The experimental studies were carried out using CV and CP methods.

#### *i) Cyclic voltammetry*

The cyclic voltammetry techniques have been employed all alloy coatings, deposited at different current densities in the potential window of 0 to 0.75 V, at a scan rate of 50 mVsec<sup>-1</sup> for 20 cycles. The corresponding voltammograms are shown in the Figure 9.5. From the graph, it is clear that (NiCo) alloy deposited at current density equal to 1.0 Adm<sup>-2</sup> showed the better OER activity compared to those at other current densities. The mechanism proposed involves initial adsorption of OH<sup>-</sup> ions from electrolyte solution onto the electrode surface, followed by electron transfer process within the system, which lead to liberation of oxygen. The anodic peak current density (*i*<sub>p</sub><sub>a</sub>) found to be decreased with increase of deposition current density. Hence, it may be inferred that (NiCo)<sub>1.0 Adm<sup>-2</sup></sub> coating has highest efficacy for even OER.

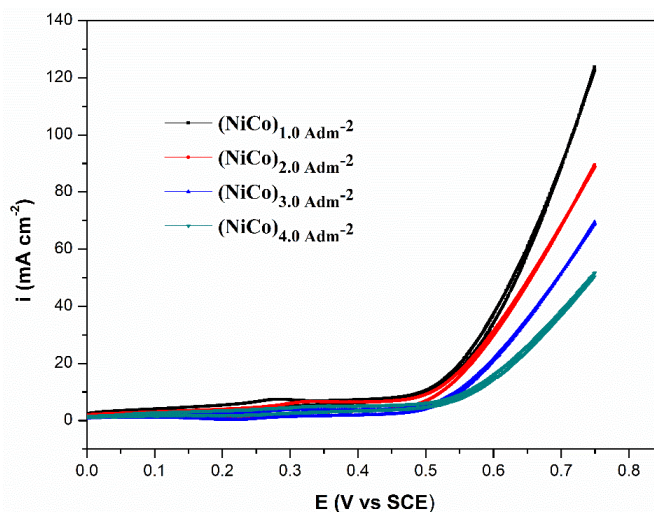


**Figure 9.5-** Cyclic voltammograms of OER on the surface of NiCo alloy coating, deposited at different current densities.

#### *ii) Chronopotentiometry*

CP study for evolution of OER on the surface of NiCo alloy coatings were carried out at a positive current + 0.3 Acm<sup>-2</sup>, and corresponding electrochemical responses are shown in Figure 9.6.

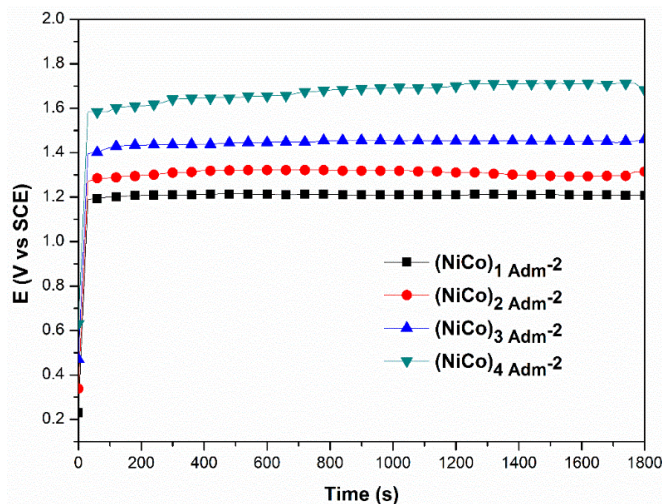


**Figure 9.6-** Chronopotentiograms of NiCo alloy coatings deposited at different current densities showing different responses for OER.

It may be observed that initially the potential has increased drastically, and then remained almost constant indicating the establishment of an equilibrium between adsorbed OH<sup>-</sup> and liberated O<sub>2</sub>. The amount of O<sub>2</sub> liberated in the initial 300 s on different coatings were measured, and is reported in Table 9.2. It may be noted that there is no significant change in the volume of oxygen liberated with deposition current density. However, from the volume of O<sub>2</sub> liberated, it may be noted that (NiCo)<sub>1.0</sub> Adm<sup>-2</sup> coating is more efficient for OER, than other coatings. The highest wt. % Co in (NiCo)<sub>1.0</sub> Adm<sup>-2</sup>, supported by EDS study may be responsible for its better efficacy for even OER.

**Table 9.2- Electrochemical parameters obtained for OER on the surface of (NiCo) alloy coatings deposited at current densities**

Coating configuration	Wt. % of Co content of the deposit	Anodic peak c.d. (mA cm <sup>-2</sup> )	Onset potential for O <sub>2</sub> evolution (V vs SCE)	Volume of O <sub>2</sub> Evolved in 300 s (cm <sup>3</sup> )
(NiCo) <sub>1.0</sub> Adm <sup>-2</sup>	70.6	125.298	0.497	7.5
(NiCo) <sub>2.0</sub> Adm <sup>-2</sup>	66.7	90.393	0.509	6.8
(NiCo) <sub>3.0</sub> Adm <sup>-2</sup>	64.2	70.244	0.517	6.2
(NiCo) <sub>4.0</sub> Adm <sup>-2</sup>	61.4	52.042	0.534	5.8

Here, it is important to note that highest electro-catalytic activity of  $(\text{NiCo})_{1.0 \text{ Adm}^{-2}}$  coatings (having definite Co content) for both HER and OER indicates that this is better bi-functional electrode (to use both as anode and cathode) for overall water splitting applications, compared to other coatings.

#### **9. 4 EFFECT OF ADDITION OF SILVER NANO-PARTICLES**

The effect of addition of silver (Ag) nanoparticles on electro-catalytic activity of NiCo-Ag composite coating has been tested, by adding it in known amount into NiCo bath. The improvement in its electro-catalytic activity, in terms of efficacy for HER have been tested using it as cathode. The experimental study have been made, and their catalytic efficiency and stability have been tested following the same CV and CP methods. Experimental results are discussed as below.

##### **9.4.1 Development of NiCo-Ag composite coating**

Guided by the literature that incorporation of nanoparticles into the electroactive alloy matrix can improve their electro-catalytic activity to large extent, Ag nanoparticles were added into NiCo bath, having composition reported in Table 3.1. Ag-electrocodeposited (NiCo) coatings, represented as NiCo-Ag composite were developed by conventional electrodeposition method, by adding three different amount of Ag nanoparticles, like 0.5 g/L, 1.0 g/L and 2 g/L. The electrolyte was sonicated for 60 minutes for uniform dispersion of Ag nanoparticles, and for 15 minutes before every use. The NiCo-Ag composite coatings were developed on the cross sectional area of mirror finished copper rod, having exposed surface area of  $1\text{cm}^2$  as cathode; and graphite sheet as anode at an optimal deposition current density of  $1.0 \text{ Adm}^{-2}$ , using the same electrolyser. Here, it may be noted that current density of  $1.0 \text{ Adm}^{-2}$  was selected as the deposition current density at which NiCo alloy showed is highest electrocatalytic activity for HER as discussed in Section 9.3. All other deposition conditions, like pH and duration of deposition were kept constant for comparison purpose. Here, NiCo-Ag composite coatings are conveniently denoted as  $(\text{NiCo-Ag})_X$ , where X stands for the amount of Ag nanoparticles (in g/L) added into the optimized NiCo bath.

## 9.4.2 Characterization of NiCo-Ag composite coating

As catalytic process is a surface phenomenon, and it depends on its very surface morphology. Hence, to explain the electro-catalytic behaviour of the NiCo-Ag composite coating, they are subjected to surface and compositional analyses, like SEM-EDS, AFM and elemental mapping.

### 9.4.2.1 SEM-EDS Analysis

The microstructure of the electro-codeposited NiCo-Ag composite coatings were analysed using SEM, and the corresponding SEM micrographs are shown in Figure 9.7. A clear difference in the surface morphology of composite coatings may be seen, when they are deposited without, and with Ag nanoparticles (in different amounts).

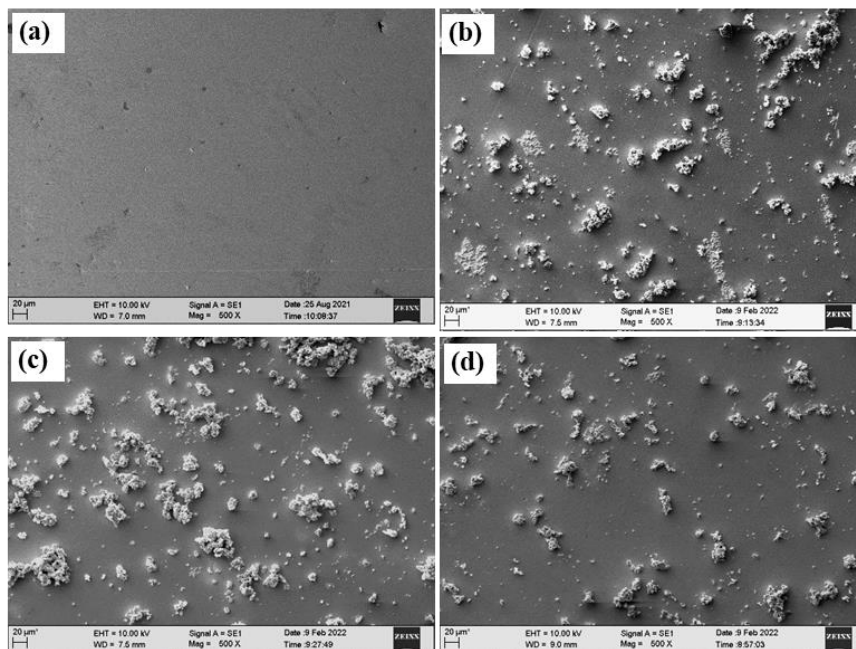


**Figure 9.7-** SEM image of NiCo alloy coating under different conditions: (a)  $(NiCo)_{1.0}Adm^{-2}$ , (b)  $(NiCo-Ag)_{0.5}$ , (c)  $(NiCo-Ag)_{1.0}$  and (d)  $(NiCo-Ag)_{2.0}$

As seen in SEM images, the nanoparticles were spread over the surface of alloy coating almost uniformly by giving almost rougher surface to earlier smooth NiCo alloy coating. The distribution of metal species in metal matrix are generally identified by *Elemental mapping* technique. Elemental mapping is a powerful technique, and gives information with regard to the spatial distribution of elements in a sample. It relied on principle of compiling extremely specific elemental composition data, across the area

of sample under test. This is typically done using SEM image interfaced with EDS data. Accordingly, high resolution image of NiCo-Ag composite coatings are collected along with their EDS data, and are shown in Figure 9.8. From elemental mapping of NiCo-Ag composite coatings, having varied quantity of Ag nanoparticles, *i.e.* 0.5g/L, 1.0g/L and 2g/L, it confirmed that Ag nanoparticles are incorporated into the alloy matrix, in compliance with the observed facts in SEM image, shown in Figure 9.7. Thus, elemental mapping corresponding to all three constituting elements, namely Ni, Co and Ag may be seen distinctly in Figure 9.8, confirming the incorporation of Ag in alloy matrix of NiCo.

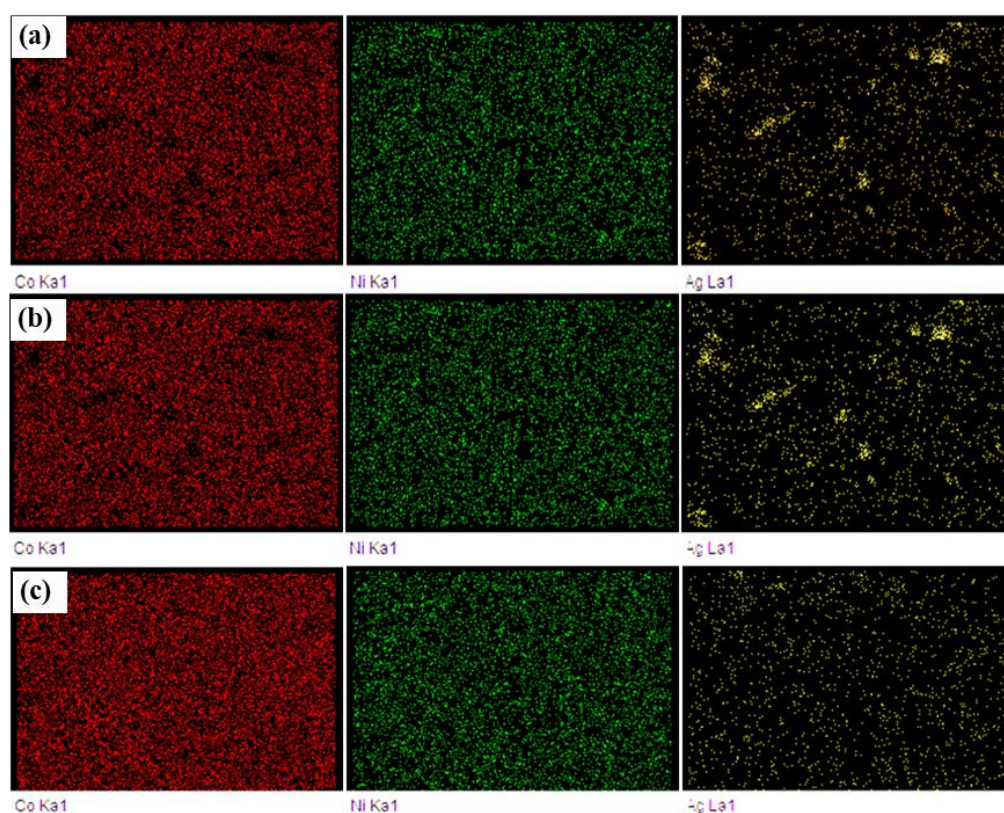


**Figure 9.8** – Elemental mapping of NiCo-Ag composite coatings deposited from optimal bath having added with varied quantity of Ag nanoparticles: a) 0.5g/L, (b) 1.0g/L and (c) 2g/L. Presence of Ni, Co and Ag may be noted in all three coatings, confirming the incorporation of Ag in alloy matrix of NiCo.

#### 9.4.2.2 AFM Study

To interpret possible reasons for improved electro-catalytic activity of NiCo coatings on incorporation of Ag nanoparticles, the surface roughness data of Ag-electrocodeposited NiCo alloy coatings were obtained through AFM analysis. The AFM image, taken in  $10\mu\text{m} \times 10\mu\text{m}$  area showing a substantial difference in the topography of  $(\text{NiCo})_{1\text{Adm}^{-2}}$  and  $(\text{NiCo-Ag})_{1.0}$  alloy coatings are shown in Figure 9.9. The corresponding surface roughness parameters, such as average roughness ( $R_a$ ) and root mean square roughness ( $R_q$ ) values are given in Table 9.3.

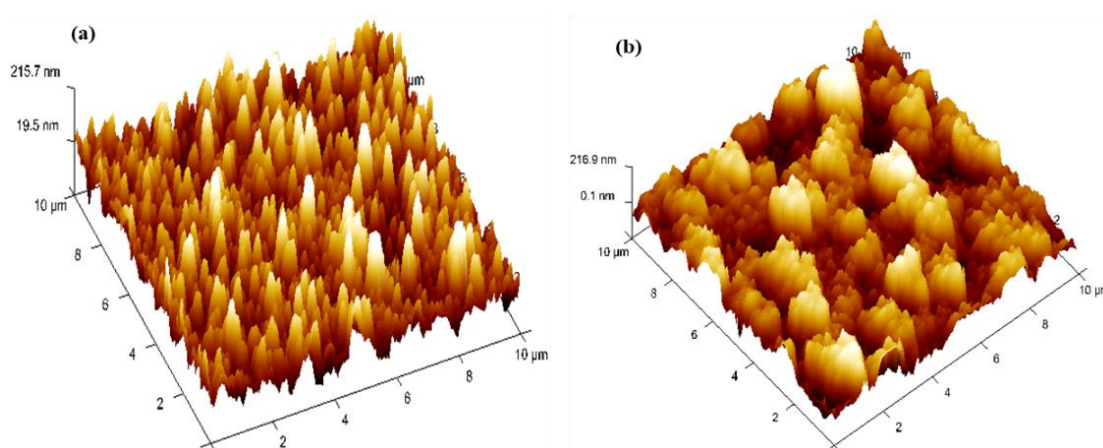


**Figure 9.9** – AFM image showing the surface roughness of a)  $(\text{NiCo})_{1\text{Adm}^{-2}}$  coating and b)  $(\text{NiCo-Ag})_{1.0}$  composite coating, deposited from same bath, A substantial difference in the topography of coatings may be seen due to addition of Ag nanoparticles.

#### 9.4.5 Electrocatalytic efficacy of NiCo-Ag composite coating

The electro-catalytic efficacy of NiCo-Ag composite coatings were put to test by conventional CV and CP methods and are discussed here.

##### 9.4.5.1 Cyclic voltammetry analysis

The electrode - ion interaction in the electrode/electrolyte interface can be obtained from the exceptionally reliable, and most widely used CV technique. Accordingly, CV study of all NiCo-Ag composite coatings have been done following the same procedure, as explained in Section 9.3. The corresponding CV responses are recorded in Figure 9.10.

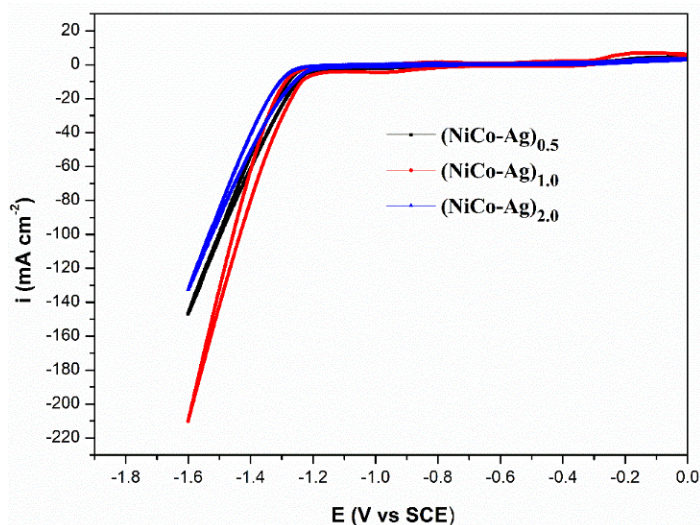


**Figure 9.10** - CV curves of HER on the surface of NiCo-Ag composite coatings deposited at  $1.0 \text{ Adm}^{-2}$  from the optimized bath, having added with different quantity of Ag nanoparticles. Highest cathodic peak current density ( $i_{pc}$ ) corresponding (NiCo-Ag)<sub>1.0</sub> indicates its highest efficacy for HER compared to other coatings.

From the nature of CV curves, shown in Figure 9.10, and electro-kinetic parameters shown in Table 9.4, it is evident that (NiCo-Ag)<sub>1.0</sub> composite coating showed the highest cathodic peak current density ( $i_{pc}$ ) value with least onset potential, compared to all other coatings. It means to understand that this particular composite electrode has higher efficacy for HER than all other coatings. Further, data given in Table 9.4 confirms that (NiCo-Ag)<sub>1.0</sub> composite coating is the best electrode material towards HER with least onset potential (1.27 V), compared with bare- NiCo alloy electrode (1.32 V). Hence, it may be inferred that incorporation of nanoparticles into the alloy matrix is considered to be responsible for increasing the effective surface area of coatings, and hence, their electrocatalytic activity. When 1.0g/L Ag nanoparticles are added to the plating bath, Co content of the deposit found to be increased slightly, compared to (NiCo)<sub>1.0Adm<sup>-2</sup></sub> coating, as shown in Table 9.4. This may be one of the reason responsible for enhanced HER of (NiCo-Ag)<sub>1.0</sub> composite coating. Thus it may be summarized that large variation in  $i_{pc}$  value for the composite electrode is attributed to both enhanced adsorption of the  $\text{H}^+$  ions on the electrode surface, influenced by the increased surface area, with no active sites affected due to incorporation of Ag nanoparticles into the alloy matrix, and increased Co content.

**Table 9.3 – Electro-catalytic parameters of NiCo-Ag composite coatings in different composition for HER alkaline water electrolysis**

Coating configuration	Wt. % of Ni in the deposit	Wt. % of Co in the deposit	Wt. % of Ag in the deposit	HER		
				Cathodic peak c.d. (mAcm <sup>-2</sup> )	Onset potential (V vs SCE)	Volume of H <sub>2</sub> evolved in 300 s
(NiCo-Ag) <sub>0.5</sub>	26.99	70.33	2.69	-148.5	-1.28	13.1
(NiCo-Ag) <sub>1.0</sub>	25.64	71.14	3.22	-212.3	-1.27	13.9
(NiCo-Ag) <sub>2.0</sub>	29.10	68.64	2.26	-132.6	-1.30	12.9
(NiCo) <sub>1.0</sub> Adm <sup>-2</sup>	29.40	70.60	-	-128.7	-1.32	12.3

#### 9.4.5.2 Chronopotentiometry analysis

The CP curves of the NiCo-Ag coatings obtained after applying -0.3A current for a time duration of 300 s are shown in the Figure 9.11. The applied constant current leads to the continuous reduction of the H<sup>+</sup> ions at the cathode surface, and thereby the continuous evolution of H<sub>2</sub>. Apart from that, during the chrono-potentiometry analysis, hydrogen evolution takes place uninterruptedly at the same rate at a particular potential, depending on the stability and efficiency of electrode material. Accordingly, the volume of H<sub>2</sub> evolved on surface of different coatings were measured, and reported in Table 9.4

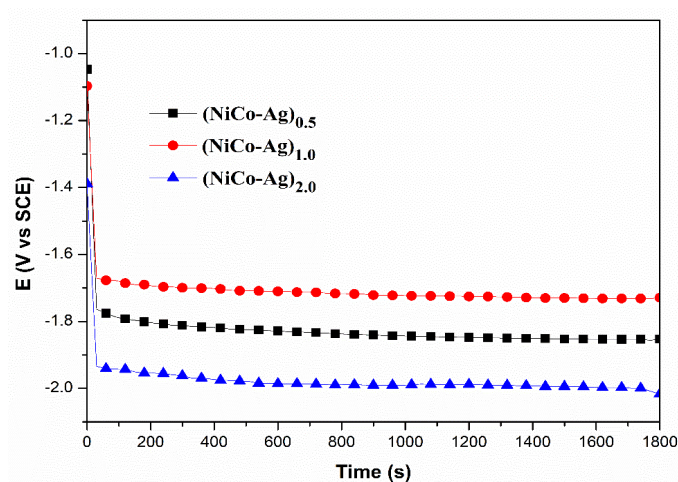


**Figure 9.11 - CP curves of HER on the surface of NiCo-Ag composite coatings deposited at 1.0 Adm<sup>-2</sup> on adding different amount of Ag nanoparticles into the optimized bath.**



The chrono-potentiogram of each coating, shown in Figure 9.11 confirms that The (NiCo-Ag)<sub>1.0</sub> composite coating is more stable and efficient as electro-catalyst for HER. The (NiCo-Ag)<sub>1.0</sub> coating exhibited the best electrocatalytic activity for HER with maximum amount of H<sub>2</sub> gas evolution, compared to all other coatings. All (NiCo-Ag) composite coatings, showed a sudden decrease in potential in the beginning of electrolysis, and eventually reached a steady state. This is due to the attainment of equilibrium between reduction of H<sup>+</sup> from electrolyte on the electrode surface and H<sub>2</sub> gas evolution from the surface. In addition, as the efficiency of electrode material increases towards HER, the potential value becomes nobler (moves close to zero). Therefore, from constant 'E-t' response of (NiCo-Ag)<sub>1.0</sub> composite coatings (by being more noble), it may be inferred that it is more stable and robust electrode material for HER, than all other coatings under given condition of electrolysis.

#### **9.4 CONCLUSIONS**

The electrocatalytic study of electrodeposited NiCo alloy coatings for alkaline water electrolysis, and effect of addition of Ag nanoparticles on it's HER efficacy have been studied to arrive the following conclusions.

1. The NiCo alloy coatings have been deposited at different current densities and their electrocatalytic study have been made, by using them as electrode material as both cathode and anode for hydrogen evolution reaction (HER) and oxygen evolution reaction (OER), respectively.
2. The electrocatalytic performance of NiCo alloy coatings were evaluated in 1M KOH medium using electrochemical techniques such as cyclic voltammetry (CV) and chronopotentiometry (CP).
3. Quantitative measurement of H<sub>2</sub> and O<sub>2</sub> gas, evolved at cathode and anode revealed that NiCo alloy deposited at low current density is good electrode material for both HER and OER, supported by CV and CP study.
4. The changed electrocatalytic activity of NiCo alloy coatings, developed at different current densities were attributed to their changed surface morphology, composition and phase structure, analyzed through SEM, AFM, EDS and XRD techniques.

5. The effect of addition of Ag nanoparticles into the bath, and electrocatalytic activity of NiCo-Ag composite coatings for HER was studied. A substantial improvement in the electro-catalytic activity of HER was found.
6. The NiCo-Ag composite coating having (NiCo-Ag)<sub>1.0</sub> configuration is considered to be the best electrode material for HER in alkaline water electrolysis, compared to other coatings.
7. The high electrocatalytic activity of NiCo-Ag composite was found to be affiliated to the incorporation Ag nanoparticles into NiCo alloy matrix, confirmed by SEM, EDS and elemental mapping analyses.
8. It was summarized that higher efficacy of (NiCo-Ag)<sub>1.0</sub> composite coating for HER is attributed to the enhanced adsorption of the H<sup>+</sup> ions on the electrode surface, influenced by the increased surface area, with no active sites affected due to incorporation of Ag nanoparticles into the alloy matrix, and its increased Co content.

## **CHAPTER 10**

### **SUMMARY AND CONCLUSIONS**



## CHAPTER 10

### SUMMARY AND CONCLUSIONS

---

*This chapter summarizes the experimental results of investigation on electrodeposition and characterization of two binary alloys of nickel, namely NiW and NiCo for improved corrosion protection and electrocatalytic activity through different methods of electroplating, reported in different chapters. Electrodeposition conditions were optimized for peak performance of alloy coatings for intended purposes of either corrosion protection or electrocatalytic activity, or both, through multilayer coating approach. Improved performance of alloy coatings were explained through the changed composition, surface morphology and phase structure of alloy coatings, depending on the current density used for electroplating. The effect of forced convections, like magnetic field (B) effects on mass transport process, and hence corrosion performance of alloy coatings have been compared. The advent of magneto-electrodeposition (MED), over the conventional electrodeposition (ED) are compared and discussed. The effect of current density and addition of Ag nanoparticle on electrocatalytic activity of NiCo alloy coatings were tested, and results are discussed. The final conclusions are presented at the end, in the form of bar charts.*

#### 10.1 THESIS LAYOUT

The research work presented in this thesis is primarily on optimization of two new Ni-based alloy baths, using glycine as the additive. Deposition conditions and operating variables have been optimized for best performance of alloy coatings, against corrosion and good electro-catalytic activity of HER and OER. The corrosion resistance and electro-catalytic activities of conventional monolayer alloy coatings, developed using direct current were tried to improve further, through different modern methods of electroplating, like composition modulated multilayer and magneto-electrodeposition methods. The flow chart of the research work carried out in titled thesis is presented in Figure 10.1.

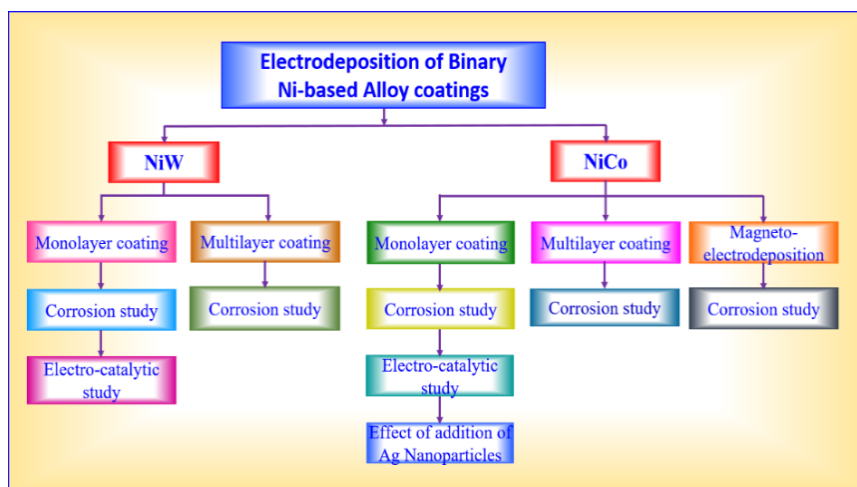


**Figure 10.1-** Flow chart of the research work presented in the thesis.

## 10.2 EXPERIMENTAL

The optimal conditions necessary to obtain quality electrodeposits of NiW and NiCo alloy coatings were achieved using Hull cell method (Kanani 2006). The various deposition techniques adopted for the development of alloy/composite coatings from optimised NiW and NiCo plating baths are schematically shown in Figure 10.2. All depositions were carried out in a rectangular PVC vessel of 250 mL capacity by keeping Graphite anode, and copper cathode (substrate) parallel, at 5 cm distance. Depositions of alloy/composite coatings were carried out for the same duration of time (10 min), for comparison purpose using DC Power Analyser (Agilent Technologies, Model: N6705), as the power source. The new class of materials, called composition modulated multilayer alloy (CMMA), or simply multilayer coatings, have been developed electrolytically by pulsing the DC between two values, taking the respective baths (Kanani 2006; Krishnan et al. 2002). The magneto-electrodeposited (MED) alloy coatings were accomplished at desired current density in conjunction with induced  $B$ , using DC power source and an electromagnet (Polytronics, Model: EM 100), respectively. The corrosion behaviours and electrocatalytic activities of alloy coatings were tested using electrochemical methods. Electrochemical impedance spectroscopy (EIS) and potentiodynamic polarization and methods were used for evaluating the corrosion behaviours of the alloy coatings, in 3.5% NaCl solution (as common corrosion medium).

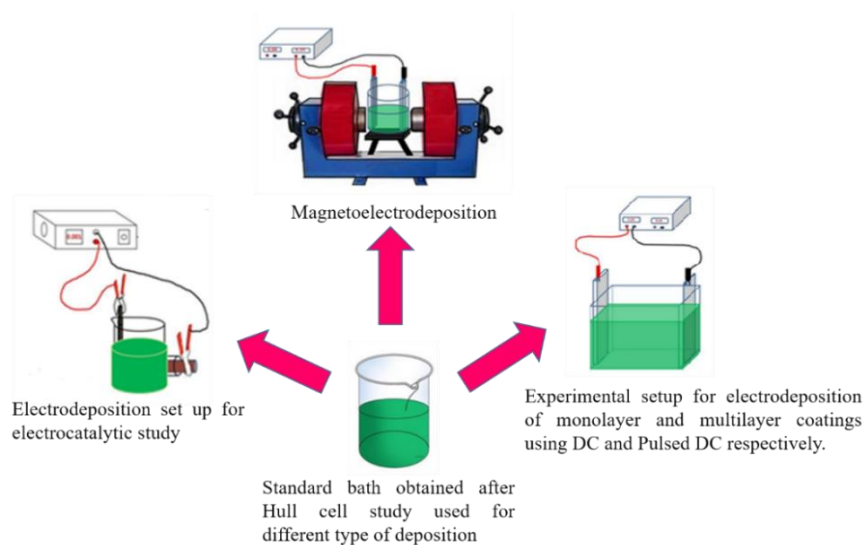


**Figure 10.2-** Schematic of the various deposition techniques used for development of different binary alloy coatings, using the same optimized bath.

The electro-catalytic activity of binary alloys, and their nanocomposite coatings were assessed through cyclic voltammetry (CV) and chronopotentiometry (CP) techniques, in 1.0 M KOH medium. All electrochemical measurements were made using computer controlled potentiostat/galvanostat (VersaSTAT-3, Princeton Applied Research Laboratory, USA). Apart from the electrochemical characterizations, coatings were analysed for their morphology, composition and structure, using SEM, AFM, EDS and XRD techniques, respectively for better insight of their structure-property relationships.

### 10.3 OPTIMIZATION OF NiW AND NiCo ALLOY BATHS

Electroplating is a process in which an inexpensive metal (substrate) is covered with a thin and uniform layer of another metal/alloy having improved properties. It is relatively an inexpensive methods. Generally, electrodeposited alloys have a better appearance than the parent metals, by being smoother and brighter. It is further asserted that relative to the single metal involved, alloy deposits can have different properties in certain composition ranges. They can be denser, harder, more corrosion resistant, and more protective of the underlying base metal. Off late, the subject of alloy plating is growing in both evolutionally and revolutionary ways. The reason for this is due to the vastness of the number of possible alloy combinations, and associated practical applications. Hence, keeping wide industrial applications of alloy plating, two

electrolytic baths, namely NiW and NiCo were optimized through standard Hull Cell method, and corresponding composition and operating variables are given in Table 10.1.

**Table 10.1- Composition and operating parameters of optimized binary alloy baths used for electrodeposition and characterization of different alloys**

Bath Constituents	NiW bath (g/L)	NiCo bath (g/L)
<b>NiSO<sub>4</sub>. 6H<sub>2</sub>O</b>	14.3	100.0
<b>Na<sub>2</sub>WO<sub>4</sub>.2H<sub>2</sub>O</b>	22.5	-
<b>KNaC<sub>4</sub>H<sub>4</sub>O<sub>6</sub>.4H<sub>2</sub>O</b>	100.0	16.6
<b>NH<sub>4</sub>Cl</b>	50.0	-
<b>NH<sub>2</sub>-CH<sub>2</sub>-COOH</b>	4.3	3.3
<b>CoSO<sub>4</sub>. 7H<sub>2</sub>O</b>	-	20.0
<i>Operating parameters</i>		
<b>Current density range</b>	1.0 - 4.0 Adm <sup>-2</sup>	1.0 - 4.0 Adm <sup>-2</sup>
<b>Temperature</b>	303 K	303 K
<b>pH</b>	8.5	3.0
<b>Anode</b>	Graphite	Graphite
<b>Cathode (substrate)</b>	Copper	Copper
<b>Deposition duration</b>	600 s	600 s

## 10.4 ELECTRODEPOSITION OF NiW AND NiCo ALLOY COATINGS

### 10.4.1 Conventional monolayer alloy coatings

In the thesis, NiW and NiCo alloy were optimized, and their monolayer (conventional) alloy coating have been accomplished using direct current (DC), and their corrosion behaviors were studied. Monolayer alloy coatings of NiW and NiCo alloy was carried out at different current densities, and optimal current density for deposition of their coatings, showing best performance against corrosion was identified.



#### **10.4.2 Development of multilayer and magneto-electrodeposited (MED) alloy coatings**

To improve the corrosion resistance property of conventional monolayer alloy coatings, deposited using DC was tried to improve further multilayer approach and magneto-electrodeposition methods as explained here. Multilayer NiW and NiCo alloy coatings of different configuration, having different number layers of alternatively different composition and thickness were developed by setting up the power source to switch between two cathode current density values. The corrosion resistance behaviour of both alloy systems were tried to enhance by multilayer approach. This effect was found to increase up to a certain number of layers, and thereafter no improvement in corrosion resistance behaviour was found. Further, the advent of magnetic field effect on electrodeposition of NiCo alloy coatings was tried, by superimposing magnetic field  $B$ , parallel to the process of deposition by keeping the current density as constant (optimal). The magneto-electrodeposited (MED) NiCo alloy coating was carried out at different intensities of  $B$ , applied both parallel and perpendicular to the direction of flow of ions.

#### **10.5 CORROSION STUDY OF ELECTRODEPOSITED ALLOY COATINGS**

The corrosion protection efficacy of monolayer, multilayer and MED coatings of NiW and NiCo are studied by electrochemical AC and DC methods. Corrosion rate values revealed that corrosion resistance of binary alloy coatings can be increased by many folds, by both multilayer and MED methods. A significant improvement in the corrosion resistance of MED coatings was found (under both parallel and perpendicular  $B$ ). It was attributed to the increased Ni content of the alloy, due to magneto-convection effect. Further, MED coating developed under perpendicular  $B$  was found to show superior properties, over the coatings developed under parallel  $B$ . The increased corrosion stability of MED coatings were attributed to the maximum MHD effect due to additional effect of Lorentz force. Experimental results of MED study revealed that coating with  $(\text{NiCo})_{4/0.3\text{T/Per}}$  configuration is showing the best corrosion performance, compare to all their coatings. To summarize, with objective of developing a better corrosion resistant Ni-based alloy coatings from two baths, namely NiW and NiCo, using different modern methods of electrodeposition, like multilayer electrodeposition and magneto-electrodeposition, a good degree of success was achieved. The corrosion

performance of all coatings, deposited for same duration (600 s) were evaluated in common corrosion medium, and their corrosion rates (CR's) are shown, in a relative scale in Figure 10.3. It was concluded that corrosion performance of monolayer coatings of both alloys can be improved to many fold better by both multilayer and MED approaches, as evidenced by their CR values.

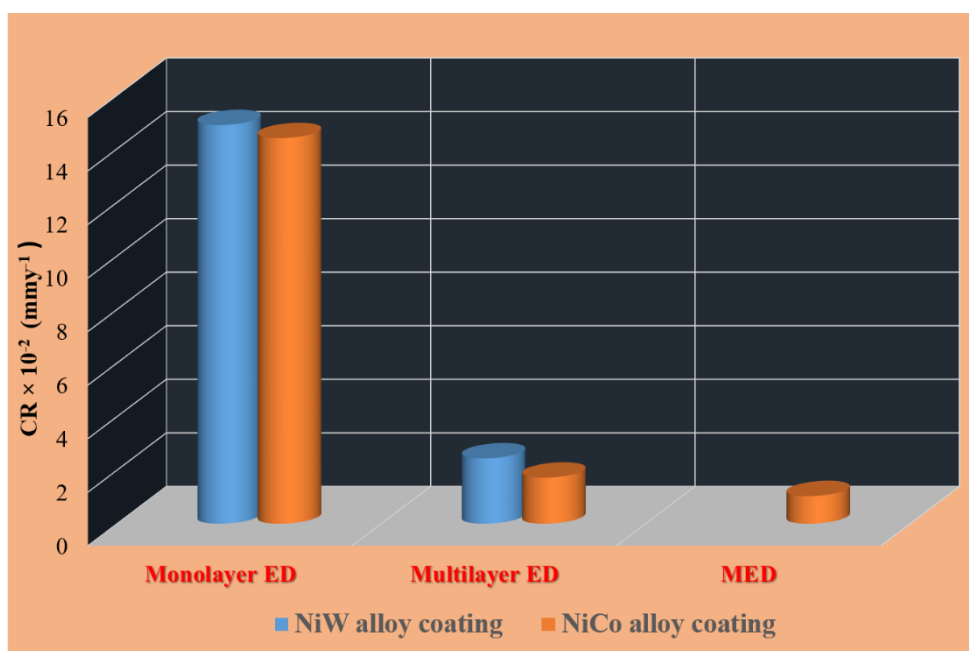


**Figure 10.3-** Histogram showing the corrosion rates (CR) of NiW and NiCo alloy coatings, achieved through different approaches in relation to that of their monolayer counterpart, deposited using DC, from same bath for same duration of time.

### 10.6 ELECTROCATALYTIC STUDY OF ALLOY COATINGS

The electrocatalytic activity of electrodeposited alloy coatings were examined by subjecting them to alkaline water electrolysis (1.0 M KOH), by using them as cathode and anode, for hydrogen evolution reactions (HER) and oxygen evolution reactions (OER), respectively. The electro-catalytic activity NiW and NiCo alloy coatings, deposited from their optimal baths, have been tested for their efficacy for both HER and OER. The effect of addition of nanoparticles, namely Ag nanoparticle into NiCo bath has been studied for its HER activity, using it as cathode in the electrolyser. To begin with, monolayer NiW and NiCo alloy coatings were electrodeposited from their optimised baths, at different current densities and their electro catalytic activity for alkaline water electrolysis were studied. Electrocatalytic efficacy of alloy coatings

(corresponding to different current density and hence different alloy compositions) were studied for their HER and OER have been studied, by measuring quantitatively the amount of H<sub>2</sub> and O<sub>2</sub> evolved on their electrode surface. The electrocatalytic stability of alloy coatings, in the medium of water electrolysis have also been studied, by chronopotentiometric methods. The experimental data revealed that NiW alloy coating developed at lower current density, having high W content is more favourable to HER, than for OER, and coating deposited at higher current density is found to be more favourable for OER than HER. This inverse dependency of alloy composition for HER and OER is attributed to the energy difference of HOMO and LUMO of associated redox processes. Similarly, (NiCo) coating deposited at lower current density was found to facilitate both HER and OER, compared to other coatings deposited at high current densities. Experimental study demonstrated that addition of Ag nanoparticles into the alloy matrix of (NiCo) increased the electrocatalytic activity of HER.

To summarize, electrocatalytic activity of NiW and NiCo alloy coatings have been measured, in terms of the amount of H<sub>2</sub> and O<sub>2</sub> gas evolved during alkaline water electrolysis. The relative performance of different alloy coatings, for HER and OER of alkaline water electrolysis is shown diagrammatically in Figure 10.4.

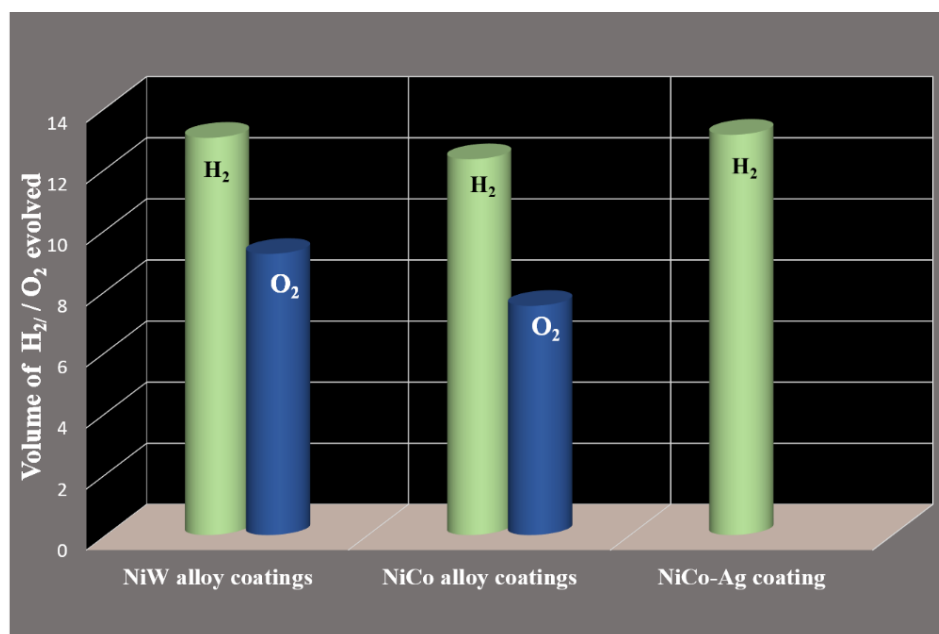


**Figure 10.4-** Diagrammatic representation showing the relative performance of Ni-based alloy coatings as electro-catalyst for alkaline water electrolysis of HER and OER (deposited for same duration of time).

It was observed that electrodeposited NiW alloy coatings are electrocatalytically more active towards both HER and OER compared to NiCo alloy coatings. Addition of Ag nanoparticles into NiCo alloy system enhanced its electrocatalytic activity towards HER, to bring its electrocatalytic activity on par with that of NiW alloy coating.

## 10.7 CONCLUSIONS

Based on experimental investigation carried out on electrodeposition of NiW and NiCo alloy coatings from newly optimized baths, through different methods for better corrosion performance and electro-catalytic activity following conclusion are drawn:

1. The proposed baths, namely NiW and NiCo alloy were found to follow, respectively induced and anomalous type of co-depositions under all conditions of bath composition and operating variables studied.
2. The corrosion study of NiW alloy coatings revealed that coating deposited at  $1.0 \text{ Adm}^{-2}$ , denoted as  $(\text{NiW})_{1.0 \text{ Adm}^{-2}}$  with highest W content (18.9 Wt. %) is the most corrosion resistant ( $\text{CR} = 14.8 \times 10^{-2} \text{ mmy}^{-1}$ ), compared to all other coatings.
3. The NiCo alloy deposited at  $4.0 \text{ Adm}^{-2}$  denoted as  $(\text{NiCo})_{4.0 \text{ Adm}^{-2}}$  having highest Ni content (38.6 Wt. %) is found to exhibit the least corrosion rate ( $\text{CR} = 14.4 \times 10^{-2} \text{ mmy}^{-1}$ ), compared to all other coatings.
4. Under optimal conditions, both multilayered NiW and NiCo alloy coatings having  $(\text{NiW})_{1.0/3.0/120}$  and  $(\text{NiCo})_{2.0/4.0/120}$  configurations were found exhibit, respectively about six times and eight times more corrosion resistance, when compared to their monolayer counterparts, deposited from same bath for same duration.
5. SEM study of corroded surface of monolayer and multilayer alloy coatings of both NiW and NiCo demonstrated that the better corrosion performance of multilayer coating is due to selective dissolution of alternate layers of alloys, having low and high noble metal content (W and Ni). In other words, it is due to selective dissolution of alternate layers of alloys having different composition, affected due to periodic pulsing of the cathodic current during deposition.
6. Increased corrosion resistance of multilayer alloy coating, both NiW and NiCo compared to their monolayer counterpart is accredited to increased number of interfaces, affected due to layering. Alternate layers of alloys are making the

corroding constituents to spread laterally through interfaces, with less scope for them to penetrate directly into the coatings to reach the substrate.

7. Increase of corrosion rate at higher degree of layering after 120 layers, in both NiW and NiCo is accredited to the diffusion of individual layers, due to very short pulsing period. *i.e.* pulsing period is too short to form alternate layers with different composition. In other words, at higher degree of layering multilayer coating reduces to monolayer coating.
8. Study of magneto-electrodeposition (MED) of NiCo coatings revealed that corrosion protection efficacy of monolayer alloy coatings can be increased to many fold of its magnitude by superimposing magnetic field ( $B$ ), both parallel and perpendicular simultaneously to the process of deposition.
9. Increased corrosion resistance of MED coatings is attributed to the increased noble metal content (Ni) of the alloy, affected due to phenomenon, called *magneto-convection*.
10. Electrocatalytic study of NiW and NiCo alloy coatings for alkaline water splitting (1.0 M KOH) of HER and OER revealed that their electro-catalytic activity has strong dependency with their deposition current density determined composition, confirmed through cyclic voltammetry (CV) and chronopotentiometry (CP) study.
11. Incorporation of Ag nanoparticles into NiCo alloy matrix was found to increase its electro-catalytic activity of HER in alkaline water electrolysis, and is attributed to increased reactive sites for evolution of H<sub>2</sub>.
12. Corrosion and electrocatalytic performance of all monolayer, multilayer, magneto-electrodeposited and nanocomposite coatings of NiW and NiCo alloy are compared and discussed, with support of different instrumental methods of analyses, such as SEM, EDS, XRD, AFM, EIS, PDP, CV and CP techniques. The experimental results are discussed with reasons responsible for improved corrosion resistance/electro-catalytic activities.

## 10.8 SCOPE FOR THE FUTURE WORK

- To study pulse electrodeposition of NiW and NiCo alloys by varying pulse frequency and duty cycle, and to examine their effect on their electrochemical properties.
- To study electrodeposition of NiWCo ternary alloy coating and compare their corrosion and electro-catalytic behavior with that of their binary counter parts.
- To study the effect of ultrasound on the process of electrodeposition of above alloy coatings, and to optimize the deposition conditions of their monolayer and multilayer alloy coatings for peak performance against corrosion.
- To study the effect of two dimensional chalcogenides such as WS<sub>2</sub>, MoS<sub>2</sub> in electro-codeposition of NiW and NiCo alloy coatings, and their electro-catalytic activity for overall water electrolysis.

## REFERENCES

---

- Allahyarzadeh, M. H., Aliofkhazraei, M., and Rouhaghdam, A. R. S. (2016a). "Functionally graded nickel – tungsten coating : electrodeposition , corrosion and wear behaviour." *Can. Metall. Q.*, 55(3), 303–311.
- Allahyarzadeh, M. H., Aliofkhazraei, M., Rouhaghdam, A. R. S., and Torabinejad, V. (2016b). "Electrodeposition of Ni-W-Al<sub>2</sub>O<sub>3</sub> nanocomposite coating with functionally graded microstructure." *J. Alloys Compd.*, 666, 217–226.
- Allen J. Bard, and Faulkner, L. R. (2000). *Electrochemical methods: Fundamentals and applications*. John Wiley Sons, Inc., New York.
- Anicai, L. (2007). "Ni-W alloys coatings as ecological alternative for Chromium plating - Evaluation of corrosion behaviour." *Corros. Rev.*, 25(5–6), 607–620.
- Arganaraz, M. P. Q., Ribotta, S. B., Folquer, M. E., Zelaya, E., Llorente, C., Ramallo-lópez, J. M., Benítez, G., Rubert, A., Gassa, L. M., Vela, M. E., and Salcarezza, R. C. (2012). "The chemistry and structure of nickel – tungsten coatings obtained by pulse galvanostatic electrodeposition." *Electrochim. Acta*, 72, 87–93.
- Arul Raj, I., and Vasu, K. I. (1990). "Transition metal-based hydrogen electrodes in alkaline solution -- electrocatalysis on nickel based binary alloy coatings." *J. Appl. Electrochem.*, 20, 32–38.
- Arunsunai Kumar, K., Paruthimal Kalaigan, G., and Muralidharan, V. S. (2012). "Pulse electrodeposition and characterization of nano Ni-W alloy deposits." *Appl. Surf. Sci.*, 259, 231–237.
- Ashraf, M. A., Li, C., Pham, B. T., and Zhang, D. (2020). "Electrodeposition of Ni–Fe–Mn ternary nanosheets as affordable and efficient electrocatalyst for both hydrogen and oxygen evolution reactions." *Int. J. Hydrogen Energy*, 45(46), 24670–24683.
- Ashraf, P. M., Thomas, S. N., and Edwin, L. (2016). "Development of graphene–nanometre-sized cerium oxide-incorporated aluminium and its electrochemical evaluation." *Appl. Nanosci.*, 6(2), 149–158.

Bahadormanesh, B., Dolati, A., and Ahmadi, M. R. (2011). "Electrodeposition and characterization of Ni-Co/SiC nanocomposite coatings." *J. Alloys Compd.*, 509(39), 9406–9412.

Bahadormanesh, B., Ghorbani, M., and Lotfi, N. (2017). "Electrodeposition of nanocrystalline Zn / Ni multilayer coatings from single bath : Influences of deposition current densities and number of layers on characteristics of deposits." *Appl. Surf. Sci.*, 404, 101–109.

Bakhit, B., and Akbari, A. (2013). "Nanocrystalline Ni-Co alloy coatings: Electrodeposition using horizontal electrodes and corrosion resistance." *J. Coatings Technol. Res.*, 10(2), 285–295.

Bakhit, B., Akbari, A., Nasirpouri, F., and Hosseini, M. G. (2014). "Corrosion resistance of Ni-Co alloy and Ni-Co/SiC nanocomposite coatings electrodeposited by sediment codeposition technique." *Appl. Surf. Sci.*, 307, 351–359.

Bang, J. H., and Suslick, K. S. (2010). "Applications of ultrasound to the synthesis of nanostructured materials." *Adv. Mater.*, 22(10), 1039–1059.

Benaicha, M., Allam, M., Dakhouch, A., and Hamla, M. (2016). "Electrodeposition and characterization of W-rich NiW alloys from citrate electrolyte." *Int. J. Electrochem. Sci.*, 11(9), 7605–7620.

Bouzit, F. Z., Nemamcha, A., Moumeni, H., and Rehspringer, J. L. (2017). "Morphology and Rietveld analysis of nanostructured Co-Ni electrodeposited thin films obtained at different current densities." *Surf. Coatings Technol.*, 315, 172–180.

Brenner, A. (1963a). *Electrodeposition of Alloys: Principles and Practice*. New York and London: Academic Press.

Brenner, A. (1963b). *Electrodeposition of alloys: principles and practice*. New York and London : Academic press.

Bull, S. J., and Jones, A. M. (1996). "Multilayer coatings for improved performance." *Surf. Coatings Technol.*, 78(1–3), 173–184.



- Bunaciu, A. A., Udriștioiu, E. gabriela, and Aboul-Enein, H. Y. (2015). “X-Ray Diffraction: Instrumentation and Applications.” *Crit. Rev. Anal. Chem.*, 45(4), 289–299.
- Burzyńska, L., and Rudnik, E. (2000). “Influence of electrolysis parameters on the composition and morphology of Co-Ni alloys.” *Hydrometallurgy*, 54(2), 133–149.
- Cai, F., Jiang, C., Fu, P., and Ji, V. (2015). “Effects of Co contents on the microstructures and properties of electrodeposited NiCo-Al composite coatings.” *Appl. Surf. Sci.*, 324, 482–489.
- Chang, L. M., Wang, Z. T., Shi, S. Y., and Liu, W. (2011). “Study on microstructure and properties of electrodeposited Ni – W alloy coating with glycolic acid system.” *J. Alloys Compd.*, 509(5), 1501–1504.
- Chi, B., Li, J., Yang, X., Gong, Y., and Wang, N. (2005). “Deposition of Ni-Co by cyclic voltammetry method and its electrocatalytic properties for oxygen evolution reaction.” *Int. J. Hydrogen Energy*, 30(1), 29–34.
- Choi, P., Al-Kassab, A., Gartner, F., Kreye, H., and Kirchheim, R. (2003). “Thermal stability of nanocrystalline nickel  $\dot{A}$  18 at .% tungsten alloy investigated with the tomographic atom probe.” *Mater. Sci. Eng. A*, 353, 74–79.
- Covington, A. K. (1973). “Ion-selective electrodes.” *C R C Crit. Rev. Anal. Chem.*, 3(4), 355–406.
- Cullity, B. (1956). *Elements of X ray diffraction*. Addison-Wesley Publishing.
- Davis, J. R. (2000). *Corrosion: understanding the basics*. ASM Int., Ohio.
- Dini, J. W. (1993). *Electrodeposition: the materials science of coatings and substrates*. *Br. Corros. J.*, New Jersey: Noyes Publications.
- Dobrzański, L. A., and Lukaszewicz, K. (2007). “Corrosion resistance of multilayer and gradient coatings deposited by PVD and CVD techniques.” *Arch. Mater. Sci. Eng.*, 28(1), 12–18.

Eaton, P., and West, P. (2010). "Atomic Force Microscopy." *At. Force Microsc.*, 9780199570, 1–256.

Elgrishi, N., Rountree, K. J., McCarthy, B. D., Rountree, E. S., Eisenhart, T. T., and Dempsey, J. L. (2018). "A Practical Beginner's Guide to Cyclic Voltammetry." *J. Chem. Educ.*, 95(2), 197–206.

Elias, L., and Chitharanjan Hegde, A. (2015). "Electrodeposition of laminar coatings of Ni-W alloy and their corrosion behaviour." *Surf. Coatings Technol.*, 283, 61–69.

Elias, L., and Hegde, A. C. (2015). "Electrodeposition and Electrocatalytic Study of Ni-W Alloy Coating." *Mater. Sci. Forum*, 830–831, 651–654.

Elias, L., and Hegde, A. C. (2016). "Modification of Ni-P alloy coatings for better hydrogen production by electrochemical dissolution and TiO<sub>2</sub> nanoparticles." *RSC Adv.*, 6(70), 66204–66214.

Elias, L., and Hegde, A. C. (2017a). "Effect of magnetic field on corrosion protection efficacy of Ni-W alloy coatings." *J. Alloys Compd.*, 712, 618–626.

Elias, L., and Hegde, A. C. (2017b). "Effect of including the carbon nanotube and graphene oxide on the electrocatalytic behavior of the Ni-W alloy for the hydrogen evolution reaction." *New J. Chem.*, 41(22), 13912–13917.

Elias, L., Scott, K., and Hegde, A. C. (2015). "Electrolytic Synthesis and Characterization of Electrocatalytic Ni-W Alloy." *J. Mater. Eng. Perform.*, 24(11), 4182–4191.

Eliasz, N., and Gileadi, E. (2008). "Induced Codeposition of Alloys of Tungsten, Molybdenum and Rhenium with Transition Metals." *Mod. Asp. Electrochem.*, (42), 191–301.

Eliasz, N., Sridhar, T. M., and Gileadi, E. (2005a). "Synthesis and characterization of nickel tungsten alloys by electrodeposition." *Electrochim. Acta*, 50(14), 2893–2904.

Eliasz, N., Sridhar, T. M., and Gileadi, E. (2005b). "Synthesis and characterization of nickel tungsten alloys by electrodeposition." *Electrochim. Acta*, 50, 2893–2904.

Elrouby, M., Sadek, M., Mohran, H. S., and El-Lateef, A. M. (2020). “A highly stable and efficient electrodeposited flowered like structure Ni-Co alloy on steel substrate for electrocatalytic hydrogen evolution reaction in HCl solution.” *J. Mater. Res. Technol.*, 9(6), 13706–13717.

Fahidy, T. Z. (1983). “Magnetoelectrolysis.” *J. Appl. Electrochem.*, 13, 553–563.

Fan, C., Piron, D. L., and Paradis, P. (1994). “Hydrogen evolution on electrodeposited nickel-cobalt-molybdenum in alkaline water electrolysis.” *Electrochim. Acta*, 39(18), 2715–2722.

Fontana, M. G. (1987). *Corrosion Engineering*. Singapore: McGraw-hill.

Fratesi, R., Roventi, G., Giuliani, G., and Tomachuk, C. R. (1997). “Zinc-cobalt alloy electrodeposition from chloride baths.” *J. Appl. Electrochem.*, 27(9), 1088–1094.

Gáliková, Z., Chovancová, M., and Danielik, V. (2006). “Properties of Ni-W Alloy Coatings on Steel Substrate.” *Chem. Pap.*, 60(5), 353–359.

Ganci, F., Cusumano, V., Livreri, P., Aiello, G., Sunseri, C., and Inguanta, R. (2021). “Nanostructured Ni–Co alloy electrodes for both hydrogen and oxygen evolution reaction in alkaline electrolyzer.” *Int. J. Hydrogen Energy*, 46(16), 10082–10092.

Ganesan, P., Kumaraguru, S. P., and Popov, B. N. (2007). “Development of compositionally modulated multilayer Zn-Ni deposits as replacement for cadmium.” *Surf. Coatings Technol.*, 201(18), 7896–7904.

Ganesh, V., Vijayaraghavan, D., and Lakshminarayanan, V. (2005). “Fine grain growth of nickel electrodeposit: Effect of applied magnetic field during deposition.” *Appl. Surf. Sci.*, 240(1–4), 286–295.

Gang Wu \*, Ning Li , Derui Zhou , Kurachi Mitsuo a, aa b. (2004). “Electrodeposited Co–Ni–Al O composite coatings 23.” *Surf. Coatings Technol.*, 176, 157–164.

Girão, A. V., Caputo, G., and Ferro, M. C. (2017). “Application of Scanning Electron Microscopy–Energy Dispersive X-Ray Spectroscopy (SEM-EDS).” *Compr. Anal. Chem.*, 75, 153–168.

Girolamo, G. Di, Brentari, A., and Serra, E. (2016). "Some recent findings on the use of SEM-EDS in microstructural characterisation of as-sprayed and thermally aged porous coatings: A short review." *AIMS Mater. Sci.*, 3(2), 404–424.

Golodnitsky, D., Rosenberg, Y., and Ulus, A. (2002). "The role of anion additives in the electrodeposition of nickel-cobalt alloys from sulfamate electrolyte." *Electrochim. Acta*, 47(17), 2707–2714.

Gómez, E., Pané, S., and Vallés, E. (2005). "Electrodeposition of Co-Ni and Co-Ni-Cu systems in sulphate-citrate medium." *Electrochim. Acta*, 51(1), 146–153.

Gómez, M. J., Benavente Llorente, V., Lacconi, G. I., and Franceschini, E. A. (2021). "Facile electrodeposition of NiCo-TiO<sub>2</sub> composite coatings for enhanced hydrogen evolution reaction." *J. Electroanal. Chem.*, 895(January).

González-Buch, C., Herraiz-Cardona, I., Ortega, E., García-Antón, J., and Pérez-Herranz, V. (2013). "Synthesis and characterization of macroporous Ni, Co and Ni-Co electrocatalytic deposits for hydrogen evolution reaction in alkaline media." *Int. J. Hydrogen Energy*, 38(25), 10157–10169.

González-buch, C., Herraiz-cardona, I., Ortega, E. M., García-antón, J., and Pérez-herranz, V. (2013). "Development of Ni-Mo, Ni-W and Ni-Co Macroporous Materials for Hydrogen Evolution Reaction Cristina." *Chem. Eng. Trans.*, 32(3), 865–870.

Hassani, S., Raeissi, K., Azzi, M., Li, D., Golozar, M. A., and Szpunar, J. A. (2009). "Improving the corrosion and tribocorrosion resistance of Ni-Co nanocrystalline coatings in NaOH solution." *Corros. Sci.*, 51(10), 2371–2379.

Hassani, S., Raeissi, K., and Golozar, M. A. (2008). "Effects of saccharin on the electrodeposition of Ni-Co nanocrystalline coatings." *J. Appl. Electrochem.*, 38(5), 689–694.

Hefnawy, A., Elkhoshkhany, N., and Essam, A. (2018). "Ni-TiN and Ni-Co-TiN composite coatings for corrosion protection: Fabrication and electrochemical characterization." *J. Alloys Compd.*, 735, 600–606.

Hinds, G., Coey, J. M. D., and Lyons, M. E. G. (2001). "Influence of magnetic forces on electrochemical mass transport." *Electrochem. commun.*, 3(5), 215–218.

Hosokawa, H., Yamasaki, T., Sugamoto, N., Tomizawa, M., Shimojima, K., and Mabuchi, M. (2004). "Bending Properties of Nanocrystalline Ni-18 at % W Alloy Produced by Electrodeposition." *Mater. Trans.*, 45(5), 1807–1810.

Indyka, P., Beltowska-Lehman, E., Tarkowski, L., Bigos, A., and García-Lecina, E. (2014). "Structure characterization of nanocrystalline Ni-W alloys obtained by electrodeposition." *J. Alloys Compd.*, 590, 75–79.

Jović, V.D., Lačnjevac, U.Č., Jović, B. M. (2014). *Electrodeposition and Surface Finishing: Fundamentals and Applications*. Springer, (S. S. Djokic', ed.), New York: Springer.

Kamel, M. M. (2007). "Anomalous codeposition of Co-Ni: Alloys from gluconate baths." *J. Appl. Electrochem.*, 37(4), 483–489.

Kamel, M. M., Alzahrani, E., Ibrahim, I. S., and Rashwan, S. M. (2021). "Electrodeposition of well-crystalline Ni-Co alloy thin films on steel substrates from aqueous solutions containing citrate anions." *Int. J. Electrochem. Sci.*, 16, 1–22.

Kanani, N. (2006). *Electroplating: Basic Principles, Processes and Practice*. Amsterdam, Netherlands: Elsevier Ltd.

Karimzadeh, A., Aliofkhazraei, M., and Walsh, F. C. (2019). "A review of electrodeposited Ni-Co alloy and composite coatings: Microstructure, properties and applications." *Surf. Coatings Technol.*, 372, 463–498.

Karpuz, A., Kockar, H., Alper, M., Karaagac, O., and Hacıismailoglu, M. (2012). "Electrodeposited Ni-Co films from electrolytes with different Co contents." *Appl. Surf. Sci.*, 258(8), 4005–4010.

Kato, T., Kubota, M., Kobayashi, N., and Suzuoki, Y. (2005). "Effective utilization of by-product oxygen from electrolysis hydrogen production." *Energy*, 30(14), 2580–2595.

Kelly, R., Scully, J., Shoesmith, D., and Buchheit, R. (2003). *Electrochemical Techniques in Corrosion Science and Engineering*. New York: Marcel Dekker, Inc.

Kołodziejczyk, K., Miękoś, E., Zieliński, M., Jaksender, M., Szczukocki, D., Czarny, K., and Krawczyk, B. (2018). “Influence of constant magnetic field on electrodeposition of metals, alloys, conductive polymers, and organic reactions.” *J. Solid State Electrochem.*, 22(6), 1629–1647.

Krishnan, K. S. R., Srinivasan, K., and Mohan, S. (2002). “Electrodeposition of compositionally modulated alloys - An overview.” *Trans. Inst. Met. Finish.*, 80(2), 46–48.

Kumar, S., Pande, S., and Verma, P. (2015a). “Factor Effecting Electro-Deposition Process.” *Int. J. Curr. Eng. Technol.*, 5(2), 700–703.

Kumar, S., Pande, S., and Verma, P. (2015b). “International Journal of Current Engineering and Technology Factor Effecting Electro-Deposition Process.” *Int. J. Curr. Eng. Technol.*, 5(2).

Lasia, A. (1999). *Electrochemical impedance spectroscopy and its applications*. Kluwer Acad. Publ.

Lasia, A. (2010). “Hydrogen evolution reaction.” *Handb. Fuel Cells*, 815.

Lee, S., Choi, M., Park, S., Jung, H., and Yoo, B. (2015a). “Mechanical properties of electrodeposited Ni-W ThinFilms with alternate W-rich and W-poor multilayers.” *Electrochim. Acta*, 153, 225–231.

Lee, S., Choi, M., Park, S., Jung, H., and Yoo, B. (2015b). “Electrochimica Acta Mechanical Properties of Electrodeposited Ni-W ThinFilms with Alternate W-Rich and W-Poor Multilayers.” *Electrochim. Acta*, 153, 225–231.

Leisner, P., Nielsen, C. B., Tang, P. T., and Moller, P. (1994). “Methods for electrodeposRing composRion-modulated alloys.” *J. Malerials Process. Teclmology*, 58, 39–44.

Li, G., and Miao, P. (2013). “Theoretical Background of Electrochemical Analysis.” 5–

18.

Li, Y., Jiang, H., Wang, D., and Ge, H. (2008). "Effects of saccharin and cobalt concentration in electrolytic solution on microhardness of nanocrystalline Ni-Co alloys." *Surf. Coatings Technol.*, 202(20), 4952–4956.

Li, Y., Zhang, X., Hu, A., and Li, M. (2018). "Morphological variation of electrodeposited nanostructured Ni-Co alloy electrodes and their property for hydrogen evolution reaction." *Int. J. Hydrogen Energy*, 3, 22012–22020.

Liu, C., Su, F., and Liang, J. (2016). "Nanocrystalline Co-Ni alloy coating produced with supercritical carbon dioxide assisted electrodeposition with excellent wear and corrosion resistance." *Surf. Coatings Technol.*, 292, 37–43.

Liu, Y., Li, H., and Li, Z. (2013). "EIS investigation and structural characterization of different hot-dipped zinc-based coatings in 3.5% NaCl solution." *Int. J. Electrochem. Sci.*, 8(6), 7753–7767.

Lokhande, A. C., and Bagi, J. S. (2014a). "Studies on enhancement of surface mechanical properties of electrodeposited Ni-Co alloy coatings due to saccharin additive." *Surf. Coatings Technol.*, 258, 225–231.

Lokhande, A. C., and Bagi, J. S. (2014b). "Studies on enhancement of surface mechanical properties of electrodeposited Ni-Co alloy coatings due to saccharin additive." *Surf. Coatings Technol.*, 258, 225–231.

Lupi, C., Dell'Era, A., and Pasquali, M. (2009). "Nickel-cobalt electrodeposited alloys for hydrogen evolution in alkaline media." *Int. J. Hydrogen Energy*, 34(5), 2101–2106.

Lupi, C., Dell'Era, A., Pasquali, M., and Imperatori, P. (2011). "Composition, morphology, structural aspects and electrochemical properties of Ni-Co alloy coatings." *Surf. Coatings Technol.*, 205(23–24), 5394–5399.

Ma, C., Wang, S. C., Wang, L. P., Walsh, F. C., and Wood, R. J. K. (2013). "The role of a tribofilm and wear debris in the tribological behaviour of nanocrystalline Ni-Co electrodeposits." *Wear*, 306(1–2), 296–303.

MacDonald, J. R. (1987). *Emphasizing solid materials and systems. Impedance Spectroscopy*. John Wiley & Sons Inc.: New York, NY, USA.

Marikkannu, K. R., Kalaigan, G. P., and Vasudevan, T. (2007). “The role of additives in the electrodeposition of nickel-cobalt alloy from acetate electrolyte.” *J. Alloys Compd.*, 438(1–2), 332–336.

Mbugua, N. S., Kang, M., Zhang, Y., Ndiithi, N. J., Bertrand, G. V., and Yao, L. (2020). “Electrochemical deposition of Ni, NiCo Alloy and NiCo-ceramic composite coatings- A critical review.” *Materials (Basel)*, 13(16).

Mehta, N. K. (2013). “EIS Equivalent Circuit Model : Electrolytic Damage Assessment of the Scribed Coated Steel Surface Embedded with Corrosion Inhibitor Capsules.” 3(5), 149–161.

Mizushima, I., Tang, P. T., Hansen, H. N., and Somers, M. A. J. (2005). “Development of a new electroplating process for Ni-W alloy deposits.” *Electrochim. Acta*, 51(5), 888–896.

Mollamahale, Y. B., Jafari, N., and Hosseini, D. (2018). “Electrodeposited Ni-W nanoparticles: Enhanced catalytic activity toward hydrogen evolution reaction in acidic media.” *Mater. Lett.*, 213, 15–18.

Monzon, L. M. A., and Coey, J. M. D. (2014). “Magnetic fields in electrochemistry: The Kelvin force. A mini-review.” *Electrochem. commun.*, 42, 38–41.

Obradović, M., Stevanović, J., Despić, A., Stevanović, R., and Stoch, J. (2001). “Characterization and corrosion properties of electrodeposited Ni-W alloys.” *J. Serbian Chem. Soc.*, 66(11–12), 899–912.

P.J.Hillson. (1952). “Adsorption and the hydrogen overpotential.” *Trans. faraday Soc.*, (48), 462–473.

Peng, X., Jin, X., Gao, B., Liu, Z., and Chu, P. K. (2021). “Strategies to improve cobalt-based electrocatalysts for electrochemical water splitting.” *J. Catal.*, 398, 54–66.

Pérez-Alonso, F. J., Adán, C., Rojas, S., Peña, M. A., and Fierro, J. L. G. (2015). “Ni-



Co electrodes prepared by electroless-plating deposition. A study of their electrocatalytic activity for the hydrogen and oxygen evolution reactions.” *Int. J. Hydrogen Energy*, 40(1), 51–61.

Perez, N. (2004). *ELECTROCHEMISTRY AND CORROSION SCIENCE*. Boston: Kluwer Academic Publishers.

Peters, P. J. L. & D. G. (1971). “Chronopotentiometry.” *CRC Crit. Rev. Anal. Chem.*, (December 2012), 587–637.

Pletcher, D. (1984). “Electrocatalysis : present and future.” *J. Appl. Electrochem.*, 14, 403–415.

Poyner, J. A. (1987). *Electroplating*. England: Argus Books Ltd.

Pramod Kumar, U., Kennady, C. J., and Zhou, Q. (2015). “Effect of salicylaldehyde on microstructure and corrosion resistance of electrodeposited nanocrystalline Ni-W alloy coatings.” *Surf. Coatings Technol.*, 283, 148–155.

Pu, Z., Amiin, I. S., Wang, M., Yang, Y., and Mu, S. (2016). “semimetallic MoP<sub>2</sub>: an active and stable hydrogen evolution electrocatalyst over the whole pH range.” *Nanoscale*, (8(16)), 8500–8504.

Radhakrishnan, S., Sekar, R., Rajasekhar, B., Mathiyarasu, J., Ragupathi, P., and Ulaganathan, M. (2021). “Electrodeposited partially oxidized Bi & NiCo alloy based thin films for aqueous hybrid high energy microcapacitor.” *J. Alloys Compd.*, 888, 161453.

Rauscher, G., Rogoll, V., Baumgaertner, M. E., and Raub, C. J. (1993). “Investigation of the Dissolution Behaviour of Electrodeposited Ni-W Layers in Concentrated Hydrogen Chloride Solution Investigation of the Dissolution Behaviour of Electrodeposited Ni-W Layers in Concentrated Hydrogen Chloride Solution.” *Trans. IMF*, 71(3), 95–98.

Raveendran, M. N., and Hegde, A. C. (2021). “Electrodeposition of multilayer NiW alloy coating for improved anticorrosion performance.” *Bull. Mater. Sci.*, 44(2).

Ribeiro, D. V., and Abrantes, J. C. C. (2016). "Application of electrochemical impedance spectroscopy (EIS) to monitor the corrosion of reinforced concrete: A new approach." *Constr. Build. Mater.*, 111, 98–104.

Roberge, P. R. (1999). *Handbook of Corrosion Engineering Library of Congress*. McGraw-hill.

Rosalbino, F., Delsante, S., Borzone, G., and Angelini, E. (2008). "Electrocatalytic behaviour of Co-Ni-R (R = Rare earth metal) crystalline alloys as electrode materials for hydrogen evolution reaction in alkaline medium." *Int. J. Hydrogen Energy*, 33(22), 6696–6703.

Rusling, J. F., and Suib, S. L. (1994). "Characterizing Materials with Cyclic Voltammetry." *Adv. Mater.*, 6(12), 922–930.

Safizadeh, F., Ghali, E., and Houlachi, G. (2015). "Electrocatalysis developments for hydrogen evolution reaction in alkaline solutions - A Review." *Int. J. Hydrogen Energy*, 40(1), 256–274.

Salehi, M., Saidi, A., Ahmadian, M., and Raeissi, K. (2014). "Characterization of nanocrystalline nickel-cobalt alloys synthesized by direct and pulse electrodeposition." *Int. J. Mod. Phys. B*, 28(6), 1–14.

San, N. O., Nazir, H., and Dönmez, G. (2012). "Evaluation of microbiologically influenced corrosion inhibition on Ni-Co alloy coatings by *Aeromonas salmonicida* and *Clavibacter michiganensis*." *Corros. Sci.*, 65, 113–118.

Sapountzi, F. M., Gracia, J. M., Weststrate, C. J. (Kee, J., Fredriksson, H. O. A., and Niemantsverdriet, J. W. (Hans. (2017). "Electrocatalysts for the generation of hydrogen, oxygen and synthesis gas." *Prog. Energy Combust. Sci.*, 58, 1–35.

Sassi, W., Dhouibi, L., Berc, P., Rezrazi, M., and Triki, E. (2012). "Effect of pyridine on the electrocrystallization and corrosion behavior of Ni – W alloy coated from citrate – ammonia media." *Appl. sur*, 263, 373–381.

Schwarzacher, W. (2006). "Electrodeposition: A Technology for the Future."

*Electrochem. Soc. Interface*, 15(1), 32–35.

She, Z., Li, Q., Wang, Z., Tan, C., Zhou, J., and Li, L. (2014). “Highly anticorrosion, self-cleaning superhydrophobic Ni-Co surface fabricated on AZ91D magnesium alloy.” *Surf. Coatings Technol.*, 251, 7–14.

Shetty, A. R., and Chitharanjan Hegde, A. (2017). “Ultrasound induced multilayer Ni-Co alloy coatings for better corrosion protection.” *Surf. Coatings Technol.*, 322, 99–107.

Shetty, A. R., and Hegde, A. C. (2018). “Effect of TiO<sub>2</sub> on electrocatalytic behavior of Ni-Mo alloy coating for hydrogen energy.” *Mater. Sci. Energy Technol.*, 1(2), 97–105.

Shi, L., Sun, C. F., Gao, P., Zhou, F., and Liu, W. M. (2006a). “Electrodeposition and characterization of Ni-Co-carbon nanotubes composite coatings.” *Surf. Coatings Technol.*, 200(16–17), 4870–4875.

Shi, L., Sun, C., Gao, P., Zhou, F., and Liu, W. (2006b). “Mechanical properties and wear and corrosion resistance of electrodeposited Ni-Co/SiC nanocomposite coating.” *Appl. Surf. Sci.*, 252(10), 3591–3599.

Shoar Abouzari, M. R., Berkemeier, F., Schmitz, G., and Wilmer, D. (2009). “On the physical interpretation of constant phase elements.” *Solid State Ionics*, 180(14–16), 922–927.

Shourgeshty, M., Aliofkhaezai, M., Karimzadeh, A., and Poursalehi, R. (2017). “Corrosion and wear properties of Zn-Ni and Zn-Ni-Al<sub>2</sub>O<sub>3</sub> multilayer electrodeposited coatings.” *Mater. Res. Express*, 4(9).

Srivastava, M., Ezhil Selvi, V., William Grips, V. K., and Rajam, K. S. (2006). “Corrosion resistance and microstructure of electrodeposited nickel-cobalt alloy coatings.” *Surf. Coatings Technol.*, 201(6), 3051–3060.

Steffani, C. P., Dini, W., Groza, R., and Palazoglu, A. (1997). “Electrodeposition and Corrosion Resistance of Ni-W-B Coatings.” *J. Mater. Eng. Perform.*, 6(August), 413–416.

Swaminathan, J., and Meiyazhagan, A. (2020). *Characterization of electrocatalyst. Methods Electrocatal. Adv. Mater. Allied Appl.*, Springer, cham.

Tacken, R. A. and Janssen, L. J. J. (1995). "Applications of magnetoelectrolysis." *J. Appl. Electrochem.*, 25, 1–5.

Tacken, R. A., and Janssen, L. J. J. (1995). "Applications of magnetoelectrolysis." *J. Appl. Electrochem.*, 25(1), 1–5.

Tahir, M., Pan, L., Idrees, F., Zhang, X., Wang, L., Zou, J. J., and Wang, Z. L. (2017a). "Electrocatalytic oxygen evolution reaction for energy conversion and storage: A comprehensive review." *Nano Energy*, 37(February), 136–157.

Tahir, M., Pan, L., Idrees, F., Zhang, X., Wang, L., Zou, J. J., and Wang, Z. L. (2017b). "Electrocatalytic oxygen evolution reaction for energy conversion and storage: A comprehensive review." *Nano Energy*, Elsevier Ltd.

Thangaraj, V., Eliaz, N., and Hegde, A. C. (2009a). "Corrosion behavior of composition modulated multilayer Zn-Co electrodeposits produced using a single-bath technique." *J. Appl. Electrochem.*, 39(3), 339–345.

Thangaraj, V., Eliaz, N., and Hegde, A. C. (2009b). "Corrosion behavior of composition modulated multilayer Zn-Co electrodeposits produced using a single-bath technique." *J. Appl. Electrochem.*, 39(3), 339–345.

Tian, L., Xu, J., and Xiao, S. (2011). "The influence of pH and bath composition on the properties of Ni-Co coatings synthesized by electrodeposition." *Vacuum*, 86(1), 27–33.

Trasatti, S. (1995). "Electrochemistry and environment: The role of electrocatalysis." *Int. J. Hydrogen Energy*, 20(10), 835–844.

Udompanit, N., Wangyao, P., Henpraserttae, S., and Boonyongmaneerat, Y. (2014). "Wear Response of Composition-Modulated Multilayer Ni-W Coatings." *Adv. Mater. Res.*, 1026, 302–309.

Ueda, Y., Kikuchi, N., Ikeda, S., and Houga, T. (1999). "Magnetoresistance and compositional modulation near the layer boundary of Co/Cu multilayers produced by

pulse electrodeposition.” *J. Magn. Magn. Mater.*, 198, 740–742.

Ul-Hamid, A. (2018). *A Beginners' Guide to Scanning Electron Microscopy. A Beginners' Guid. to Scanning Electron Microsc.*

Ullal, Y., and Hegde, A. C. (2014a). “Electrodeposition and electro-catalytic study of nanocrystalline Ni-Fe alloy.” *Int. J. Hydrogen Energy*, 39(20), 10485–10492.

Ullal, Y., and Hegde, A. C. (2014b). “Electrofabrication of multilayer Fe-Ni alloy coatings for better corrosion protection.” *Appl. Phys. A Mater. Sci. Process.*, 116(4), 1587–1594.

Venkatakrishna, K., and Chitharanjan Hegde, A. (2010). “Electrolytic preparation of cyclic multilayer Zn-Ni alloy coating using switching cathode current densities.” *J. Appl. Electrochem.*, 40(11), 2051–2059.

Vernickaite, E., Tsyntaru, N., Sobczak, K., and Cesiulis, H. (2019a). “Electrochimica Acta Electrodeposited tungsten-rich Ni-W, Co-W and Fe-W cathodes for efficient hydrogen evolution in alkaline medium.” *Electrochim. Acta*, 318, 597–606.

Vernickaite, E., Tsyntaru, N., Sobczak, K., and Cesiulis, H. (2019b). “Electrodeposited tungsten-rich Ni-W, Co-W and Fe-W cathodes for efficient hydrogen evolution in alkaline medium.” *Electrochim. Acta*, 318, 597–606.

Wagner, N. (2011). “Electrochemical impedance spectroscopy.” *PEM Fuel Cell Diagnostic Tools*, (1), 37–70.

Wang, C., Huang, J., Chen, J., Xi, Z., and Deng, X. (2019). “Progress in Electrocatalytic Hydrogen Evolution Based on Monolayer Molybdenum Disulfide.” *Front. Chem.*, 7(March), 1–9.

Wang, J., Shao, H., Ren, S., Hu, A., and Li, M. (2021). “Fabrication of porous Ni-Co catalytic electrode with high performance in hydrogen evolution reaction.” *Appl. Surf. Sci.*, 539(October 2020).

Wang, L., Gao, Y., Xue, Q., Liu, H., and Xu, T. (2005). “Microstructure and tribological properties of electrodeposited Ni-Co alloy deposits.” *Appl. Surf. Sci.*,

242(3–4), 326–332.

Wasekar, N. P., Gowthami, S., Jyothirmayi, A., Joardar, J., Sundararajan, G., Wasekar, N. P., Gowthami, S., Jyothirmayi, A., Joardar, J., and Sundararajan, G. (2019). “Corrosion behaviour of compositionally modulated nanocrystalline Ni – W coatings.” *Surf. Eng.*, 36(952–959), 1–8.

Wasekar, N. P., Latha, S. M., Ramakrishna, M., Rao, D. S., and Sundararajan, G. (2016). “Pulsed electrodeposition and mechanical properties of Ni-W/SiC nano-composite coatings.” *Mater. Des.*, 112, 140–150.

Wendt, H., Rausch, S., and Borucinski, T. (1994). “Advances in Applied Electrocatalysis.” *Adv. Catal.*, 40(C), 87–176.

Wilcox, G. D., and Gabe, D. R. (1993). “Electrodeposited zinc alloy coatings.” *Corros. Sci.*, 35(5–8), 1251–1258.

Wu, G., Li, N., Dai, C. S., and Zhou, D. R. (2004). “Electrochemical preparation and characteristics of Ni-Co-LaNi<sub>5</sub> composite coatings as electrode materials for hydrogen evolution.” *Mater. Chem. Phys.*, 83(2–3), 307–314.

Wu, Y., Chang, D., Kim, D., and Kwon, S. (2003). “Influence of boric acid on the electrodepositing process and structures of Ni – W alloy coating.” *Surf. Coatings Technol.*, 173(03), 259–264.

Xing, S., Wang, L., Jiang, C., Liu, H., Zhu, W., and Ji, V. (2020). “Influence of Y<sub>2</sub>O<sub>3</sub> nanoparticles on microstructures and properties of electrodeposited Ni–W–Y<sub>2</sub>O<sub>3</sub> nanocrystalline coatings.” *Vacuum*, 181(July), 109665.

Yahalom, J., and Zadok, O. (1987). “Formation of composition-modulated alloys by electrodeposition.” *J. Mater. Sci.*, 22(2), 499–503.

Yang, L. (2008). *Techniques for corrosion monitoring*. (L. Yang, ed.), Cambridge, England: Woodhead Publishing Limited.

Yogesha, S., and Chitharanjan Hegde, A. (2011). “Optimization of deposition conditions for development of high corrosion resistant Zn-Fe multilayer coatings.” *J.*

*Mater. Process. Technol.*, 211(8), 1409–1415.

Yogesha, S., and HEGDE, A. (2011). “Development of Composition Modulated Multilayer Alloy Coatings and their Corrosion Behavior.” *J. Met. Mater. Miner. Vol. 21 No.1*, 21(1), 83–92.

You, B., and Sun, Y. (2018). “Innovative Strategies for Electrocatalytic Water Splitting.” *Acc. Chem. Res.*, research-article, 51(7), 1571–1580.

You, S., Jiang, C., Wang, L., Xing, S., and Zhan, K. (2021). “Effect of CeO<sub>2</sub> nanoparticles on the microstructure and properties of the NiCo-CeO<sub>2</sub> composite coatings.” (November).

Zamani, M., Amadeh, A., and Lari Baghal, S. M. (2016). “Effect of Co content on electrodeposition mechanism and mechanical properties of electrodeposited Ni-Co alloy.” *Trans. Nonferrous Met. Soc. China (English Ed.)*, 26(2), 484–491.

Zhang, F., Yao, Z., Moliar, O., Zhang, Z., and Tao, X. (2020). “Ultra-low-power preparation of multilayer nanocrystalline Ni[ $\text{Ni}$ ]Co binary alloy coating by electrochemical additive manufacturing.” *Surf. Coatings Technol.*, 403(June), 126404.

Zhu, L., Younes, O., Ashkenasy, N., Shacham-Diamand, Y., and Gileadi, E. (2002). “STM/AFM studies of the evolution of morphology of electroplated Ni/W alloys.” *Appl. Surf. Sci.*, 200(1–4), 1–14.





## **LIST OF RESEARCH PUBLICATIONS**

1. Neethu, R. M. and Hegde, A. C. (2020). "Development of Ni-W alloy coatings and their electrocatalytic activity for water splitting reaction." *Phys. B Condens. Matter*, 597, 412359.
2. Raveendran, M. N. and Hegde, A. C. (2021). "Effect of Potassium Sodium Tartrate on Composition and Corrosion Performance of Ni-W Alloy Coatings." *Surf. Eng. Appl. Electrochem.*, 57(2), 268–276.
3. Raveendran, M. N. and Hegde, A. C. (2021). "Electrodeposition of multilayer NiW alloy coating for improved anticorrosion performance." *Bull. Mater. Sci.*, 44(2), 1-11.
4. Raveendran, M. N. and Hegde, A. C. (2022). "Anomalous codeposition of NiCo alloy coatings and their corrosion behaviour." *Mater. Today Proc.*, 62(8), 5047-5052.

## **PAPERS PRESENTED AT CONFERENCES**

1. Raveendran, M. N., Gonsalves C.N. and Hegde, A. C. "Electroplating of Cu-Ni alloy for protection of mild steel." XXXVII Annual National Conference of the Indian Council of Chemists, held at NITK, Surathkal on December 12-14, 2018.
2. Raveendran, M. N. and Hegde, A. C. "Development of multilayer NiW alloy coating for better corrosion protection" Twelfth International Symposium on Advances in Electrochemical Science and Technology (iSAEST-12), held at SAEST, Karaikudi, Tamil Nadu on January 08-10, 2019.
3. Raveendran, M. N. and Hegde, A. C. "Development of NiW alloy coatings and their electrocatalytic activity for water splitting reaction" International conference on Current Trends in Functional Materials (CTFM-2020), held at Physics department, NITK Surathkal on January 15-17, 2020.
4. Raveendran, M. N. and Hegde, A. C. "Effect of magnetic field on the electrodeposition of Ni-Cd alloy coating" International conference on

Electrochemistry in Industry, Health and Environment (EIHE – 2020), held at DAE convention centre, BARC, Anushaktinagar, Mumbai on January 21-25, 2020.

5. Raveendran, M. N. and Hegde, A. C “Anomalous codeposition of NiCo alloy coatings and their corrosion behaviour.” International conference on Emerging Trends in Materials Science and Technology – ICETMT 2022 held online on February 10-11, 2022.

## BIO-DATA

### PERSONAL INFORMATION:

Name : NEETHU RAVEENDRAN M  
Father's name : Raveendran K V  
Gender : Female  
Nationality : Indian  
Date of birth : 20-06-1994  
Permanent Address : Thayambath House  
South Mambalam  
Payyanur P.O.  
Kannur -670307  
Kerala  
Contact No. : +919746096862  
Email-id : [neethurm94@gmail.com](mailto:neethurm94@gmail.com)

### EDUCATIONAL QUALIFICATION:

Qualification	University	Year of Passing	Percentage of Marks/CGPA
M.Sc.	National Institute of Technology Karnataka, Surathkal	2016	7.85
B.Sc.	Kannur University	2014	3.49
HSE	Board of Higher Secondary Examinations, Kerala	2011	86.75%
SSLC	Board of Public Examinations, Kerala	2009	9 A+ & 1A
<b>Qualified for Lectureship (NET) on 18 December 2016 with 31<sup>st</sup> Rank</b>			

### **PROJECT COMPLETED:**

M.Sc. Project on “*Synthesis of Transition Metal Complexes for C-C Coupling Reactions*” under Prof. Badekai Ramachandra Bhat, NITK Surathkal (2016).

### **AREA OF RESEARCH: Electroplating**

#### **Research Experience:**

- Skillful in developing alloy coatings by different methods of electrodeposition and analyzing their practical utility in corrosion and water electrolysis applications
- Hands-on experience in using electrochemical workstations like VersaSTAT 3, Biologic-SP 150, Gill AC instruments
- Good in material characterization techniques like Electrochemical Impedance Spectroscopy, Cyclic Voltammetry, XRD, Scanning Electron Microscopy and FT-IR
- Assisted students in completing M.Sc project on Electroplating

### **WORKSHOP ATTENDED**

Two days’ workshop on Metal Finishing Technologies on Electroplating, organized by The Electrochemical Society of India, IISc Bangalore – February 1& 2 -2018.

### **LIST OF PUBLICATIONS:**

1. Neethu, R. M. and Hegde, A. C. (2020). “Development of Ni-W alloy coatings and their electrocatalytic activity for water splitting reaction.” *Phys. B Condens. Matter*, 597, 412359.
2. Raveendran, M. N. and Hegde, A. C. (2021). “Effect of Potassium Sodium Tartrate on Composition and Corrosion Performance of Ni–W Alloy Coatings.” *Surf. Eng. Appl. Electrochem.*, 57(2), 268–276.
3. Raveendran, M. N. and Hegde, A. C. (2021). “Electrodeposition of multilayer NiW alloy coating for improved anticorrosion performance.” *Bull. Mater. Sci.*, 44(2), 1-11.

4. Raveendran, M. N. and Hegde, A. C. (2022). “Anomalous codeposition of NiCo alloy coatings and their corrosion behaviour.” Mater. Today Proc., 62(8), 5047-5052.

**IN CONFERENCES:**

1. Neethu Raveendran M, Cindrella N Gonsalves and A C. Hegde (2018). “Electroplating of Cu-Ni alloy for protection of mild steel.” 37<sup>th</sup> Annual National Conference of the Indian Council of Chemists, held at NITK, Surathkal on December 12-14, 2018.
2. Neethu Raveendran M and A C. Hegde (2019) “Development of multilayer NiW alloy coating for better corrosion protection” International Symposium, iSAEST-12, held at SAEST, Karaikudi, Tamil Nadu on January 08-10, 2019.
3. Neethu Raveendran M and A C. Hegde (2020) “Development of NiW alloy coatings and their electrocatalytic activity for water splitting reaction” International conference, CTFM-2020, held at Physics department, NITK Surathkal on January 15-17, 2020.
4. Neethu Raveendran M and A C. Hegde (2020) “Effect of magnetic field on the electrodeposition of Ni-Cd alloy coating” International conference, EIHE – 2020, held at DAE convention centre, BARC, Mumbai on January 21-25, 2020.
5. Neethu Raveendran M and A C. Hegde (2022) “Anomalous codeposition of NiCo alloy coatings and their corrosion behaviour.” International conference, ICETMT - 2022 held online on February 10-11, 2022.

